A study of liquid bridges in random sphere packing in relation to the properties of fine wet coal.

Mason, G.

Award date:
1968

Awarding institution:
University of Bath

A STUDY OF LIQUID BRIDGES IN RANDOM SPHERE PACKINGS IN RELATION TO THE PROPERTIES OF FINE WET COAL

by G. Mason

A thesis submitted for the Degree of Doctor of Philosophy of the Council for National Academic Awards, 24 Park Crescent, London, W.1.

June, 1968.

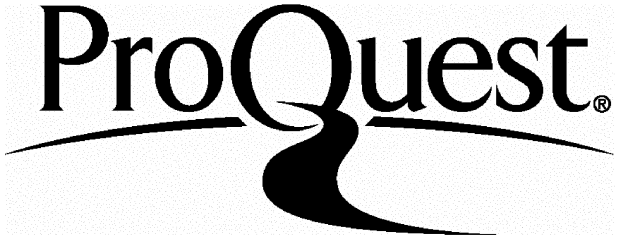

To the memory of

my late father

MEMORANDUM

The work described in this thesis was carried out by me in the School of Physics at Bristol College of Science and Technology (now Bath University of Technology) between February 1963 and April 1966 under the joint supervision of Dr. W.C. Clark (of the College) and Dr. J.O. Cutress (of the Central Electricity Generating Board South Western Regional Research Laboratories). No part of this thesis has previously been submitted by me for any other higher degree, and the work described herein is original and unaided except where specific reference or acknowledgment has been made.

G. Mason.....

11 June, 1968.

ACKNOWLEDGMENTS

I wish to thank Dr. W.C. Clark (then at Bristol College of Science and Technology) and Dr. J.O. Cutress (then at the Central Electricity Generating Board South Western Regional Research Laboratories) for their help and guidance during the course of this work. I am further indebted to Dr. W.C. Clark for his help and encouragement in the production of this thesis - a part which I have found more difficult than the work contained within it.

I thank the Central Electricity Generating Board for their financial support; and my parents for giving me both the opportunity of a University education and the will to continue with it.

Some of the work contained in this thesis is already published:-

1. "Zero force liquid bridges between spherical particles". G. Mason and W. Clark. Brit. Chem. Eng., 10, 327-8 (1965).

2. "Distribution of near neighbours in a random packing of spheres." G. Mason and W. Clark. Nature, 207, 512, (1965).

3. "Liquid bridges between spheres." G. Mason and W. Clark. Chem. Eng. Sci., 20, 859-66, (1965).

4. "Fine structure in the radial distribution function from a random packing of spheres". G. Mason and W. Clark. Nature, 211, 957, (1966).

5. "Tensile strength of wet granular materials". W.C. Clark and G. Mason. Nature, 216, 826-7, (1967).

SUMMARY

This thesis is concerned with the effects of oil on the cohesion of wet coal. Two approaches are described - the analysis of the behaviour of an ideal system of equal spheres and an experimental investigation of the spreading of oil on wet coal.

Chapter 1 describes some experiments and calculations carried out to determine radial distribution functions at small separations for dense random packings of equal spheres. The measurement of a packing of table tennis balls cast in agar yielded the near neighbour distribution function to a greater accuracy than has been achieved hitherto.

Chapter 2 is concerned with the properties of liquid bridges between particles particularly for the limiting cases of two spheres and a sphere and a plane. For these cases the bridge volumes, neck radii, tensile strengths, pressure deficiencies, rupture distances, and the work required for rupture of the bridges have been measured experimentally assuming a zero contact angle. In addition the conditions for a zero force bridge between unequal spheres have been calculated.

The results from Chapters 1 and 2 have been combined in Chapter 6 in an attempt to explain the tensile strength behaviour of packings of wet spheres. The assumption that the cohesion is due to forces exerted by liquid bridges between particles is examined. It is proposed that the tensile strength remains at a constant value over a critical extension of the packing. It is argued that this extension is a little more than one particle diameter. The tensile

strength is derived from the work required to rupture the bed which is spread over this extension. The results are in agreement with experimental results.

The addition of fuel oil or gas oil is known to improve the flow from bunkers of many wet high rank fine coals. Not all coals respond to oiling and a coal which is responsive to oiling when fresh becomes unresponsive when weathered. Chapters 3, 4 and 5 are an account of experiments to determine whether oil spreads spontaneously on wet coal by measuring the advancing contact angle of oil over wet coal. An original modification of a suction potential technique, which obviates the need to pack identical beds of wet coal, is described. A mechanism whereby oiling improves flow is proposed and discussed in the light of these measurements. The contact angle for weathered surfaces is always less than for fresh surfaces. A critical angle of 36° is the demarcation between responsive and unresponsive coals.

CONTENTS

INTRODUCTION

The work presented in this thesis is spread over a wide range of subjects. Consequently the usual thesis format has been modified so as to keep the various related subjects completely together. References are included at the rear of each chapter, together with any appendices. Where one chapter refers to another, a short summary of the relevant section of one is included in the other.

This format has broken up the usual thesis theme. A theme does exist, and it can best be expressed as a "tree" of questions. (Figs. 1 and 2).

The general problem posed was the improvement of the flow of wet coal from the large bunkers of power stations. The Central Electricity Generating Board had already initiated studies of bunker design and carried out many tests of additives, finding that fuel oil was helpful in some cases. A contract was awarded to the then Bristol College of Science and Technology (now Bath University of Technology), to continue trials with additives, The terms of reference were later extended to cover the mechanisms of particle cohesion. There were two main approaches to this; to find why a wet powder was cohesive - involving detailed knowledge of geometry and properties of the liquid bridges; or to find how oil improved the flow from the host of possible mechanisms. Both these approaches soon reached the threshold of knowledge; the various properties of sphere packings had not been measured accurately enough and very little experimental work on the properties of liquid bridges between particles was available; coal surfaces and the action of surface active agents had been studied in the flotation sciences but it was not known whether oil spread

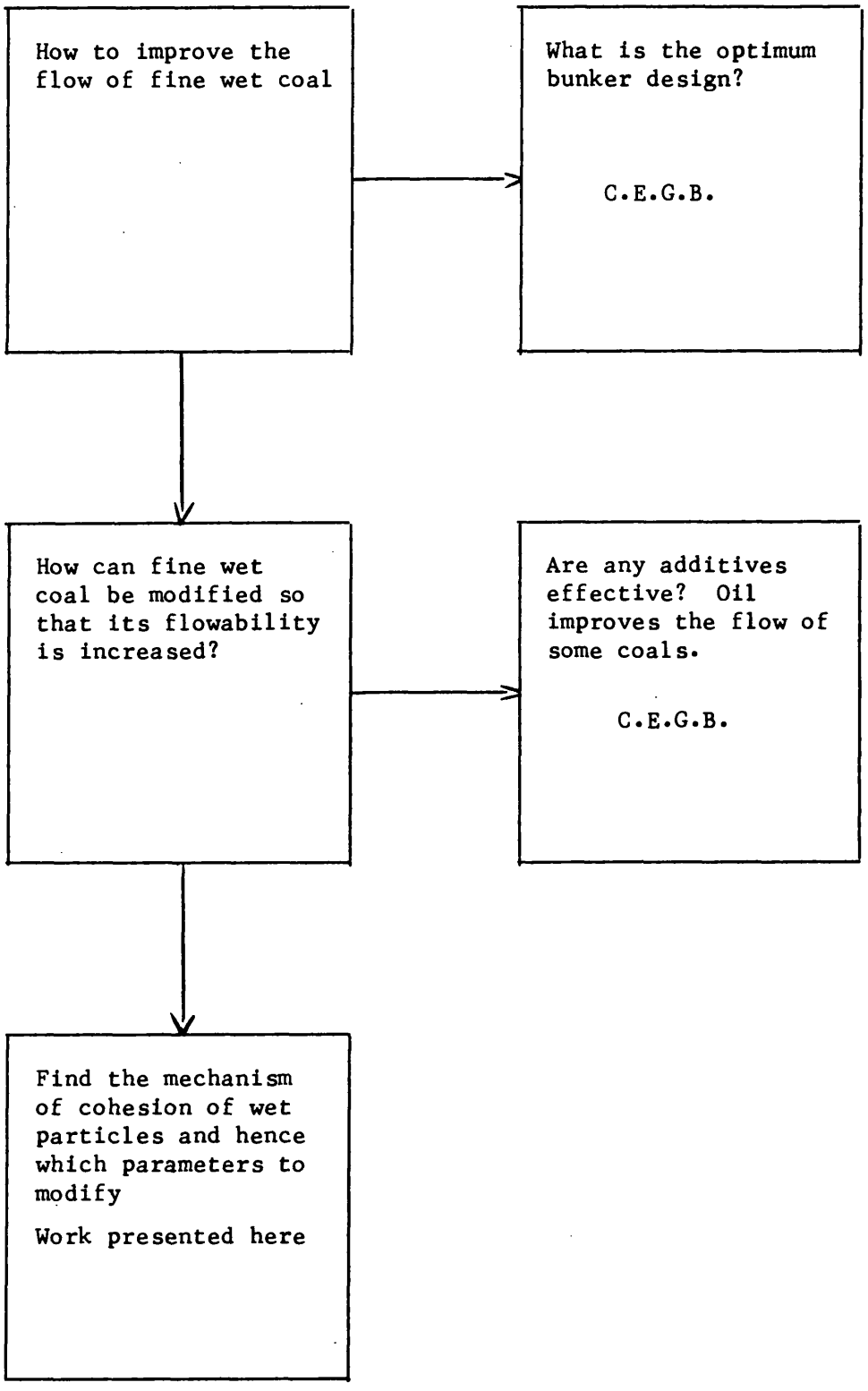
How to improve the flow of fine wet coal
What is the optimum bunker design?
C.E.G.B.
How can fine wet coal be modified so that its flowability is increased?
Are any additives effective? Oil improves the flow of some coals.
C.E.G.B.
Find the mechanism of cohesion of wet particles and hence which parameters to modify
Work presented here

FIG. 1.

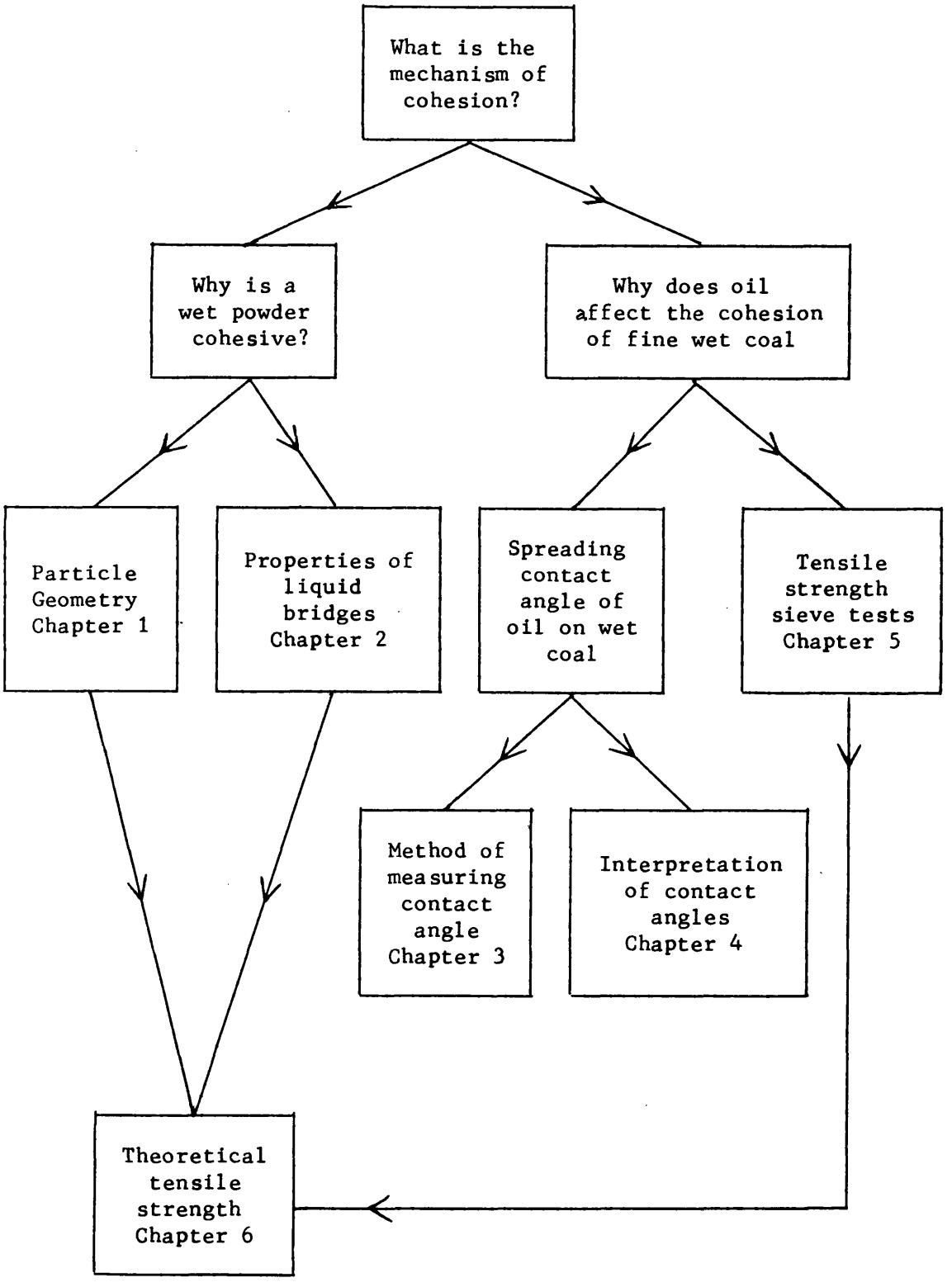
What is the mechanism of cohesion?
Why is a wet powder cohesive?
Why does oil affect the cohesion of fine wet coal
Particle Geometry Chapter 1
Properties of liquid bridges Chapter 2
Spreading contact angle of oil on wet coal
Tensile strength sieve tests Chapter 5
Method of measuring contact angle Chapter 3
Interpretation of contact angles Chapter 4
Theoretical tensile strength Chapter 6

FIG. 2.

spontaneously on wet coal displacing the water.

In the final chapter, an attempt has been made to calculate the tensile strength of beds of wet spheres from first principles and to formulate new equations.

CHAPTER ONE

GEOMETRICAL PROPERTIES OF PARTICLE PACKINGS

INTRODUCTION

1. Porosity
2. Packing Density
3. Co-ordination Number
4. Radial Distribution Function
5. Angular Distribution Function
6. Boundary Effects.
   (i) Statistical effects
   (ii) Regularities propagated from the boundary
   (iii) Local voidage at the boundary
7. Subdivision of packings

SPHERES

EQUAL-SIZED

A. REGULAR PACKINGS

1. Exact properties
2. Unit cell

B. IRREGULAR PACKINGS

1. Packing density limits
2. Dilation and packing density
3. Theoretical restrictions on packing density
4. Co-ordination Number
   (i) From acid and lead shot
   (ii) From spheres set in paint
   (iii) From spheres set in wax
5. Polyhedra and co-ordination number
   (i) Plasticene spheres
   (ii) Soap froth, compressed lead shot
6. Voronoi Polyhedra
7. 5-membered rings

8. Theoretical co-ordination number

9. Addition of spheres to small packings

10. Liquids and irregular packings

11. Experiment with a random packing

(i) Theory and method

(ii) Practical details

(iii) Correction for boundary effect.

(iv) Results. Fine structure. Co-ordination number.

SPHERES

UNEQUAL SIZED

A. REGULAR PACKINGS

1. Geometry of interstices

2. Limit of packing density

B. IRREGULAR PACKINGS

1. Packing density of binary mixtures

2. Theoretical approach of Wise.

NON SPHERICAL PARTICLES

A. REGULAR PACKINGS

1. Interest to biologists

B. IRREGULAR PACKINGS

1. Difficulties of theoretical study.

REFERENCES

APPENDIX I

1. Calculation of size of gap in pentagonal ring.

2. Calculation of other small gaps.

APPENDIX II

Derivation of 13.39 (7) as the maximum number of spheres that can be packed around a central sphere assuming a dense regular covering.

INTRODUCTION

1. Porosity

Porosity is the most easily measured property of a packing. It is defined as either the fractional void space or the percentage void space.

Either $$\varepsilon = \frac{V_o}{V + V_o}$$

or $$\varepsilon = \frac{V_o}{V + V_o} \times 100\%$$

where ε = porosity

V_o = volume of the voids

V = volume of the solids.

2. Packing Density

This is the inverse of porosity. It is defined as the fractional solids volume

$$\text{Packing Density} = \frac{V}{V + V_o}$$

3. Co-ordination Number

If a single sphere in a packing is considered, the co-ordination number of that sphere is the number of spheres in contact with it. The term is sometimes widened to include all spheres within a certain distance of the central sphere and not merely contacts. The co-ordination number of an individual sphere is not a very useful parameter and it is customary to quote the "average co-ordination number" of a packing or the co-ordination number distribution function.

4. Radial Distribution Function (Pair Distribution Function)

The radial distribution function expresses the probability of finding a sphere at a certain distance from another sphere. If

a particular sphere in a pack is taken as a centre and its distance from every other sphere in the pack calculated, then the histogram plot of "number of spheres" against "distance" gives the radial distribution function of the central sphere. Usually a number of centres are taken and the radial distribution function plotted as the average of this number. The probability of a sphere centre lying within two limits at a distance from the central sphere is dependent upon the square of this radial distance, because the volume of the sample shell is proportional to its surface area and thickness. It is therefore more useful for demonstrating ordering effects in radial distribution functions to normalize by plotting the "number"/$4\pi r^2$ where 'r' is the radial distance from the central sphere.

5. Angular Distribution Function

If a central sphere is taken as an origin and two adjacent co-ordinated spheres considered in conjunction, then one of these spheres defines a pole from the central sphere and the second sphere defines a plane containing the polar axis. The angular positions of all the other spheres in the same co-ordination shell are calculated with reference to these co-ordinates, and the system repeated for all the other possible combinations of three adjacent spheres. The average of all these angles is plotted on a hemisphere centred on the central sphere. There is an area on the top of the hemisphere obscured by the first co-ordinated sphere and another adjacent area obscured by the second co-ordinated sphere defining the reference plane. Other peaks and hollows can be assessed as an indication of the regularity of the packing. (See Scott[10]).

6. Boundary Effects

(i) In any real packing of spheres there is always a boundary to the packing and this boundary can give effects leading well into the packing. The pack has to be of such a size that the number of spheres on the surface is small relative to the total number. If one considers a cubic open packing of 1,000 spheres then there are on average 81 spheres on each of the six faces. The total number of spheres in the outside layer is thus 486, or approximately one half of the total number. To reduce the effect of the boundary, a very large packing has to be considered or some means of limiting its importance devised.

(ii) A random packing can suffer from the effect of a boundary in a more serious manner[34]. A plane wall or spherical surface will induce a regularity which can extend over several particle diameters into the packing. This is because the wall forms a regular layer of particles and successive layers occupy the sockets or depressions in the first layer and extend the regularity. All supposed random packings of spheres in containers with flat or smooth sides must be regarded with suspicion.

(iii) If the porosity of a packing is to be calculated one has to determine the volume occupied by the packing and the volume can be found from a measurement of weight and density or calculated from the number of particles. The volume occupied by the packing is subject to a wall effect in that the porosity near the wall is much higher than the rest of the packing. In the case when the particles near the wall comprise a large percentage of the total this wall effect can be serious. Scott[2] measured the porosity of ball bearings in different sized containers in order to find the porosity unaffected by walls. Using different sized copper

Fig. 1(a)

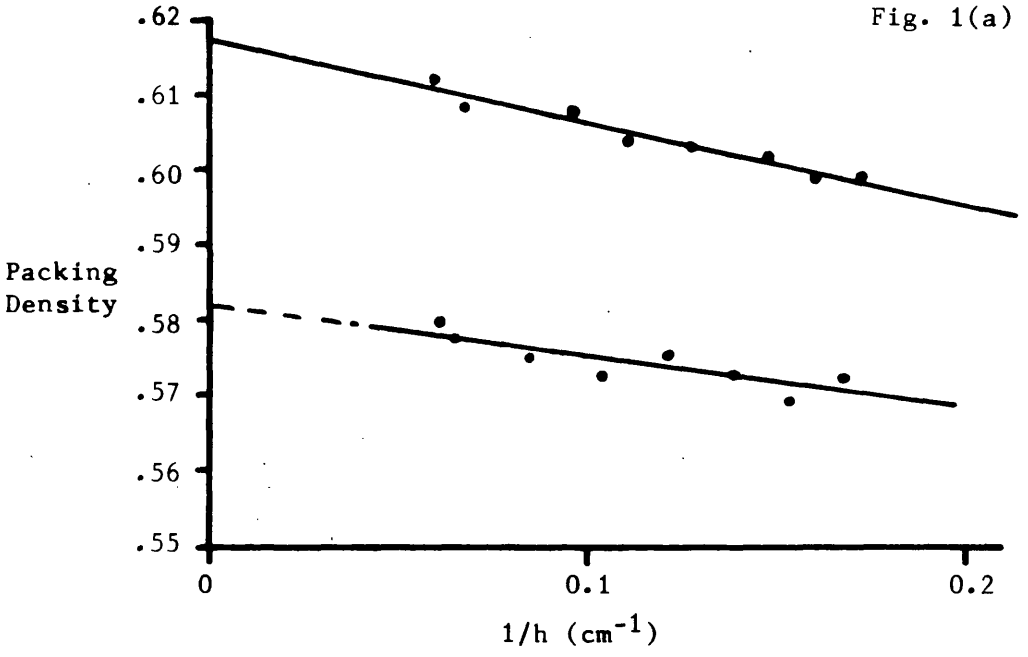

Packing density of balls in a dimpled copper cylinder. h is the depth to which the balls fill the cylinder.

Fig. 1(b)

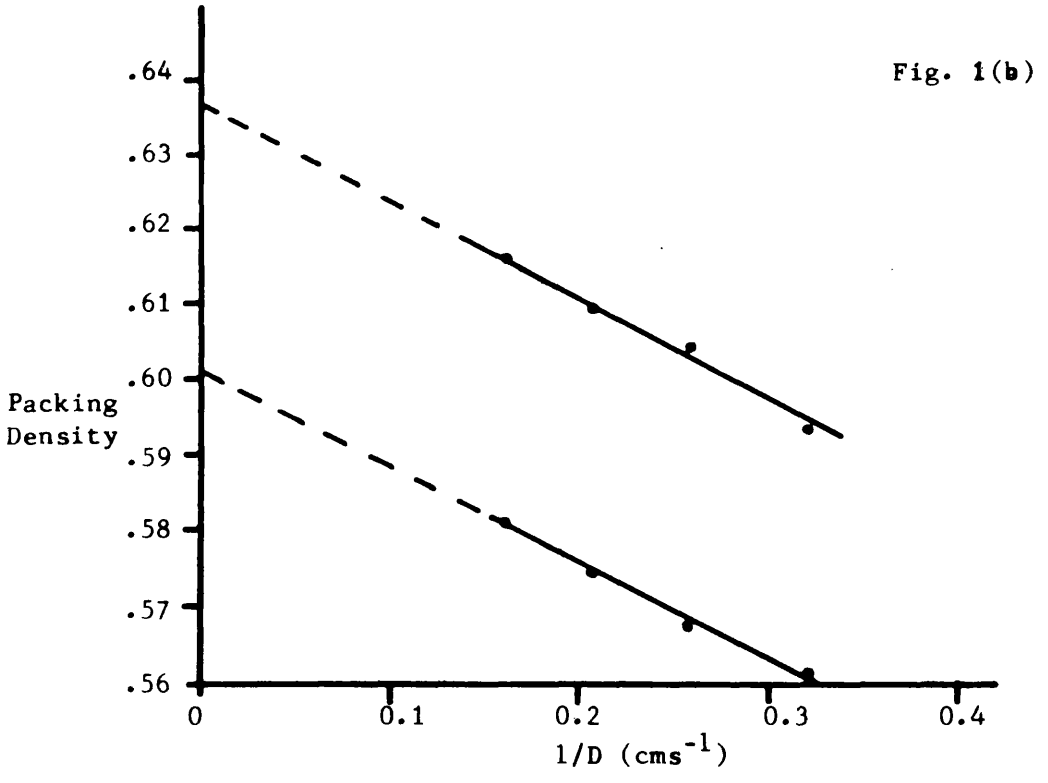

Packing density in a cylinder of infinite length, obtained from extrapolation as in Fig. 1(a) plotted against reciprocal diameter. D is the diameter of the cylinder. After Scott. Ref. 2.

cylinders with dimpled walls he packed them first with different depths of balls and extrapolated the resulting porosities to infinite depth. Then, extrapolating the relation between these values and the cylinder diameter to infinite diameter he obtained the corrected porosity of the packing accurate to 0.2%

7. Subdivision of space

Any array of spheres can be subdivided into irregular tetrahedra by joining adjacent centres with lines. Other methods of subdivision include unit cells for regular arrays and, more generally, Voronoi polyhedra. A Voronoi polyhedron about a sphere is formed by constructing planes, each a surface equidistant from the central sphere and a near neighbour, about a sample sphere. The basic property of these various sub-units is that they can be packed together to completely fill the space. This is well known in crystallography as the explanation for the absence of five-fold or seven-fold symmetry in regular arrays.

SPHERES EQUAL SIZED

A. REGULAR PACKINGS

1. The regular packings have been well defined by crystallographers[1], and their space-filling properties fully investigated. The highest packing density is 0.7405.... for cubic closest packing and in this arrangement each sphere has twelve near neighbours. Details of the other packings are given in Fig. 2. The radial distribution functions of the regular packings contain discrete peaks as several near neighbours occur at identical distances. These functions are shown in Fig. 3. for the denser packings.

A regular packing can be divided into unit cells and the properties of one such cell gives the properties of the overall packing. The unit cell represents the total packing but contains far fewer spheres thus making an analysis much easier. (Spheres. Equal Sized).

B. IRREGULAR PACKINGS

1. The study of irregular packing is complicated by the absence of a unit cell with the result that the packing has to be considered as a whole with a corresponding increase in complexity. It was established by Scott[2] that the packing density of ball bearings could vary between two limits which he termed "loose random packing" and "dense random packing". Taking care to correct for the wall effects he arrived at the packing density of 0.63(7) for the dense packing and 0.60(1) for the loose packing. These densities differ from the closest packed limit of 0.7405.. by about 16% Of the two packings, the "random close packing" is the easiest to handle because distortion and compression have little effect and the packing can be restored by vibration. Open

Name	Packing Density	Co-ordination Number
Cubic closest	0.7405	12
Body-centred tetragonal	0.6981	10
Body-centred cubic	0.6801	8
Simple hexagonal	0.6046	8
Simple cubic	0.5236	6

FIG. 2. Details of some lattice packings.

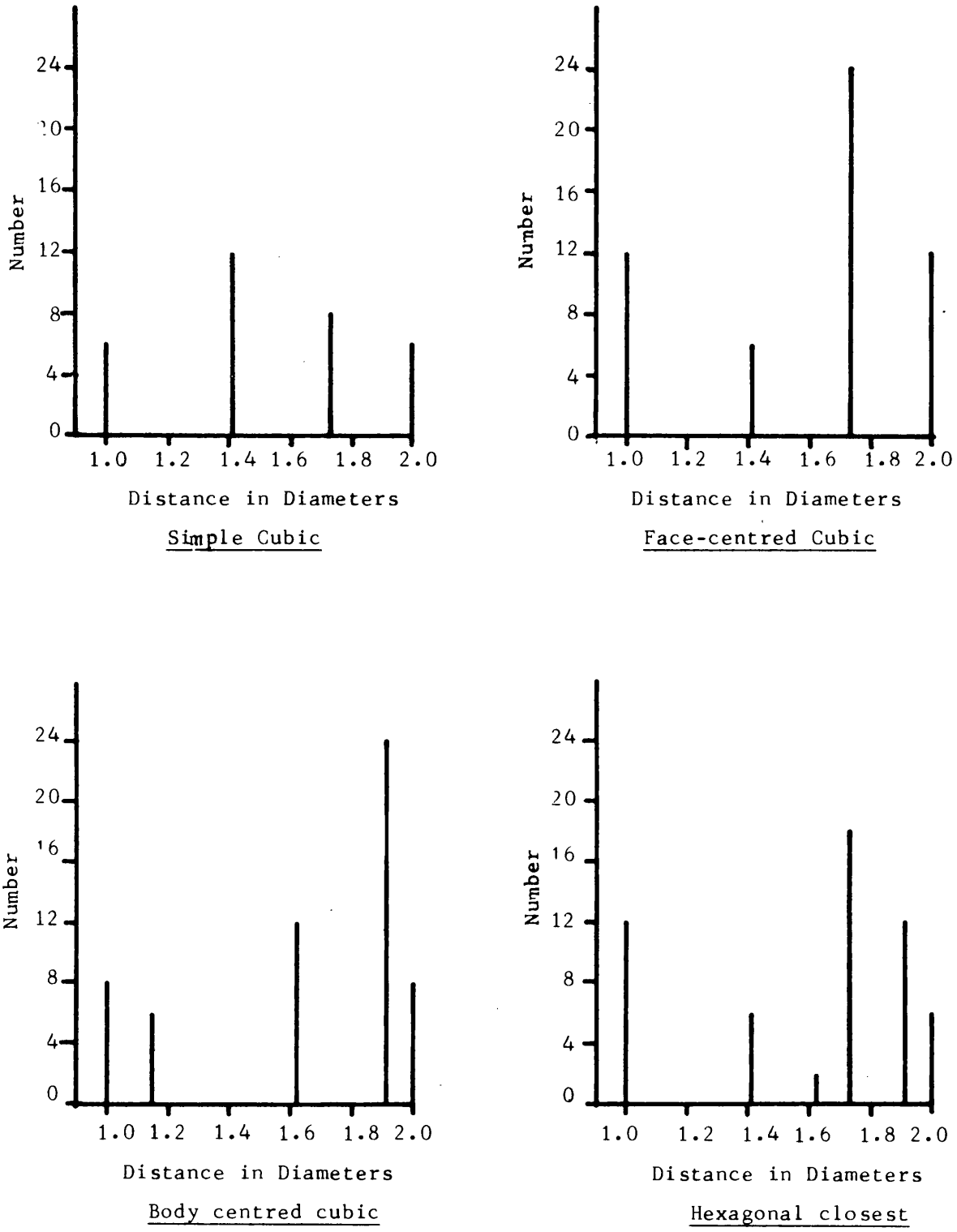

FIG. 3. Radial distribution functions of some lattice packings.

packings are more difficult because they collapse when disturbed and have to be expanded and repacked to restore their porosity. The ease of handling has resulted in the close packings receiving the greatest attention with respect to their radial distribution function and angular distribution function.

2. It is known that dense particulate masses have to dilate in order to be sheared[3],[4]. A random close packed array has to open slightly in order to permit the particles free passage. In a series of experiments with steel balls Roscoe, Schofield and Wroth[5] found the critical porosity to be 39% corresponding to a packing density of 0.61. This is nearly the packing density of random open packing and the significance of this agreement has been dealt with thermodynamically by Morgenstern[4].

3. Sphere packings have also been investigated by mathematicians[13],[14],[15], who have introduced new and useful concepts. It can be shown that the packing density of an array of four spheres, each of which touches the other three is

$$\sqrt{18} \cdot (\cos^{-1} 1/3 - \pi/3) = 0.7797.[38].$$

This is the density of the tetrahedron spanned by their four centres. This compares with 0.7405... for the closest lattice packings. Consequently it can be seen that an irregular array of spheres could conveivably have a density greater than that of the closest regular packings[18]. However, it is impossible to completely fill space with regular tetrahedra and it would seem that a packing density greater than 0.7405.. is impossible for a large packing, although this cannot be proved. Boerdijk[39] has shown that the maximum number of equal spheres simultaneously touching a similar sphere is twelve and Fejes[40], assuming this

as an experimental fact, showed that the mean density over all space was less than $4\pi/30\sqrt{2(65 - 29\sqrt{5})} = 0.7547...$ which would appear to reduce the limit for any packing. However, Fejes Tóth[13] only mentions such a proof as applying to a packing having a unit cell of a dodecahedron with the twelve surrounding spheres attached through the twelve faces of the dodecahedron. Dodecahedra cannot fill space and so the proof must be an idealised case and invalid in general.

4. (i) In an early series of experiments Smith, Foote and Busang[6] attempted to find a relationship between the co-ordination number and packing density. They packed lead shot in a beaker filled with acetic acid and drained it. Wherever two balls were close or touching, a liquid bridge of acetic acid was formed, which attacked the lead forming the basic acetate. This left white deposits on the balls at all the contacts and near contacts. The packing was dismantled and the number of spheres with different numbers of contacts counted. The result of this was a series of histograms of "the number of spheres" against "contacts per sphere" for different porosities. It also proved possible to propose a function of the variation of "Average number of contacts per sphere" with porosity.

4. (ii) Bernal and Mason[7] performed a similar experiment using ball bearings and black paint. The pack of balls was drained and the paint allowed to set, whereupon the mass was dissected. The number of paint spots per sphere was counted throughout the pack. In a further experiment[8] the co-ordinates of every sphere centre were measured before the ball was removed. The sphere centre co-ordinates were used to calculate a radial distribution function.

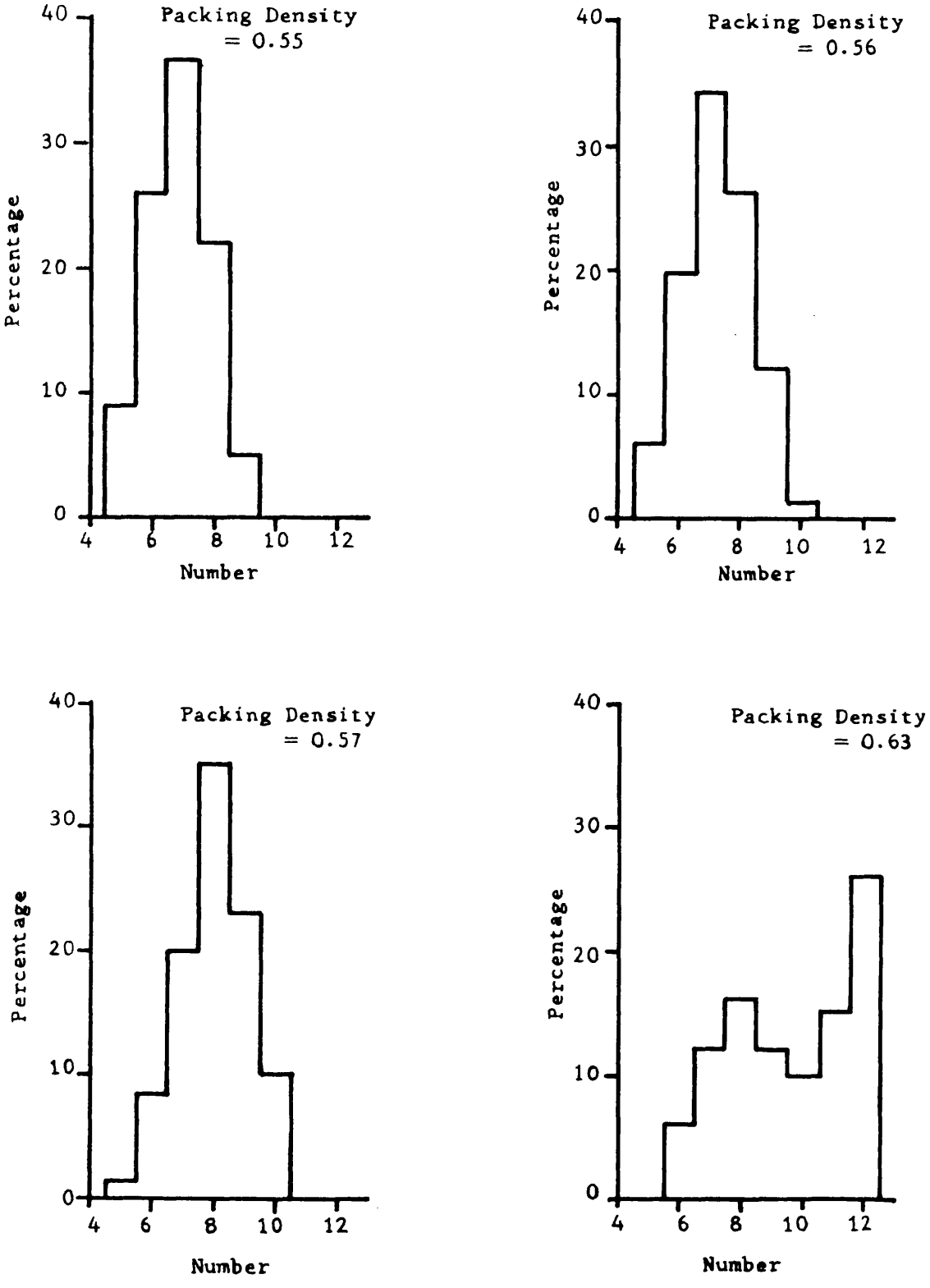

FIG. 4. Co-ordination Number Distribution Functions.
(After Smith, Foote & Busang[6].)

4. (iii) Similar work by Scott[9] in which the balls were cast in paraffin wax and their co-ordinates measured with an optical comparator resulted in a similar, although more accurate radial distribution function. Scott and Mader[10] went further and produced an angular distribution function which showed that angular effects did not stretch beyond the second co-ordination shell.

5. (i) Bernal[8],[11],[12] had also packed chalk covered "plasticene" spheres together in a balloon, evacuated the mass, and compressed it. The balls were distorted into polyhedra and the numbers of the various pentagonal and hexagonal faces counted. This showed an overwhelming number of five-sided faces.

5. (ii) Such experiments had been performed before. As long ago as 1727 Hales[35] compressed peas in a pot and found that they were formed into "pretty regular dodecahedrons" and Marvin[36] and Matzke[37] repeated Hales[35] experiment using lead shot, finding in general 14 sided bodies were formed. Matzke[37] also examined 600 central bubbles of a 1,900 bubble froth and found an average number of contacts of 13.70 as well as the most common body which had 1 quadrangular, 12 pentagonal and 2 hexagonal faces.

6. There is about every point in an array a region containing all space which is closer to that point than any other point. In two dimensions these regions will be polygons and in three dimensions polyhedra. They are called either Voronoi[16] polyhedra or Dirichlet[17] zones after the mathematicians who formalized them. By constructing these polyhedra, an array can be subdivided into units which can be studied individually. The

units can be repacked to completely fill the space. Any point around a central point which contributes a face to the Voronoi polyhedron of the central point is classed as a geometric neighbour. Clearly the number of faces of the Voronoi polyhedron equals the number of geometric neighbours. A count of Bernal's plasticene packing (5 (i)) gave the average number of faces as 13.6. This agrees with a result of Coxeter[18] who obtained 13.56 from an investigation of four and five dimensional polytopes. Coxeter[18] was not completely certain of his derivation of 13.56 as an equally plausible equation gave a co-ordination number of 13.398. This second value was obtained by considering the space around a central sphere to be filled with tetrahedra of four touching spheres, one sphere of the tetrahedron being the central sphere. Assuming that tetrahedra can be placed in this manner, one arrives at the co-ordination number of 13.398 (see Appendix II), whereas the maximum number that can actually be placed like this is only 12[39]. Bernal's[11] plasticene Voronoi polyhedra demonstrate all the geometric neighbours of a sphere, whereas Coxeter's[18] "proof" demands that the co-ordinated spheres touch the central sphere. The agreement of the results must be somewhat fortuitous. What is needed is some analysis of sphere packing that considers all the near neighbours as significent. This can be illustrated by considering an array of spheres giving a network of Voronoi polyhedra around the sphere centres co-ordinates. If now the spheres are slightly reduced in size but retain their former centres, then the Voronoi polyhedra network is unchanged, yet no sphere touches any other. Meijering[41] analysed a set of random co-ordinates using classical statistical methods and obtained a value of $48\pi^2/35 + 2 = 15.54...$ for the average number

of geometric neighbours of any point. This is for points occupying any position in space and does not apply to spheres which have the restriction that they cannot overlap. That the value for the average number of geometric neighbours is 12 for the most regular array of spheres yet only 15.54 for a random array of points leads one to suppose that these are the two limits, and any other sphere packing must have an average geometric co-ordination number between these two values. Smith[43] mentions a paper by von Federow[44] in which it is shown that space filling polyhedra cannot be convex if they have more than 14 faces. Voronoi polyhedra must always be convex, since normals to the faces always pass through a certain point inside the polyhedron so this theorem of von Federow[44] would apparently place doubts upon the calculation of Meijering[41] which showed that there were on average 15.54 geometric neighbours. Although I have not seen the proof of von Federow[44] it is possible that he was referring to regular space filling polyhedra, in which case fourteen sides seems a reasonable number, as the truncated octahedron which has fourteen sides can be packed to completely fill space.

7. Using a geometric co-ordination number of 13.56, Bernal[12] calculated the average number of edges of each face of the Voronoi polyhedra. Euler's formula[15] connecting the number of faces, edges and vertices for three dimensional polytopes is

$$V - E + F = 2 \qquad \ldots\ldots\ldots\ldots\ldots\ldots\ldots \quad (1)$$

However, there are three edges at every vertex (an experimental fact[11]), so

$$3V = 2E \qquad \ldots\ldots\ldots\ldots\ldots\ldots\ldots \quad (2)$$

since each edge contributes to two vertices.

Thus $2E/F = \frac{6(F-2)}{F}$ ..... (3)

and $\frac{2E}{F} = 5.115$ ..... (4)

as $F = 13.56$.

The average number of edges to each face is thus 5.115, and so there will be a predominance of pentagons on the Voronoi polyhedra. For a packing of spheres there will be a predominance of five-membered rings; these in general being around the equator of two touching spheres.

8. If a sphere is taken as an origin, it is found that at most twelve other spheres can be placed upon it[13],[39]. There is, however, an infinite number of ways in which this shell of touching neighbours can be arranged. There is sufficient area available for the thirteenth sphere but it is impossible to arrange the other twelve to leave only one large hole and not several small ones. Furthermore, any attempt at placing twelve spheres upon a central one invariably creates rings of five spheres. The arrangements that do not produce these rings of five spheres are the regular packings.

9. If one starts packing spheres such that each sphere touches three others, the rings can be seen building up. (Fig. 5). There is only one way of placing two spheres in contact. On adding the third it can either form an open chain of three or a triangular arrangement. As we are aiming for a dense packing, it is clear that the densest arrangement of three spheres is the triangle. Similarly, on adding the fourth sphere a tetrahedron is formed. There is only one place to add the fifth sphere to continue dense packing, and that is on one of the faces, or rather in one of

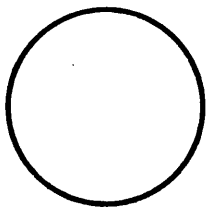

(i)

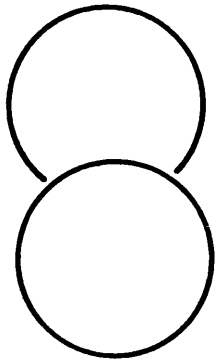

(ii)

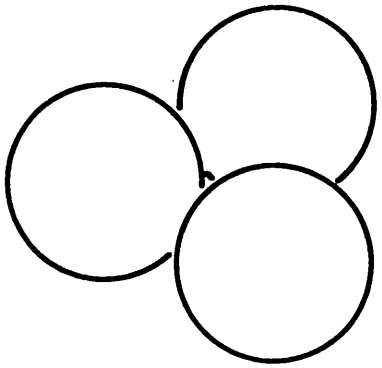

(iii)

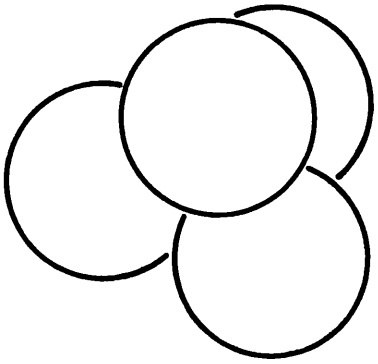

(iv)

FIG. 5.

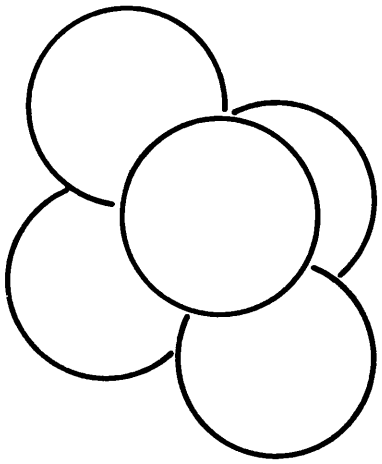

(v)

(vi) a

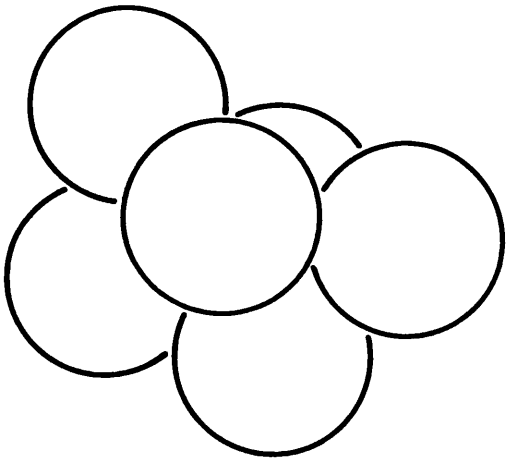

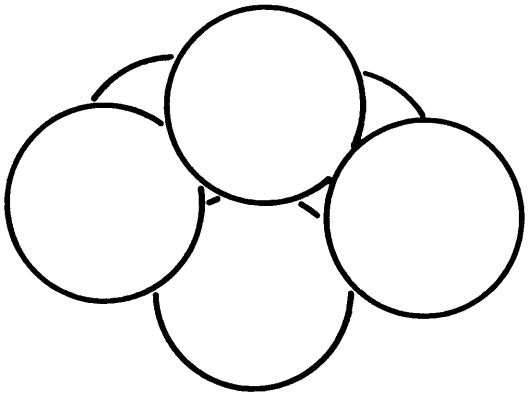

(vi) b

FIG. 5.

holes on the faces of the tetrahedron. This gives a system of two tetrahedra base to base containing five spheres. Upon adding the sixth sphere the packing becomes irregular. There is only one place where this sphere can be added to continue as a close packed array and that is on one of the exposed tetrahedron faces. Thus the rather surprising fact emerges that there is one, and only one, closest packed array of six spheres. Furthermore, adding the sixth sphere in this manner makes a lattice packing impossible.

The seventh sphere can be added to the six in several ways, but the number of different structures totals only four, of which two are mirror images of one another. One of these structures has a small gap where five spheres have been placed around the equator of two touching spheres and another has a three-fold axis of symmetry.

Adding the eighth sphere can give ten possible structures of which five are similar, in that the position of a small gap is their only difference. There is also the start of a left-handed and right handed "rope" of tetrahedra and one structure with four three-fold axes of symmetry where a sphere has been attached to every face of a tetrahedron.

Adding the ninth sphere would give over twenty new structures but this was not undertaken because the "eight" structures had already made the point that a packing of spheres of infinite volume of density 0.7797 can exist, provided the space it fills is of special shape. The two "rope" structures can be grown indefinitely from each end without any small gaps forming between the spheres. In order to branch one of these chains, a small gap has to be formed which implies a reduction in the packing density.

10. A liquid may be considered for some purposes to be a random array of moving hard sphere atoms and the small packings of spheres described above might be assumed to exist in the mass. The fact that a regular array is impossible for more than five close-packed spheres may go some way towards explaining the need for "seeding" a liquid in order to grow crystals. With the aid of a large model of a packing of spheres, Bernal[8] discovered regions of tetrahedra, packed similar to the "ropes" and proposed the name pseudo-nuclei. The existence of these nuclei had already been suggested by Eyring[19] and demonstrated by Boerdijk[39]. However, Bagley[20] devised a dense packing (packing density 0.7257) with five-fold symmetry which had an orthorhombic unit cell. Whiskers of nickel, iron and platinum have shown this five-fold symmetry[26].

11. (i) A drop of liquid between two spheres will form a small bridge which holds the spheres together. (see Chapter 2). The maximum span of such bridges in a packing of spheres is about 0.2 diameters, and therefore, in any calculation of bulk tensile strength from the liquid bridge properties, the radial distribution function in this nearly touching range will be of importance. The published results of Bernal[7],[8],[11],[12] and of Scott[2],[9] do not show sufficient detail because these workers used ball bearings of small size ($\frac{1}{4}$ or $\frac{1}{8}$ ins. diameter). They were also interested in spheres as far apart as four diameters and were forced to measure the co-ordinates of each sphere and to calculate the radial distribution distances. The narrow range between 1 and 1.3 diameters is different because it is impossible for two spheres, whose centre separation is 1.3 diameters, to have the space between them obscured by another sphere. Consequently it is possible to measure such separations directly.

11. (ii) Experimental

If a mass of spheres is cast in some non-adhesive wax or jelly and a sphere removed leaving a clean socket, the separations between its near neighbours can be measured directly with a simple depth probe. For such a direct measurement the spheres have obviously to be as large as practicable and high grade table tennis balls (dia. 1.5 $\pm$ 0.010 ins) proved suitable. Potato agar was selected as a casting liquid because it did not set when cooling until about 30°C and when set, proved rigid enough to hold the balls easily. The agar did not stick to the balls and this enabled a ball to be removed leaving the clean cut socket cast in the agar. As the agar had to be poured at about 45°C a few table tennis balls were tested at this temperature for distortion and this proved to be negligible for "One-Star" balls. However, a cheaper and thinner ball did distort appreciably. Heat distorted table tennis balls are non spherical.

A simple probe device was made for measuring the distance through the agar from a socket to the adjacent sphere and it was accurate to approximately 0.25 mms. (See Fig. 6).

The container for the balls had to be irregular to reduce wall effects and a special polythene bag was made for the purpose. It was roughly cylindrical and the surface was dimpled with no particular order by heating the polythene with a cloth soaked in hot water and then striking it with a large ball-pein hammer. A soft anvil of hard rubber foam was found to give the best effect. The indentations thus produced varied in size but were a maximum of an inch across and half an inch deep. The 1006 balls were packed in the bag from time to time to study visually whether this indenting of the bag surface was effective. Initially the

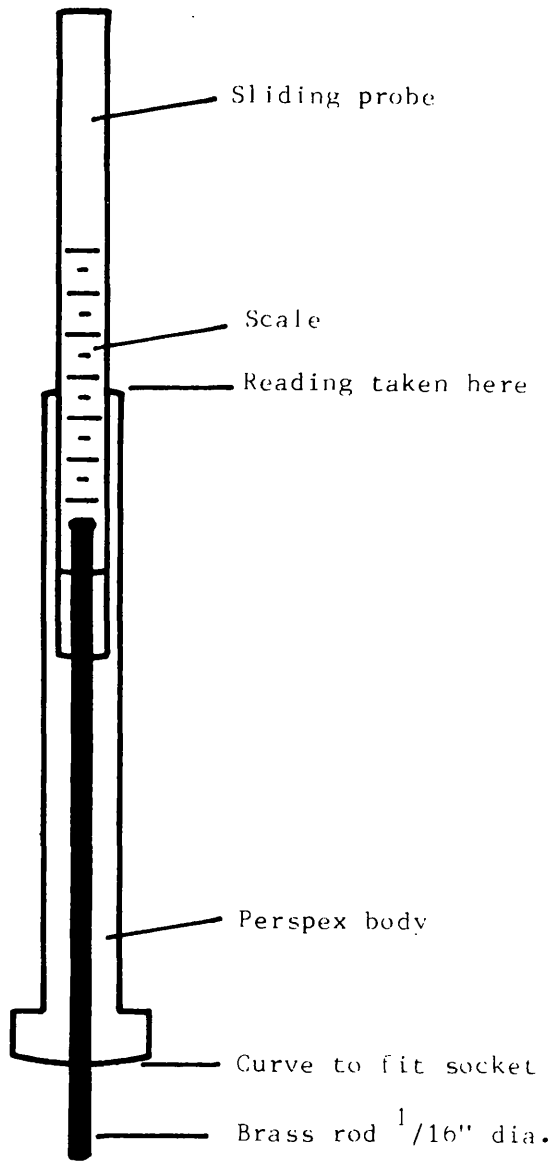

FIG. 6. Diagram of probe.

Treatment	Diameters in cms.		
	A	B	C
At room temperature	3.810	3.808	3.816
2 mins. at 30°C	3.813	3.810	3.818
5 mins. at 40°C	3.814	3.811	3.819

Typical effect of temperature on the dimensions of "One Star" table tennis balls. The three diameters were taken to be approximately perpendicular to each other.

FIG. 7. Effect of temperature on table tennis balls.

surface layer was quite regular but finally, although regularities could still be seen, there was obviously far more disorder. The packing so formed was approximately cylindrical about two feet high and eighteen inches in diameter. This packing was placed in a dustbin and the external space filled with sand so as to support the walls of the bag when the agar was added. A polythene tube was run down one side of the packing into the bottom of the bag before the top of the bag was tied and covered over with sand. Only the tube remained visible and a large funnel was fastened into the polythene filler tube.

A 2% W/V mixture of Oxoid Agar No.3 was made up and after allowing the agar to cool to 45°C it was run down the polythene tube and into the packing. About 24 hours later, when the mass was fully cooled, the sand was removed from the bin and the packing carefully lifted out. The excess agar on the outside was cut away and the packing was weighed. Since the agar occupied the void space and the number of balls, their individual weight and volume were known, it was possible to calculate the packing density. The density of the agar was taken as that of water.

The packing was now cut apart using a small knife to ease balls from their sockets and the number of contacts and near contacts for each socket measured. Thus on removal of the next sphere any contact or near contact which had previously been counted was observed to be between two sockets and so could be ignored. In this manner it was possible to avoid counting a contact twice. Only contacts or near contacts between a socket and a sphere were measured, never between two sockets. If a record were kept for each individual sphere it would be possible to determine the co-ordination number distribution function.

Weight of the polythene bag	= 125 gms
Weight of polythene bag plus the balls	= 2900 gms
Weight of polythene bag and balls plus the agar	= 20,335 gms
Diameter of the balls	= 3.81 cms
Volume of agar ≡ Volume of voids	= 20,335 - 2,900
Assuming density of agar = 1 gm/cc	= 17,435 ccs.
Total volume of the balls	$= 1{,}006 \times \frac{4}{3} \pi \times (\frac{3.81}{2})^3$
	= 29,131 ccs
Total volume of the pack	= 46,566 ccs

Hence packing density = $\frac{29{,}131}{46{,}566} = 0.625(6)$

FIG. 8. Calculation of packing density.

However, the added complexity of documentation and the time taken to record the measurements would have turned this simple experiment into something much larger. Furthermore, it would only be a check on the work of Bernal[11] and would have ideally needed measurements out to 1.5 sphere diameters.

11. (iii) The results can be plotted graphically in a number of ways. However, care has to be taken that the wall effect is not neglected. If the packing is taken as having the general dimensions of approximately fifty-five spheres in cross section and eighteen spheres in length then the number of spheres in the outside layer is about 450. Each of these spheres will only have a fraction of their full number of contacts and an indication of this fraction can be obtained from consideration of hexagonal closest packing. In hexagonal closest packing each sphere has twelve nearest neighbours, six of which form a ring around an equator of the central sphere. The remaining six are split into two groups of three which are placed one above the ring of six and the other below. However the outside layer is curved into a cylindrical shell and each sphere can be considered to be four neighbours short or one third of the total. Thus the present packing can be considered, as far as the number of contacts is concerned, to be of only $(1006 - 450/3) = 856$ spheres.

11. (iv) As there appeared to be considerable scatter on the original histogram (Fig. 9) an attempt was made to eliminate this by taking a running three-fold average of the results. This consists of adding three adjacent results together, dividing the sum by three and re-plotting this as the middle result. On taking this average again, it was found that there were three peaks on the

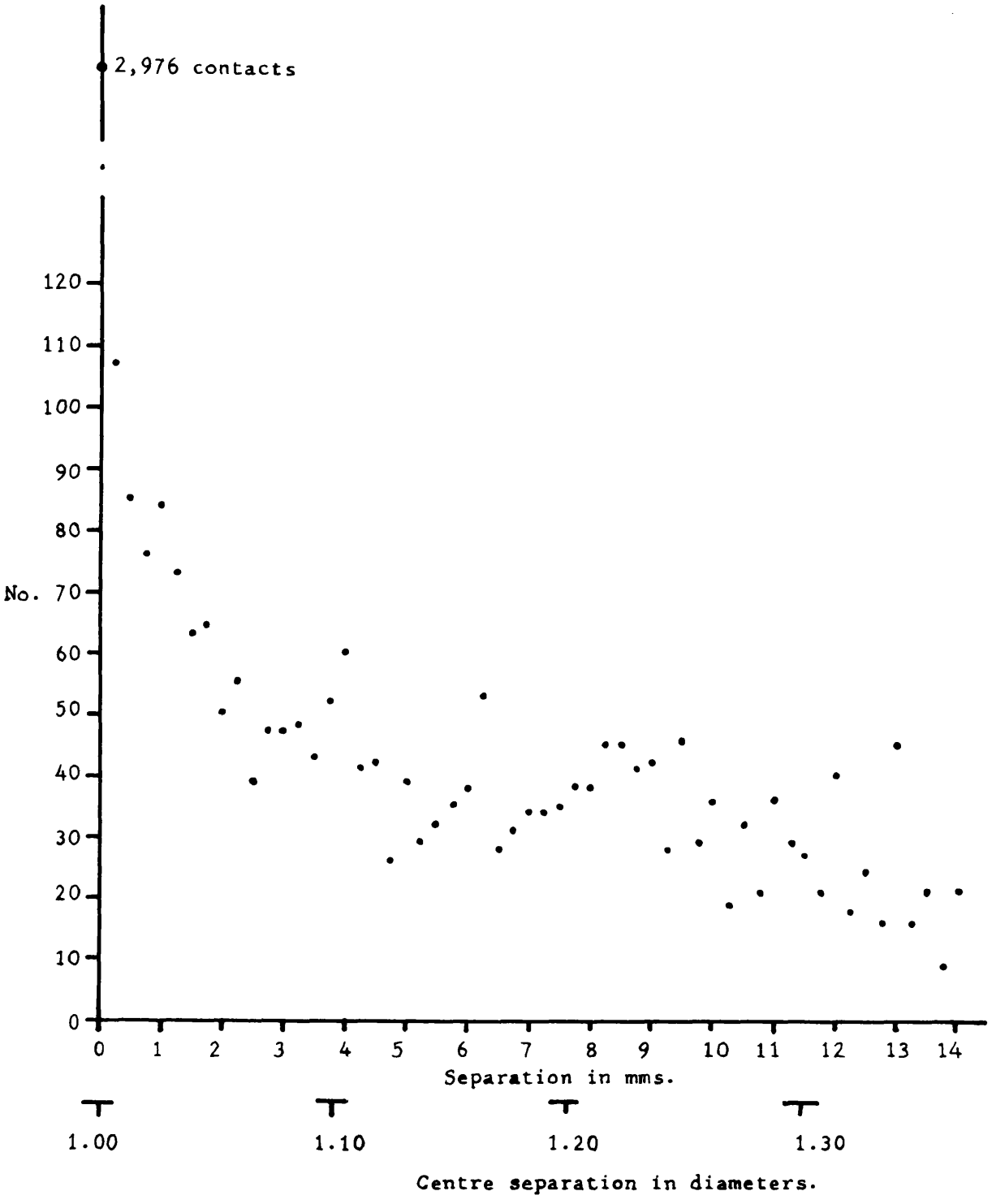

FIG. 9. Basic results of Number vs Separation.

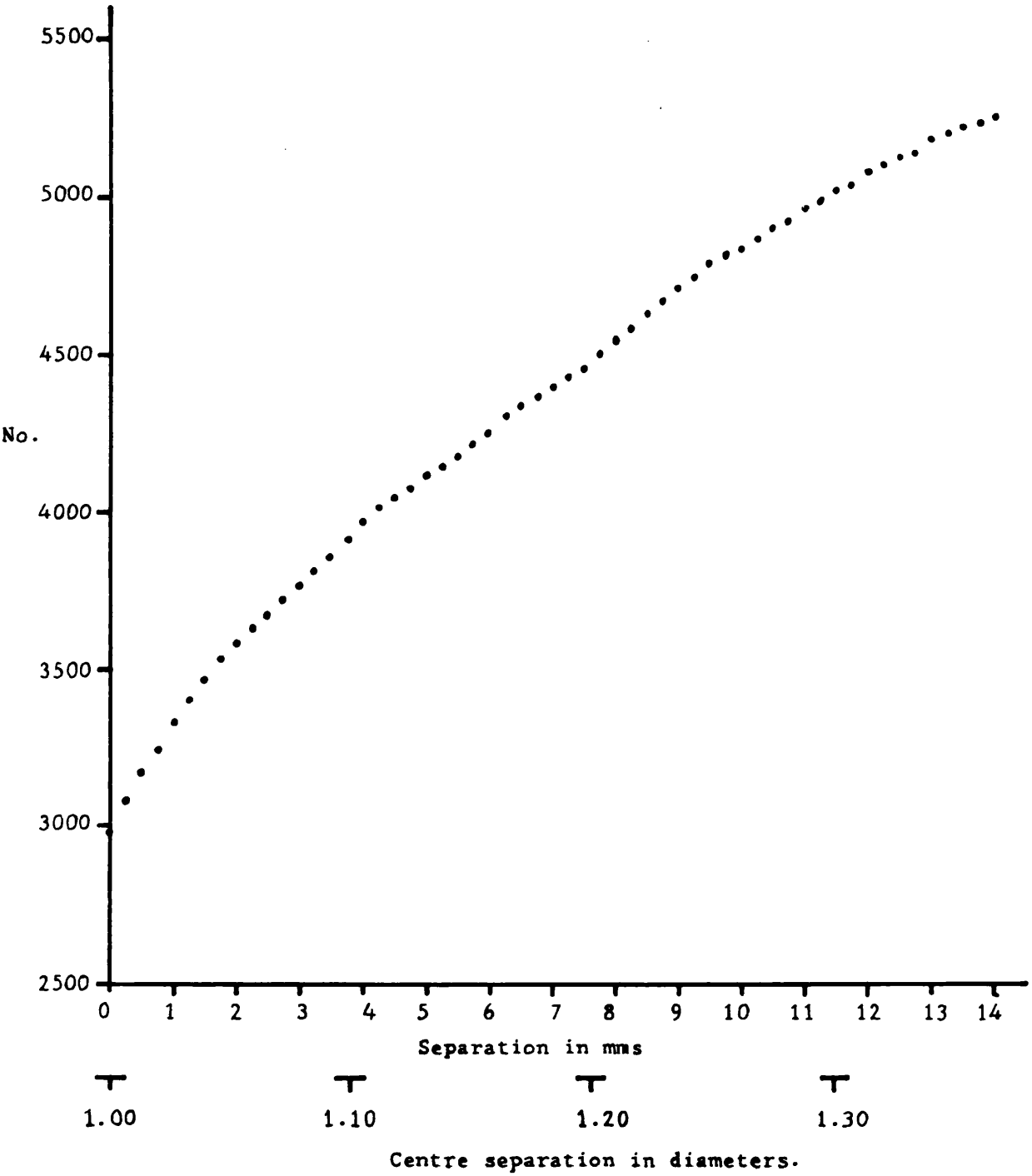

FIG.10. The number of pairs with separations less than a fixed separation.

histogram at approximately 1.10, 1.16, and 1.22 sphere diameters (Fig. 11). This fine structure was unexpected. However, on consideration of a random close packed array of spheres, small gaps can be postulated. For the case of seven spheres, five of which form a ring around the equator of two touching spheres, a small gap is found to exist between two spheres of the ring. The sphere centre separation can be calculated as $\frac{4\sqrt{2}}{3\sqrt{3}} = 1.0886$ sphere diameters.

If another ring of five spheres is added to this first ring such that each sphere touches two adjacent spheres of the ring as well as one of the central pair, then five gaps are observed between these added spheres. Three of the gaps can be shown to be caused by a sphere centre separation of $\frac{4\sqrt{2}}{3\sqrt{3}}$ diameters, but the other two are greater. They are larger because one of the new ring of spheres occupies a site above the original small gap and is therefore slightly below the plane of the other four spheres. The sphere centre separation for these larger gaps can be shown to be $5/\sqrt{19} = 1.14707$ diameters (see Appendix I).

These separations agree approximately with the first two peaks on the histogram but both are smaller than the histrogram separations. It requires at least seven spheres and fifteen contacts to form the smallest gap. If one small separation is introduced somewhere in the fifteen contacts, then it is found that in five cases the $\frac{4\sqrt{2}}{3\sqrt{3}}$ separation is reduced, whereas in ten cases it is increased. For the $5/\sqrt{19}$ separation it requires at least nine spheres and twenty-one contacts to form a configuration where this separation is possible. If each of these contacts is opened in turn then it is found that five have little effect, six close the $5/\sqrt{19}$ separation and ten open it. A rigourous reasoning is

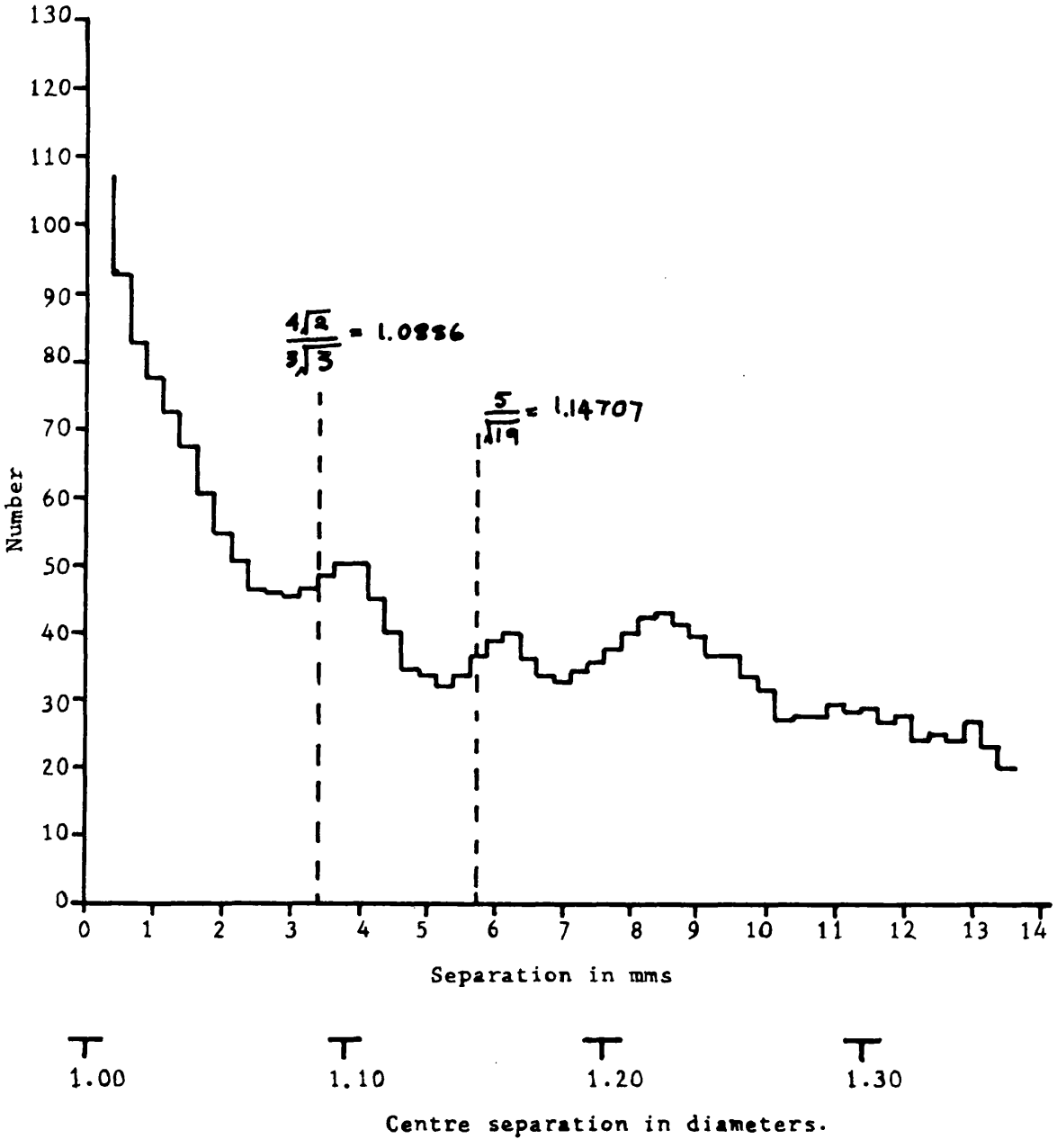

FIG.11. Number of pairs vs separation.
Smoothed twice by running threefold average.

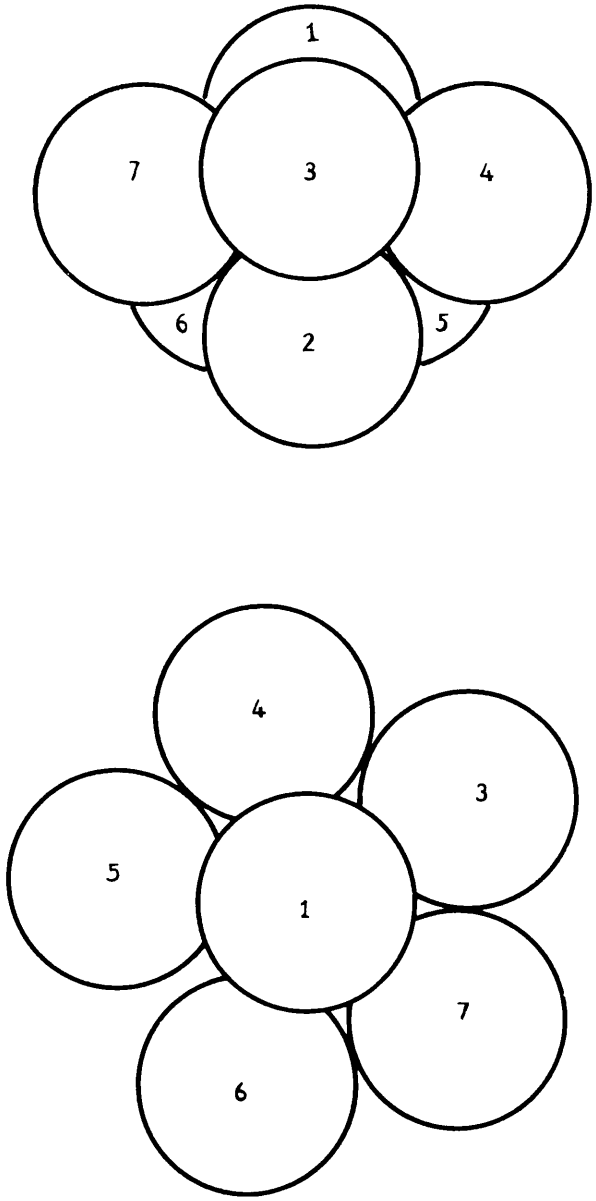

FIG. 12 Configuration containing one small gap.

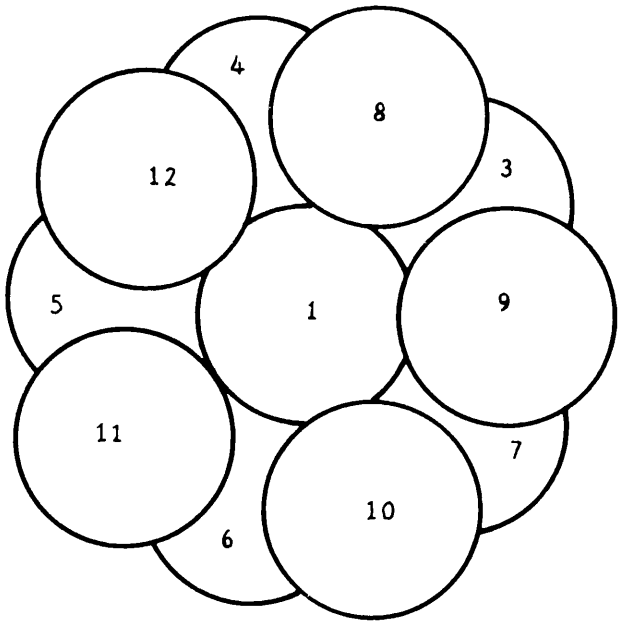

FIG. 13. Configuration containing several small gaps.

more difficult than in the first case, because there are $5/\sqrt{19}$ separations in the new layer but, in general, a small gap introduced into the structure is more liable to open the two main separations than to close them.

Bernal[21] has calculated a radial distribution function for the narrow range considered here, and on smoothing this by running a three-fold average, three similar peaks appear. Bernal[21] also provided a computer tape of Scott's[9] co-ordinates and a computer program was written to calculate the radial distribution function in this narrow range. When Scott's[9] separations were smoothed and plotted as a histogram small peaks were again evident (Fig. 14). The first peak was very large but the second small, and the third apparently absent. The separations for the first two peaks agreed with the table-tennis ball results and also with those of Bernal[21].

A histogram of the average number of spheres within a certain distance can be found as this is the integral of the number against separation curve. The plot of Scott's results and those of the table-tennis balls revealed an approximately straight line (Fig. 15). This is surprising because the "average number" computed from the packing density and the volume of each sampling sphere rises as a cubic function. Scott[9] gives a co-ordination number of 9.3 ± 0.8 for all neighbours within 1.10 diameters. Bernal[7] gives an independent co-ordination number of 6.4 close-contacts and 8.5 within 1.05 diameters. All these values agree with the two curves plotted. However, Levine and Chernick[22], who generated unit cells of a random packing on a computer obtained 8.5 contacts per sphere and 9.2 within 1.35 diameters. This gives a line which differs considerably from the others and indicates that

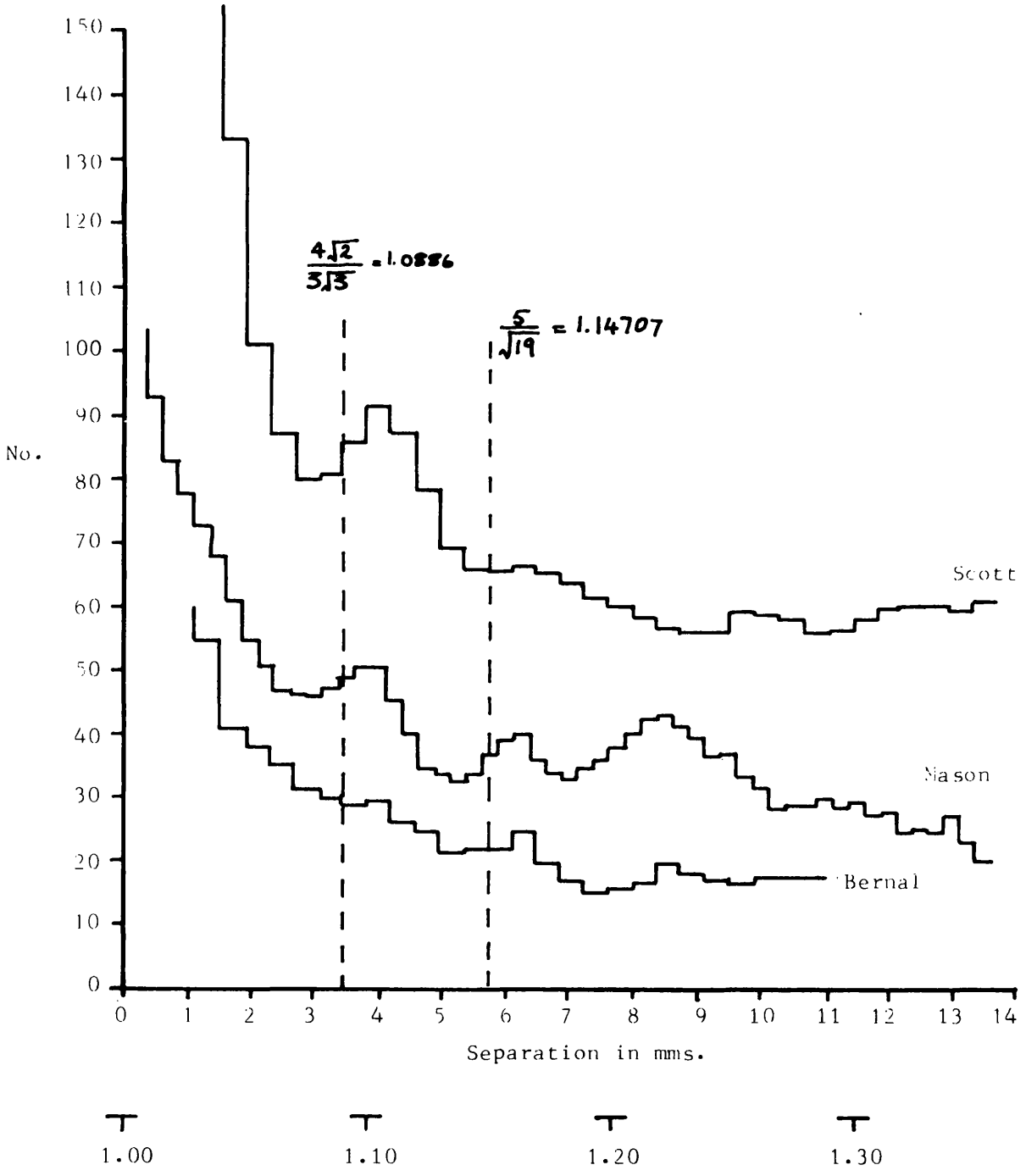

FIG.14. Number of pairs vs separation. Collected results. All smoothed twice by running threefold average.

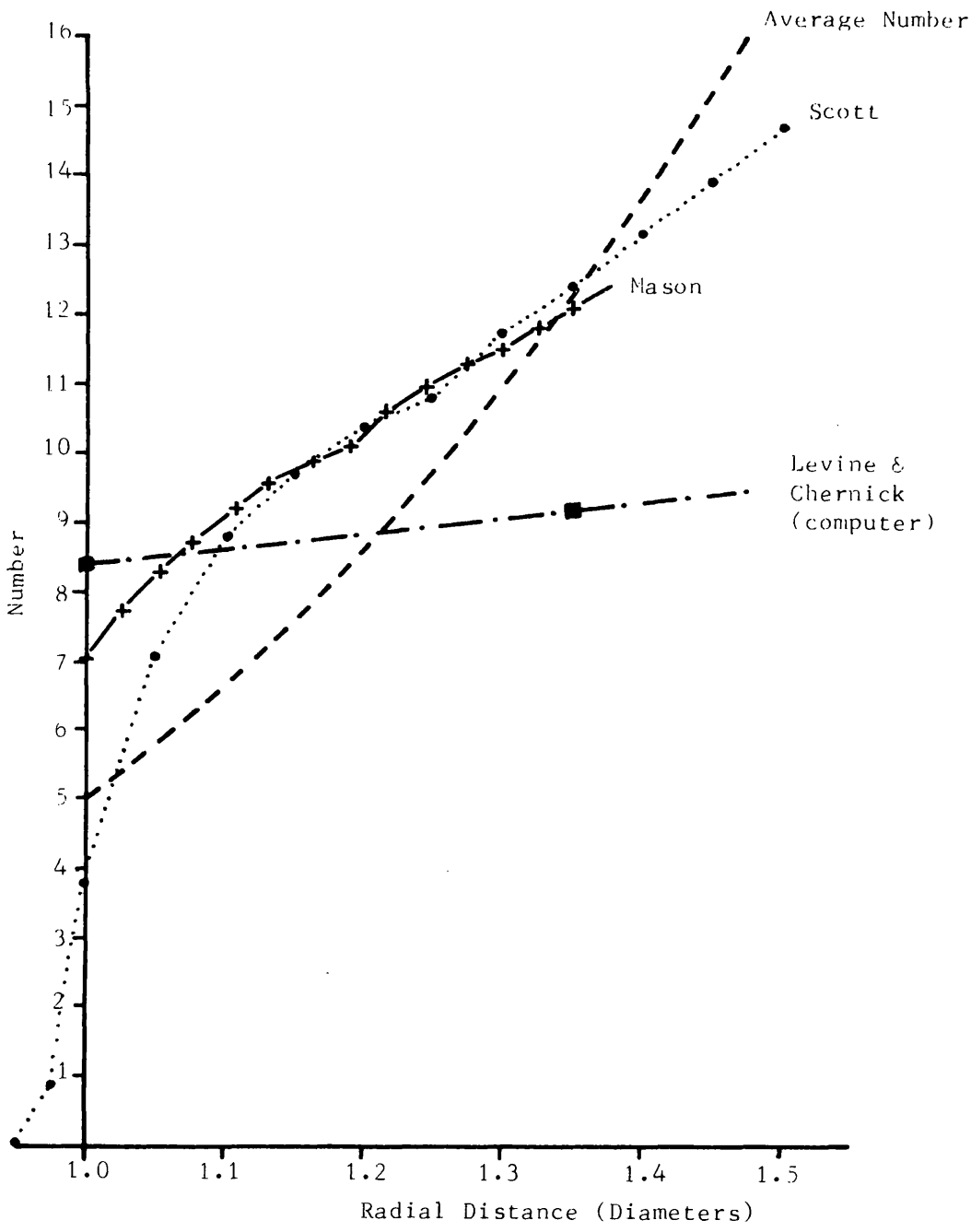

FIG.15 Co-ordination Number vs Sample Radius.
Collected results.

their computer model is not satisfactory. The curves from the results of Scott and the table-tennis balls intersect the completely random distribution cubic curve at about 1.38 diameters. It is possible that Bernal's[8] approximation of 13.6 spheres within a $\sqrt{2}$ diameter sphere agrees with Coxeter's[18] calculated value of 13.56 because of this intersection at approximately 1.38 diameters.

It can be seen from Fig. 15 that for random close packing, density 0.63, there are on average 7.0 contacts per sphere and 10.4 within a 1.20 diameter range. About one third of the neighbours can be classed as "near neighbours" defined by there being a small gap between them which can be spanned by a liquid bridge.

A graph can be plotted of the number of contacts against packing density (Fig. 16). A maximum of 13.4 contacts at a packing density of 0.7797 is theoretically possible but practically unobtainable. The regular lattice structures give several points which fall on no apparent smooth curve. (12,0.7405 . 10,0.6981 . 8,0.6801 . 8,0.6046, 6,0.5236 . 4,0.3401 . 4,0.1235, [1]. Results for lower packing densities can be obtained from Hutchison and Sutherland[23] who synthesised a random floc of particles using a computer. The figures of Smith, Foote and Busang[6] from packings of lead shot moistened with acetic acid, of other workers from capillary condensation and absorption have been neglected because liquid bridges are possible between spheres not in contact. Such graphs have been plotted by several workers[6],[31],[32],[33] and curve fitting equations can be devised. No theory exists. The dotted line on Fig. 16 gives the contact number calculated simply from the number of spheres around the central one, assuming no ordering and no peaks on a radial distribution function. The number of

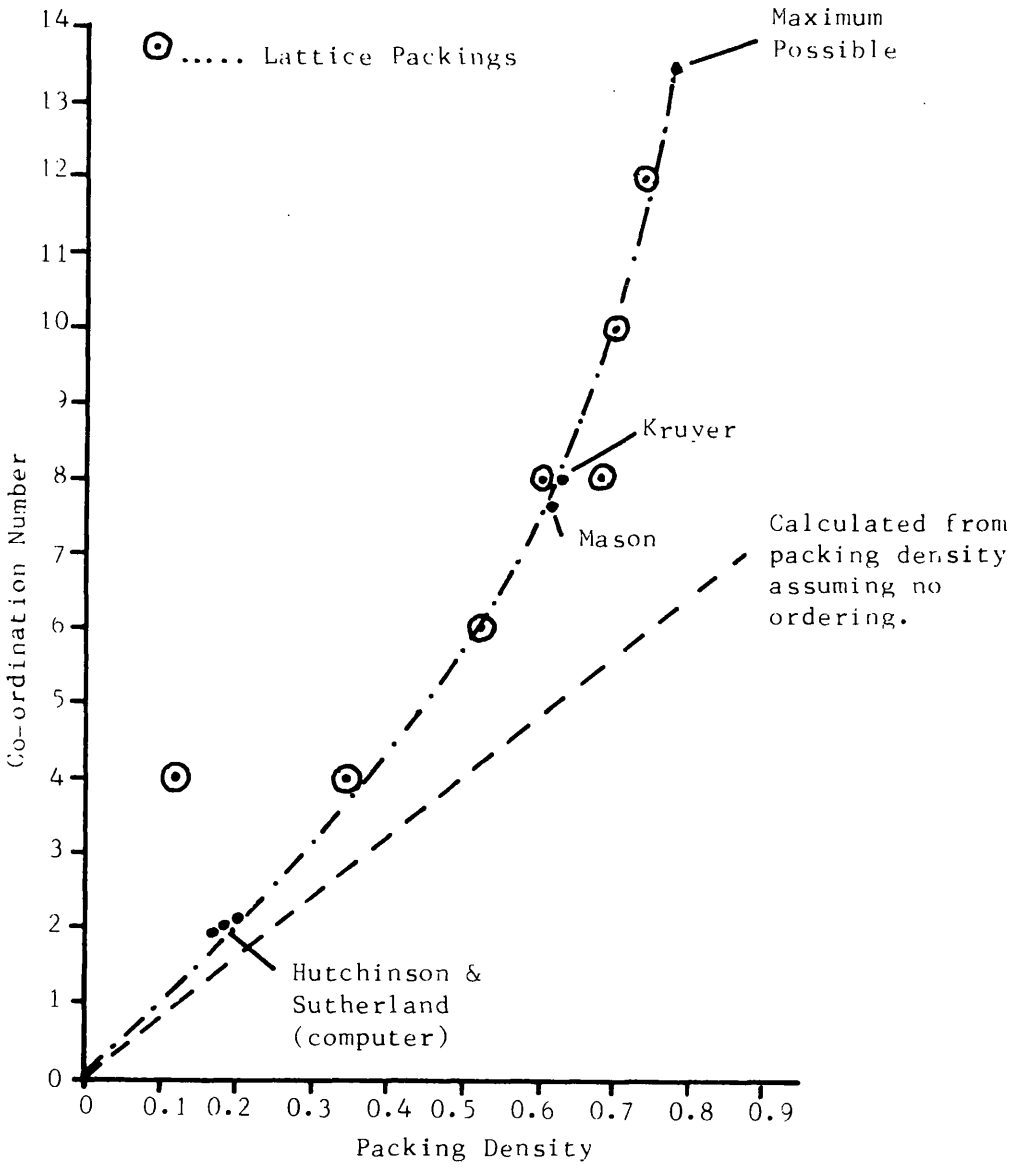

FIG.16 Co-ordination Number vs Packing Density.

contacts per sphere should always come above this line as the packing is ordered by the limitation that the same space cannot be occupied by two spheres.

SPHERES UNEQUAL SIZED

A. REGULAR PACKINGS

1. The size of sphere required to fill the interstices of a regular array can be found from the intelligent application of Pythagoras' Theorem[24]. The sphere that just fits into the largest interstices is called the secondary sphere. The next largest sphere that fits into a hole is the tertiary sphere and so on for the quaternary and quinternary spheres. The relative sphere sizes, numbers of each size and the effect on the packing density have been calculated by Horsfield[25] and also by White and Walton[26]. Hudson[24] added even further to previous work with a reference to interstitial compounds and metallic solid solutions.

2. However, all work on regular packing is somewhat idealised and it is doubtful if the packing density of 0.96 (Horsfield[25]) will ever be achieved in practice.

(Spheres. Unequal sized)

B. IRREGULAR PACKINGS

1. Binary mixtures of spheres have been considered experimentally by several workers because of the importance of producing a dense packing for ceramics and sintered metals. Ayer and Soppet[27] vibrated large spheres into a pack and then introduced smaller spheres on the top, which they shook down into the pack of the large spheres. They developed an equation to fit their results.

Yerazunis, Bartlett and Nissan[28] developed a theory for the density of packing of random binary mixtures and fitted this to their results. In a later paper Yerazunis, Cornell and Wintner[29] report packing binary mixtures for six different diameter ratios. They developed another equation which, as they pointed out, did not

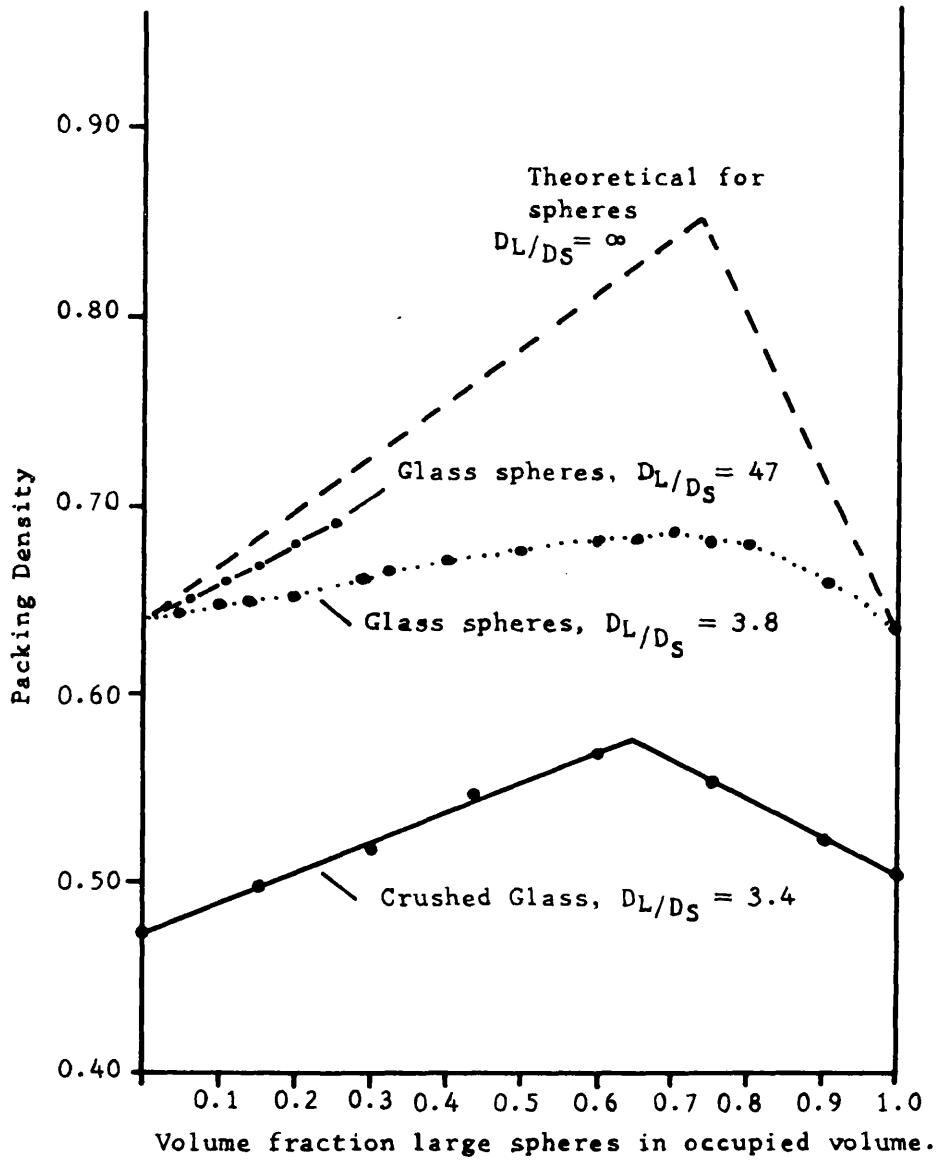

FIG. 17 Packing Density of Binary Mixtures.
After Yerazunis, Bartlett & Nissan (Ref. 28).

extrapolate to the limit of constant packing density for different compositions of equal spheres.

2. Wise[30] in 1952 devised a mathematical model in a paper entitled "Dense Random Packing of Unequal Spheres". His definition of dense packing is that there should be no small gaps between any particles and states that this can only be possible if the particle size distribution is wide. This is not unrealistic, as Wise considers assembling a packing by sorting out those particles which will not fit. When such a system is dissected into tetrahedra by lines connecting adjacent centres, and a particle size distribution assumed, it is possible to calculate various properties. He shows that the average number of spheres touching any one sphere is about twelve. This is for a wide size distribution and compares in practice with about seven for equal spheres. However, in a packing with no near contacts, such as that of Wise, the number of contacts equals the number of geometric neighbours. This, in the case of a random packing of equal spheres, has been shown to be about thirteen[8]. Wise also discussed the effects of small gaps on his packings and decided that they would complicate the calculations considerably. The method could be used for equal spheres if a radial distribution function for geometric neighbours were known. The packing density, average number of contacts, size of various holes, etc. could be calculated. This has been recently accomplished by Collins[42] working on the liquid state. He divides his packing into tetrahedra by connecting the centres of geometric near neighbours and postulates a radial distribution function. Unfortunately, the mathematics prove too awkward, but in principle it would be possible to compute

properties of gases and liquids. Conversely the properties of sphere packings could be revealed from the study of the rare gas isotherms.

NON-SPHERICAL PARTICLES

A. REGULAR PACKINGS

1. There seems to be very little theoretical work on these packings, although they are of interest to biologists considering the structure of enzyme complexes and viruses. The difficulty seems to be to find and define the shape of the particles being packed.

B. IRREGULAR PACKING

1. A random array of non-spherical particles would seem to be extremely difficult to consider theoretically. Practically, it is the most important, being concerned in the simpler cases with such materials as wheat, rice and peas, and in the more complex cases with broken minerals in which the shape of no particle approximates to that of any other. The behaviour under shear stresses has been studied and equations formulated, but no fundamental properties have been discovered. A simple experiment in this field would be to cast part of a pebble beach in agar and dissect the resulting mass.

REFERENCES

(1) Close Packing. A.L. Patterson & J.S. Kaspar. International Tables for X-ray Crystallography. Vol. 1. 342. Kynoch Press. Birmingham. 1959.

(2) Packing of Equal Spheres. G.D. Scott. Nature 188, 908, (1960).

(3) Experiments showing dilatancy. O. Reynolds. Collected Scientific Papers. 2, 217. (1901).

(4) Maximum Entropy of Granular Materials. M. Morgenstern. Nature. 200, 559. (1963).

(5) On the Yielding of Soils. K.H. Roscoe, A.N. Schofield and C. P. Wroth. Geotechnique 8, 22, (1958).

(6) Packing of Homogeneous Spheres. W.O. Smith, P.D. Foote, and P.F. Busang. Phys. Rev. 34, 1271, (1929).

(7) Co-ordination of Randomly Packed Spheres. J.D. Bernal and J. Mason. Nature 188, 910, (1960).

(8) The Geometry and Structure of Liquids. J.D. Bernal. Proceedings of Symposium on Liquids: structure, properties, solid interactions. General Motors Research Laboratories. Warren. Michigan. 1963. Elsevier 1965.

(9) Radial Distribution of the Random Close Packing of Equal Spheres. G. D. Scott. Nature 194, 956, (1962).

(10) Angular Distribution of Random Close Packed Equal Spheres. G.D. Scott and D.L. Mader. Nature 201, 382, (1964).

(11) A Geometrical Approach to the Structure of Liquids. J. D. Bernal. Nature 183, 141, (1959).

(12) The Structure of Liquids. J. D. Bernal. Proc. Roy. Soc., 280A, 299, (1964).

(13) Regular Figures. L. Fejes Tóth. Macmillan. New York. 1964.

(14) Packing and Covering. C.A. Rogers. Cambridge. 1964.

(15) Introduction to Geometry. H.S.M. Coxeter. John Wiley & Sons, Inc., New York. 1960.

REFERENCES (Cont'd).

(16) Nouvelles applications des paramètres continus à la théorie des formes quadratiques, Deuxième Mémoire, Recherches sur les parallélloèdres primitifs. G. Voronoi. Journal für die reine und angewandte Mathematik. 134, 198, (1908).

(17) Über die Reduction der positiven quadratischen Formen mit drei unbestimmten ganzen Zahlen. G.L. Dirichlet. Journal für die reine und angewandte Mathematik. 40. 209, (1850).

(18) Close Packing and Froth. H.S.M. Coxeter. Illinois J. Math. 2, 746, (1958).

(19) Viscosity, plasticity and diffusion as examples of Absolute Reaction Rates. H. Eyring. J. Chem. Phys. 4, 283, (1936).

(20) A Dense Packing of Hard Spheres with five-fold Symmetry. B. G. Bagley. Nature. 208, 674, (1965).

(21) J. D. Bernal. Private Communication.

(22) A Numerical Model of Random Packings of Spheres. M.M. Levine and J. Chernick. Nature. 208, 68, (1965).

(23) An open-structured Random Solid. H.P. Hutchison and D.N. Sutherland. Nature. 206, 1036, (1965).

(24) Density and Packing in an Aggregate of Mixed Spheres. D. R. Hudson. J. Applied Phys. 20. 154, (1949).

(25) The Strength of Asphalt Mixtures. H. T. Horsfield. J. Soc. Chem. Ind. 53, 107T, (1934).

(26) Particle Packing and Particle Shape. H.E. White and S. F. Walton. J. Am. Ceram. Soc. 20, 155, (1937).

(27) Vibratory Compaction: I, Compaction of Spherical Shapes. J. E. Ayer and F. E. Soppet. J. Am. Ceram. Soc. 48, 180, (1965).

(28) Packing of Binary Mixtures of Spheres and Irregular Particles. S. Yerazumis, J.W. Bartlett and A.H. Nissan. Nature. 195, 33, (1962).

(29) Dense Random Packing of Binary Mixtures of Spheres. S. Yerazumis, S.W. Cornell and B. Wintner. Nature. 207, 835 (1965).

(30) Dense Random Packing of Unequal Spheres. M. E. Wise. Philips Research Reports. 7, 321, (1952).

(31) The Penetration of Mercury and Capillary Condensation in Packed Spheres. S. Kruyer. Trans. Farad. Soc. 54, 1758, (1958).

(32) Structure of drying gels, their pores and particles. A. V. Kiselev. Doklady Akad. Nauk. SSSR. 98, 431, (1954).

(33) Crushing strength of Zinc Oxide Agglomerates. H.P. Meissner, A. S. Michaels and R. Kaiser. Ind. Eng. Chem. Process Design and Development. 3, 202, (1964).

(34) The Internal Flow of Granular Masses. R.L. Brown and P.G.W. Hawksley. Fuel. 26, 159, (1947).

(35) Vegetable Staticks. S. Hales. Exp. 32. pp 94-96, London, 1727.

(36) The Shape of Compressed Lead Shot and its Relation to Cell Shape. J.W. Marvin. Am. J. Bot. 26, 280, (1939).

(37) In the twinkling of an eye. E. B. Matzke. Bulletin of the Torrey Botanical Club. 70, 222, (1950).

(38) The Packing of Equal Spheres. C.A. Rogers. Proc. London Math. Soc. 8, 609, (1958).

(39) Some Remarks concerning Close Packing of Equal Spheres. A. H. Boerdijk. Philips Research Reports. 7, 303, (1952).

(40) Über die dichteste Kugellagerung. L. Fejes. Mathematische Zeitschrift. 48, 676, (1943).

(41) Interface Area, Edge length and number of vertices in crystal aggregates with random nucleation. J. L. Meijering. Philips Research Reports. 8, 270, (1953).

(42) On the Entropy of the Liquid State. R. Collins. Proc. Phys. Soc. 86, 199, (1965).

(43) Further Notes on the shape of metal grains. Space filling polyhedra with unlimited sharing of corners and faces. C.S. Smith. Acta Metallurgia. 1, 295, (1953).

(44) Elemente der Gestaltenlehre. E. von Federow. Zeitschrift für Krystallographie und Mineralogie. 21, 689-92, (1893).

APPENDIX I

Pentagon around the equator of a pair.

let the spheres have a diameter of 2.0.

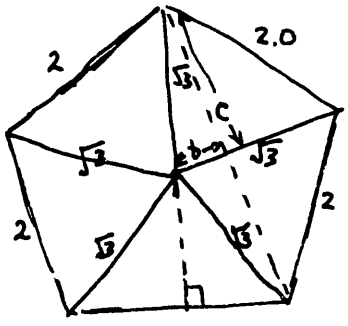

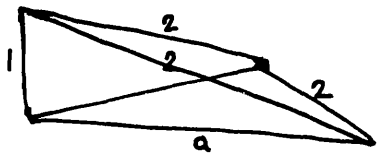

$a^2 + 1 = 4$

$\therefore a = \sqrt{3}$

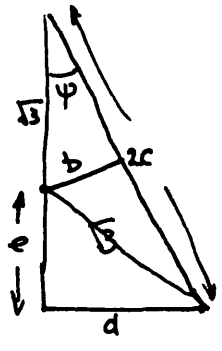

(i) $b^2 + c^2 = 3$

(ii) $4 - (\sqrt{3}-b)^2 = 4 - 3 + 2\sqrt{3}b - b^2 = c^2$

Hence $b^2 + c^2 = 1 + 2\sqrt{3}b$

And $b = 1/\sqrt{3}$ $\quad c = \frac{2\sqrt{2}}{\sqrt{3}}$

$$\cos\psi = \frac{\sqrt{3}+e}{\frac{4\sqrt{2}}{\sqrt{3}}} = \frac{2\sqrt{2}}{\sqrt{3}.\sqrt{3}}$$

Hence $e = \frac{7}{9}\sqrt{3}$

$$\sin\psi = \frac{d\sqrt{3}}{4\sqrt{2}} = \frac{1}{\sqrt{3}.\sqrt{3}} \qquad d = \frac{4\sqrt{2}}{3\sqrt{3}}.$$

$$\text{Gap 1} = \frac{4\sqrt{2}}{3\sqrt{3}} = 1.0886.....$$

Aim

Gap between sphere above gap 1 and one adjacent sphere.

Method

Determine the two sphere centres as distances and angles upon the plane of the pentagonal set. Calculate the projected separation and actual separation.

Irregular side

Face triangle.

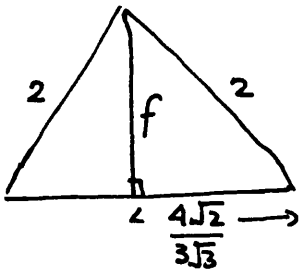

$f^2 = 4 - \frac{16}{9} \cdot \frac{2}{3}$

Hence $f = \frac{2}{3\sqrt{3}}\sqrt{19}$

Triangle in pentagonal set.

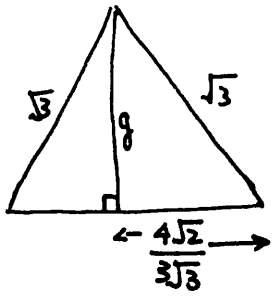

$g^2 = 3 - \frac{16}{9} \cdot \frac{2}{3}$

$g = \frac{7}{3\sqrt{3}}$

Section from the centre of the pentagonal set through the centre of gap 1.

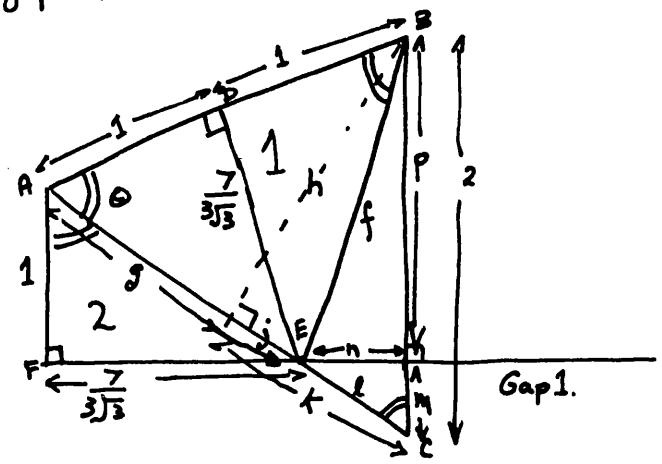

$$g^2 = 1 + \frac{49}{27} \quad . \quad g = \frac{2\sqrt{19}}{3\sqrt{3}}$$

$\triangle$ ABE is isosceles.
ADE congruent with. AFE

$$\sin\theta = \frac{h}{2} = \frac{7}{3\sqrt{3}} \cdot \frac{3\sqrt{3}}{2\sqrt{19}} \qquad \therefore \; h = \frac{7}{\sqrt{19}}$$

$$j^2 = f^2 - h^2 = \frac{4}{9} \cdot \frac{19}{3} - \frac{49}{19} \quad . \quad \therefore \; j = \frac{11}{3\sqrt{3}\cdot\sqrt{19}}$$

$$k^2 = 2^2 - h^2 = 4 - \frac{49}{19} \qquad \therefore \; k = \frac{3\sqrt{3}}{\sqrt{19}}$$

$$l = k - j = \frac{3\sqrt{3}}{\sqrt{19}} - \frac{11}{3\sqrt{3}\cdot\sqrt{19}} \qquad \therefore \; l = \frac{16}{9} \cdot \frac{\sqrt{3}}{\sqrt{19}}$$

$$\sin\theta = \frac{n}{l} = \frac{7}{3\sqrt{3}} \cdot \frac{3\sqrt{3}}{2\sqrt{19}} \qquad \therefore \; n = \frac{56\sqrt{3}}{9.19}$$

$$\cos\theta = \frac{m}{l} = \frac{3\sqrt{3}}{2\sqrt{19}} \qquad \therefore \; m = \frac{8}{19}$$

$P = 2 - m = 2 - 8/19$ $\quad\therefore\quad P = 30/19$

Centre to foot of perp (B to Gap 1)

$= n + \frac{7}{3\sqrt{3}} = \frac{21}{19}\sqrt{3}$

Height of perp $P = \frac{30}{19}$

Regular side

Face triangle

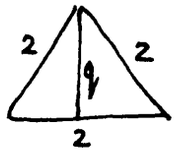

$q^2 = 4 - 1$
$\therefore q = \sqrt{3}$

Triangle in pentagonal set.

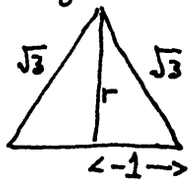

$r^2 = 3 - 1$
$r = \sqrt{2}$

Section from the centre of the pentagonal set through ~~to~~ a contact in the pentagonal set.

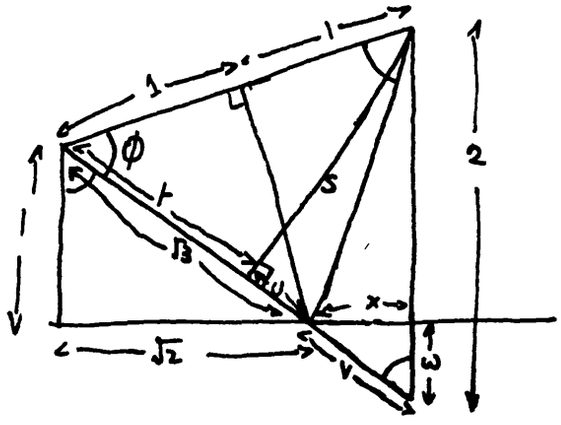

$\sin\phi = \frac{s}{2} = \frac{\sqrt{2}}{\sqrt{3}}$ $\quad\therefore\ s = \frac{2\sqrt{2}}{\sqrt{3}}$

$\cos\phi = \frac{t}{2} = \frac{1}{\sqrt{3}}$ $\quad\therefore\ t = \frac{2}{\sqrt{3}}$

$u^2 = 3 - s^2 = 3 - \frac{4\cdot 2}{3}$ $\quad\therefore\ u = \frac{1}{\sqrt{3}}$

Hence $v = t - u = \frac{2}{\sqrt{3}} - \frac{1}{\sqrt{3}}$ $\quad\therefore\ v = \frac{1}{\sqrt{3}}$

$\sin\phi = \frac{x}{v} = \frac{x\sqrt{3}}{1} = \frac{\sqrt{2}}{\sqrt{3}}$ $\quad\therefore\ x = \frac{\sqrt{2}}{\sqrt{3}}$

$\cos\phi = \frac{w}{v} = w\sqrt{3} = \frac{1}{\sqrt{3}}$ $\quad\therefore\ w = 1/3$

Centre to foot of perp $= \sqrt{2} + x = \frac{4\sqrt{2}}{3}$

Height of perp $= 2 - \frac{1}{3} = \frac{5}{3}$

Combination of irregular + regular sides

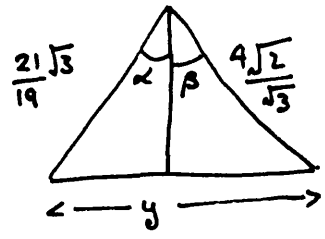

but

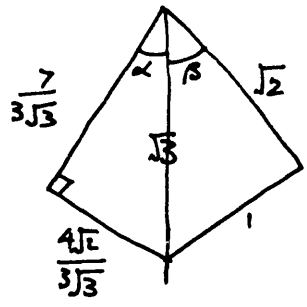

(vi)

$$\cos(\alpha+\beta) = \cos\alpha\cos\beta - \sin\alpha\sin\beta$$

$$= \frac{7}{3\sqrt{3}.\sqrt{3}} \cdot \frac{\sqrt{2}}{\sqrt{3}} - \frac{4}{3}.\frac{\sqrt{2}}{\sqrt{3}} \cdot \frac{1}{\sqrt{3}.\sqrt{3}}$$

$$= \frac{\sqrt{2}}{3\sqrt{3}}$$

Applying cosine formula.

$$y^2 = \frac{21^2}{19^2}.3 + \frac{4^2}{9}.2 - 2.\frac{4\sqrt{2}}{3} \cdot \frac{21}{19}\sqrt{3}.\frac{\sqrt{2}}{3\sqrt{3}}$$

Hence $y = \dfrac{5\sqrt{683}}{3.19}$

This is the distance apart projected on the plane of the pentagonal set.

At right angles.

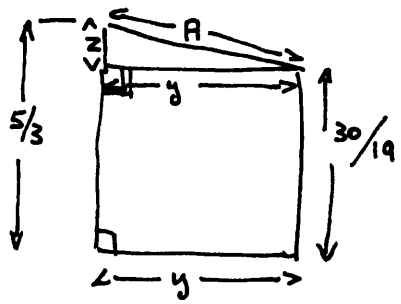

$$z = \frac{5}{3} - \frac{30}{19}$$

$$= \frac{5}{3.19}$$

$$A^2 = y^2 + z^2 = \frac{25.683}{9.19^2} + \frac{25}{9.19^2}$$

Hence $A = \dfrac{5\times 2}{\sqrt{19}}$

Gap 2 $= \dfrac{5}{\sqrt{19}} = 1.14707$ sphere diameters.

APPENDIX II

Calculation of the maximum number of geometric neighbours.

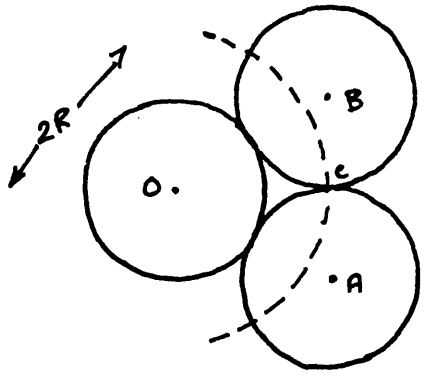

The sphere, centre O, which passes through the points of contact of the shell spheres will have a radius of $\sqrt{3}R$. The area of the cap of this sphere cut off by sphere A will be $= 2\pi\sqrt{3}R \times (\sqrt{3}-\frac{3}{2})R$

The density of a close packed covering of a sphere can be found from consideration of a tetrahedron of equal spheres. The area of the spherical triangle of one face of the tetrahedron $= (3\cos^{-1}\frac{1}{3} - \pi) \times 3R^2$

The area of the three partial sphere caps is $= 3\sqrt{3}R^2 \times (\sqrt{3}-\frac{3}{2}) \times \cos^{-1}\frac{1}{3}$. Hence the packing density of this covering is $= \dfrac{\sqrt{3}(\sqrt{3}-\frac{3}{2})\cos^{-1}\frac{1}{3}}{3\cos^{-1}\frac{1}{3} - \pi}$

(viii)

Since the surface area of the sphere with radius $\sqrt{3}R$ is $4\pi . 3R^2$ the number of spheres that can be accomodated on a central sphere assuming ~~area~~ overall close packing is

$$\frac{4\pi . 3R^2}{2\pi\sqrt{3}R^2(\sqrt{3}-3/2)} \times \frac{\sqrt{3}\cos^{-1}\frac{1}{3}(\sqrt{3}-3/2)}{(3\cos^{-1}1/3 - \pi)}$$

$$= \frac{6}{(3 - \pi/\cos^{-1}1/3)}$$

as $\cos^{-1}1/3 = 70.529...^{\circ}$

The number of spheres is = 13.39.(7).

CHAPTER TWO

LIQUID BRIDGES BETWEEN PARTICLES

INTRODUCTION

1. Basic problem involved.
2. Surfaces of minimum surface area.
3. Variables involved.
4. Simplifications. Solid of revolution.
5. Curvature and pressure differential.

LIQUID BRIDGES BETWEEN EQUAL SPHERES

(i) ZERO CONTACT ANGLE

(a) Equal spheres in contact

1. Haines' toroid approximation.
2. Exact solution by Fisher.
3. Adsorption.
4. Other toroid approximations.
5. Hyperboloid approximation.

(b) Equal spheres separated

1. No exact solution.
2. Toroid approximation.

(ii) NON-ZERO CONTACT ANGLE

(a) Equal spheres in contact

1. Toroid approximation.
2. Hyperboloid approximation.

(b) Equal spheres separated

1. Toroid approximation for small separations.

LIQUID BRIDGES BETWEEN UNEQUAL SPHERES

(i) ZERO CONTACT ANGLE

(a) Unequal spheres in contact

1. Toroid approximation.
2. By a graphical method.
3. Toroid approximation for a sphere and plate.
4. Some experimental results.

LIQUID BRIDGES BETWEEN UNEQUAL SPHERES (Cont'd).

(b) Unequal spheres separated

1. An experimental observation.

(ii) NON-ZERO CONTACT ANGLE

(a) Unequal spheres in contact

1. Toroid approximation for small liquid volumes.

2. Equal spheres and sphere and plate.

3. Experimental difficulties with contact angles.

4. Properties of a bridge with zero attractive force.

(b) Unequal spheres separated

1. Properties of a bridge with zero attractive force.

EXPERIMENTAL SECTION

(i) Theoretical considerations

1. Elimination of gravitational effects.

2. Application of force to the bridge.

3. Hydrometer of variable weight.

(ii) Practical details

1. Mixture of oils with density 1.0.

2. Sample tank and thermostat.

3. Construction of hydrometer float.

4. Use of micrometer syringe.

5. Optical arrangement.

6. Calibration of float.

7. Details of a run.

(iii) Measurement of surface tension

1. Difficulties of two liquids of equal density.

2. Modified Sentis' method.

3. Instability of the system.

4. Practical details

5. Results.

(iv) Results from the apparatus

1. Force and separation.
2. Maximum force and volume.
3. Neck diameter and volume.
4. Curvature and bridge volume.
5. Curvature and neck diameter.
6. Significance of the peak force when separating spheres.
7. Work done to rupture bridge and volume.
8. Rupture distance and volume.

INTRODUCTION

1. In the absence of a gravitational field, the calculation of various properties of liquid bridges is, in essence, straightforward. If the equation of the liquid surface is known, then all the other properties can be derived. The problem thus reduces to finding the equation of a free liquid surface.

2. At equilibrium, the surface adjusts to have a minimum surface energy, and this implies a minimum surface area. It can be shown[1],[2] that a surface of minimum area will have a zero curvature, but if the volume contained by the surface is specified, then the surface of minimum area will only have constant, not zero curvature.

The solution of such a problem was first investigated by Plateau, and his lack of success led him to formulate his famous problem; namely, that given the boundary conditions to calculate the surfaces of constant curvature that fit them; (see for example[51],[52],[53]). In the general case, this is the solution of a differential equation.

3. The variables in any complete solution, even when the equation of the surface is known, are numerous. For example, considering two particles, the size and shape of both these can be varied as can their separation, and the volume of liquid in the bridge. The parameters of interest are the force between two such particles, the curvature of the liquid surface and the neck diameter of the liquid bridge. One other variable remains, which is the contact angle (see Chapter 3), which is the angle that the free liquid surface makes with the solid surface of the particles.

4. As there are so many parameters, it is natural that simplifications should be made. The most popular of these is to consider the liquid surface to be a surface of revolution, by giving the bridge an axis of symmetry. The particles will also have similar symmetry and are normally taken to be spheres. The surfaces of revolution of constant curvature have certain properties: the meridional curves are the roulettes of the foci of conic sections. That is, when a conic section, such as an ellipse or hyperbola is rolled along a straight line, the foci trace out a section, taken along the axis, of a surface of constant curvature. The ellipse yields an unduloid, and the straight line a sphere[3],[4].

The solution of these roulettes involves the use of Elliptic Integrals[5], except in the case of the sphere and catenoid. To avoid such integrals approximations have to be made. The meridianal curve can be assumed to be a circular arc, the so-called toroid approximation, or some other figure such as a hyperbola.

5. The pressure across a liquid interface is related to the curvature by the surface tension.

$$P = \gamma . C. \qquad \ldots\ldots\ldots\ldots\ldots\ldots\ldots\ldots (1)$$

where P is the pressure differential, γ the surface tension and C the curvature of the surface. The sphere and unduloid have a positive curvature, the catenoid zero curvature and the nodoid negative curvature. The pressure differential varies in a similar manner.

In Cartesian co-ordinates, with the axis of symmetry along

the x-axis the curvature of a surface of revolution can be expressed as:-

$$C = 1/y \left\{1 + (dy/dx)^2\right\}^{\frac{1}{2}} \pm (d^2y/dx^2) \; / \; \left\{1+ (dy/dx)^2\right\}^{3/2} \quad \ldots\ldots \; 2$$

LIQUID BRIDGES BETWEEN EQUAL SPHERES

(i) ZERO CONTACT ANGLE

For a zero contact angle, the boundary condition is that the liquid meets the sphere surface tangentially.

(a) Equal spheres in contact

This is the simplest case of a liquid bridge between spheres, and has been studied by an astonishing number of workers independently. This is partly due to a confusion in the literature with papers in such different journals as Soil Science and Nuclear Technology.

1. The first major publication was by Haines[6] who made two approximations to obtain his result. Firstly, he assumed that only the internal pressure deficiency was holding the spheres together, neglecting the attractive force from the liquid surface itself. Secondly, Haines[6] assumed that the meridianal curve of the liquid surface was a portion of a circle - the toroid approximation.

2. Haines[6] approximations were corrected by Fisher[7], who calculated exactly the force binding the two spheres together, as well as the neck diameter of the bridge for different liquid volumes. Fisher's[7] results are summarised in Fig. 1 and Fig. 2.

Haines[6] calculated the pressure deficiency as

$$P = \gamma (\cot^2 \alpha/2 - \cot \alpha/2 - 2)/2R \quad \ldots\ldots\ldots\ldots\ldots\ldots (3)$$

which is positive for values of $\alpha < 53.2^{o}$. Above this value the pressure tends to push the spheres apart.

Haines[6] calculated the force as

$$F = 2\pi R \gamma (1 - 2 \tan \alpha/2)/(1 + \tan \alpha/2) \quad \ldots\ldots\ldots\ldots\ldots\ldots (4)$$

which Fisher[7] corrected partially by incorporating the surface tension force as well as the pressure to

$$F = 2\pi R \gamma /(1 + \tan \alpha/2) \quad \ldots\ldots\ldots\ldots\ldots\ldots (5)$$

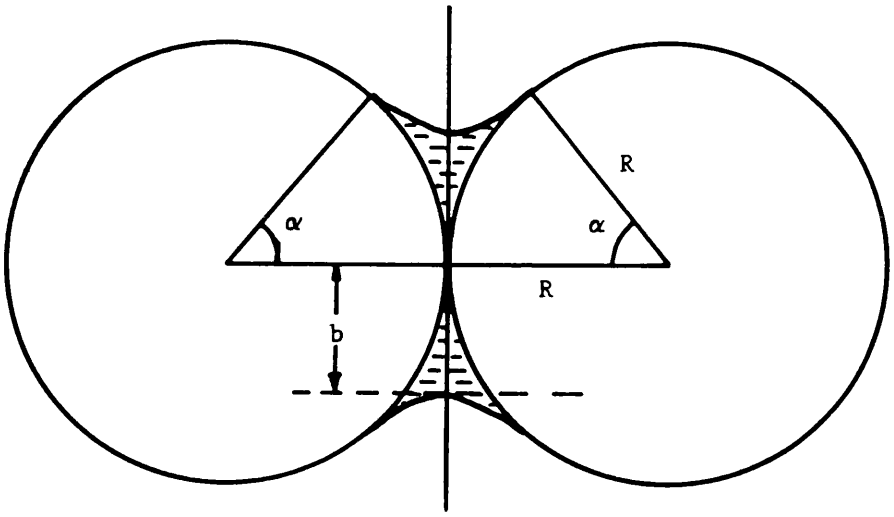

FIG. 1. Diagram of liquid bridge.

Modular Angle / α		Neck Radius $\frac{}{R}$	Tensile Force $\frac{}{2\pi R\gamma}$	Pressure Deficiency $\frac{}{\gamma/R}$	Volume* $\frac{}{R^3}$
25°	5° 25'	0.092292	0.963711	214.265	0.0000542701
30°	7° 46'	0.127068	0.948449	101.742	0.000216306
35°	10° 31'	0.168361	0.930955	53.8069	0.000678672
40°	13° 39'	0.213255	0.911521	30.7079	0.00178112
45°	17° 8'	0.260807	0.890450	18.5134	0.00406621
50°	20° 56'	0.310087	0.868073	11.6061	0.00829561
55°	24° 59'	0.360217	0.844741	7.46819	0.0154213
60°	29° 15'	0.410401	0.820801	4.87329	0.0265071
65°	33° 40'	0.459939	0.796594	3.18284	0.0426105
70°	38° 10'	0.508249	0.772438	2.08527	0.0646502
75°	42° 40'	0.554863	0.748619	1.25868	0.0932762
80°	47° 8'	0.599421	0.725383	0.701137	0.128805

*The Volume is that volume associated with one sphere.

i.e. half the total volume of liquid.

γ is the surface tension of the liquid.

FIG. 2. FISHER'S RESULTS

Haines[6] found the volume of half a bridge to be

$$V = \pi R^3 (\sec\alpha - 1)^2 \left\{ 1 - (\pi/2 - \alpha)\tan\alpha \right\} \quad \ldots\ldots\ldots\ldots (6)$$

Von Engelhardt[9] partially repeated Fisher's[7] exact calculations and produced the relationship between the pressure differential and bridge volume. He was not concerned with inter-particle forces.

Woodrow[19] detailed the exact surface profiles and forces between two spherical particles for differing contact angles, assuming a value of the pressure differential across the surface. Woodrow, Chilton and Hawes[20] elaborated further and quoted examples for the cohesion of particles in liquid metal slurries.

3. Radushkevich[10] also partially repeated Fisher's[7] calculations, concerning himself with the volume of the bridges at sphere contacts for different partial vapour pressures. In adsorption isotherms of gases upon particulate matter, there comes a stage when the gas condenses at the contacts between the particles forming liquid bridges. The pressure differential, and hence the curvature, is a function of the pressure of the gas[11].

$$RT \log \frac{P_1}{P} = C \gamma \frac{M}{\rho - \rho^1} \quad \ldots\ldots\ldots\ldots\ldots\ldots (7)$$

where R = the gas constant

T = the absolute temperature

P_1 = the vapour pressure of the curved surface

P = the vapour pressure of a flat surface

γ = the surface tension of the liquid

M = the molecular weight of the liquid

C = the curvature of the surface

ρ = the density of the liquid

ρ^1 = the density of the vapour.

The limiting case is clearly the catenoid when C = 0.

4. Smith, Foote and Busang[12] derived an equation, using the toroid approximation for the volume of a bridge between two spheres. However, they used parameters which complicated the equation, and upon elimination of these parameters, their result reduced to that of Haines[6]. Rose[16] made reference to Smith et al.[12], but did not realize that they made the toroid approximation, and so he regarded their equation as exact. Rose's[16] equation does, in fact, reduce to that of Haines[6]. Carman[22] and Higuti and Utsugi[23],[25] both made the toroid approximation which had been fully solved before by Haines[6] and Fisher[7].

5. Kruyer[21] considered the meridional curve to be part of a hyperbola and found almost perfect correlation between this approximation and the exact solution of Raduskevich[10].

(b) Equal spheres separated

1. It is difficult to calculate the variation of bridge strength with sphere centre separation, because it entails finding the shape of the liquid surface knowing only its volume and boundary conditions.

2. Carr[26] attempted this, using the toroid approximation, and found that the force decreased with sphere centre separation. For a zero contact angle and a fairly large bridge, the initial force versus separation curve falls approximately linearly, The point of instability when the bridge breaks into two halves does not seem to have been calculated.

Also using the toroid approximation, Smith[14] derived an equation for the volume of liquid in a bridge between two separated spheres as a function of the pressure differential. He did not concern himself with capillary forces.

(ii) NON-ZERO CONTACT ANGLE

(a) Equal spheres in contact

1. Carr[26] derived an expression for the force between two contacting spheres with a non-zero contact angle, by following the method of Batel[27][28]. This uses the toroid approximation, and hence is liable to be seriously in error for large bridges. The volume can be calculated in a similar manner.

2. Kruyer's[21] approximation of a hyperbola for the meridional curve is better, and he lists values of volume and curvature for differing contact angles. His method could be extended to give force/volume relationships, although the accuracy would be doubtful for large contact angles.

(b) Equal spheres separated

1. Carr[26] calculated the force/distance relationship by making the toroid approximation, and found that for a zero contact angle the force decreased with separation, whereas for a non-zero angle there is a well-defined maximum. Carr[26] assumed that the initial contact angle fell to zero when the liquid was retreating from the solid surface.

LIQUID BRIDGES BETWEEN UNEQUAL SPHERES

Surprisingly little seems to have been accomplished for liquid bridges between unequal spheres, except for the limiting case of a sphere and a plane surface. It is, perhaps, because the system of higher symmetry (equal spheres) has to be simplified which has deterred progress with the more complex systems.

(i) ZERO CONTACT ANGLE

(a) Unequal spheres in contact

1. Rose[16] calculated the surface area and volumes of the liquid bridges between two unequal spheres for different radii ratios. He used the toroid approximation and found that if the volumes and surface areas were plotted against the semiangle subtended by the liquid bridge at the centre of the largest sphere, then the variation with radius ratio was quite small. This implied that, as far as the large sphere was concerned, it was the volume of liquid that defined the semi-angle subtended by the liquid bridge, and not the size of the smaller sphere. Rose[16] did not calculate the attractive force between the two particles but this must vary because the maximum attractive force between a sphere and a plate is twice that between two equal spheres.

2. Cross and Picknett[29] solved the surface profile of a liquid bridge between a sphere and a plate by a graphical approximation method. They checked the accuracy of their solution by measuring the pressure across the liquid interface, together with the dimensions of the bridge.

3. Haynes[30] used the toroid approximation to calculate values of the curvature, volume and neck diameter and found agreement with Cross and Picknett[29] to within 7% for the range of bridge sizes considered.

However, Haynes[30] original expression was in error, and a recalculation of volumes[55] gave the expression:

$$V = 2\pi R^3 \left\{\frac{1 - \cos\alpha}{1 + \cos\alpha}\right\}^2 \left\{2 - (\pi - \alpha)\frac{\sin\alpha}{(1 + \cos\alpha)}\right\} \quad \ldots\ldots\ldots (8)$$

as opposed to

$$V = \frac{\pi R^3}{3}\left\{\frac{1 - \cos\alpha}{1 + \cos\alpha}\right\}^3 \left\{1 + \frac{3(\pi - 2\alpha)}{\sin\alpha}(1 + \cos\alpha) + 12(1 + \cos\alpha)^2\right\} \quad \ldots (9)$$

α is the semiangle subtended by the bridge at the sphere centre, and R is the sphere radius. (see Fig. 3).

4. In a later paper, Cross and Picknett[31] reported measurements of the cohesion between spheres of different sizes, using a sensitive microbalance based on a design by El-Badry and Wilson[32]. The balance was sensitive to 10^{-3} dynes and spheres were made by fusing the end of the quartz fibres. A microscope slide was used as the plane surface, and di-n-butyl phthalate as the involatile liquid. From these experiments Cross and Picknett[31] showed that for unequal spheres of radii R_1 and R_2, the attractive force was equal to that between two spheres of radius $\frac{2R_1R_2}{R_1+R_2}$, provided that the spheres were not too dissimilar.

Cross and Picknett[31] used as their major parameter, the semi-angle subtended by the liquid bridge at the sphere centre. All their results related the force to this angle and not to the volume of the bridge, but clearly the bridge volume increases with the angle. The results showed that the attractive force decreased with increasing angle (i.e. volume). This was expected, as Fisher's[7] calculations for two spheres in contact showed a similar effect.

McFarlane and Tabor[34] built a sensitive pendulum type apparatus in which a spherical bead was suspended freely upon the end of a fine thread. The bead was brought into contact with a plate and a drop of liquid placed at the junction. The plate was

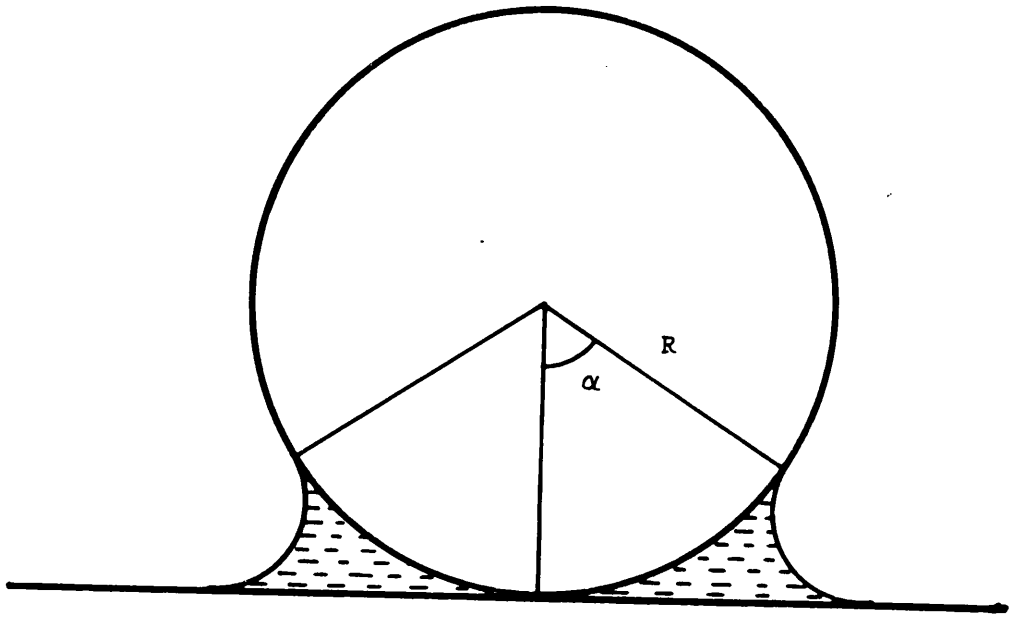

FIG. 3. Sphere on a plate.

$$\frac{\text{Volume}}{2R^3} = \pi\left(\frac{1 - \cos\alpha}{1 + \cos\alpha}\right)^2 \cdot \left[2 - \sin\alpha\,\frac{(\pi - \alpha)}{(1 + \cos\alpha)}\right]$$

$$\frac{\text{Neck Radius}}{R} = \frac{(2\sin\alpha + \cos\alpha - 1)}{(1 + \cos\alpha)}$$

$$\frac{\text{Pressure Deficiency}}{\gamma/R} = 2 \cdot \frac{(1 + \cos\alpha)}{(1 - \cos\alpha)} \cdot \frac{(\sin\alpha + \cos\alpha - 1)}{(2\sin\alpha + \cos\alpha - 1)}$$

$$\frac{\text{Peak Force}}{2\pi R\gamma} = \frac{(2\sin\alpha + \cos\alpha - 1)}{\sin\alpha}$$

FIG. 4. Toroid approximation for sphere and plate.

Angle α	$\frac{\text{Volume}}{2R^3}$	$\frac{\text{Waist Radius}}{R}$	$\frac{\text{Pressure Deficiency}}{\gamma/R}$	$\frac{\text{Tensile Force}}{2\pi R\gamma}$
2.5	0.0000014	0.043164	2077.13	1.97818
5.0	0.0000213	0.085416	512.873	1.95634
7.5	0.0001045	0.126791	224.890	1.93446
10.0	0.0003203	0.167323	124.670	1.91251
12.5	0.0007592	0.207041	78.5440	1.89048
15.0	0.0015297	0.245973	53.6300	1.86835
17.5	0.0027565	0.284140	38.6930	1.84609
20.0	0.0045784	0.321563	29.0536	1.82367
22.5	0.0071470	0.358259	22.4829	1.80109
25.0	0.0106262	0.394241	17.8100	1.77831
27.5	0.0151912	0.429520	14.3726	1.75530
30.0	0.0210284	0.464102	11.7735	1.73205
32.5	0.0283355	0.497990	9.76262	1.70853
35.0	0.0373222	0.531184	8.17643	1.68470
37.5	0.0482100	0.563679	6.90430	1.66055
40.0	0.0612339	0.595466	5.86928	1.63603
42.5	0.0766430	0.626531	5.01650	1.61112
45.0	0.0947024	0.656854	4.30602	1.58579

FIG. 5. Toroid approximation for sphere and plate.

then moved back until the bead fell under the force of the gravity component. The results showed that the adhesion depended directly upon the radius of the bead and experiments with different liquids showed that the adhesion also varied directly as the surface tension.

(b) Unequal spheres separated

1. There seems to be nothing recorded on this subject, except that Cross and Picknett[31] reported that when pulling a sphere from either another sphere or a plane, the bridge stretched slightly before rupturing if there was more than a certain critical quantity of liquid in the bridge. The graphical results suggested that the sphere lifting before the bridge ruptured was the true continuation of the force/semiangle relationship. Points obtained with the same quantities of liquid with the bridge rupturing cleanly appeared to lie on a separate line.

(ii) NON-ZERO CONTACT ANGLE

(a) Unequal spheres in contact

1. McFarlane and Tabor[34] quoted an equation

$$F = 4\pi R\gamma \cos\theta \qquad \ldots\ldots\ldots\ldots\ldots\ldots\ldots\ldots \quad (10)$$

for the adhesion (F) of a sphere to a plane surface, where R is the radius of the bead, γ the surface tension and θ the contact angle between the liquid and the solid. They offered no derivation but suggested that it was obtained from "a simple calculation".

2. Cross and Picknett[31] made the toroid approximation and showed that in the limit as the volume (or the semi-angle) was decreased to zero, the cohesive force F was

$$F = 4\pi R\gamma \cos\theta \quad \text{(for sphere on plane)} \qquad \ldots\ldots\ldots\ldots \quad (11)$$

$$F = 2\pi R\gamma \cos\theta \quad \text{(for equal spheres)} \qquad \ldots\ldots\ldots\ldots \quad (12)$$

where R was the sphere radius, γ the surface tension and θ the contact angle. Fisher[7] had derived this limit for two equal spheres with zero contact angle.

3. Using surfaces coated with silicones Cross and Picknett[31] measured the adhesion for a contact angle of about 40°. They found only qualitative agreement between experiments and their calculations, and the discrepancy increased with the semi-angle (and hence volume). It is unfortunate, but it seems that there is no simple and reliable method of producing a system with a non-zero angle.

4. It is possible to find the contact angle between solid and liquid which makes the bridge non-cohesive for different sizes of particles. Consider a liquid bridge which is symmetrical about the x-axis (Fig. 6). The force F which acts on a section of the bridge through AA^1 has a pressure component and a surface tension component. If F tends to pull towards the left it will be considered positive.

The horizontal surface tension component of F will be given by $2\pi y \gamma \cos \theta$ where γ is the surface tension and θ the gradient of the liquid meniscus.

The pressure component of F will be given by $\pi y^2 p$, where 'p' is the pressure differential between the inside and outside of the surface.

Therefore

$$F = 2\pi y \gamma \cos \theta - \pi y^2 p \quad \ldots\ldots\ldots\ldots\ldots\ldots\ldots (13)$$

For the case $F = 0$

$$2\pi y \gamma \cos \theta = \pi y^2 p \quad \ldots\ldots\ldots\ldots\ldots\ldots\ldots (14)$$

and hence $$2 \gamma \cos \theta = y p \quad \ldots\ldots\ldots\ldots\ldots\ldots\ldots (15)$$

But $$\tan \theta = dy/dx \quad \ldots\ldots\ldots\ldots\ldots\ldots\ldots (16)$$

and $$\cos \theta = 1 \Big/ \sqrt{1 + (dy/dx)^2} \quad \ldots\ldots\ldots\ldots\ldots\ldots\ldots (17)$$

However, $$p = \gamma C \quad \ldots\ldots\ldots\ldots\ldots\ldots\ldots (1)$$

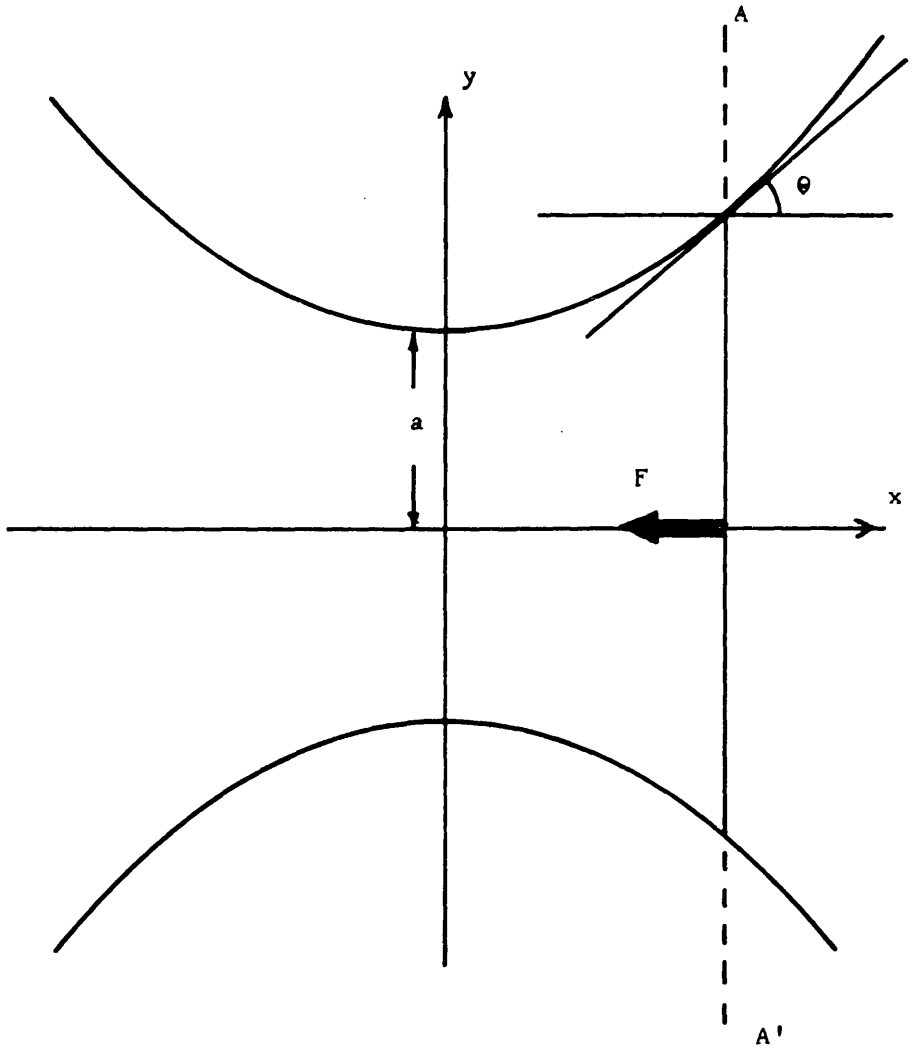

FIG. 6. Section through a liquid bridge.

where C is the curvature of the surface and

$$C = \frac{1}{\rho_1} + \frac{1}{\rho_2}$$

where ρ_1 and ρ_2 are the radii of curvature at any point on the surface and are given by

$$\rho_1 = \pm \left[1 + (dy/dx)^2\right]^{3/2} \Big/ d^2y/dx^2 \qquad \ldots\ldots\ldots\ldots (18)$$

$$\rho_2 = \pm y \left[1 + (dy/dx)^2\right]^{1/2} \qquad \ldots\ldots\ldots\ldots (19)$$

For a surface of revolution ρ_2 must always be positive, hence

$$C = \frac{1}{y\left[1+(dy/dx)^2\right]^{1/2}} \pm \frac{d^2y/dx^2}{\left[1 + (dy/dx)^2\right]^{3/2}} \qquad \ldots\ldots\ldots\ldots (20)$$

when $\frac{d^2y}{dx^2}$ is negative the meridional curve is convex and vice-versa, hence for the zero force film

$$2\gamma \cos\theta = y\rho \qquad \ldots\ldots\ldots\ldots (15)$$

becomes

$$1 + \left(\frac{dy}{dx}\right)^2 = \pm y \frac{d^2y}{dx^2} \qquad \ldots\ldots\ldots\ldots (21)$$

Integrating gives

$$x + y\frac{dy}{dx} + K_1 = 0 \qquad \ldots\ldots\ldots\ldots (22)$$

but at $x = 0$ $\frac{dy}{dx} = 0$ and so $K_1 = 0$

Integrating again

$$\frac{1}{2} y^2 = -\frac{1}{2}x^2 + K_2 \qquad \ldots\ldots\ldots\ldots (23)$$

but at $x = 0$ $y = a$, hence $K_2 = \frac{1}{2}a^2$

Thus the meridional curve is a circle given by

$$y^2 = a^2 - x^2 \qquad \ldots\ldots\ldots\ldots (24)$$

Therefore the surface of constant curvature which will give a zero force bridge will be a sphere or a portion of a sphere. The properties of such a bridge may be illustrated by considering the case of two spheres of two different radii connected by the bridge (Fig. 7).

Let the large sphere, radius R and centre A, be in contact with the small sphere radius r and centre C.

Let the spherical bridge have a radius W and a centre B which will be on the line of centres of the large and small spheres.

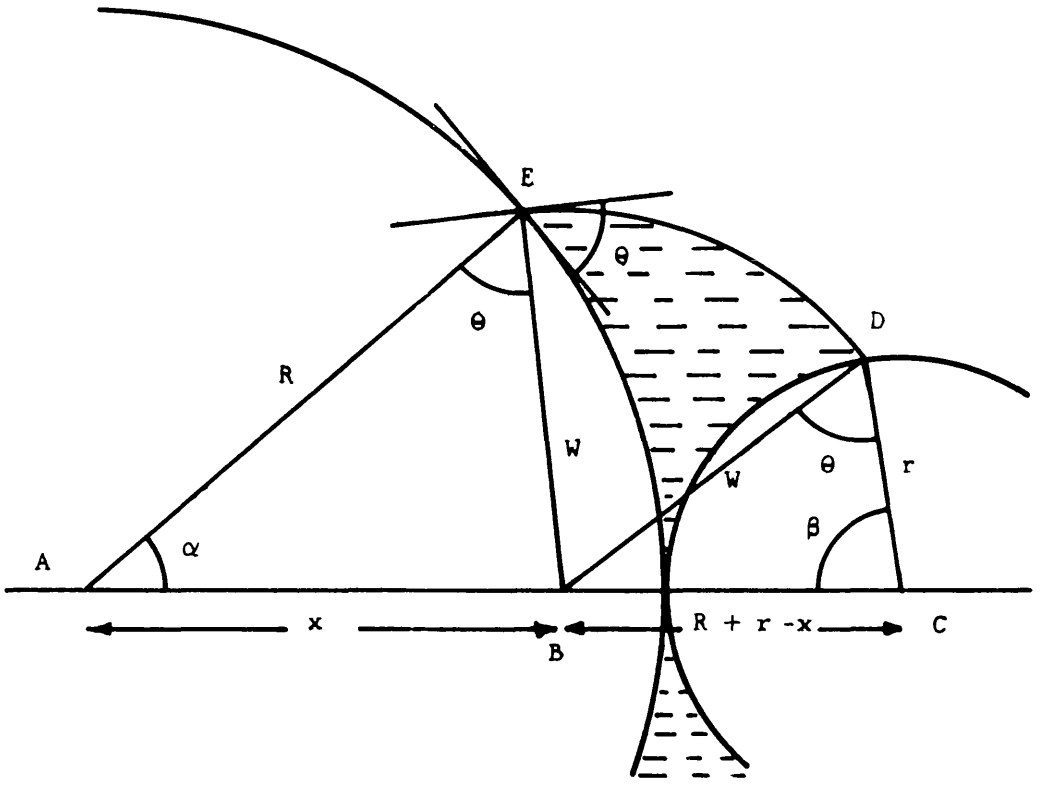

FIG. 7. A zero-force liquid bridge between two spherical particles.

Let the liquid/solid contact angle be θ and the semiangles subtended by the liquid bridge at the centres A and C be α and β respectively.

The problem consists of examining the relationship between R, r, θ and the moisture content.

Consider the triangles AEB and BDC in Fig. 7. Then EB = BD. If the triangle BDC is pivoted around B until E and D coincide then we will have a diagram as in Fig. 8.

Now $A^1D^1 + D^1C^1 = R + r$

and $A^1B^1 + B^1C^1 = R + r$

This means that D^1 and B^1 lie upon the same ellipse which has the points A^1 and C^1 as foci. A simple construction of this figure will enable one to solve all of the dimensions in the example. More generally, if we are given the ratio R:r then, by varying the distance A^1C^1, we can study how α, β, x and w vary as θ varies.

In a wet granular material α and β can only have limited values and these are defined by the packing. If these two angles are too large then the liquid bridges coalesce, giving the funicular state[35].

If α has to be limited to 20° and β to 90° for a R:r ratio of 10:1, then some idea of the magnitude of θ can be gained from Fig. 6.

$\alpha = 20^\circ$. $\beta = 90^\circ$. $A\hat{B}C < 180^\circ$

Hence $2\theta > 70^\circ$ or $\theta > 35^\circ$

Thus we need a receding contact angle of more than 35° to realise the zero force condition in this particular case.

The case when R = r, and $\theta = 90^\circ$ is interesting because Carr[26] states that "for a liquid having a 90° contact angle there is no cohesion between the spheres at any stage of moisture content".

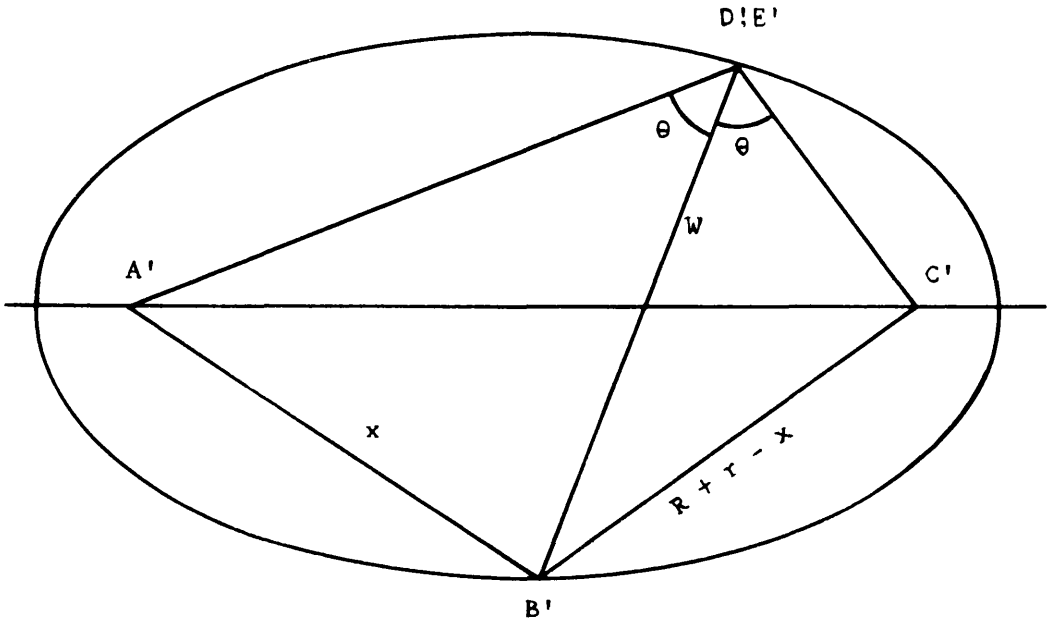

FIG. 8. An ellipse for the analysis of a zero force liquid bridge.

The ellipse construction demonstrates that for $\theta = 90^{o}$ the ellipse is merely a straight line and hence $W = 0$. This means that the only spherical surface between the two spheres will occur when there is no liquid between them. The equations

$$F = 4\pi R \gamma \cos\theta \quad \text{(sphere on plane)} \quad \ldots\ldots\ldots\ldots (11)$$

$$F = 2\pi R \gamma \cos\theta \quad \text{(equal spheres)} \quad \ldots\ldots\ldots\ldots (12)$$

derived by Cross and Picknett[31] are supposed to hold for all values of θ. McFarlane and Tabor[34] only considered them to apply to small values of θ. It can be seen that there is no circle which cuts two touching circles in four places normally and no circle which cuts a circle and its tangent in four places normally. This demonstrates that in the limit as $\theta \rightarrow 90^{o}$ the system becomes impossible, although the attractive force is apparently reduced.

(b) Unequal spheres separated

2. The ellipse construction for a non-cohesive bridge can be extended to non-touching spheres but point B^{1} lies outside the ellipse and $(A^{1}B^{1} + B^{1}C^{1})$ is greater than $(R + r)$.

If we consider a spherical bridge of zero cohesive force and imagine the two spheres to be pulled apart, then, keeping the contact angle unchanged, the bridge will recede into the gap between the spheres and lose its spherical shape. This will result in an attractive force between the two spheres and so the cohesion increases with separation for these special circumstances.

Carr[26] considered the more realistic situation of the contact angle falling to zero as the liquid receded from the surface. Under these conditions the attraction rose with separation until it met the force/separation condition for a bridge with a zero contact angle. It then behaved as a zero contact angle bridge until it ruptured.

The force required to remove a narrow glass slide or wire ring from a liquid surface is commonly used to measure the surface tension of that liquid[49]. Walker[50] used this method to measure the force necessary to pull small pieces of coal from a reservoir of water, when the water surface was treated with different additives. This method gives the combined effects of contact angle and surface tension, provided separation is effected fairly slowly.

EXPERIMENTAL SECTION

(i) Theoretical considerations

The various theories and approximations for the cohesive strength of liquid bridges more than outweighed the experimental results. Clearly there was need for the study of the effect of separation, volume and contact angle on the attractive force. There were, however, two obvious difficulties.

1. To reduce the effects of gravity any experiments have either to be performed in a situation of weightlessness, the apparatus made small, so that the capillary forces dominate or the liquid bridge supported by a surrounding bath of an immiscible liquid of equal density.

2. The method of applying a force to the bridge has to be such that the applied force decays rapidly with displacement of the bridge, otherwise the decline of bridge strength with separation cannot be followed, because the bridge simply breaks. This is what happened with Cross and Picknett's[31] microbalance and they were only able to record maximum forces. However, the method of applying the force has to be sufficiently sensitive to enable quite small forces to be measured.

The micrometer syringe[37] is able to dispense liquid quantities of the order of 2×10^{-4} mls which enables fairly small bridges to be made with precision,

3. Consideration of the design of the experiment led to a system based on the principle of a hydrometer of variable weight. The technique of Boys[4] and Plateau[36] using two immiscible liquids of equal density was used and one of the spheres was at the bottom of a form of hydrometer floating in a bath of liquid. The hydrometer was

raised and lowered by removing or adding liquid to a small attached bath and the force measured by the amount that the float was pulled down from its equilibrium position. The sensitivity of the hydrometer to displacement forces could be varied by having different diameter stems on the hydrometer.

(ii) Practical details

1. Various formulations of immiscible liquids of equal density are known. Boys[4], for instance, used salad oil in aqueous alcohol and he gave precise details of how this was prepared. Di-n-butyl phthalate in a saline solution was a possibility, but initial tests with this showed that the water evaporated, concentrating the saline. Salad oil in aqueous alcohol is similarly unsuitable, and it is obviously more convenient to use water as the bulk phase and find some mixture of oils, immiscible and inert in water, of unit density. Di-n-butyl phthalate, of density 1.042 gms/ml at 25°C[33],[38] was almost suitable alone, but some oil of lesser density was needed to mix with it. Turpentine (density 0.855 - 0.865[39])/di-n-butyl phthalate mixtures proved reactive with water, in that the surface developed a white deposit. This must almost inevitably result in an interfacial surface tension which fluctuates with time. A mixture of di-n-butyl phthalate and liquid paraffin (S.G.0.830 - 0.837) proved more stable and a quantity of mixture with the correct density was made up by trial using a hydrometer to indicate density changes. The mixture was subsequently adjusted to the exact density by floating large drops (1 cm diameter) in a bath of water thermostatted at 25°C ($\pm$ 0.2°C). This proved exceedingly sensitive as the drops rose or fell depending on their density. The density was finally adjusted so that the drops just floated at 25°C. It was then possible to

clean all excess oil from the sample tank without draining the tank as the oil drops could be simply sucked up with an eye dropper. It also had advantages in the determination of the water level in the tank, as will be seen later in the determination of the interfacial tension.

2. The external chamber of the apparatus consisted of a rectangular glass box made from old photographic plates (size 3¼"x 4¼"), in order to reduce any errors due to imperfections in the glass[40]. A copper coil which circulated water up and down the four vertical edges of the tank was inserted to keep the temperature constant. This coil did not obstruct the working space in the tank and kept the temperature at $25^{o}C \pm 0.2^{o}C$. Water at $25^{o}C \pm 0.05^{o}C$ was circulated through the copper coil at about five litres/minute from a thermostat tank containing fifteen litres of water. This bath contained a mercury contact thermometer which actuated a mercury relay switch to control the heaters.

3. The hydrometer float was constructed from a high grade table tennis ball. Other floats made of differing materials such as perspex and nitrocellulose sheet were eventually found to leak, but the table tennis ball proved ideal. One disadvantage was that the oil mixture seemed to soak into the ball and soften it (di-n-butyl phthalate is used as a plasticiser in the plastics industry) and care had to be taken to prevent contact by removing, with an eye dropper, excess oil which accumulated at the liquid surface.

The hydrometer stem was made from a 6 mm ignition tube as the exterior produced the correct force/displacement ratio. Several floats with different diameter tubes were made and 6 mm selected as the right diameter. The thin wall of the ignition tube enabled a sufficient quantity of water to be placed inside

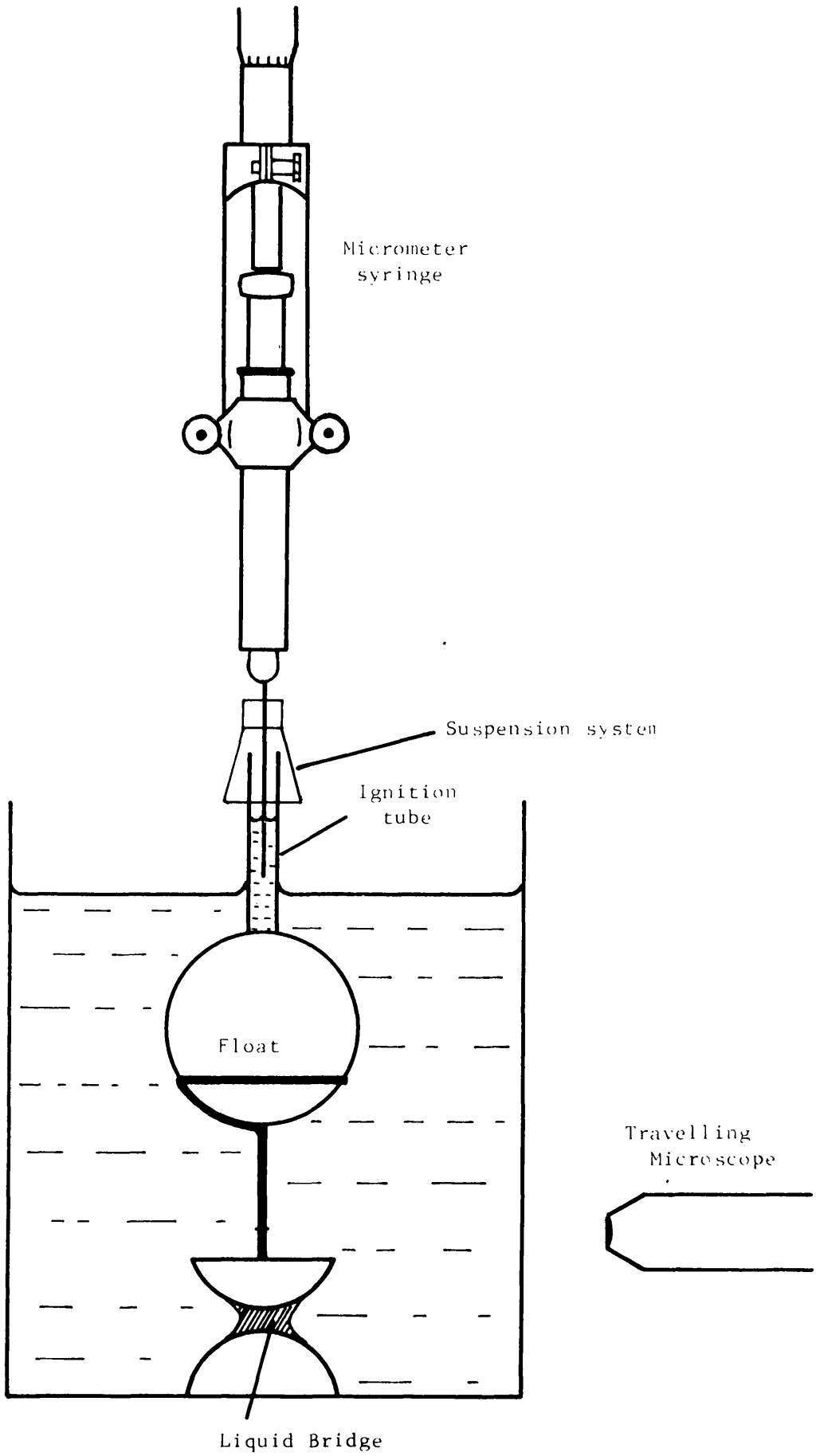

FIG. 9. Diagram of the Apparatus.

for it to act as a reservoir. Water removed or added to the inside of the ignition tube allowed the float to be raised or lowered. As the tube had thin walls, the level of liquid in the ignition tube remained approximately constant as the float was raised and lowered. The ignition tube was selected to have a uniform diameter as measured with a micrometer and was ground with fine emery paper to produce a matt finish. The tube was attached to the table tennis ball with Araldite, and a jig made to ensure that the tube was accurately perpendicular to the sphere surface. A copper wire, 2 mm diameter, was attached to the opposite side of the sphere with Araldite and this led down to one of the hemispherical surfaces.

Some hard-polythene centrifuge tubes were found to have hemispherical ends and these ends were cut from the tubes. The polythene surface was slightly roughened with fine abrasive to remove the smooth surface and then rubbed well with the di-n-butyl phthalate/liquid paraffin mixture. This was found necessary, in order to make the oil mixture wet the polythene under water. One of the polythene hemispheres was weighted and attached to the bottom of the float and weights added to give the correct trim. The wire at the base was bent until the ignition tube and the straight part of the wire were on the same straight line, such that when the float was rotated, neither the wire nor the ignition tube oscillated from the vertical position.

4. A micrometer syringe was used to remove or add water to the ignition tube. The syringe was fitted with a rubber band which pulled the piston hard against the micrometer face. This permitted water to be removed without the need for pulling up the syringe barrel with the fingers. The piston of the syringe was lubricated with di-n-butyl phthalate as it was found that water evaporated

from the region where the piston entered the barrel and fresh water was being drawn up from inside the ignition tube by capillary rise. Thus the float slowly rose from the liquid over a period of hours, which was inconvenient. A two inch hypodermic needle was fitted to the syringe and a delicate cotton suspension arranged, so that the needle was kept in the centre of the ignition tube against the surface tension force trying to move it to the edge. Attempts to exploit the surface tension repulsion of surface, one of which is wetted and the other not[45] failed.

5. The float could be made to rise and fall by adjustment of the micrometer syringe. The change in height was observed by a travelling microscope reading to 0.01 mm focused on an engraved mark on the copper wire of the float. When water alone was used in the tank it was found that the float did not return to its initial position when a quantity of water was removed and then added to the ignition tube. It could be seen visually that the contact angle of the water advancing on the glass of the ignition tube was not zero, and this hysteresis of contact angle was giving a hysteresis on the height of the float. The surface of the ignition tube was cleaned with an abrasive cleaner (Briz) and the tank filled with a 0.2% V/V Teepol L solution. The surface tension of the water was reduced by the Teepol but so also was the hysteresis.

6. In order to calibrate the float, it was submerged to its maximum depth and increments of water removed from the ignition tube, whilst corresponding readings were taken of the height of the etch mark on the wire. The size of these increments (V) and the height of the scratch (h) were recorded and a graph plotted. As expected, this was a straight line, the gradient corresponding to the cross-sectional area of the ignition tube. Correlation was

good between the value obtained from the dimensions of the tube and this volumetric method.

7. Another polythene hemisphere, loaded with lead, and with a carefully prepared surface, was lowered into the tank so that it lay, curved side up, on the bottom. Another micrometer syringe, this time with a very fine needle and filled with di-n-butyl phthalate/liquid paraffin mixture was lowered point down, until the needle touched the lower hemisphere. A drop of known volume was injected on to the top of this hemisphere and the syringe removed.

The float and its associated micrometer syringe were then swung over the drop and the float carefully sunk. When contact was made between the spherical surfaces, a bridge of the oil mixture was formed between them. If the bridge did not seem symmetrical, then the float was moved to assist spreading of the oil on the polythene. The bridge was finally centered by raising the float a little, allowing it to centralise over the lower hemisphere and then lowering it back into a touching position. The neck diameter was then measured with the travelling microscope. The scratch on the copper wire of the float was now observed as water was removed from the ignition tube in known increments. Details of the height (h) and the syringe reading (V) were taken as the bridge was slowly stretched until finally it ruptured. This point was noted and further readings were taken to make sure that the float was not sticking to the suspension.

It is interesting to note that the so-called Plateau's spherule[45],[48], the small drop formed when a large drop separates from a tube, was not observed when the bridge ruptured. This may be due to the "slowness" of the system due to the low interfacial tension and the viscosity of the oil, or alternatively, due to the drop not rupturing with a large gravitational acceleration as happens

with a free drip.

Fig. 10 illustrates graphically the method used to calculate the variation of force with separation, although in fact, both the separation and the force were calculated directly from the results.

The sensitivity of the apparatus was such that a force of 0.004 gms produced a displacement of 0.0142cms. Forces of the order of 0.3 milligrams could be observed.

(iii) Measurement of surface tension

1. The measurement of the inter-facial tension between two liquids of the same density poses several interesting problems. All of the conventional methods utilising differential density to measure pressure will not work and the method of Mack and Bartell[42] which is a modification of the well-known differential capillary rise method[43] has the disadvantage of trapping the oil/water interface in capillary tubes. Equilibrium is reached by one interface advancing and the other receding, and the respective contact angles are unlikely to be zero under these conditions.

2. The following method which is based on that of Sentis[44] (see also Smith[45]) was devised. Consider a drop of liquid suspended from a tube under the surface of another liquid (Fig. 11). If the liquids are of equal density then a simple analysis gives:-

$$dfg = \frac{2\gamma_1}{r} + \frac{2\gamma_2}{R} \qquad \ldots\ldots\ldots\ldots\ldots (25)$$

where d is the height of the meniscus above the liquid surface, f is the density of the liquids, g the acceleration due to gravity,

γ_1 is the surface tension of the liquid in the capillary,

γ_2 is the interfacial tension between the bulk liquid and the liquid in the capillary, r is the radius of the capillary tube, and R is the radius of the spherical drop.

If the volume of liquid in the tube is varied, then d and R will vary. However, they will always be connected by the above

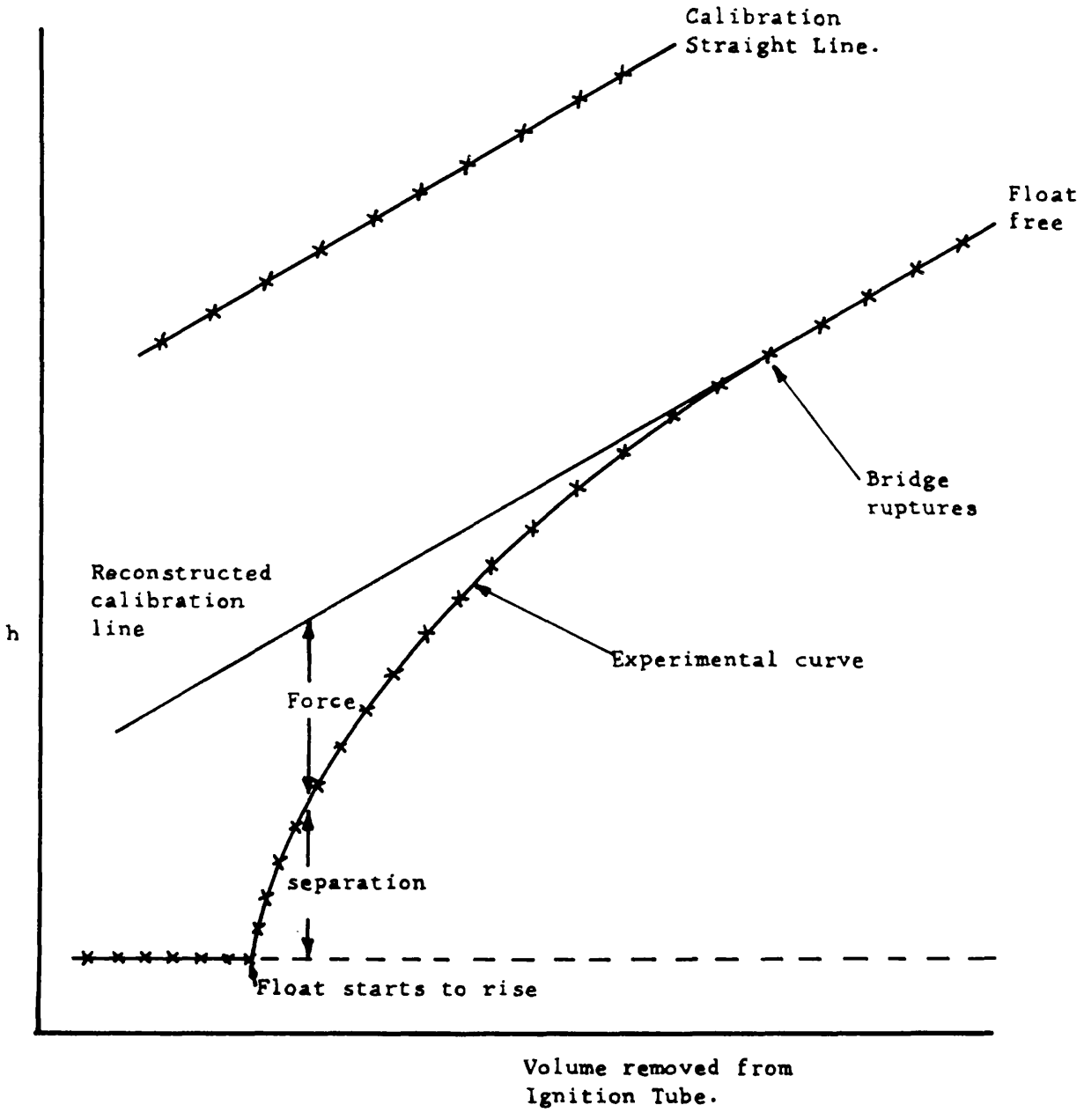

FIG. 10. The graphical method for calculating force and separation.

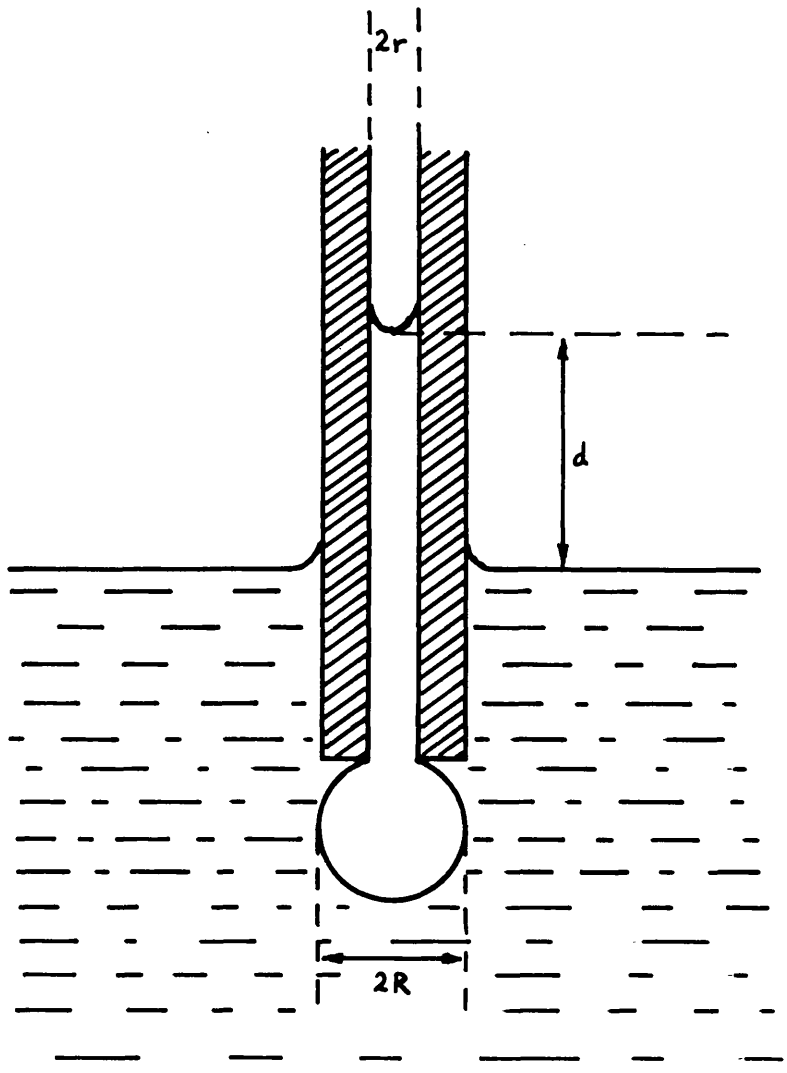

FIG. 11. Measurement of surface tension.

relationship (Eqn. 25) so that a graph of d against $^1/R$ will be a straight line of gradient $2\gamma_2/\rho g$ and intercept $2\gamma_1/\rho g$ r

3. It is important that the system be stable and the drop will reach instability when the rates of change of pressure with R for both the column and the sphere are equal.

If V is the volume of the liquid and P the pressure in the capillary/sphere system.

For the column:-

$$P_c = \frac{\rho g V}{\pi r^2} - \frac{4}{3}\frac{\pi R^3 \rho g}{\pi r^2} - \frac{2\gamma_1}{r} \qquad \ldots\ldots\ldots\ldots\ldots\ldots (26)$$

and $$\frac{dP_c}{dR} = -4\pi R^2 \frac{\rho g}{\pi r^2} \qquad \ldots\ldots\ldots\ldots (27)$$

For the sphere:-

$$P_s = K\rho g + \frac{2\gamma_2}{R} \qquad \ldots\ldots\ldots\ldots (28)$$

where K is a constant

$$\frac{dP_s}{dR} = -\frac{2\gamma_2}{R^2} \qquad \ldots\ldots\ldots\ldots (29)$$

At the critical point, using Equns. (27) and (29).

$$-\frac{4\pi R \rho g}{\pi r^2} = -\frac{2\gamma_2}{R^2} \qquad \ldots\ldots\ldots\ldots (30)$$

Hence $$R^4 = \gamma_2 r^2 / 2\rho g \qquad \ldots\ldots\ldots\ldots (31)$$

At this value of R the spherical drop will shrink away up the tube and this places a maximum on the value of 1/R. Since the minimum of 1/R is zero, only a portion of the graph can be drawn.

4. The experimental arrangement used the cell previously mentioned, which was half filled with 0.2% Teepol L solution and thermostatted at $25^\circ C \pm 0.2^\circ C$. A 0.5 mm internal diameter Veridia capillary tube about 12 inches long with a rubber tube on the end was filled with di-n-phthalate/liquid paraffin by sucking through the rubber tube. It was then transferred to the cell and mounted in a vertical position dipping about 2 cms into the Teepol solution. A large spherical drop then grew from the bottom of the tube as the meniscus in the capillary fell. At equilibrium the diameter

of the drop and the height of the meniscus above the tank water level were measured with a travelling microscope. In order to see the water level accurately a small quantity of oil was introduced into the tank by squirting from a glass dropper. This atomised the large oil drops and some of the smaller drops attached themselves to the surface. The hour-glass shape of the sphere and its image in the surface enabled the water level to be determined accurately.

The experiment was repeated with different quantities of the oil. For the small drops, a convenient way of reducing the volume of oil was to suck part of the drop back up the capillary tube and to break off the remaining part by tapping the capillary. A smaller drop would then regrow. It is not advisable to grow all the drops in this way, as a systematic error can be incurred from changes in the capillary bore, affecting the height. Several runs were taken, remounting the capillary at a different depth each time.

5. The height (d) was found to vary by about 2 mms for the maximum and minimum values of 1/R. The capillary rise in the tube, due to the oil/air interface was approximately 2 cms, consequently any error in the position of the meniscus due to the capillary rise could result in a larger error in the change due to the spherical oil drop. Errors of this type were most likely to occur, because of variations in the tube bore. The diameter of the tubing was quoted as 0.50 mm $\pm$ 0.01 mm, but this error was very unlikely to occur over the small length of the tube used. Furthermore, Haynes[30] measured the variation of bore of a 0.4 mm diameter Veridia tube, and found it to be no more than $\pm$ 0.001 mms. Fig. 12 is a graph of d against 1/R and shows the scatter of the points. The gradient of the line was found giving a value of the interfacial tension of 2.45 $\pm$ 0.2 dynes/cm. The surface tension of the di-n-butyl phthalate/ liquid paraffin mixture was found to be 31.8 dynes/cm from the intercept value.

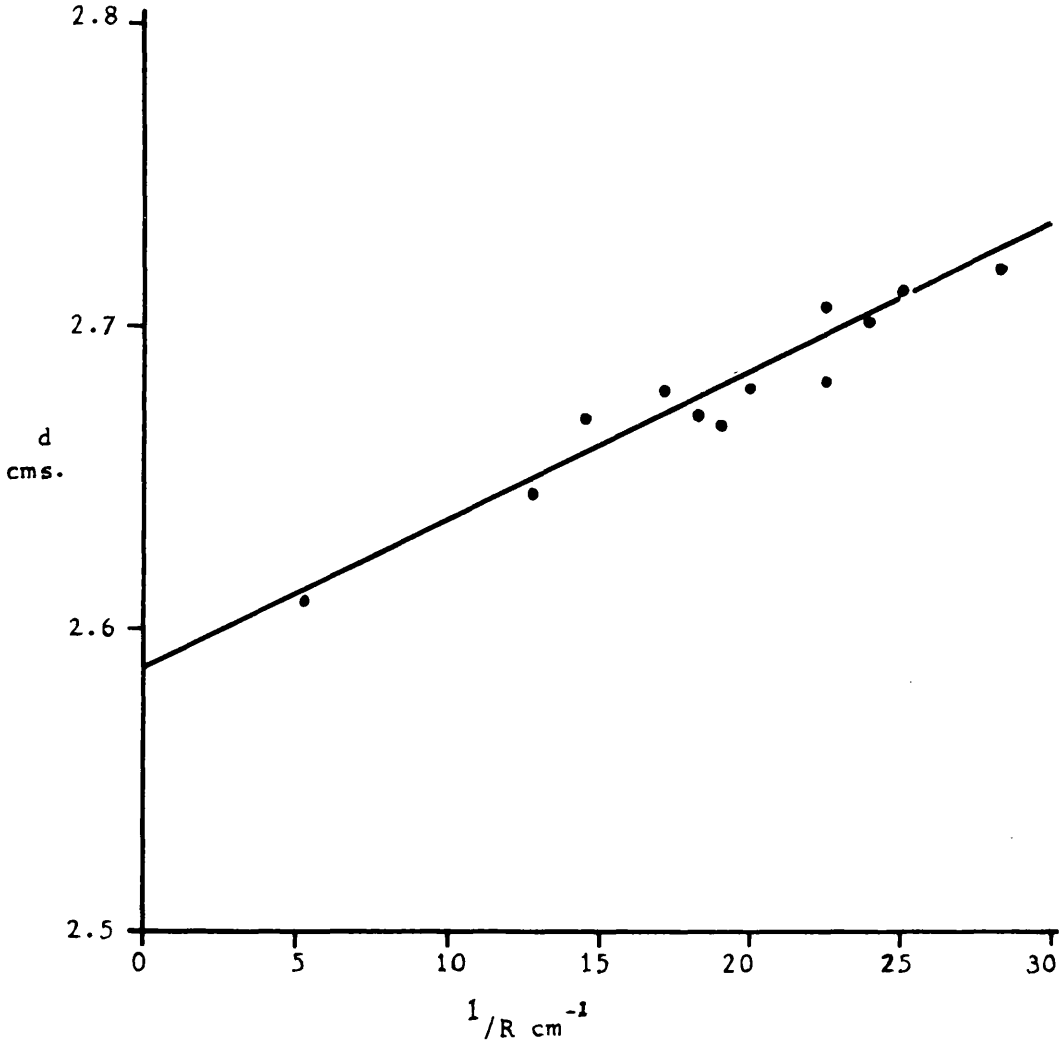

FIG. 12. Plot of d against $^{1}/R$ for measurement of the surface tension.

The low interfacial tension of 2.45 dynes/cm was due to the Teepol L solution, since the surface tension of water is reduced from approximately 70 dynes/cm to between 30 and 40 dynes/cm, by such detergents. Antonow's Rule states that for two mutually saturated liquids the interfacial tension is equal to the difference of their surface tensions[46][47][11] and as the surface tension of the oil does not change by more than a few dynes/cm[30] any reduction of the surface tension of the water reduces the surface tension of the interface by an almost equal amount.

(iv) Results from the apparatus

The calibration straight line (Fig. 10) had a gradient of 14.2 (units of 0.01 mm) per 4×10^{-3} mls (20 divisions on the micrometer syringe) of water removed from the ignition tube. Calculations from the diameter gave 14.16 (units of 0.01 mms) per 4×10^{-3} mls.

1. For two spheres the force/separation curves are shown in Fig. 13 (a - e). In general the form of the curves is similar with an expansion along the separation axis as the volume of oil increases. At higher oil volumes the curves can be approximated by a straight line. Fig. 14 lists the major properties of bridges between spheres.

Force/separation curves for a liquid bridge between a sphere and a plate are shown in Fig. 15 (a - e) and these are generally similar in shape to the curves for two spheres. Fig. 16 lists the major properties of bridges between a sphere and a plate.

2. The peaks of all the force/separation curves were taken as the maximum force and plotted against volume (Fig. 17). Fisher's[7] theoretical results of the force between two spheres are shown, as are theoretical results of the force between a sphere and a plate using the toroid approximation. The force between the two spheres was about half that between the sphere and the plate.

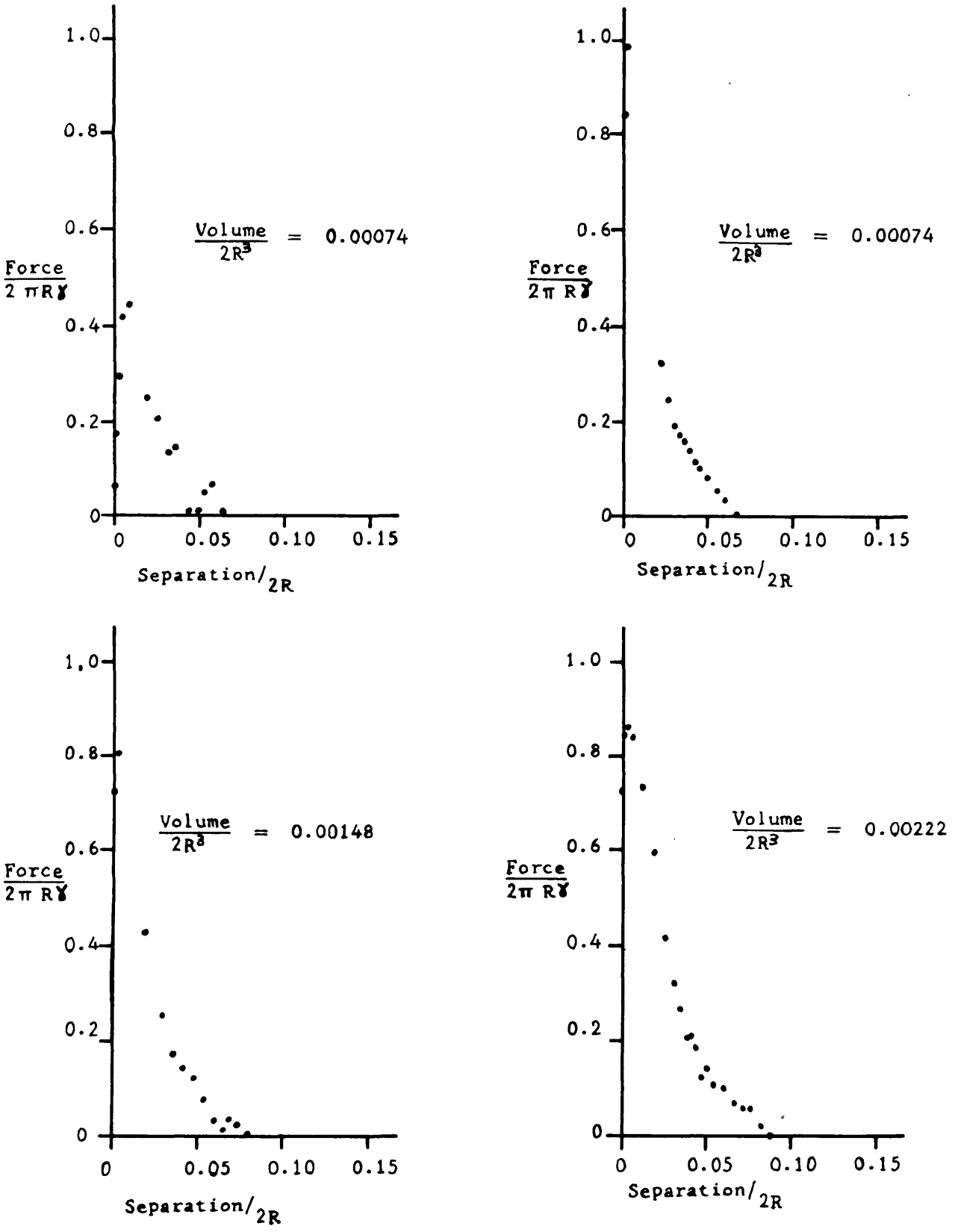

FIG. 13(a) Force/separation curves. Two spheres.

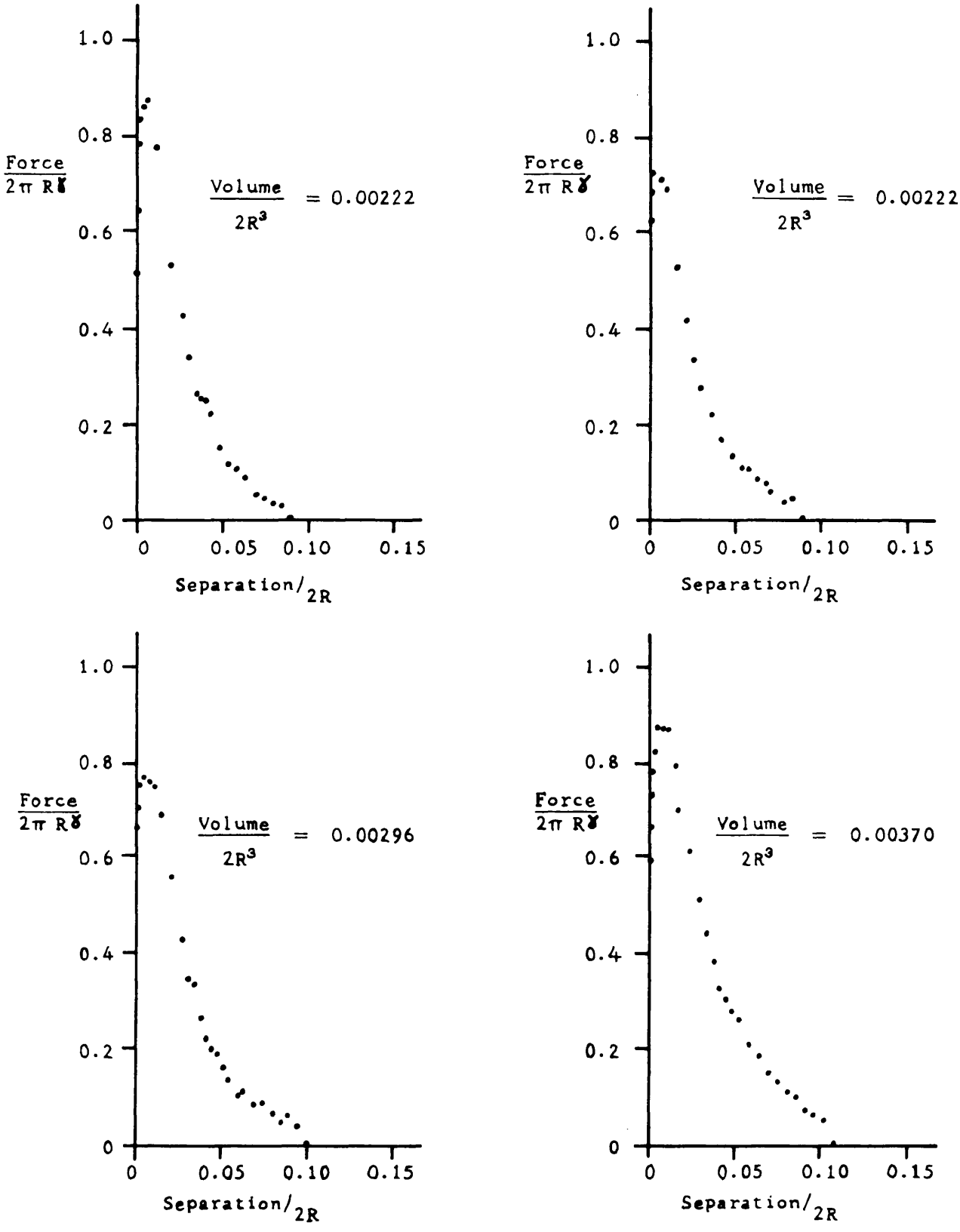

FIG. 13(b) Force/separation curves. Two spheres.

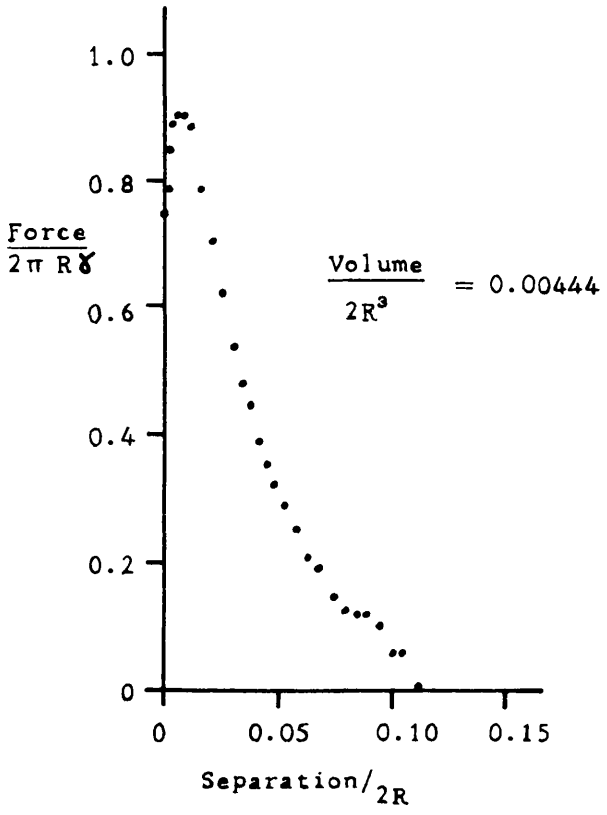

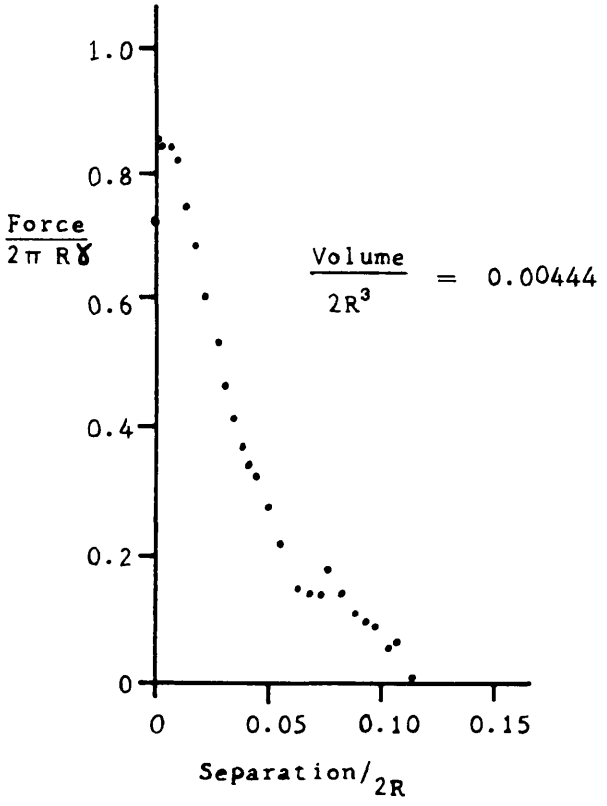

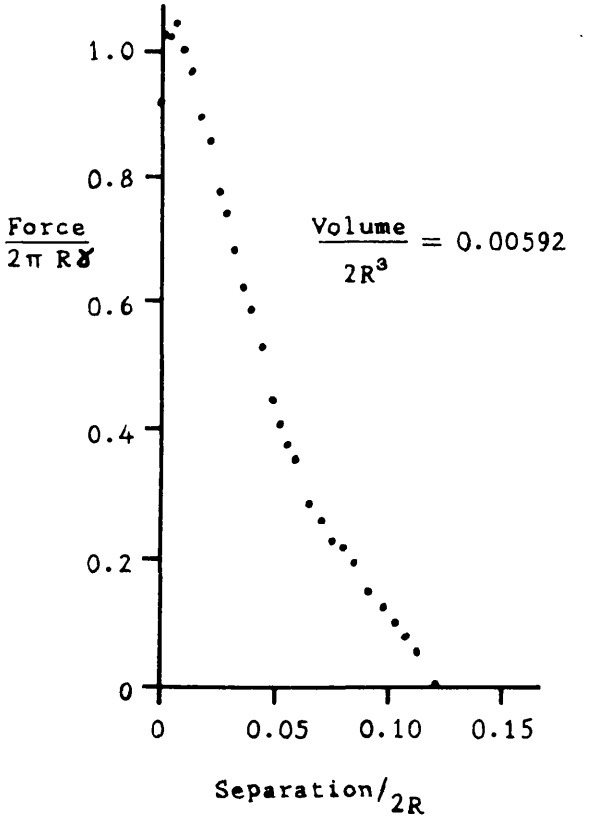

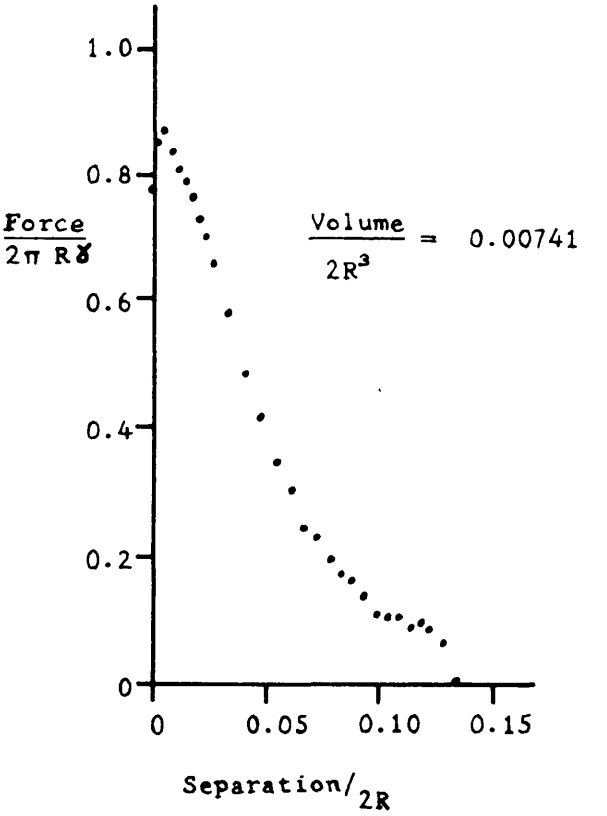

FIG. 13(c) Force/separation curves. Two spheres.

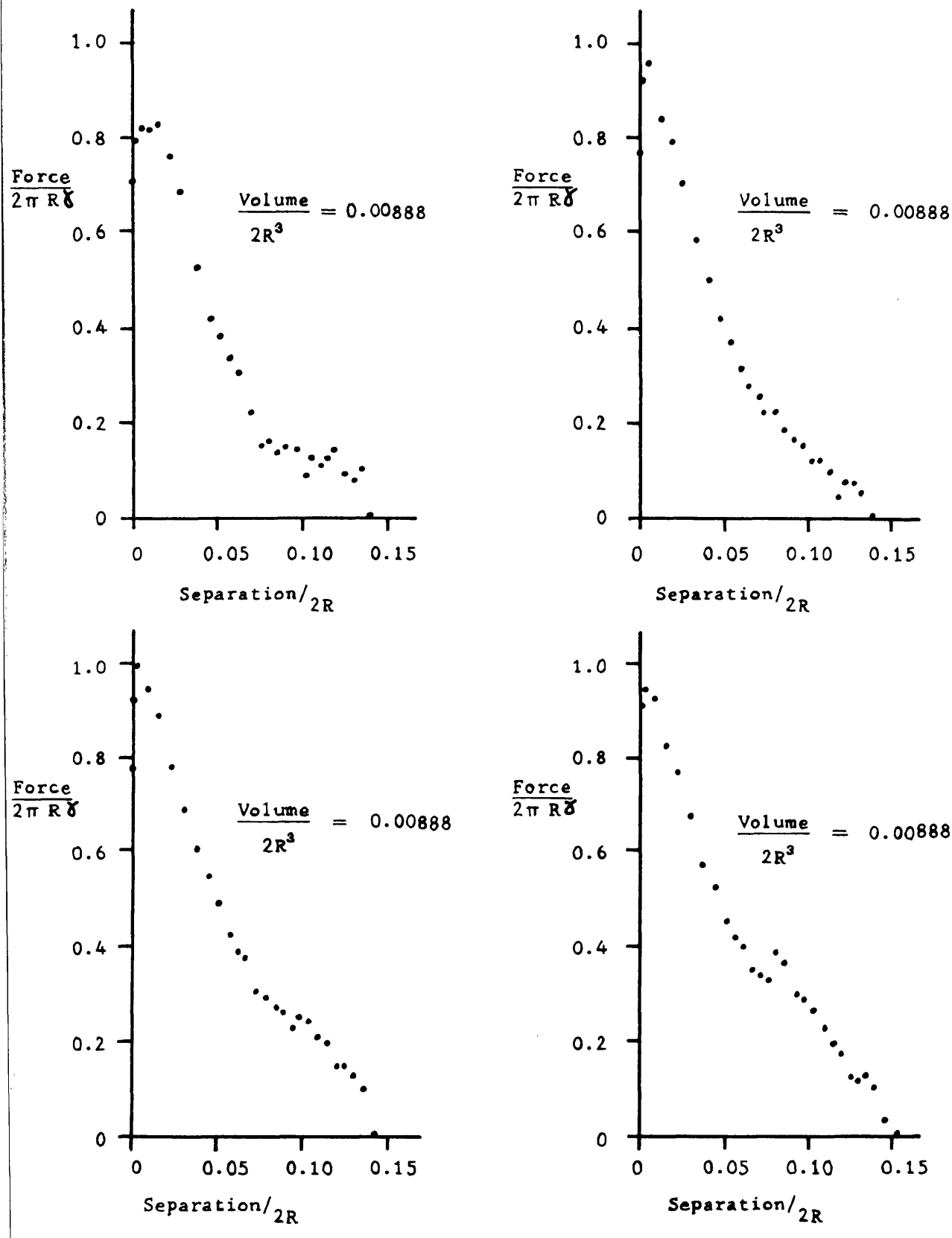

FIG. 13(d) Force/separation curves. Two spheres.

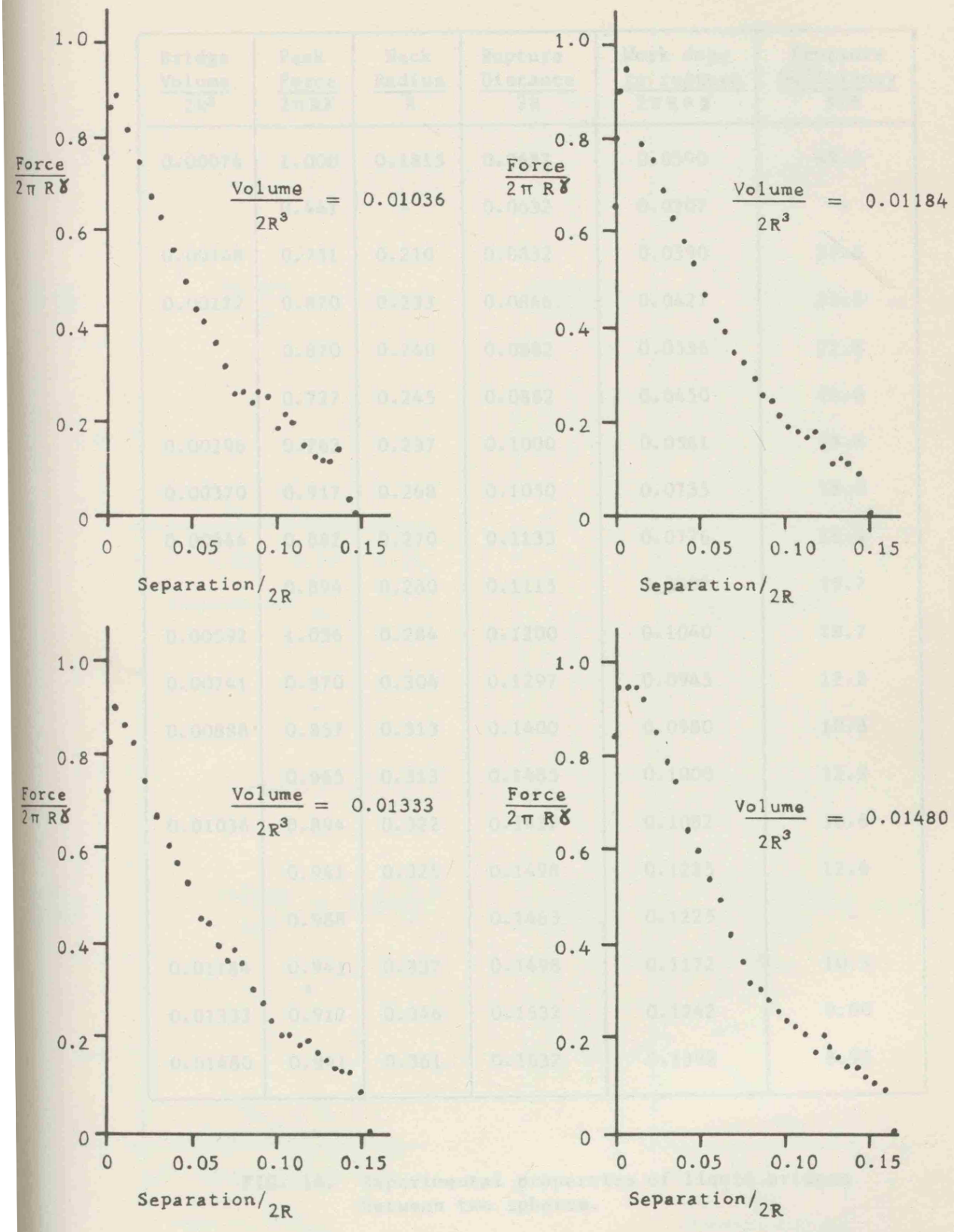

FIG. 13(e) Force/separation curves. Two spheres.

Bridge Volume $2R^3$	Peak Force $2\pi R\gamma$	Neck Radius R	Rupture Distance 2R	Work done to rupture $2\pi R^2\gamma$	Pressure Deficiency γ/R
0.00074	1.000	0.1815	0.0632	0.0390	49.0
	0.441	-	0.0632	0.0207	-
0.00148	0.751	0.210	0.0832	0.0390	27.6
0.00222	0.870	0.233	0.0866	0.0427	23.5
	0.870	0.240	0.0882	0.0536	21.8
	0.727	0.245	0.0882	0.0450	16.0
0.00296	0.763	0.237	0.1000	0.0561	18.8
0.00370	0.917	0.268	0.1050	0.0735	18.0
0.00444	0.882	0.270	0.1133	0.0726	16.9
	0.894	0.280	0.1115	0.0802	15.7
0.00592	1.036	0.284	0.1200	0.1040	18.7
0.00741	0.870	0.304	0.1297	0.0945	12.2
0.00888	0.857	0.313	0.1400	0.0980	10.8
	0.965	0.313	0.1465	0.1000	12.9
0.01036	0.894	0.322	0.1432	0.1082	10.6
	0.941	0.325	0.1498	0.1225	12.6
	0.988	-	0.1465	0.1225	-
0.01184	0.941	0.337	0.1498	0.1172	10.5
0.01333	0.917	0.346	0.1532	0.1242	9.00
0.01480	0.941	0.361	0.1632	0.1392	8.95

FIG. 14. Experimental properties of liquid bridges between two spheres.

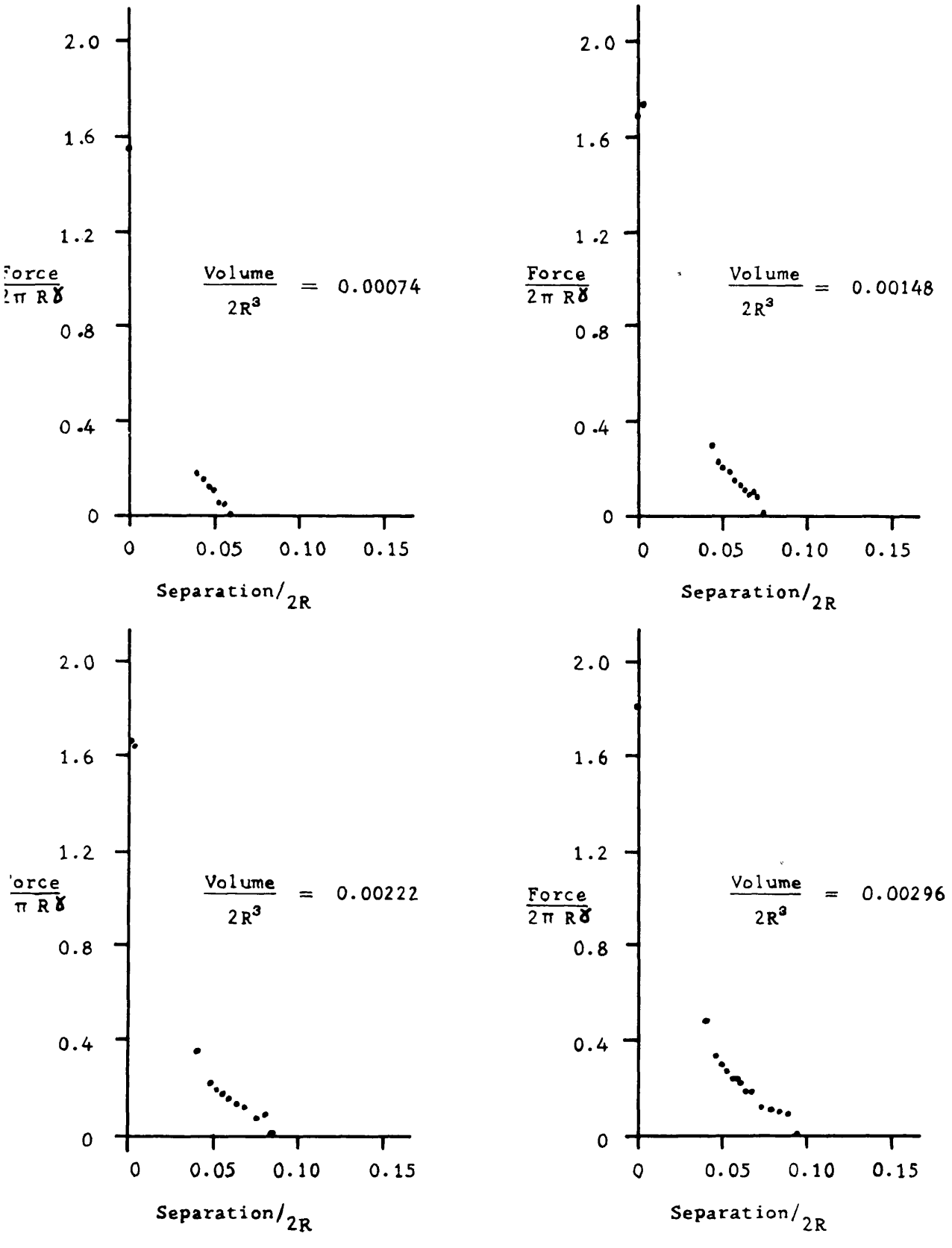

FIG. 15(a) Force/separation curves. Sphere and plate.

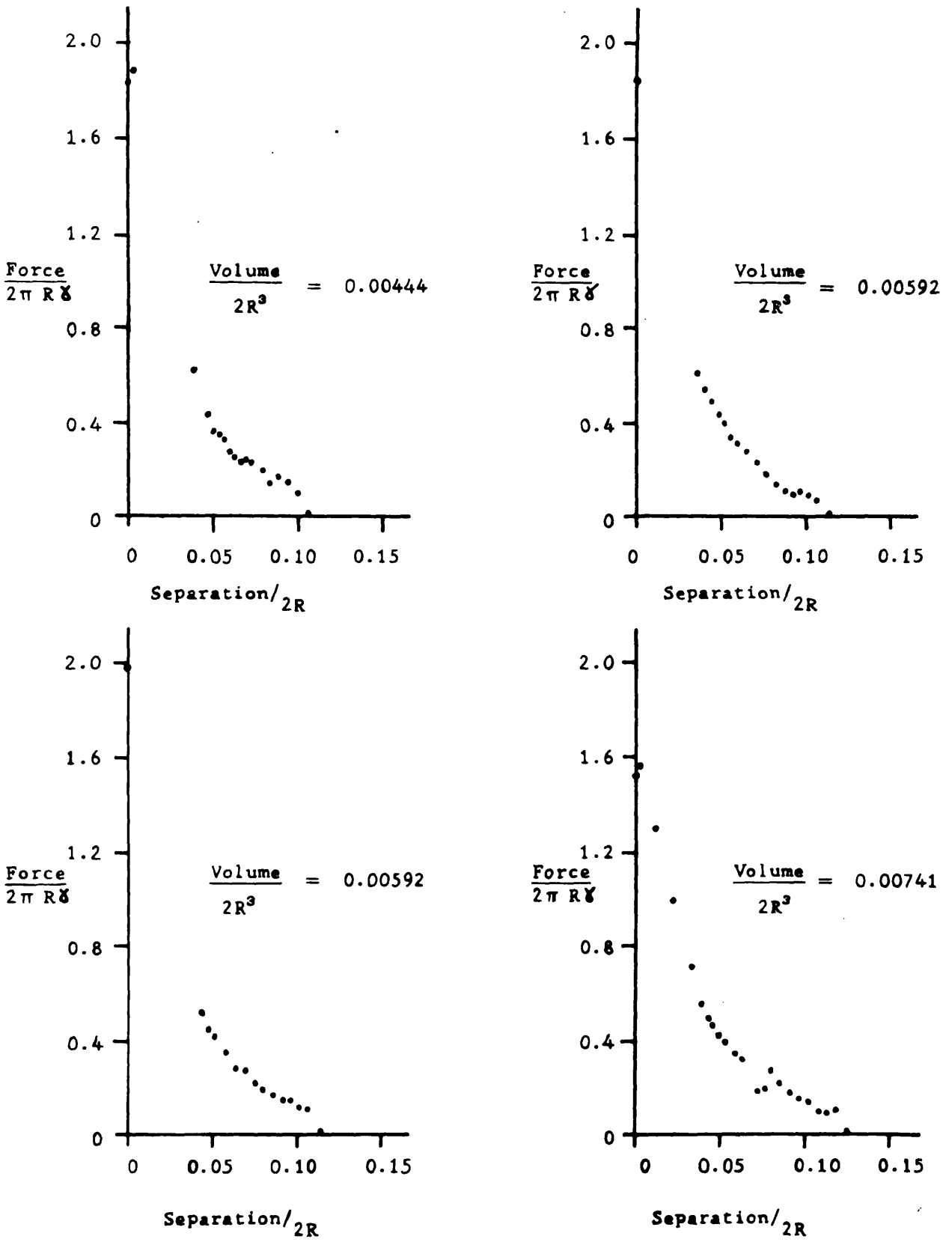

FIG. 15(b) Force/separation curves. Sphere and plate.

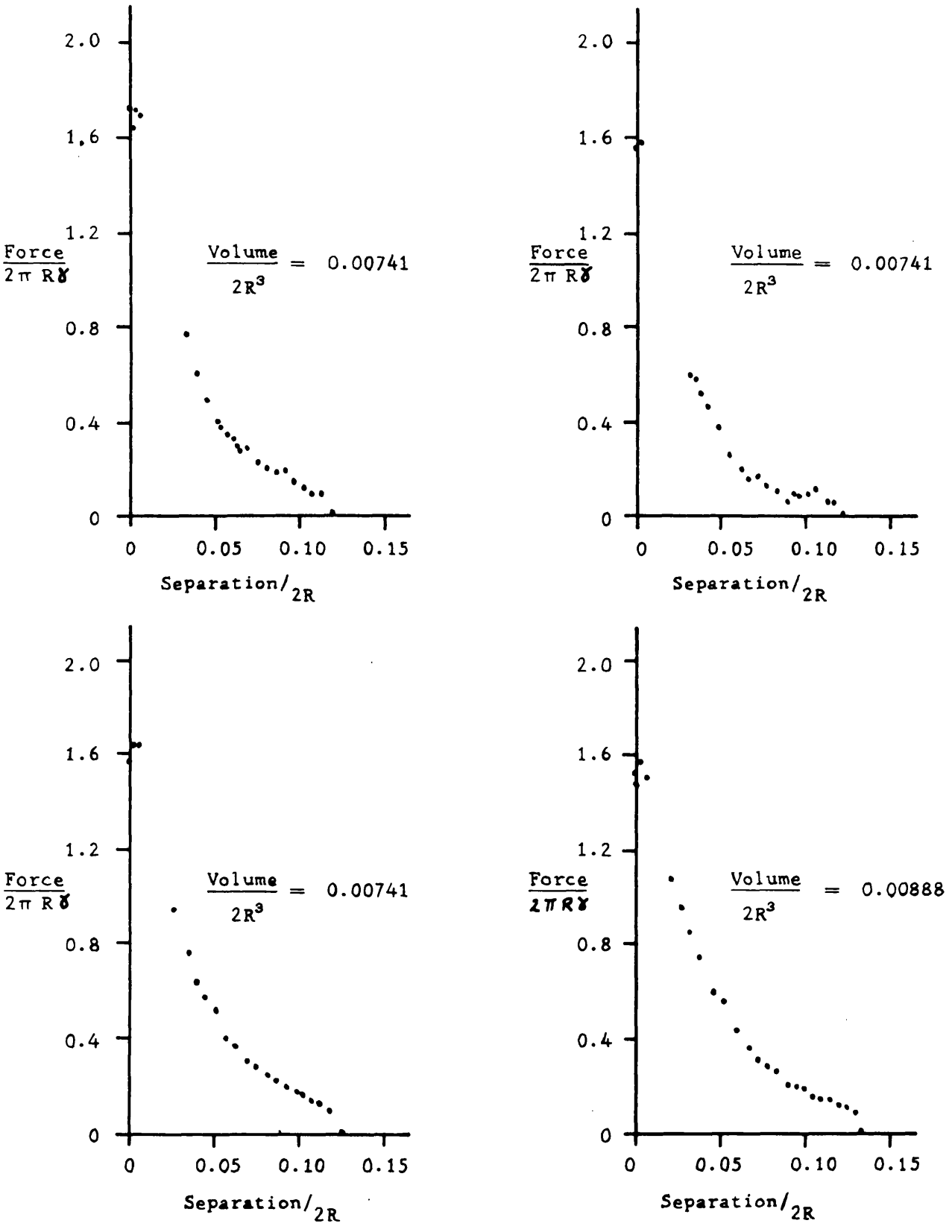

FIG. 15(c) Force/separation curves. Sphere and plate.

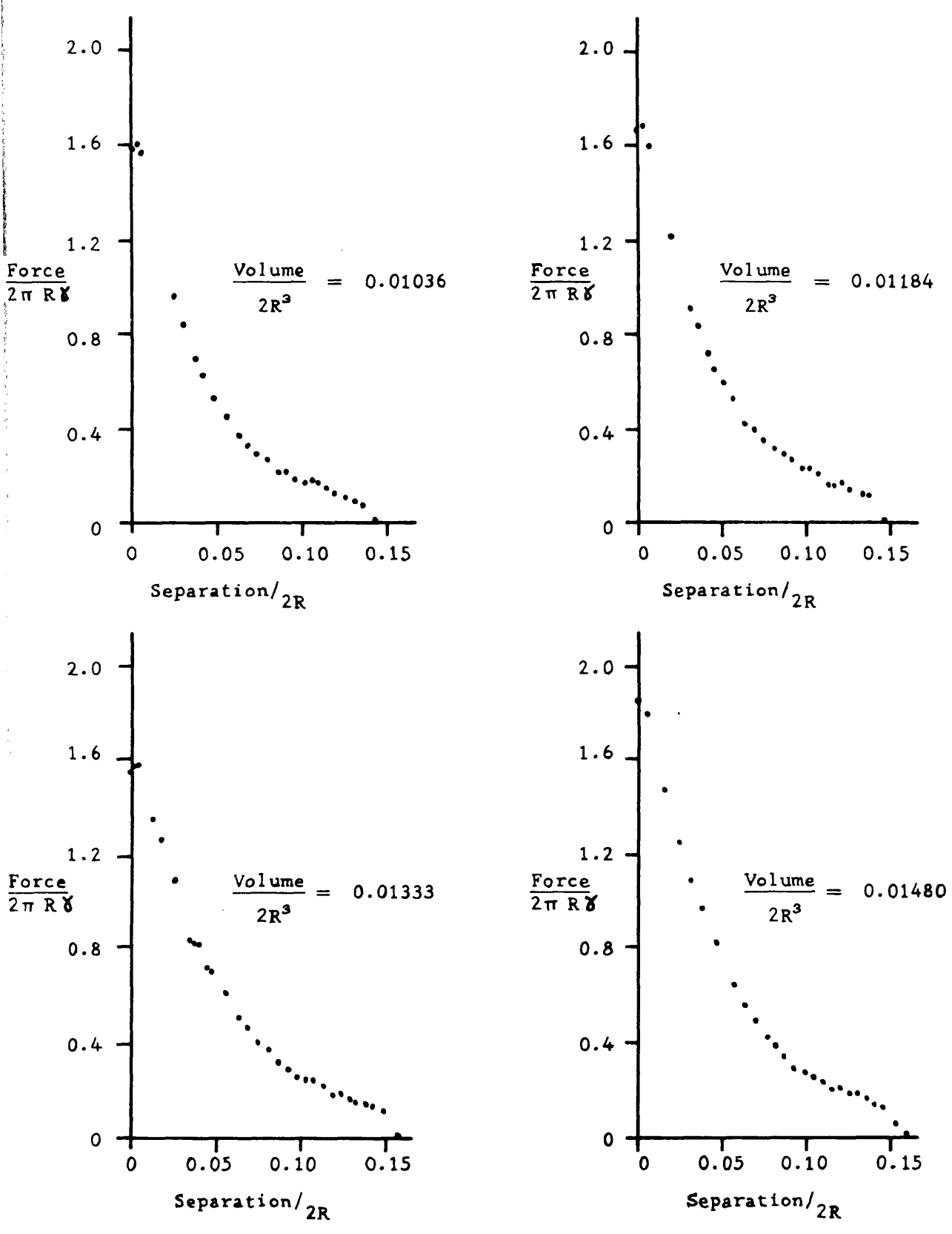

FIG. 15(d) Force/separation curves. Sphere and plate.

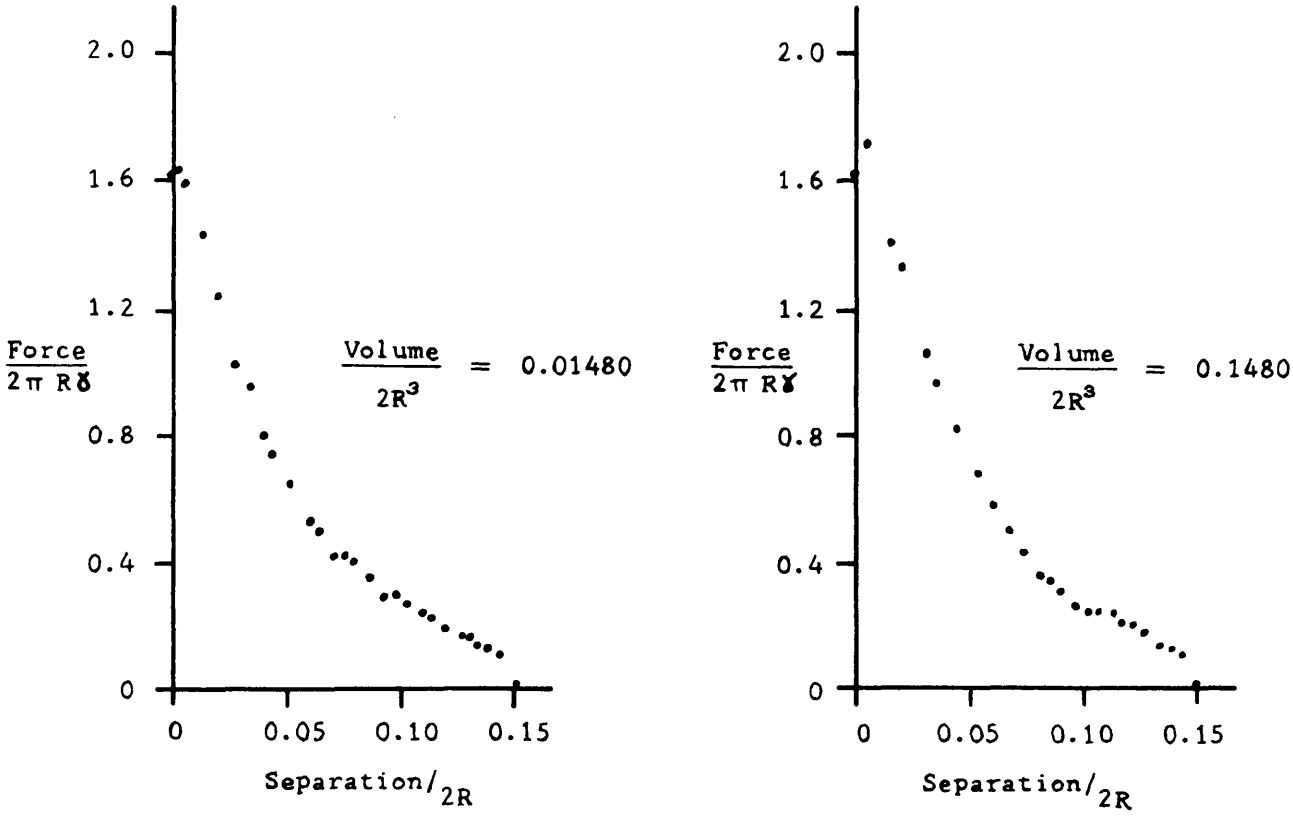

FIG. 15(e) Force/separation curves. Sphere and plate.

Bridge Volume $\frac{}{2R^3}$	Peak Force $\frac{}{2\pi R\gamma}$	Neck Radius $\frac{}{R}$	Rupture Distance $\frac{}{2R}$	Work done to rupture $\frac{}{2\pi R^2\gamma}$	Pressure Deficiency $\frac{}{\gamma/R}$
0.00074	1.536	-	0.0590	0.0590	-
0.00148	1.975	-	0.0704	0.0854	-
0.00222	1.665	0.257	0.0850	0.0970	42.6
0.00296	1.810	0.287	0.0953	0.1090	37.1
0.00444	1.881	0.300	0.1070	0.1302	35.3
0.00592	1.830	0.343	0.1139	0.1250	25.7
	1.965	0.340	0.1142	0.1320	26.7
0.00741	1.571	0.347	0.1245	0.1258	21.8
	1.726	0.347	0.1200	0.1338	23.5
	1.571	0.340	0.1222	0.1105	23.8
	1.667	0.350	0.1255	0.1412	22.1
0.00888	1.595	0.371	0.1339	0.1424	22.5
0.01036	1.620	0.385	0.1432	0.1402	16.7
0.01184	1.666	0.393	0.1450	0.1575	16.2
0.01333	1.595	0.412	0.1565	0.1686	14.9
0.01480	1.870	0.431	0.1540	0.1942	14.5
	1.750	-	0.1515	0.1815	-
	1.631	-	0.1515	0.1750	-

FIG. 16 Experimental properties of liquid bridges between a sphere and a plate.

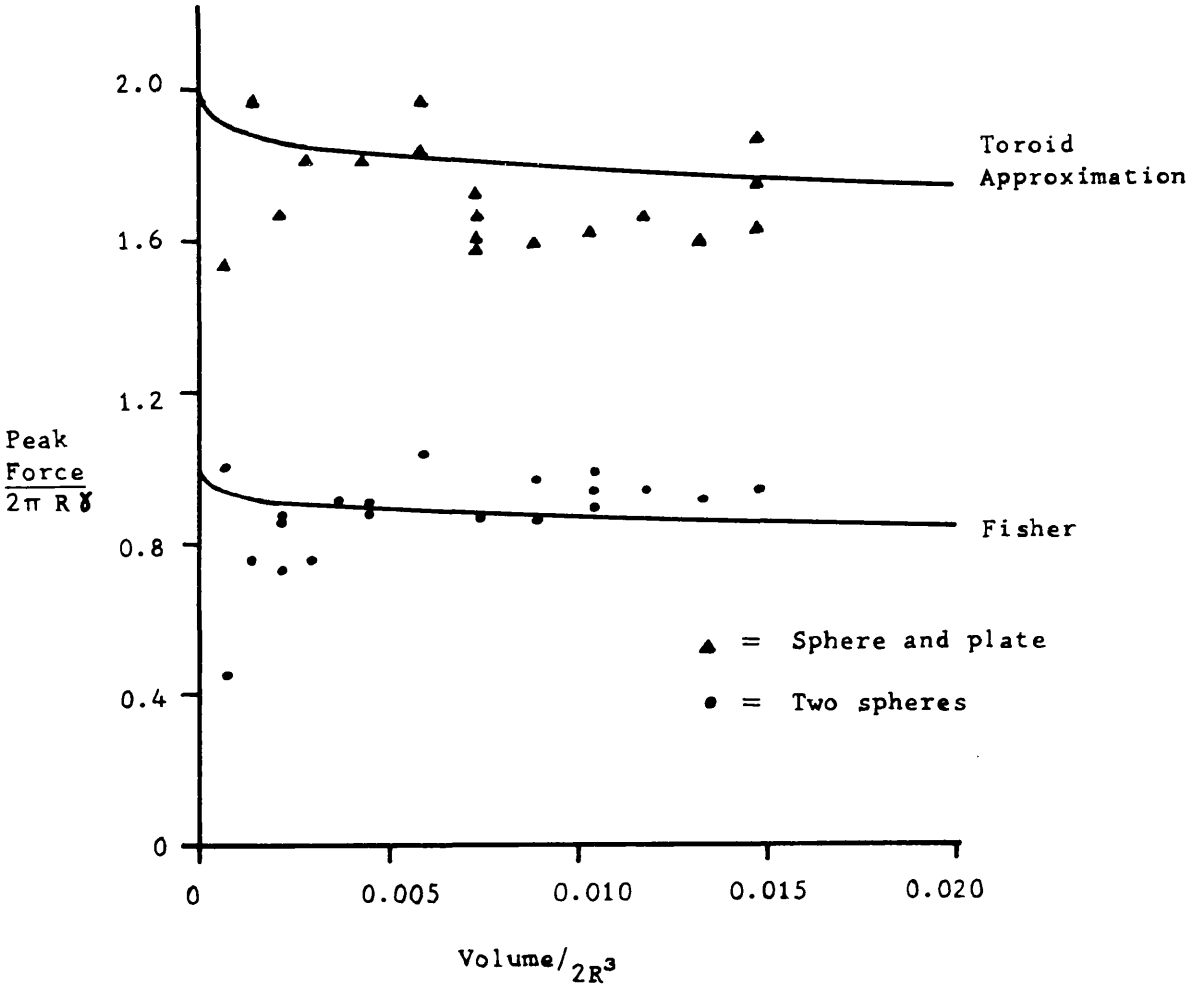

FIG. 17. Variation of maximum force with volume for liquid bridges between two spheres and between a sphere and a plate.

3. The neck diameters were compared with Fisher's[7] calculations for the two spheres and with the toroid approximation for the sphere and the plate (Fig. 18). Agreement is generally good between the theory and the experiments, but the toroid approximation for the sphere and the plate seems to overestimate the neck radius for a given bridge volume. This is not unexpected, as the simplification approximates a nodoid as a part of a toroid. The nodoid is more highly curved than the toroid, and so the neck diameter is always less than the toroid approximation (Fig. 19).

4. Fig. 20 shows the variation of pressure deficiency with bridge volume. The pressure was calculated from the equation

$$\text{Pressure deficiency} = \frac{2\gamma}{R}\left(\frac{f-a}{a^2}\right) \qquad \ldots\ldots\ldots\ldots (32)$$

where f = Peak force/$2\pi R\gamma$

a = Neck diameter/2R

This equation is a simple rearrangement of the equation for the cohesive force containing a cohesion due to the surface tension directly and a cohesion due to the pressure deficiency. Fisher[7] and von Engelhardt[9] have calculated the values for the two spheres. The values for the sphere and plate were calculated using the toroid approximation.

5. Fig. 21 shows the variation of pressure deficiency with neck radius. The values at low curvatures for the sphere and plate are due to Haynes[30] and it can be seen that the toroid approximation is relatively more accurate in this case than in the others. Again the results for two spheres fit the theoretical results of Fisher[7].

We can conclude that the theoretical work of Fisher[7] on the nodoid between two spheres has been given a practical test and has in every way proved adequate. The toroid approximation for a

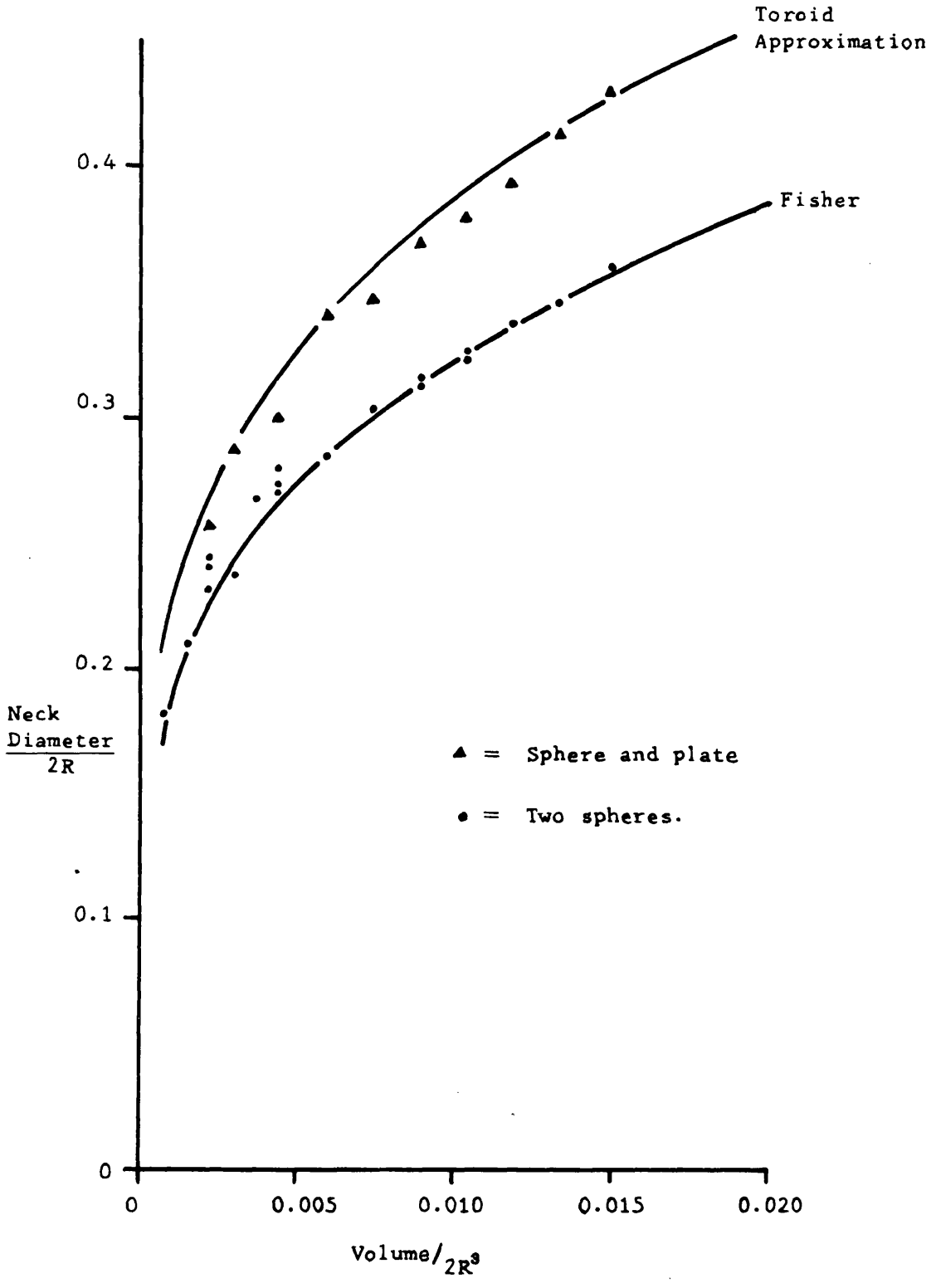

FIG. 18. Variation of neck diameter with volume for liquid bridges between two spheres and between a sphere and a plate.

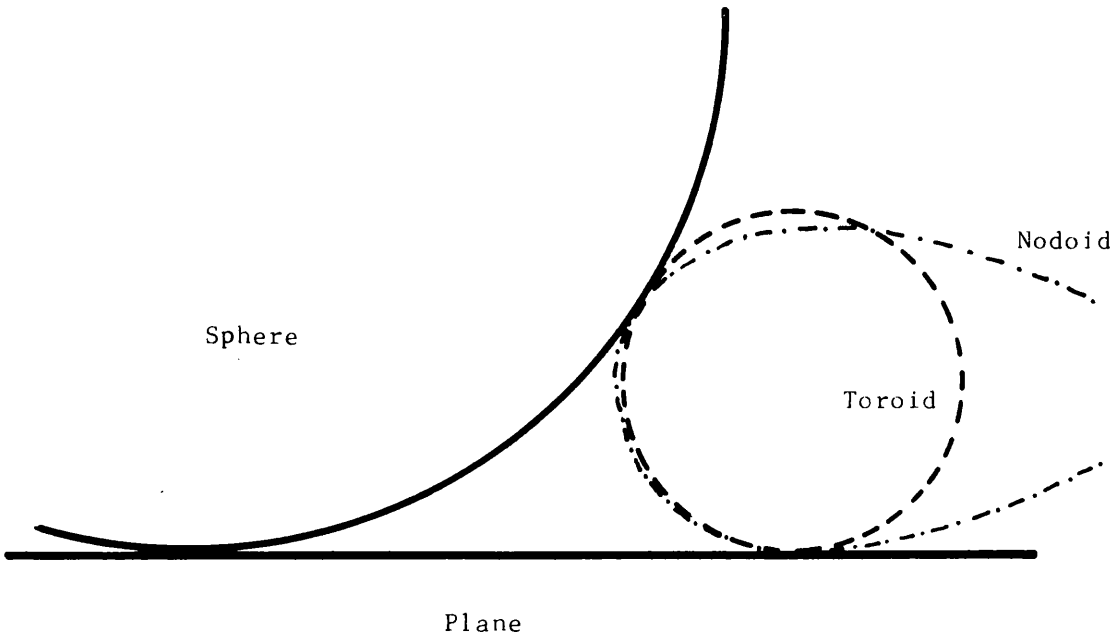

FIG. 19. Comparison of Nodoid and Toroid approximation for a sphere and plate.

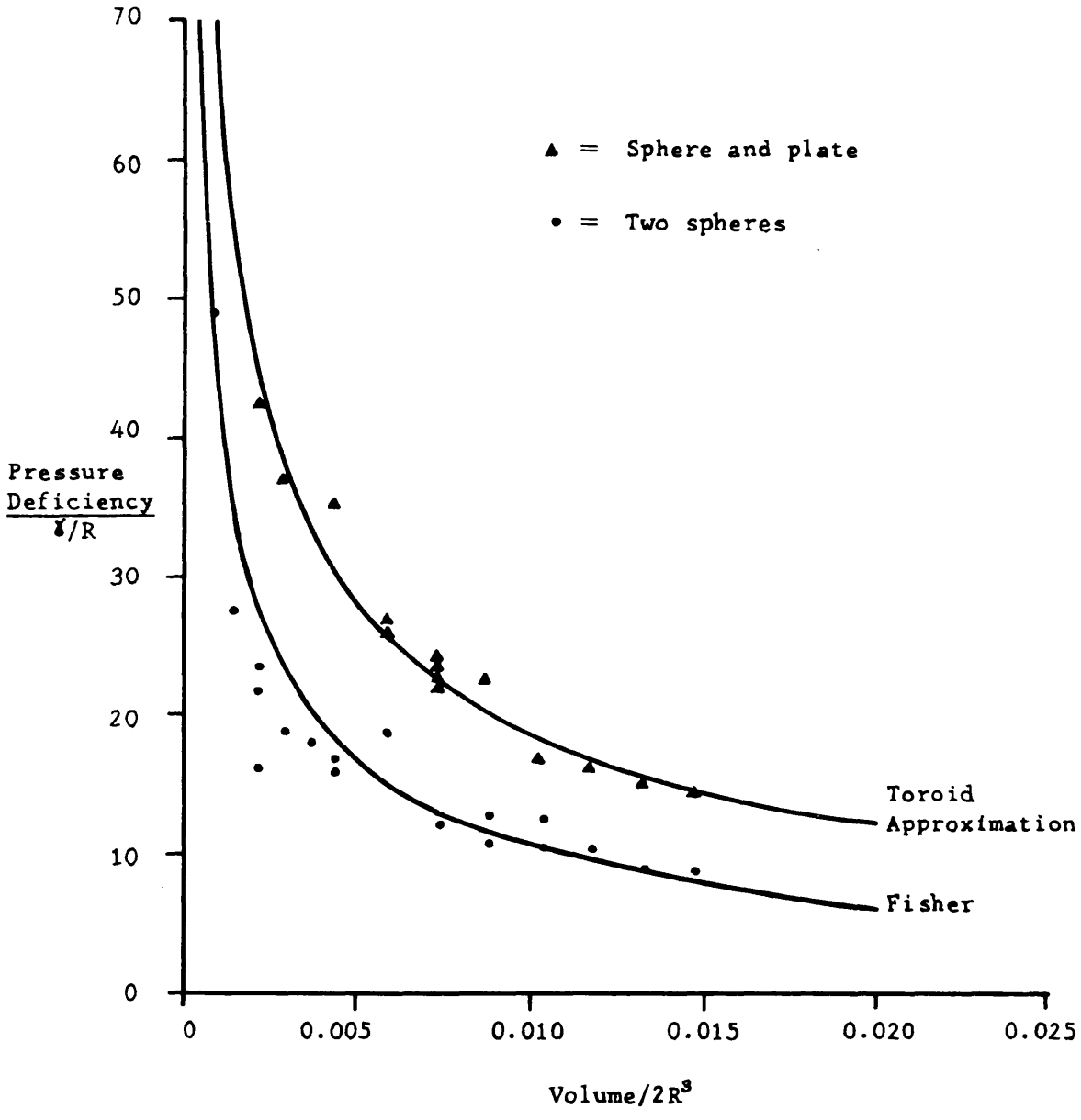

FIG. 20. Variation of pressure deficiency with volume for liquid bridges between two spheres and between a sphere and a plate.

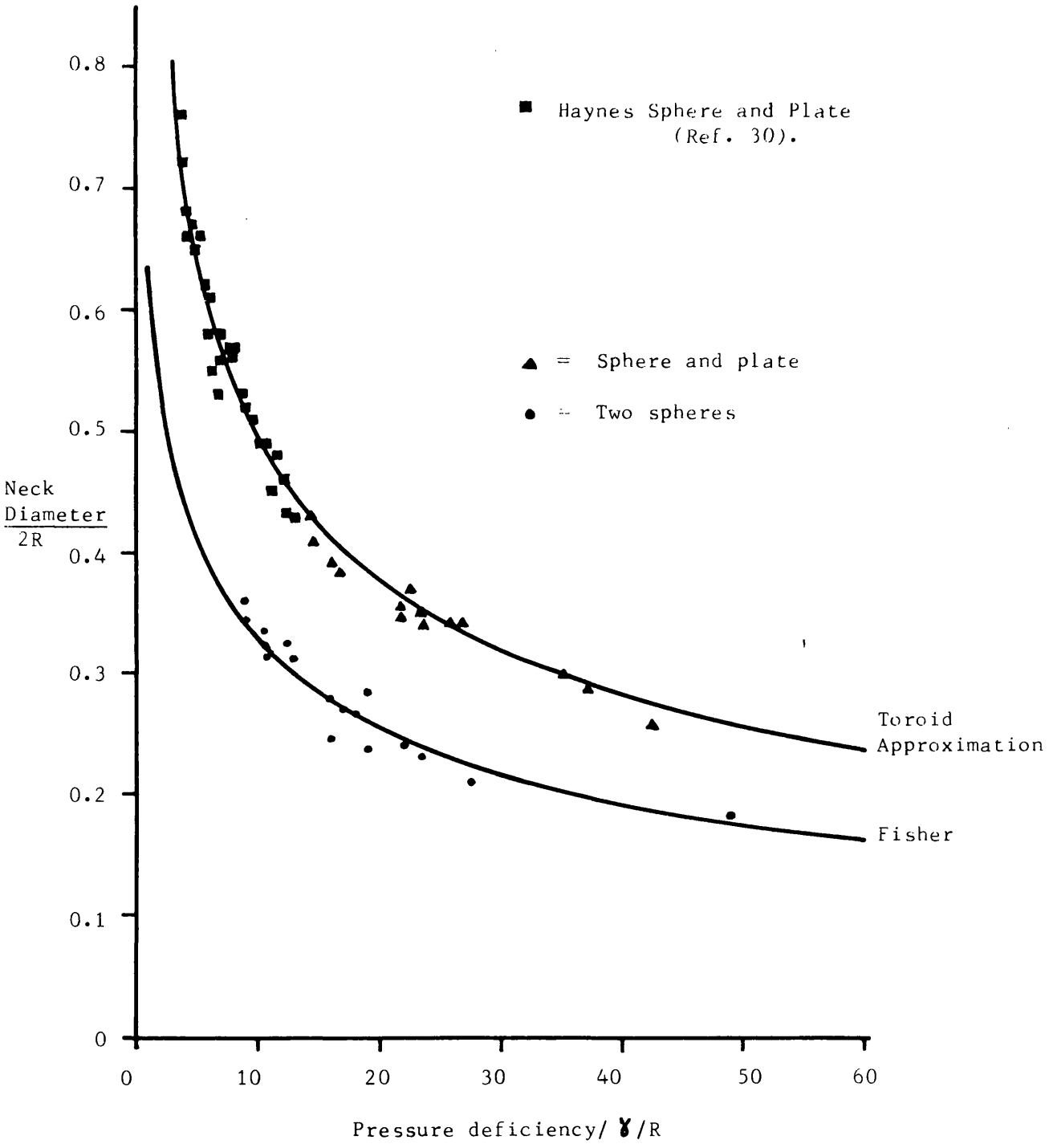

FIG. 21. Variation of neck diameter with pressure deficiency for liquid bridges between two spheres and between a sphere and a plate.

sphere on a plate has also been given a practical test, but has not been so successful.

6. Several of the force/separation curves for two spheres show that the force appears to pass through a maximum, whilst at small sphere separations. This maximum appears to be significant and may be due either to a finite initial contact angle which tended to zero as the separation increased or to the point of contact not being on the axis of the top spherical surface. The possibility of a small contact angle was minimised experimentally by wetting the sphere surfaces with bridge liquid before commencing a run. Visual examination indicated good wetting and any contact angle would have to be small. To minimise non-axial alignment, the hydrometer was raised slightly and allowed to sink into contact from above, whilst being centralised by the bridge. The maximum may well be a property of the bridges as Cross and Picknett[31] noted that there was a slight displacement before bridge rupture when using a microbalance on a similar system.

7. The work done in rupturing a bridge is particularly difficult to calculate, as it involves a limiting instability (i.e. rupture). Indeed, the calculations of the force/separation function would seem to be so laborious as to be hardly justified, even without the complications of a further integration for the work done in rupturing the bridge. The areas under the force/separation curves were measured with a planimeter and are produced in graphical form (Fig. 22). As would be expected, the work done in rupture rises with the quantity of oil, although not linearly. Thus, for equal volumes of liquid, a few large bridges will contain less energy than a host of small ones.

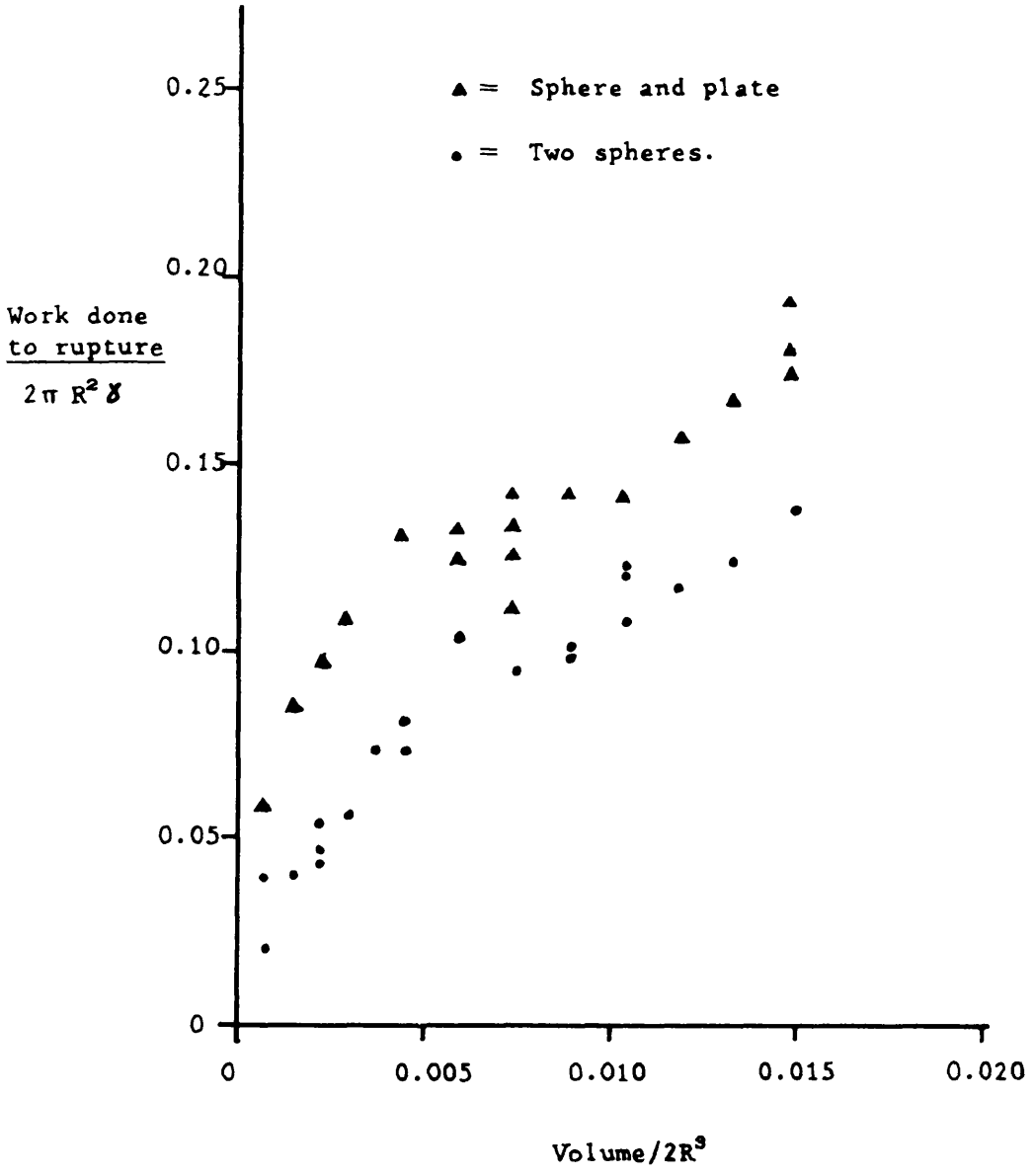

FIG. 22. Variation of the work needed to rupture the bridge with volume for liquid bridges between two spheres and a sphere and a plate.

8. The bridge rupture distances for different volumes of liquid are shown in Fig. 23, and the maximum sphere centre separation that can sustain a bridge is about 1.16 diameters for the bridge volumes considered here. This gives some idea of the near neighbours that can be spanned by bridges of liquid in a random packing of spheres.

For a small fixed sphere separation a bridge will increase in strength as liquid is added. If, however, the spheres were in contact, then the bridge strength would be almost unchanged with increasing liquid. Thus, we can see that near neighbours could cause an increase in the tensile strength of a bed of wet granular material for an increase in moisture content.

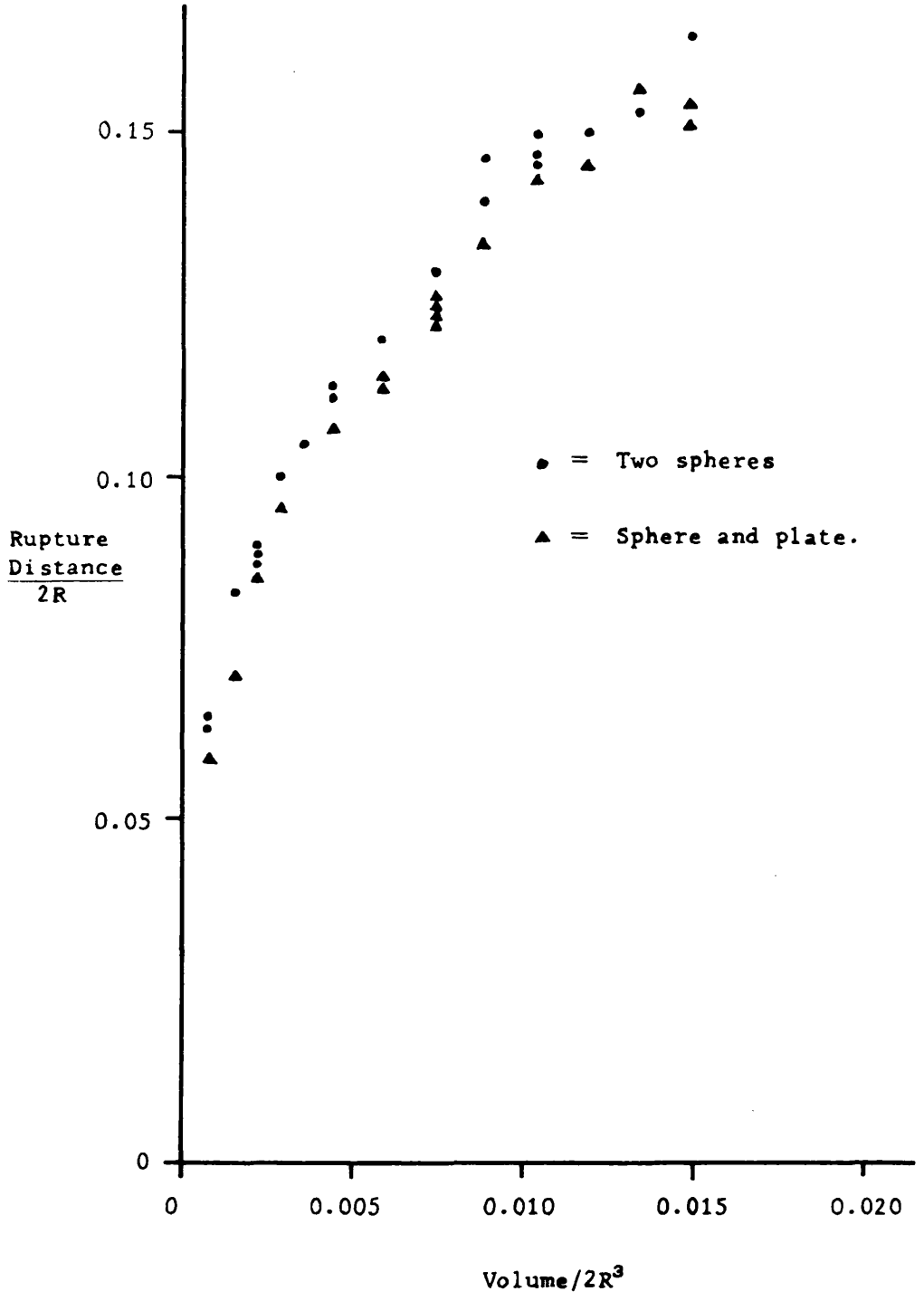

FIG. 23. Variation of Rupture distance with volume for liquid bridges between two spheres and between a sphere and a plate.

REFERENCES

(1) An essay on the cohesion of fluids.
T. Young. Phil. Trans. Pt. 1, 65, (1804).

(2) Mechanique Céleste. Laplace. Supplement to Book 10 (1806).

(3) Capillary action. J.C. Maxwell. Encyclopaedia Britannica.
9th Ed. Vol. 5, 1876.

(4) Bubbles and the forces which mould them.
C. V. Boys. Reprinted by Heinemann. 1960.

(5) The application of Elliptic functions. A.G. Greenhill.
p.98. First published 1892. Reprinted by Dover Publications.
N.Y. 1959.

(6) Studies on the physical properties of soils II.
W. B. Haines. J. Agric. Sci. 15, 529, (1925).

(7) On the capillary forces in an ideal soil.
Correction of formulae given by W.B. Haines.
R. A. Fisher. J.Agric. Sci. 16, 492, (1926).

(8) The moisture retention properties of fine coal. Part I.
C. C. Harris and H. G. Smith, Proceedings of the second
symposium on coal preparation. Leeds. 1957.

(9) Interstitial water of oil bearing sands and sandstones.
W. von Engelhardt. Proceedings of the Fourth World
Petroleum Congress. 1, c, 399, (1955).

(10) Studies of capillary condensation of vapours in highly
dispersed systems. Part 1. Calculation of capillary
condensation in the vicinity of points of contact of
spherical particles. V. Radushkevich. Ivz. Akad. Nauk SSSR.
Otdel Khim. Nauk. 1952. 1008.
English translation. Bull. Acad. Sci. USSR. Div. Chem. Sci.
1952, 885.

(11) The general properties of matter. F. H. Newman and V.H.L. Searle.
Edward Arnold and Co. London. 1951.

(12) Capillary retention of liquids in assemblages of homogeneous
spheres. W.O. Smith, P.D. Foote and P. F. Busang.
Phys. Rev. 36, 524. (1930).

(13) Capillary rise in sands of uniform spherical grains. W.O. Smith, P.D. Foote and P.F. Busang. Physics 1, 18, (1931).

(14) The final distribution of retained liquid in an ideal uniform soil. W.O. Smith. Physics 4, 425, (1933).

(15) Studies on the physical properties of soils. IV. A further contribution to the theory of capillary phenomena in soil. W.B. Haines. J. Agric. Sci. 17, 264, (1927).

(16) Volumes and surface areas of pendular rings. W. Rose. J. App. Phys. 29, 687, (1958).

(17) Studies of waterflood performance 1. Causes and character of residual oil. W. Rose. Illinois State Geol. Survey Bull. 80, 147, (1957).

(18) Fluid flow in petroleum reservoirs. 1. The Kozeny Paradox. W. Rose. Illinois State Geol. Survey Circ. 236 (1957).

(19) Effect of surface tension and contact angle on the settling of slurries. J. Woodrow. A.E.R.E. Report ED/M. 13 (1954).

(20) Forces between slurry particles due to surface tension. J. Woodrow, H. Chilton and R. I. Hawes. Nuclear Energy. Part B. Reactor Technology 1, 229, (1961).

(21) The penetration of mercury and capillary condensation in packed spheres. S. Kruyer. Trans. Farad. Soc. 54, 1758. (1958).

(22) Properties of capillary held liquids. P.C. Carman. J. Phys. Chem. 57, 56, (1953).

(23) Capillary condensation phenomenon in sorption of vapours on non-porous powders. I. Higuti and H. Utsugi. Sci. Repts. Tohoku University. 1st Series. 36, 27, (1952).

(24) Mercury porosimetry - Breakthrough pressure for penetration between packed spheres. R.P. Mayer and R.A. Stowe. J. Colloid Sci. 20, 893, (1965).

(25) Capillary condensation in contact zones between non-porous particles of a powder. I. Higuti and H. Utsugi. J. Chem. Phys. 20, 1180, (1952).

(26) Basic studies of coal flow : Surface tension forces in wet powders. J.F. Carr. C.E.G.B. S.W. Region. Research Memo No.14. (1964).

(27) Discussion of "The influence of the wetting of coal underground for dust suppression on prescreening and dedusting in coal preparation" by K. Thein (Paper AV2). W. Batel. Proceedings of The Second International Coal Preparation Congress. Essen. 1954. Page 43.

(28) The behaviour of granular materials during sieving. W. Batel. The Refractories Journal. No.8, 1955, 468.

(29) The liquid layer between a sphere and a plane surface. N.L. Cross and R.G. Picknett. Trans. Farad. Soc. 484, 846, (1963).

(30) Capillary properties of some model pore systems. J.M. Haynes. Ph.D. Thesis. Bristol. March 1965.

(31) Particle adhesion in the presence of a liquid film. N.L. Cross and R. G. Picknett. Int. Conf. on Mechanism of Corrosion by Fuel Impurities. C.E.G.B. Marchwood Eng. Labs. England 1963.

(32) The construction of a quartz microgram balance. H.M. El-Badry and C.L. Wilson. Rept. of Symposium on microbalances. Royal Inst. Chem. 1959. p.36.

(33) The rate of evaporation of droplets. II. The influence of changes of temperature and of the surrounding gas on the rate of evaporation of drops of di-n-butyl phthalate. J. Birks and R.S. Bradley. Proc. Roy. Soc. 198A, 226, (1949).

(34) Adhesion of solids and the effect of surface films. J. S. McFarlane and D. Tabor. Proc. Roy. Soc. 202A, 224, (1950).

(35) Die Kapillarität der Boden. J. Versluys. Intern. Mitt. Bodenk. 7, 117, (1917).

(36) Statique experimentale et théorique des liquides soumis aux seules forces moleculaires. J.A.F. Plateau. Paris 1873. English translation in Smithsonian Institute Annual Reports. 1863, 1864, 1865, 1866.

(37) The micrometer syringe. J.W. Trevan. Biochem. J. 19, 1111, (1925).

(38) Density of di-butyl phthalate. A.I. Kemppinen and N.A. Gokcen. J. Phys. Chem. 60, 126, (1956).

(39) Tables of physical and chemical constants.
G.W.C. Kaye and T. H. Laby. Longmans. 1956.

(40) The determination of surface tension (free surface energy) and the weight of falling drops: The surface tension of water and benzene by the capillary height method. W.D. Harkins and F. E. Brown. J. Am. Chem. Soc. 41, 499, (1919).

(41) A textbook of physics. Properties of matter.
J. H. Poynting and J. J. Thomson. London. 1907. p.154.

(42) A double capillary method for the measurement of interfacial tension. G. L. Mack and F. E. Bartell. J. Am. Chem. Soc. 54, 936, (1932).

(43) A device for the determination of the surface tension of small amounts of liquid. S. Natelson and A. H. Pearl.
J. Am. Chem. Soc. 57, 1520, (1935).

(44) Méthode pour la determination de la tension superficielle.
Sentis. J. de Physique. 6, 571, (1887).

(45) General properties of matter. C. J. Smith.
Edward Arnold. London. 1960. p. 493.

(46) Surface tension and the spreading of liquids.
R.S. Burdon. Cambridge Monographs on Physics. 1949. p.50.

(47) Surface tension at the limit of two layers.
G.N. Antonow. J. Russ. Phys. Chem. Soc. 93, 342, (1907).
Reprinted J. Chim. Phys. 5, 372, (1907).

(48) Experimental study of the shape and weight of stationary and moving drops. Ph-A. Guye and F.-Louis Perrot.
Arch. Sci. Phys. Nat. (Geneva). 15, 178, (1903).

(49) A new apparatus for measuring surface tension.
P. Lecomte du Noüy. J. Gen. Physiol. 1. 521, (1919).

(50) An investigation into the effect of additives on the flowability of damp coal. D.M. Walker. C.E.G.B. S.W. Region Research and Development Rept. No. 9. 1962.

(51) Associate minimal surfaces. J.K. Whittemore.
Am. J. Maths. 40, 87, (1918).

(52) Solution of the problem of Plateau. J. Douglas. Trans. Am. Math. Soc. 33, 263, (1931).

(53) Green's function and the problem of Plateau. J. Douglas. Am. J. Maths. 61, 545, (1939).

(54) Packing of homogeneous spheres. W. O. Smith, P. F. Foote and P. F. Busang. Phys. Rev. 34, 1271, (1929).

(55) J. M. Haynes. Private communication.

CHAPTER THREE

MEASUREMENT OF CONTACT ANGLES

INTRODUCTION

1. Definitions
2. The Young equation
3. Hysteresis of contact angle
4. Dynamic variations

METHODS OF MEASUREMENT

1. Tilting plate
2. Bubble at surface
3. Drop at a surface
4. Micromethods
5. Sliding drop
6. Suction potential
7. Modified suction potential

DESCRIPTION OF THE APPARATUS

1. Properties of the membrane
2. Constant head device
3. Manometer
4. Burette
5. Formation of a sample bed
6. Model hopper

EXPERIMENTAL PROCEDURE

1. Filling sample funnel with water
2. Experimental formation of the bed
3. Details of a run
4. Measurement of surface tension

RESULTS

1. Pressure/volume relationships
2. Not step-functions
3. Importance of a compact bed
4. Time of equilibration
5. Interpretation

INTRODUCTION

1. When a drop of liquid is placed upon a solid surface, it either spreads out flat or stops spreading whilst still convex. At equilibrium the liquid is observed to meet the surface at a particular angle, and it is this angle between the solid surface and the liquid surface that is termed the "contact angle" (Fig. 1)[1].

If a drop of liquid is placed on a plate and the surface tilted until the drop moves, then the contact angle at the advancing edge is always greater than the contact angle at the receding edge. (Fig. 2). This effect is called the hysteresis of contact angle. The angle between the liquid and the unwetted solid is called the "advancing contact angle" and that between the liquid and the wetted solid the "receding contact angle". These two values represent the limits of the angle for the particular solid and liquid.

2. The basic equation connecting surface tensions and contact angles is the Young[2] Equation which can be written

$$\gamma_{SV} - \gamma_{SL} = \gamma_{LV} \cos\theta \qquad \ldots\ldots\ldots\ldots\ldots\ldots (1)$$

It can be derived from the equilibrium shown in Fig. 3. There has been a certain amount of controversy about the reliability of the Young equation[1] but since there seems to be no conclusive proof or any alternative equation, its continuing use seems inevitable. Of the parameters in the Young equation, only the contact angle θ and the liquid/vapour surface tension (γ_{LV}) can be measured directly. The interfacial tension between solid and liquid (γ_{SL}) and solid and vapour (γ_{SV}) are inferred quantities.

3. That a contact angle does exist and has two limiting values is an experimental fact. The hysteresis has been explained in several ways, although none of the explanations cover all cases.

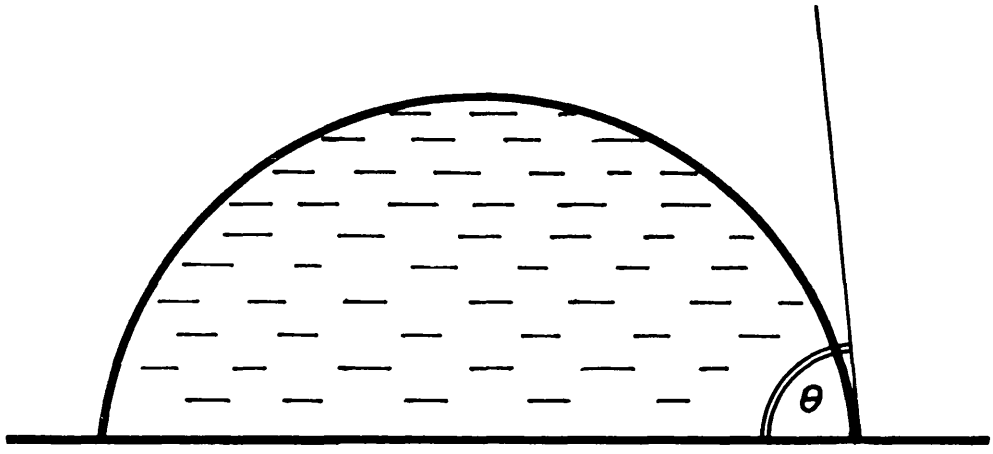

FIG. 1. The contact angle (θ). A sessile drop on a plate.

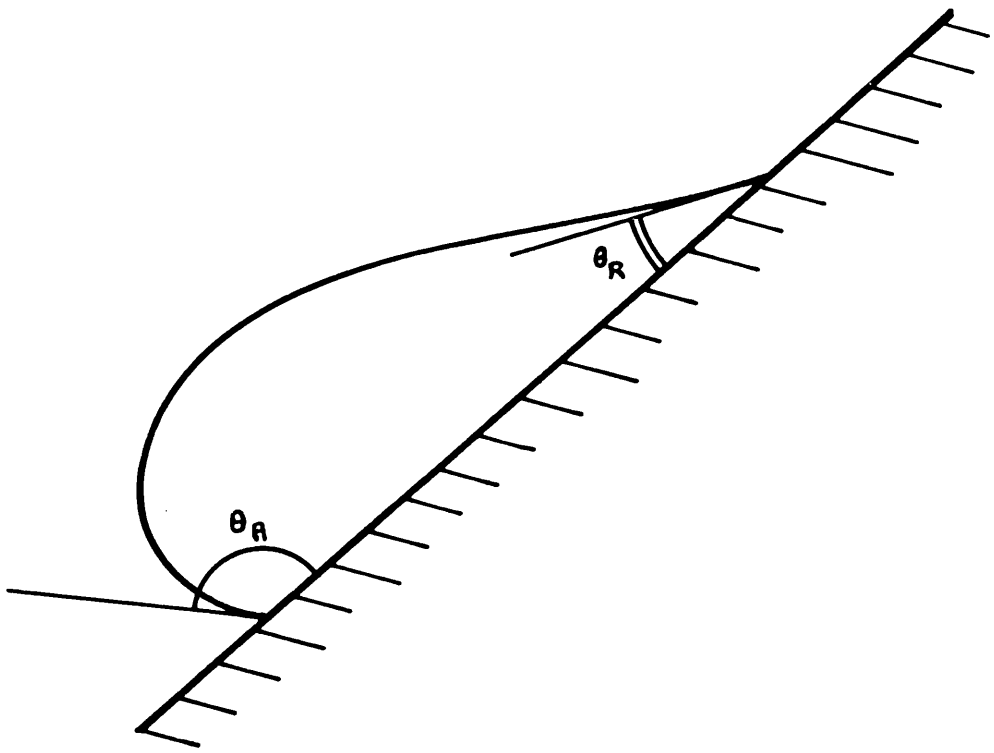

FIG. 2. Drop on a sloping plate showing advancing (θ_A) and receding (θ_R) contact angles.

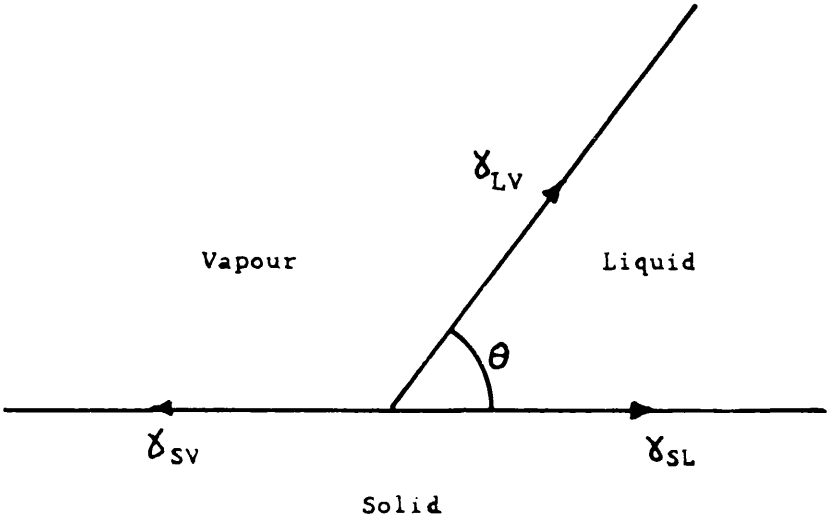

FIG. 3. Equilibrium at a solid surface. γ is an interfacial tension. The subscripts indicate between which two phases.

Surface roughness[3] obviously plays a part as is known in textile waterproofing and more elegantly in the insect kingdom where water repellent hairs and thin fibres give insects unexpected properties[4].

4. Contact angles vary dynamically as well as the static advancing and receding values. The receding angle is reduced when the liquid is moving and the advancing angle is increased. The initial study of this phenomenon was by Ablett[15], who observed the contact angle at the interface between a rotating wax drum and a bath of water. The liquid level was adjusted until the surface appeared plane at the interface with the drum. The angle could then be obtained from geometry. This is a modification of the tilting plate method. The work has been followed by Rose et al[16, 17], who postulated equations for rate dependence of contact angles. They studied the flow of liquids in and out of capillary tubes.

METHODS OF MEASUREMENT

1. There are several standard methods of measuring contact angles. As they are rather irreproducible sophisticated apparatus is rarely needed. Possibly the simplest method uses a plate of the solid, partially immersed in the liquid. This plate is rotated until optical tests show that the liquid and solid meet on one side in a sharp line without curvature[5], The angle between the plate and the liquid is measured with a protractor. Whether this method can measure advancing and receding angles is uncertain, but the major disadvantage is that a flat uniform surface is required. If a spherical surface is available the contact angle may be measured with a method similar to Yarnold[6] which measures the apparent weight of the sphere as it is raised and lowered through the liquid surface.

2. The bubble method of contact angle determination is popular in work concerning theflotation of minerals[7,8]. In this case a

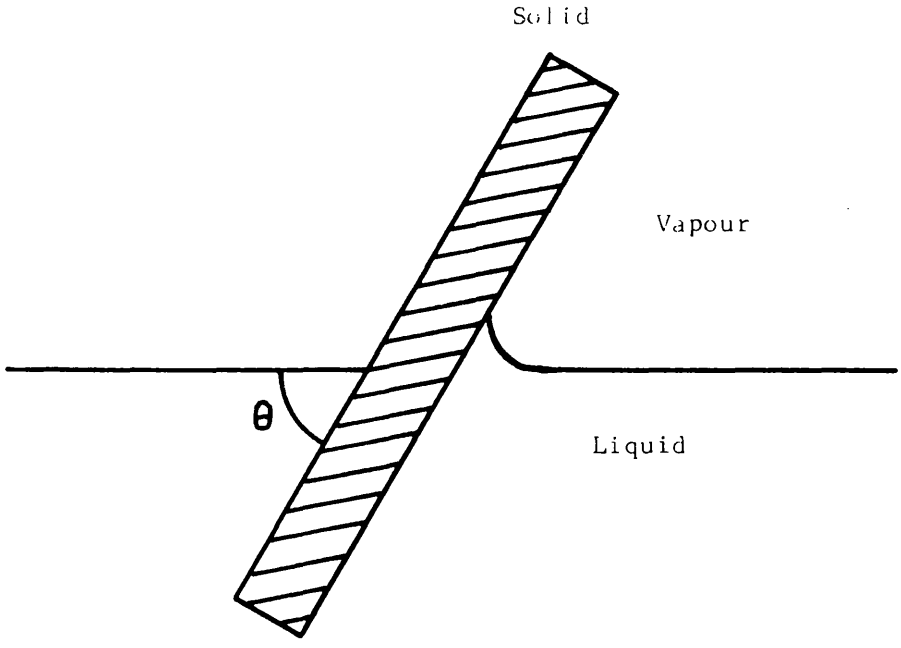

FIG. 4. Tilting plate method.

plane mineral surface is immersed in liquid and a small bubble pressed against the surface. The bubble should adhere to the surface and after allowing time for equilibrium the contact angle is observed directly. The angle observed is somewhere between the advancing and receding angles, but is often termed the "equilibrium contact angle".

3. Contact angles of sessile drops on plane surfaces can be measured directly[10,11], or calculated by assuming very small drops to be spherical. A more accurate method is to calculate the contact angle using the tables of Bashforth and Adams[12], although contact angles are rarely reproducible enough for this to be necessary.

4. Eissler[13] used a micro-method of inserting small particles through the liquid surface of sessile drops and observing the contact angle directly with a high powered microscope (X300). He was troubled by the illumination system in that he observed his water sessile drops evaporating unless special care was taken to saturate the atmosphere with water vapour.

5. Olsen et al.[14] analysed a sliding liquid drop assuming that the entire initial resistance to sliding was at the rear of the drop. This gave a method of determining the receding contact angle.

6. Another method of measuring contact angles which does not have a particularly secure theoretical basis, but which does have the advantage of not requiring a regular solid surface is the so-called suction potential method. This measures the pressure required to displace liquid from a packed bed of solid. By making certain assumptions about the bed, it is possible to derive a contact angle. The method was originated by Bartell and Osterhof[18] and has been used and studied by many workers since. The initial simplification

is that a bed of porous material can be considered as a mass of independent, equidimensional capillary tubes, running parallel from the top of the bed to the bottom. If the tubes are initially filled with liquid and an increasing suction pressure applied to the bottom of the capillaries, then there will come a critical pressure when the menisci enter the capillaries and the capillaries drain. This will be evident as liquid will be removed from the bottom of the bed.

Applying the simple capillary rise equation

$$P = \frac{2\ \gamma_{LV}\ \cos\theta}{R} \qquad \ldots\ldots\ldots\ldots\ldots\ldots\ldots\ (2)$$

where P is the suction pressure

γ_{LV} the liquid/vapour surface tension

R the radius of the capillary

θ the contact angle.

The suction pressure can be measured directly and the surface tension can be obtained in a separate experiment. The radius of the capillaries cannot be obtained in such a direct manner because their existence is a gross simplification. Bartell[18] obtained "R" by using the flow of liquid through the bed and also by capillary rise of a perfectly wetting liquid. This second method involves packing two identical beds - one to be used to measure "cos θ" and the other one to determine "R". Bailey and Gray[19] used a similar method of packing two identical beds, one filled with the test liquid and the other filled with a perfectly wetting liquid. They measured the suction pressure to draw liquid from each, which enabled "R" and "cos θ" to be determined.

The more complex case of beds of differing porosity containing different liquids has been reported by Harris, Jowett and Morrow[28] and an equation linking these effects with contact angle given.

7. In the particular case of oil spreading on wet coal the system can be simplified to only one bed and two interfaces pulled through successively. Suppose a bed of wet coal is saturated with water and a thick layer of oil poured on the water surface. As suction is applied to the bottom of the bed there will come a pressure when the oil/water interface is drawn into the bed. This interface will continue to move until the oil/air interface meets the bed surface. A further increase in suction is required to draw the oil/air interface into the bed. Two equations can be written

$$P_{o/w} = \frac{2\gamma_{o/w}\cos\theta_{o/w}}{R} \qquad \ldots\ldots\ldots\ldots (3)$$

$$P_{o/A} = \frac{2\gamma_{o/A}\cos\theta_{o/A}}{R} \qquad \ldots\ldots\ldots\ldots (4)$$

where $P_{o/w}$ is the suction pressure of the oil/water interface.

$P_{o/A}$ is the suction pressure of the oil/air interface.

$\gamma_{o/w}$ is the surface tension of the oil/water interface.

$\gamma_{o/A}$ is the surface tension of the oil/air interface.

$\cos\theta_{o/w}$ is the advancing oil/water contact angle.

$\cos\theta_{o/A}$ is the receding oil/air contact angle.

Eliminating R from 3 and 4 gives

$$\frac{\cos\theta_{o/w}}{\cos\theta_{o/A}} = \frac{P_{o/w}}{P_{o/A}} \cdot \frac{\gamma_{o/A}}{\gamma_{o/w}} \qquad \ldots\ldots\ldots\ldots (5)$$

$P_{o/w}$, $\gamma_{o/A}$, $P_{o/A}$, $\gamma_{o/w}$ can all be determined experimentally. $\theta_{o/A}$, the receding angle of oil against coal may be taken as zero, and so $\theta_{o/w}$ can be determined.

The method has the advantage of measuring an overall contact angle, averaged over the surface of every particle - something of particular importance when coal or some other non-homogeneous surface is being considered.

DESCRIPTION OF THE APPARATUS

An apparatus was constructed (Fig. 5) following the design of Gray[19] which is a modification of Haines[20] original suction apparatus.

1. An essential part of the apparatus is the fine membrane which will allow moisture to pass through, but will not pass air because of surface tension forces. In older devices filter papers or porcelain discs were used, but fine sintered glass membranes[21, 22] have superseded these. A sintered glass membrane has to be strong enough to support the forces developed by the partial vacuum applied to the system as well as having a reasonable permeability. The No. 5 sintered glass membranes have a pore size of approximately two microns, but if made thick enough to support themselves would have a very large resistance to liquid flow. Consequently a very thin layer of No. 5 sintered glass is made on top of a No. 3 disc and the pair termed "5 on 3". Morrow[22] performed some experiments on the water drained from various membranes with pressure, and showed conclusively that sintered glass was the best. A "5 on 3" sintered glass disc Buchner funnel was used as a sample cell in this apparatus.

2. A system for applying a constant pressure to the lower half of the membrane is required and a form of Mariotte bottle was devised for this purpose. In essence, it consisted of a deep reservoir of water with a tube open to atmospheric pressure through a seal in the top of the airtight lid on the reservoir. This tube could be raised or lowered to different depths in the water. If a vacuum was developed in the chamber above the water in the reservoir, air was drawn down the tube and bubbled out from the bottom. This provided a constant pressure and as the pumping speed was adjustable with a needle valve the bubbling rate could be set at any desired value. Some difficulty

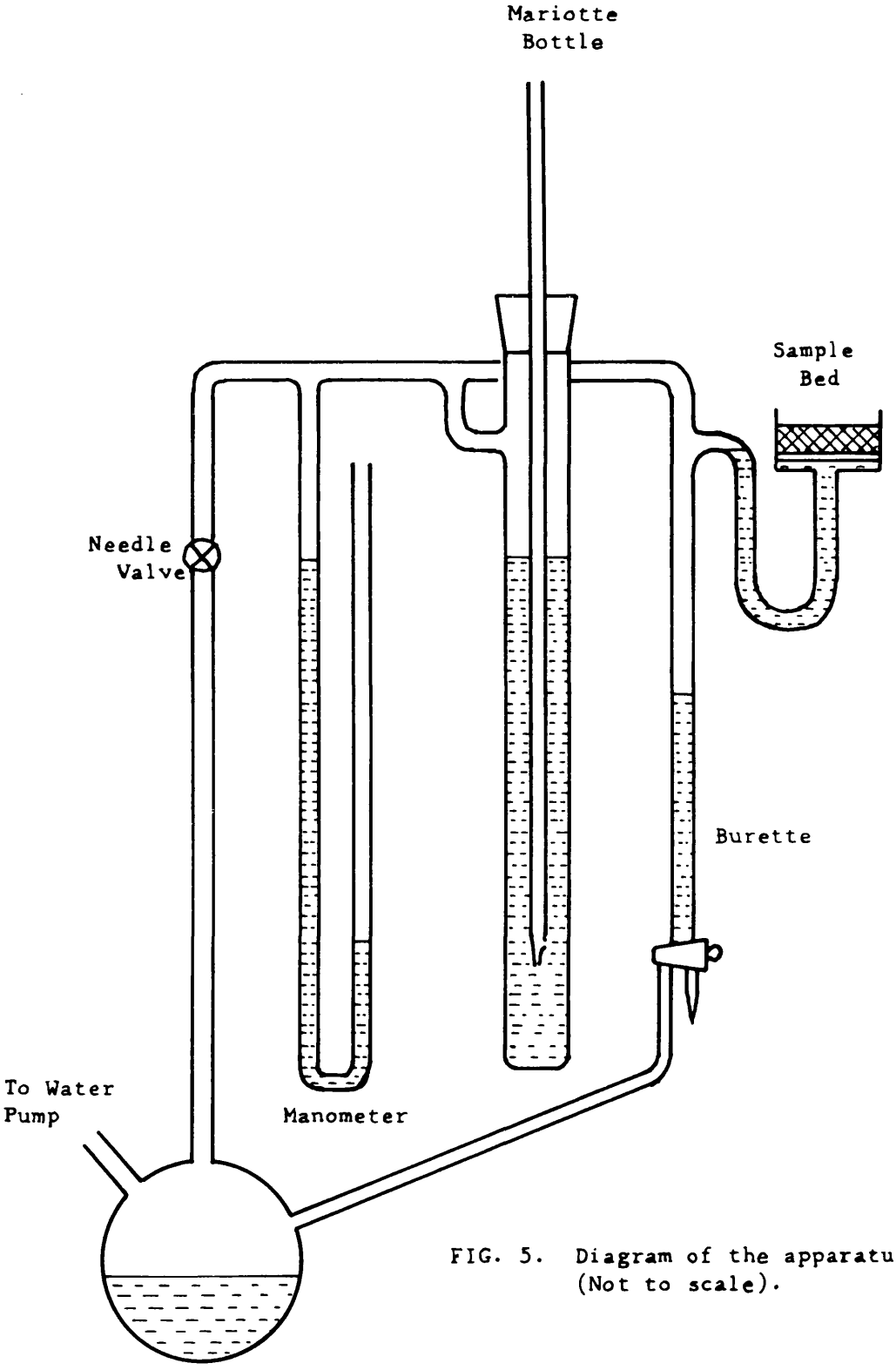

FIG. 5. Diagram of the apparatus (Not to scale).

was experienced in arranging that the pressure did not fluctuate as bubbles were drawn from the bottom of the adjustable tube. Some pressure fluctuation is inevitable as the system is similar to the bubble pressure method[23] of surface tension determination. However, by modifications to the base of the bubbler, mainly by trial and error, a shape was devised which gave a pressure fluctuation of only 1 mm water. This is shown diagramatically in Fig. 6. The seal where the adjustable tube left the bottle contained two "O" ring seals and is shown in Fig. 7.

3. The manometer was of conventional design, containing water, and had a metre mirror scale behind it, enabling pressures to be determined to 1 mm. water.

4. The burette had a calibrated volume of 50 ccs. There was a two-way tap at the bottom which allowed the burette to be drained even when there was a partial vacuum in the system. This was a useful feature when the bed was being packed and excess liquid had to be drained. Liquid drawn from the bottom of the sinter travelled down round the U tube and finally drained over into the burette. Trouble was initially experienced with large drops forming at the lip where the water drained over. This was partially overcome by reducing the diameter of the tube at this place. However, it was eventually found necessary to introduce a small plug of thread wound on a wire former to prevent drops forming. Also passing steam over this point for 48 hours removed all traces of grease which may have aggravated the trouble. No further difficulty was experienced and drained liquid rose smoothly in the burette.

5. Gray[19] drew attention to the difficulties of forming the sample bed. For good results it has to have a uniform packing density, yet must be strong enough not to compress under the suction pressure

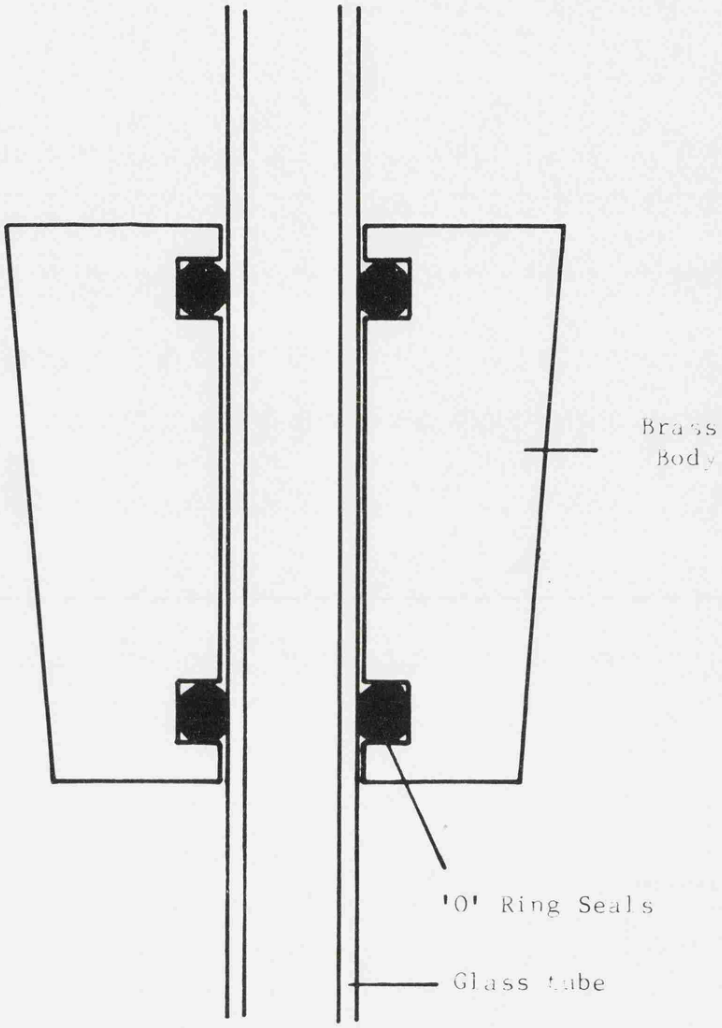

FIG. 7. Diagram of top seal of Mariotte bottle.

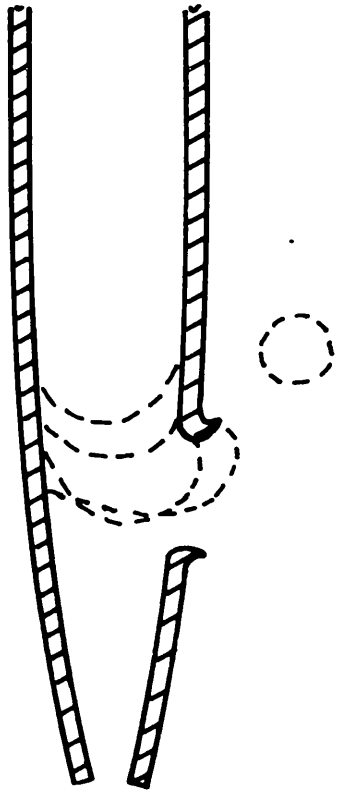

FIG. 6. Diagram of the bubbler in the Mariotte bottle.

and change its pore size distribution. Bartell and Osterhof[18] compressed their sample under high pressure, but Brown and Hawksley[24] found from a study of ball bearing packings that a packing that has been deformed is never uniform. Furthermore, they showed that a loose packing of balls was more uniform than one which had been shaken to maximum density. At maximum density there are regions of loose packing and tight packing. Kolbuszewski[25] investigated the conditions which lead to loose or dense deposits of sand and found that the packing density depended on the rate of deposition and the velocity of the deposited grains. His work is not strictly applicable to coal due to the differing densities of sand and coal, but the methods are generally applicable. Roscoe[26] explained that a uniform packing is only formed when a whole mass of particles is poured rapidly. Any break or irregularity in the pouring rate leaves discontinuities which can be observed as different densities on x-ray photographs.

The bed of coal in the sinter funnel was formed by releasing a slurry of coal particles from a small hopper. This hopper was stirred continually, even whilst the slurry was being released, and the motor was allowed to continue running to gently vibrate the bed to a maximum density. Coal particles nearly float in water, so this vibration should not have caused discontinuities. Furthermore, as the lower part of the bed settled into position the upper part of the bed was partially fluidised on the water moving upward. The vibration thus helped to lay the bed evenly and fairly densely. Without vibration a very porous bed was formed, which collapsed slightly when suction was applied. A graph showing this effect is Fig. 26 .

6. The model hopper is shown diagramatically in Fig. 8. The body of the hopper was machined from solid aluminium, so as to leave no junctions or rough edges. The release mechanism was made of brass

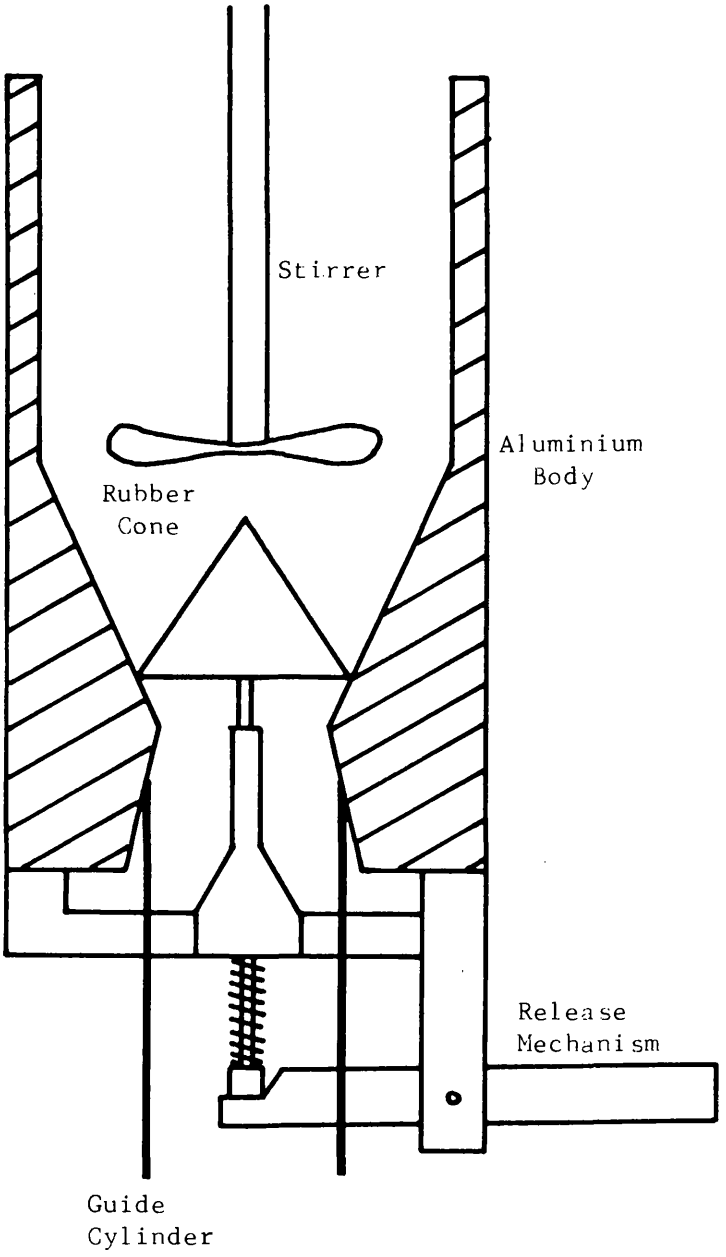

FIG. 8. Diagram of the model hopper.

to reduce the possibility of corrosion. An interesting feature was the rubber cone, which was a watertight seal at the hopper bottom. This cone was machined from a rubber bung which had been frozen in liquid nitrogen. The system was watertight and capable of discharging 50 gms of coal and 100 mls of water in about three seconds. A guide cylinder was necessary to prevent parts of the hopper load missing the bed funnel top.

EXPERIMENTAL PROCEDURE

1. In order to make a measurement of the advancing contact angle of oil against wet coal, the apparatus was checked for leaks and the sample funnel placed in position. It is important that there are no air bubbles between the sinter face and the top of the opposite limb of the U-tube (see Fig. 5), as these will expand when the system is evacuated and cause erroneous readings. With the funnel removed it was possible to fill the U-tube with boiled distilled water until the water was raised in a high meniscus above the glass socket. Similarly, it was possible to fill the inverted funnel. With some practice it was possible to invert the funnel into its proper orientation without allowing air to enter. The funnel could then be placed in position with a continuous water column from the sinter through the U-tube.

2. Details of the preparation of the coal samples are given in Chapter 4, and it will suffice here to say that they were of 50 gms. The 50 gms of coal were added to 100 mls of distilled water, and the mixture either boiled[19] or evacuated to remove air from the bed. The mixture was then added to the top of the model hopper and the stirrer set in motion. After a few seconds, the slurry was released into the sample funnel by raising the cone in the hopper. The stirrer was not switched off so the sample settled under gentle vibration. A suction pressure of about 2 cms water was used to speed up the removal

of excess water and when only a thin layer of water was left, 15 mls of domestic paraffin oil were pipetted on to the surface of the water. The system was allowed to equilibrate when all excess water was drained from the burette and the run could commence.

The pressure was increased in increments of 2 cms water head and at each pressure the volume of water withdrawn was recorded with time. When no more than 0.05 mls were withdrawn in an hour the system was assumed to be in equilibrium and the total volume withdrawn recorded together with the pressure. It often took 24 hours for equilibrium to be reached.

Finally, when further increases in pressure yielded no more water the run was completed, usually at about 40 cms water. The apparatus was stripped and cleaned in preparation for the next run.

4. The interfacial tension between paraffin and water was measured with a du Nuoy tensiometer[27], as it was felt that this would give sufficient accuracy (5%) to be compatible with the results from the suction potential apparatus. With liquids of such a small differential density as paraffin and water the ring pulls the interface up a distance of several millimetres and a little more care then usual is required to obtain consistent results.

The tensiometer was calibrated with distilled water, acetone and benzene.

Results

1. The pressure/volume relationships for several coals are shown in Figs. 11-26, and the ratio of the two steps quoted on the graphs.

2. The steps on each graph were somewhat diffuse, and the "average pressures" were obtained by finding the pressures corresponding to the midpoints between the three "volume" plateaux. Some samples were "weathered" in an oven and further details of this are given in

Chapter 4. It is evident from the results that simple step functions are not obtained. An explanation is to consider the bed to be a mass of cylindrical pores with a pore size distribution. Gray[19] used this model to calculate the pore size distribution from the width and shape of the step.

3. A particular sample (Rhas. Fig. 26) was not compacted properly and it can be seen that the bed became compressed under the reduced pressure and yielded a relatively large volume at the second plateau. The experiment was repeated. (Fig. 18).

4. The equilibration time for each point varied considerably. Fig. 27 is an example of the way in which the volume of liquid removed varied with time for a step increase in pressure from 10 cms water to 12 cms water.

5. The interpretation of these results requires a detailed knowledge of coal and its properties. These are reviewed in Chapter 4 and the present results discussed more fully.

Distilled water

Readings:	76.6	75.8	76.2	75.4
	75.2	76.3	75.9	75.0
	76.0	76.0	75.9	74.7
	76.4	76.2	75.5	74.6
	75.8	75.8	75.5	74.6

The mean of these results is 75.7 $\pm$ 0.3

Kaye & Laby[29] quote a value of 73.5 dynes/cm for water.

Acetone

Readings:	27.0	27.5
	27.0	27.0
	27.0	

The mean of these results is 27.1 $\pm$ 0.1

Kaye & Laby[29] quote a value of 23.7 dynes/cm for acetone.

Benzene

Readings:	32.6	32.0
	31.7	32.0
	31.7	32.0

The mean of these results is 31.9 $\pm$ 0.1

Kaye & Laby[29] quote a value of 28.9 dynes/cm for benzene.

FIG. 9. Calibration of tensiometer.

The correction factor for the tensiometer was 0.890 for surface tensions of about 30 dynes/cm.

Surface tension of paraffin

Readings:	29.2	28.5	29.2
	28.7	28.2	28.7
	28.2	28.4	28.2
	28.3	28.2	28.2

The mean of these readings is 28.5 $\pm$ 0.2

The surface tension of paraffin was found to be 25.4 $\pm$ 0.2 dynes/cm.

Water/paraffin interfacial tension

Readings:	35.5	32.5	35.5
	34.9	35.1	32.5
	34.8	35.2	

The mean of these readings is 35.2 $\pm$ 0.3.

The interfacial tension between water and paraffin is 31.4 $\pm$ 0.3 dynes/cm

FIG. 10. Surface tensions of paraffin and the paraffin/water interface.

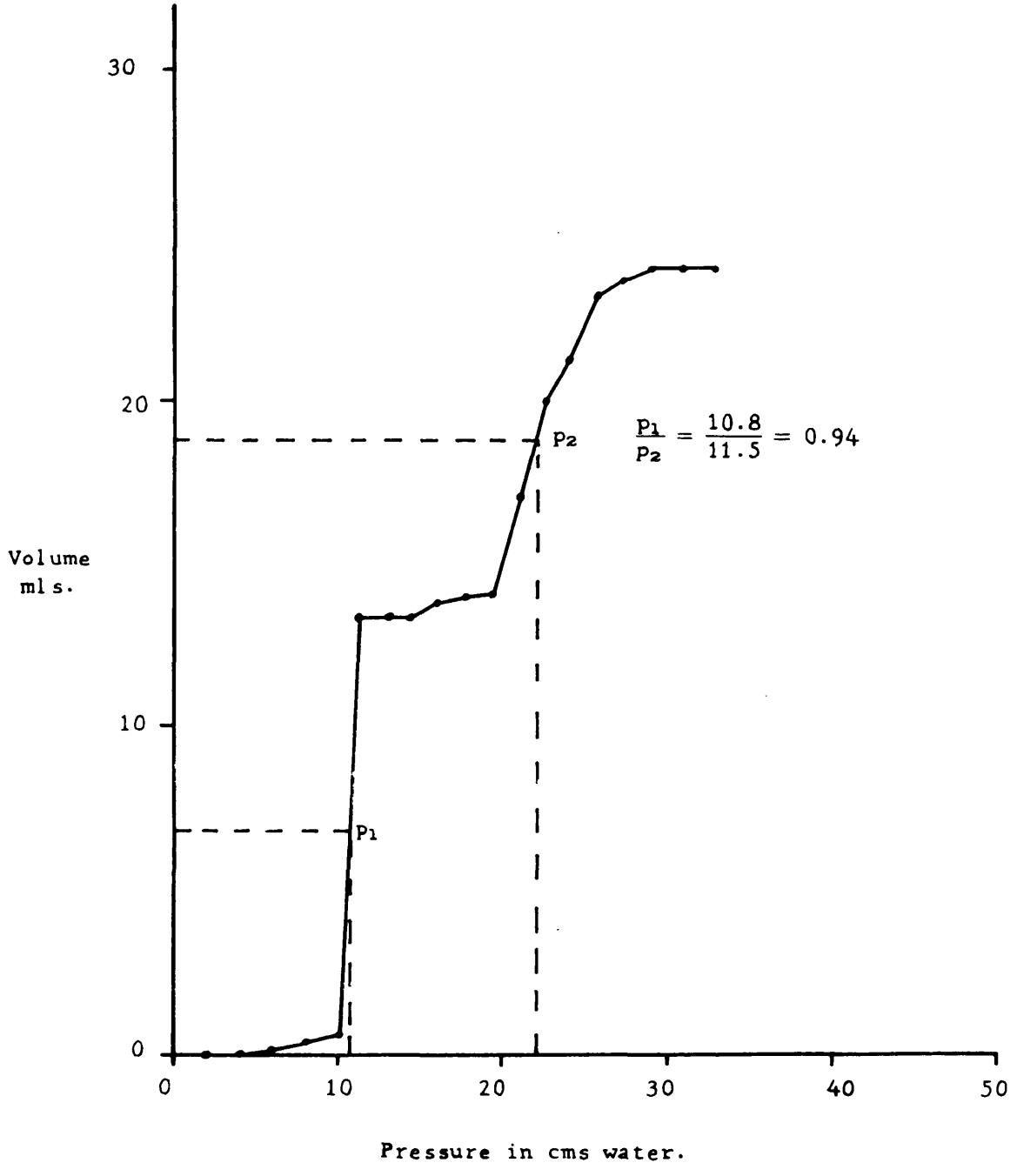

FIG. 11. Pressure/volume relationship for Lady Windsor Fines.

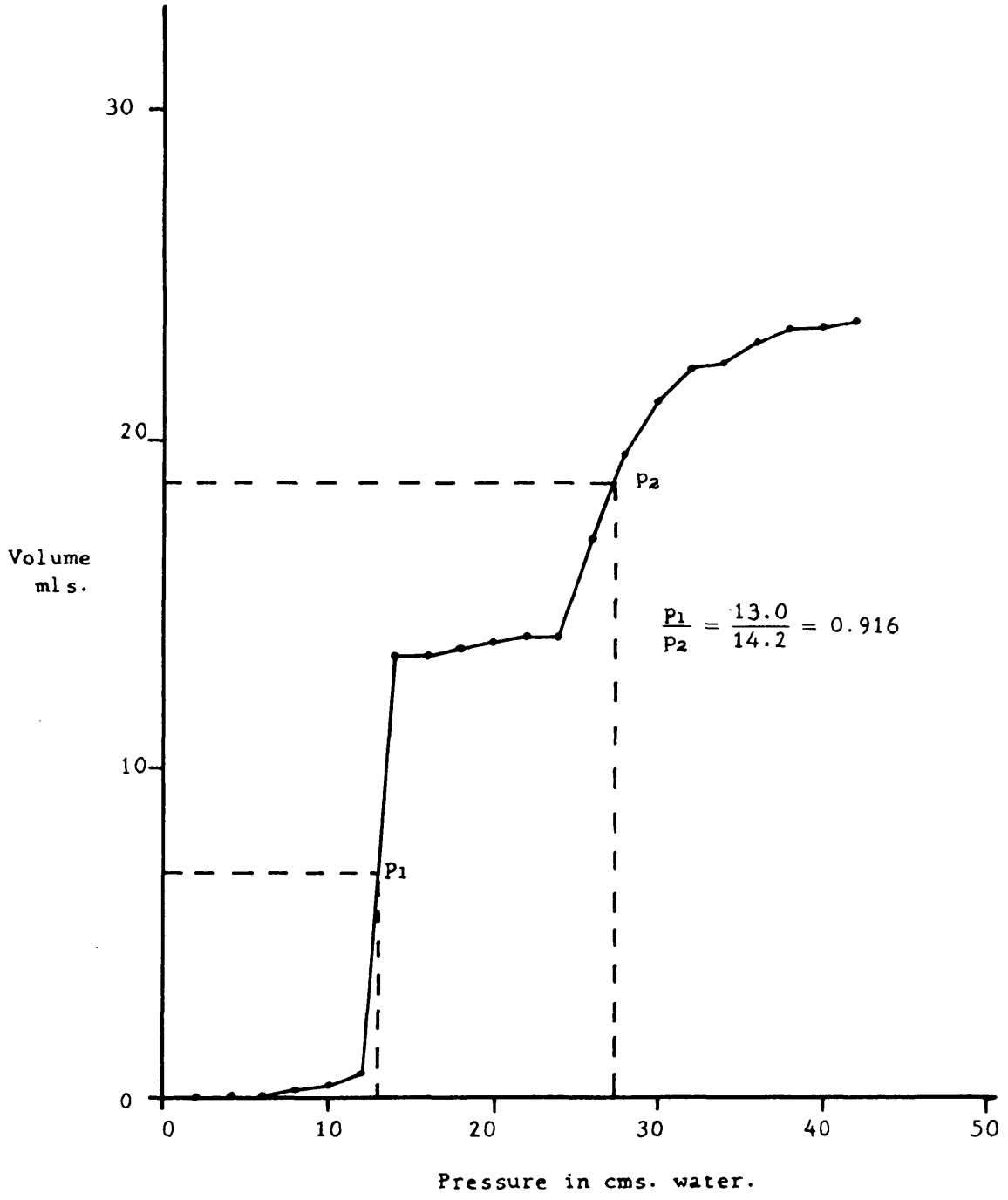

FIG. 12. Pressure/volume relationship for Lady Windsor Fines.

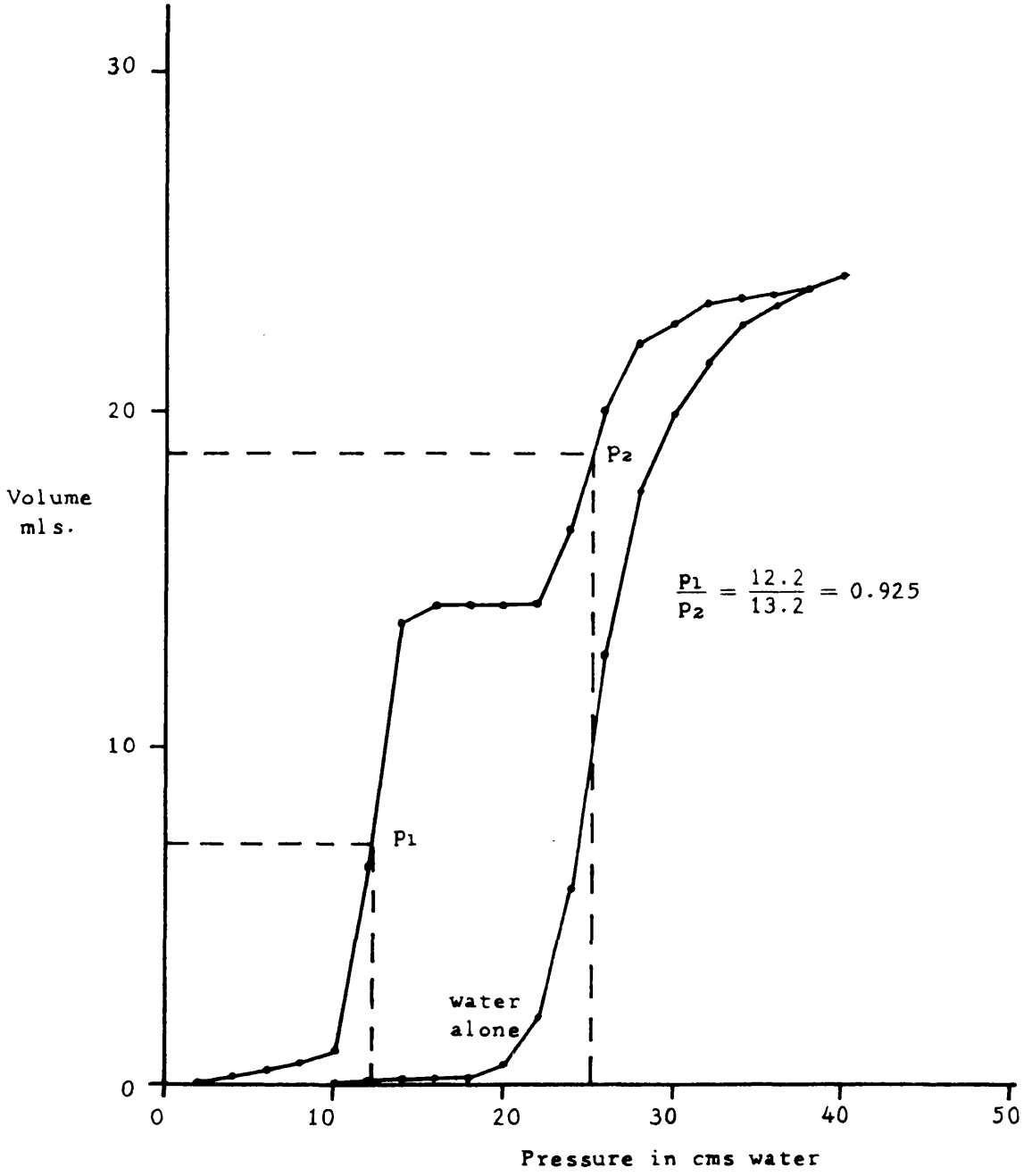

FIG. 13. Pressure/volume relationships for Lady Windsor Fines.

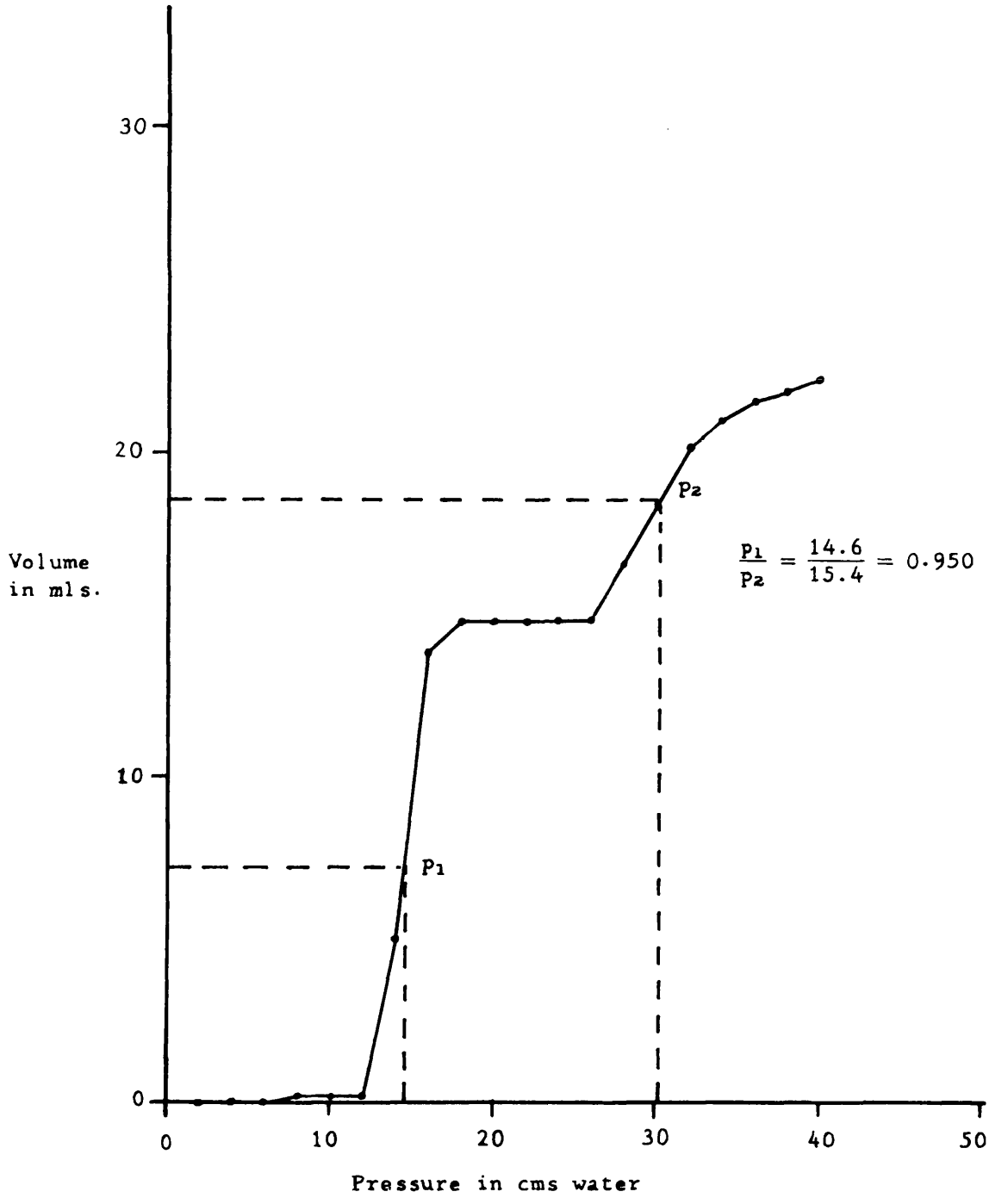

FIG. 14. Pressure/volume relationship for Lady Windsor Fines.

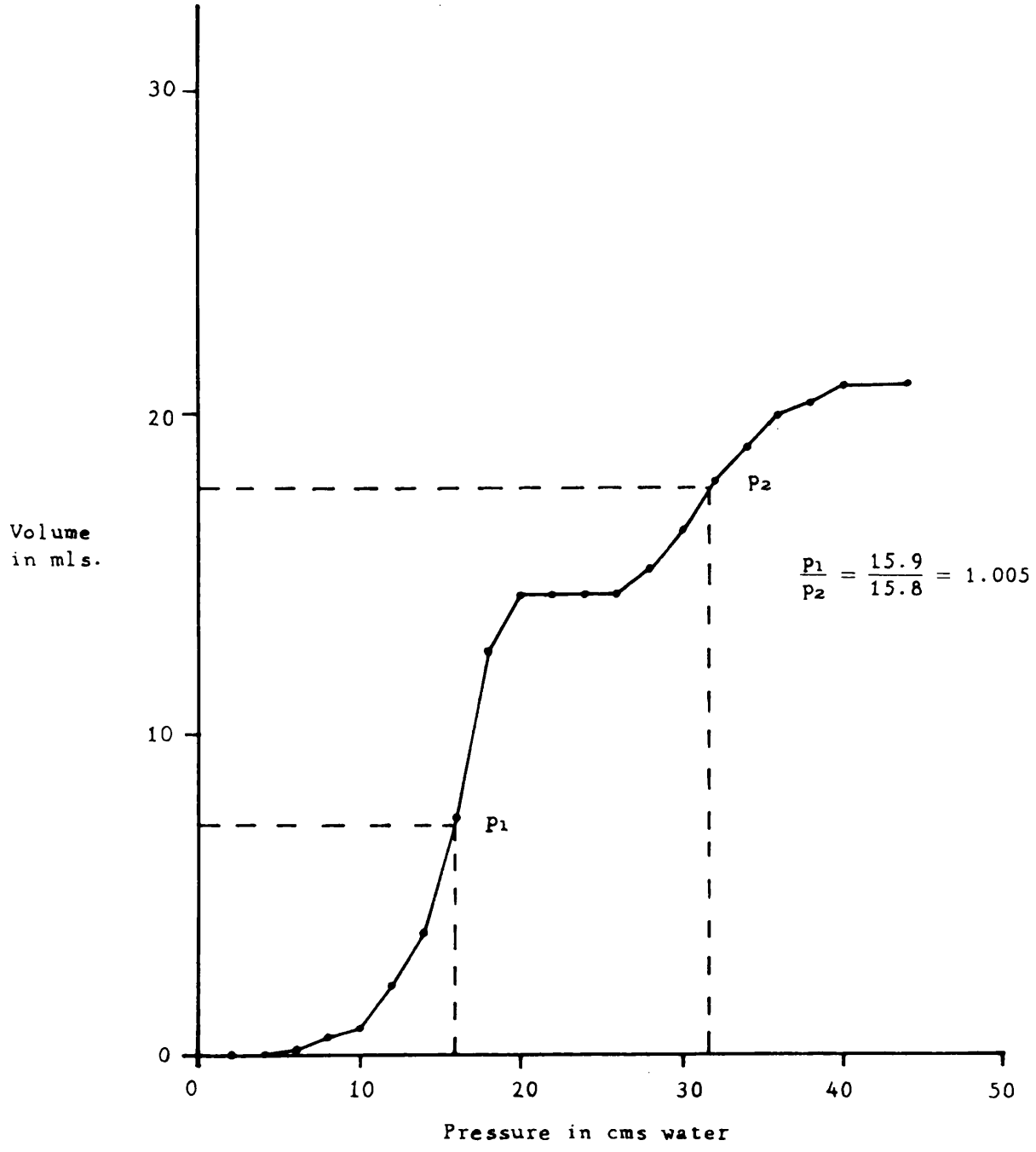

FIG. 15. Pressure/volume relationships for weathered Lady Windsor Fines.

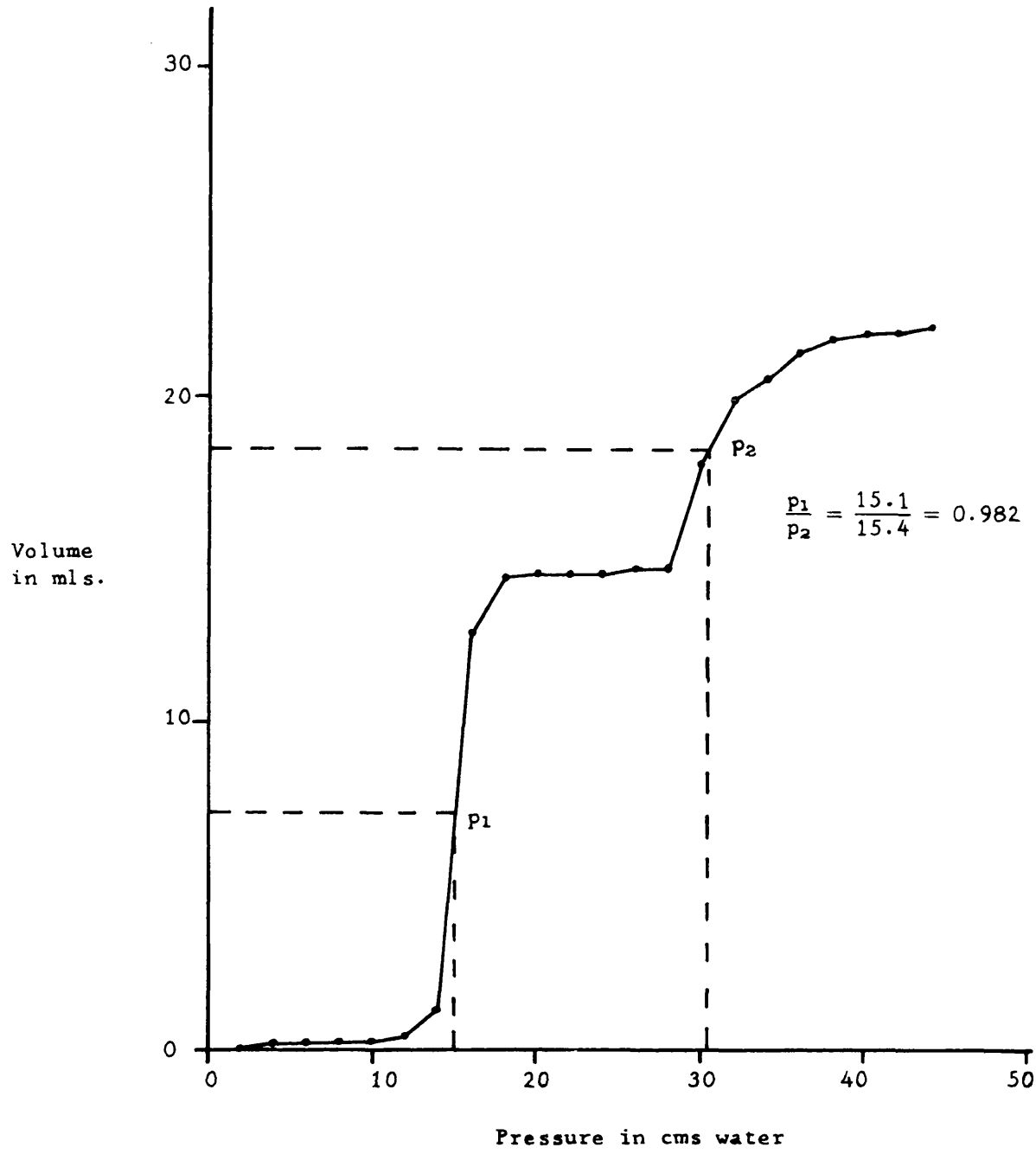

FIG. 16. Pressure/volume relationship for Felinferan Untreated Smalls.

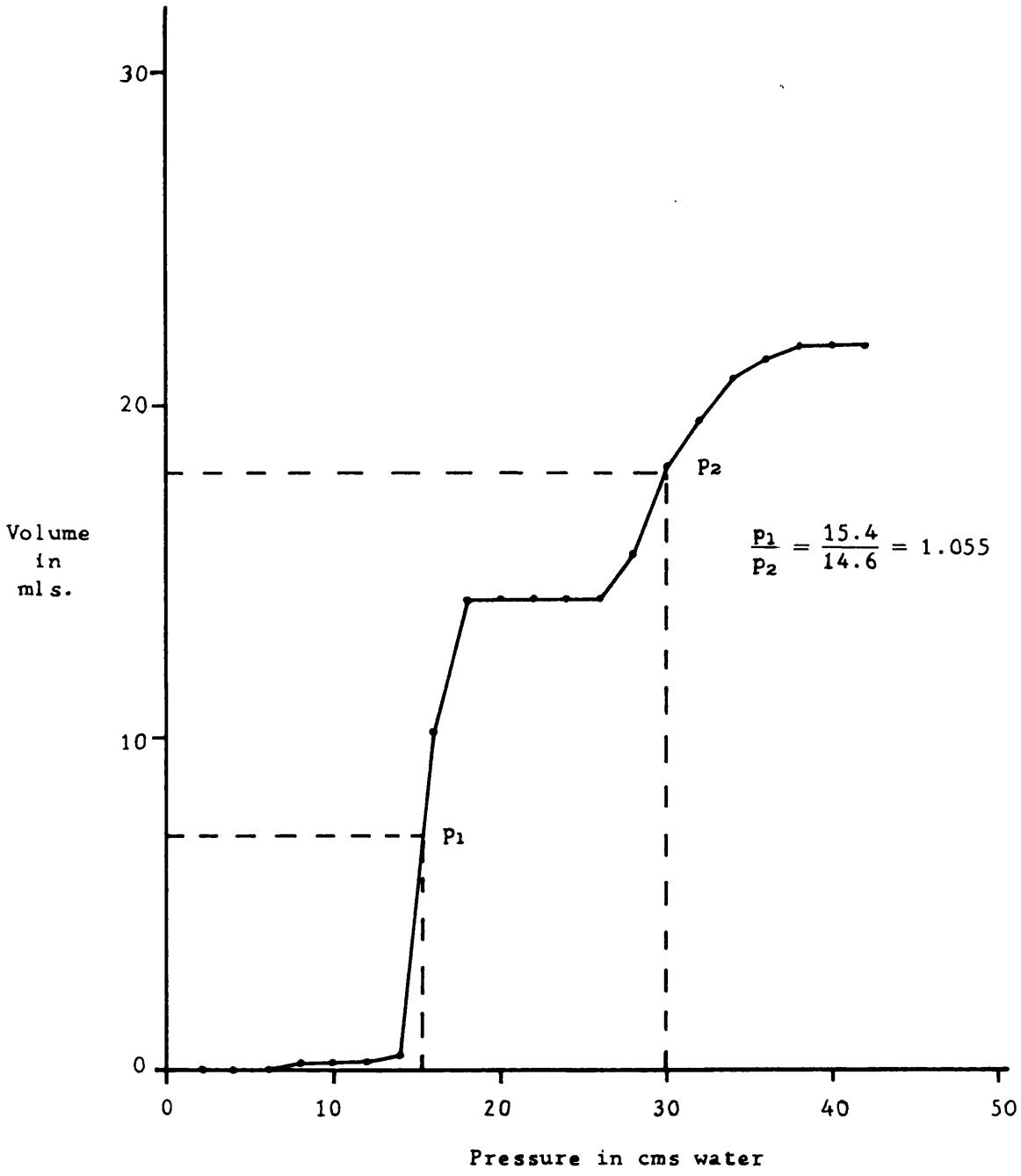

FIG. 17. Pressure/volume relationship for weathered Felinferan Untreated Smalls.

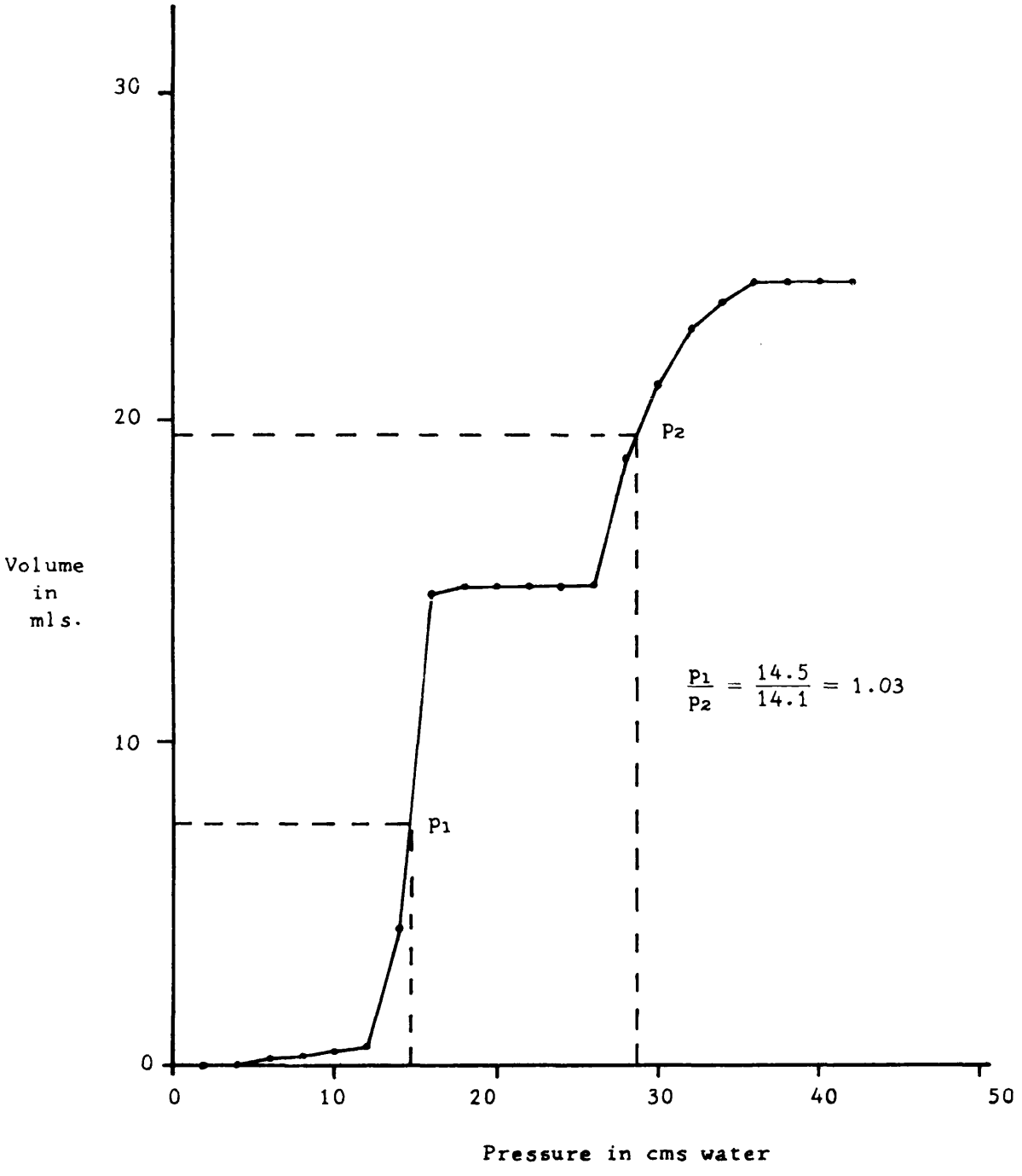

FIG. 18. Pressure/volume relationship for Rhas Untreated Smalls.

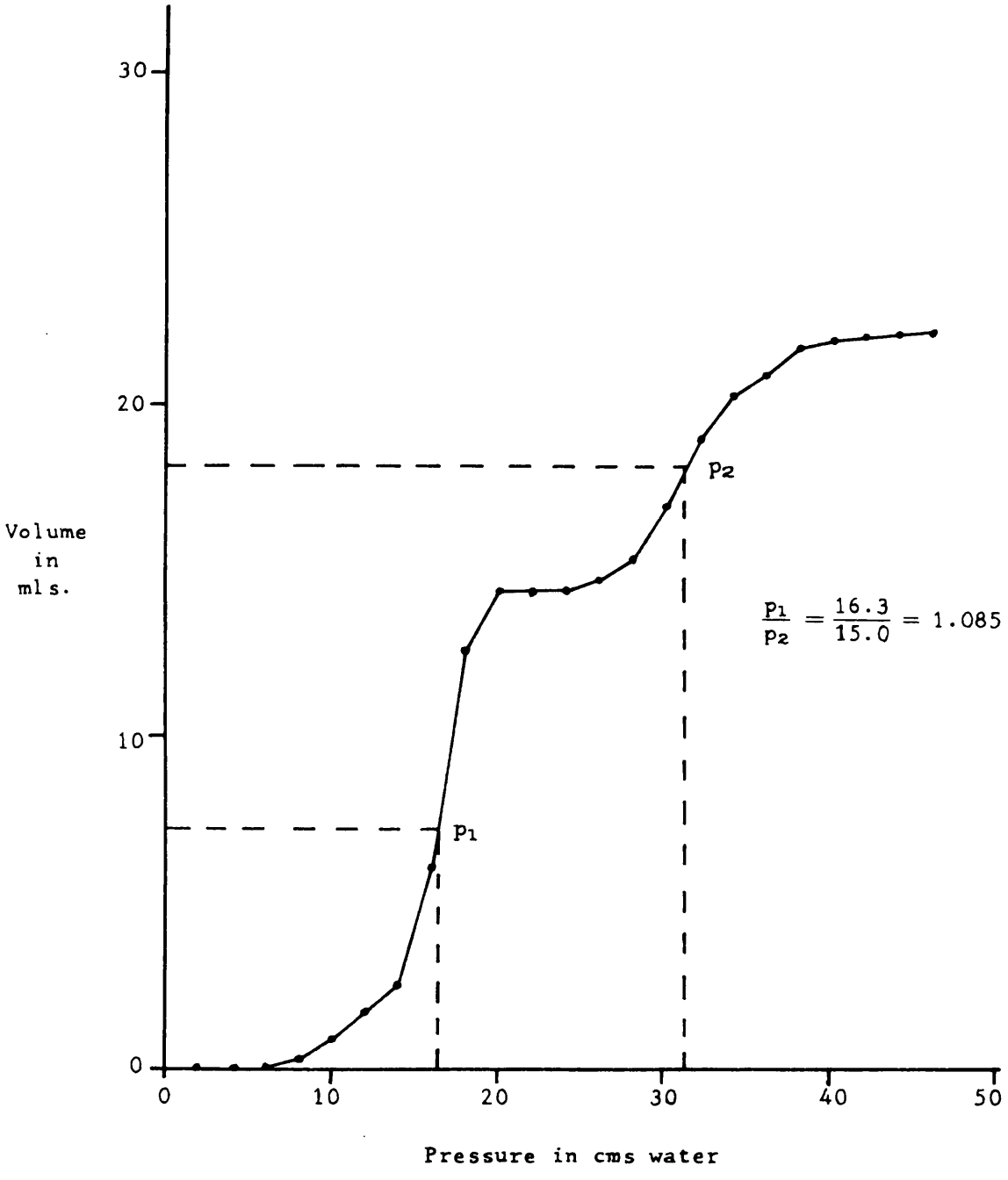

FIG. 19. Pressure/volume relationship for Weathered Rhas Untreated Smalls.

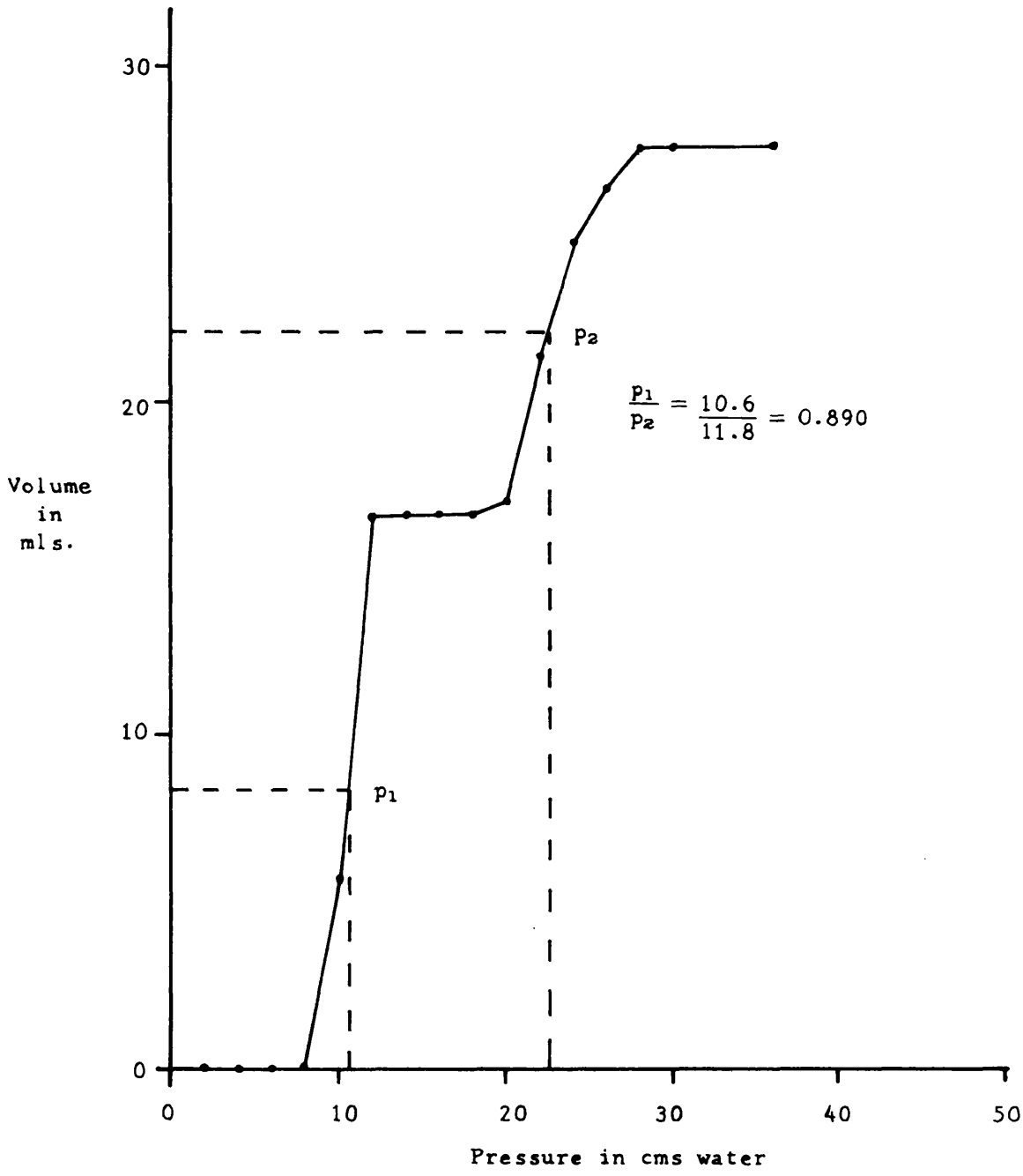

FIG. 20. Pressure/volume relationship for Ogilvie Washed Duff.

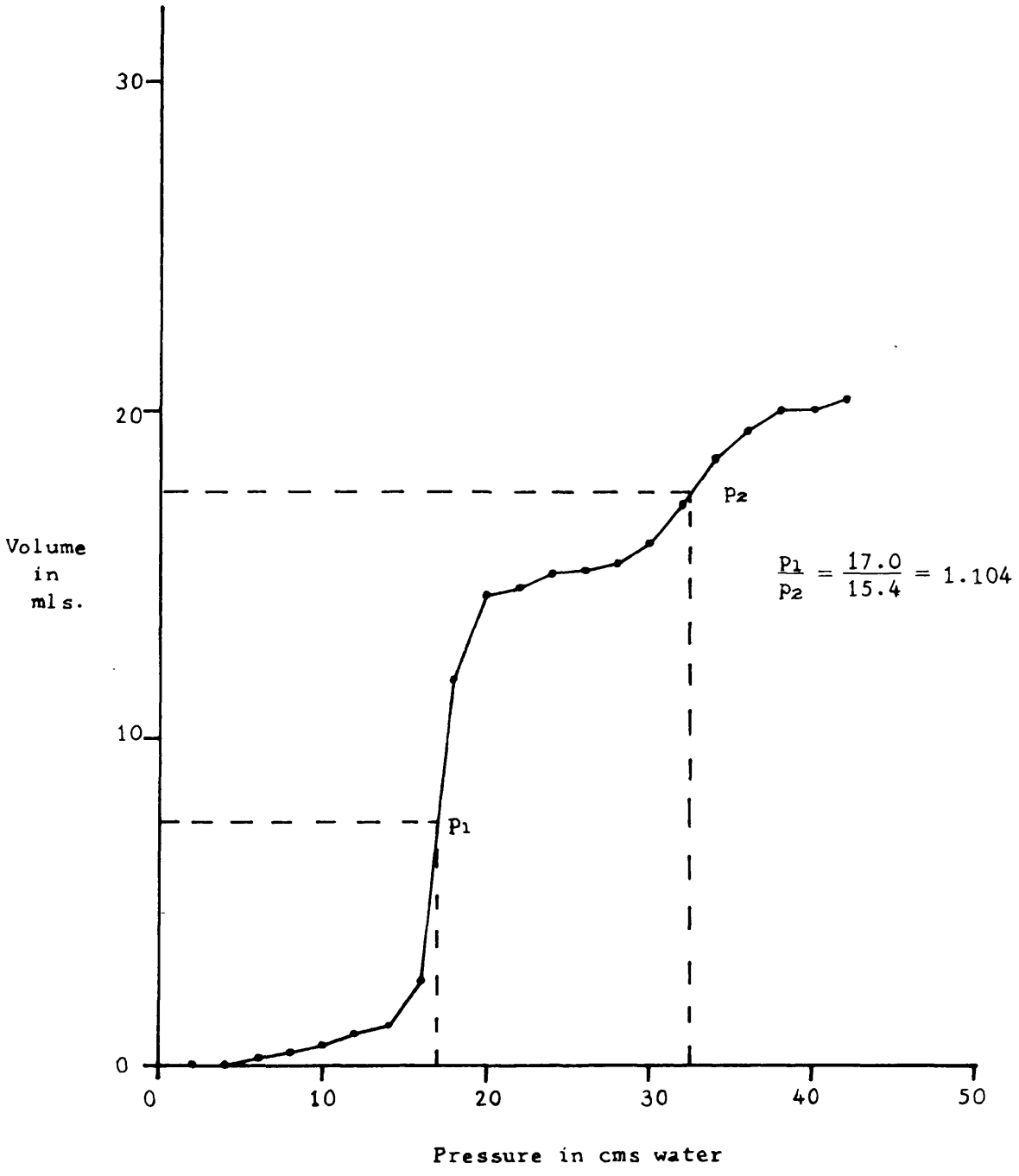

FIG. 21. Pressure/volume relationship for Weathered Ogilvie Washed Duff.

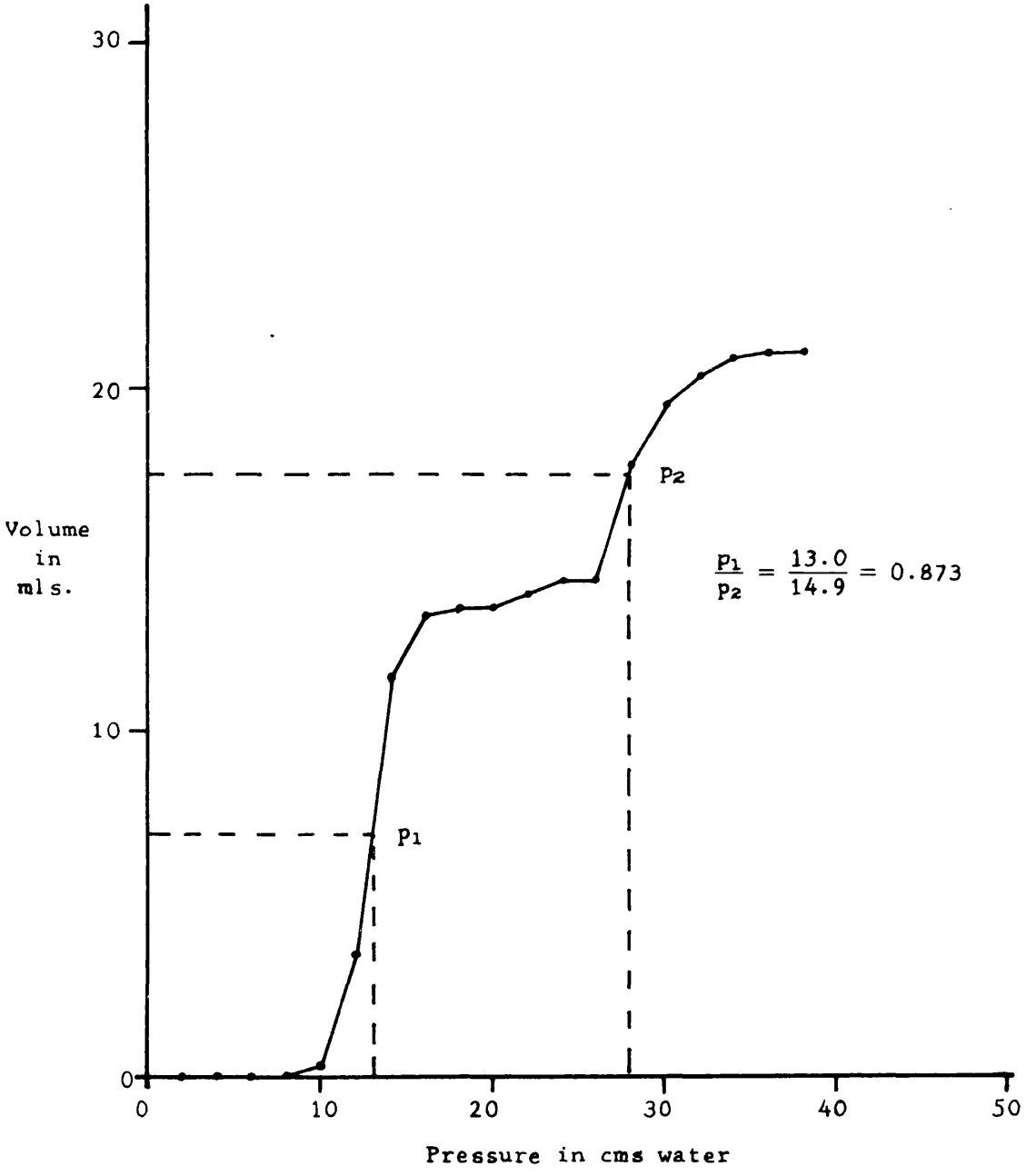

FIG. 22. Pressure/volume relationship for Brynlliw Dry Duff.

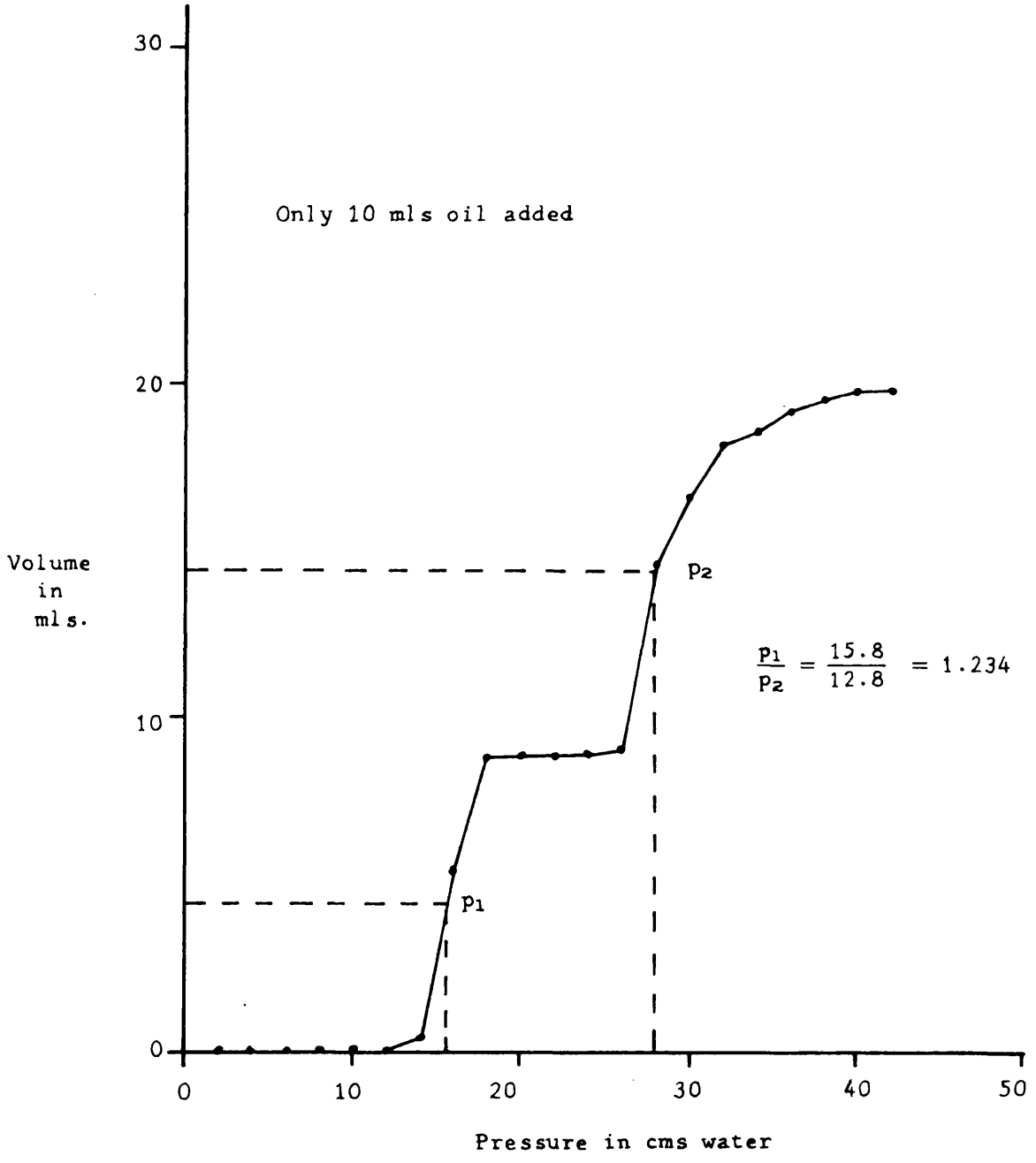

FIG. 23. Pressure/volume relationship for Weathered Brynlliw Dry Duff.

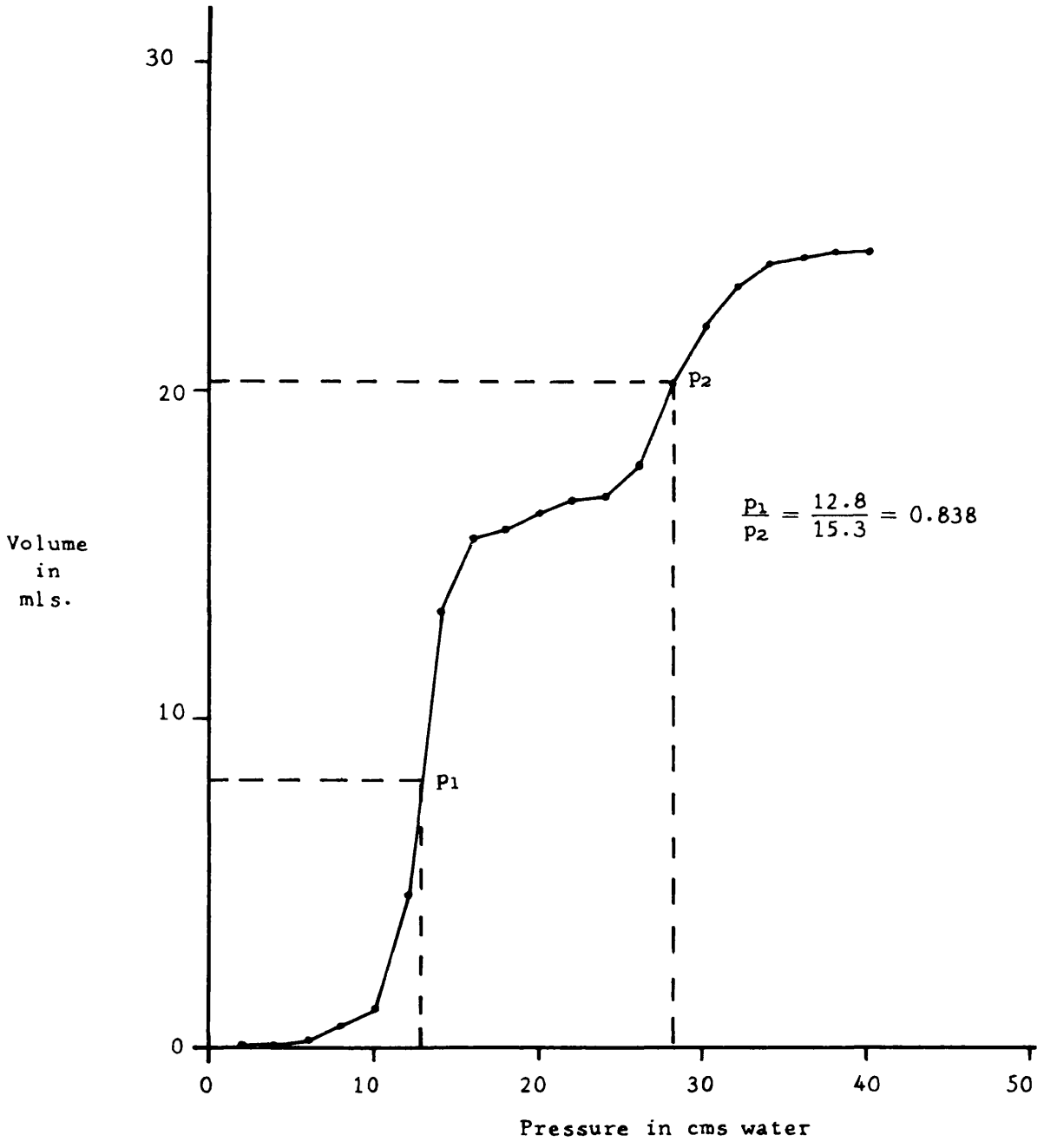

FIG. 24. Pressure/volume relationship for Morlais Untreated Smalls.

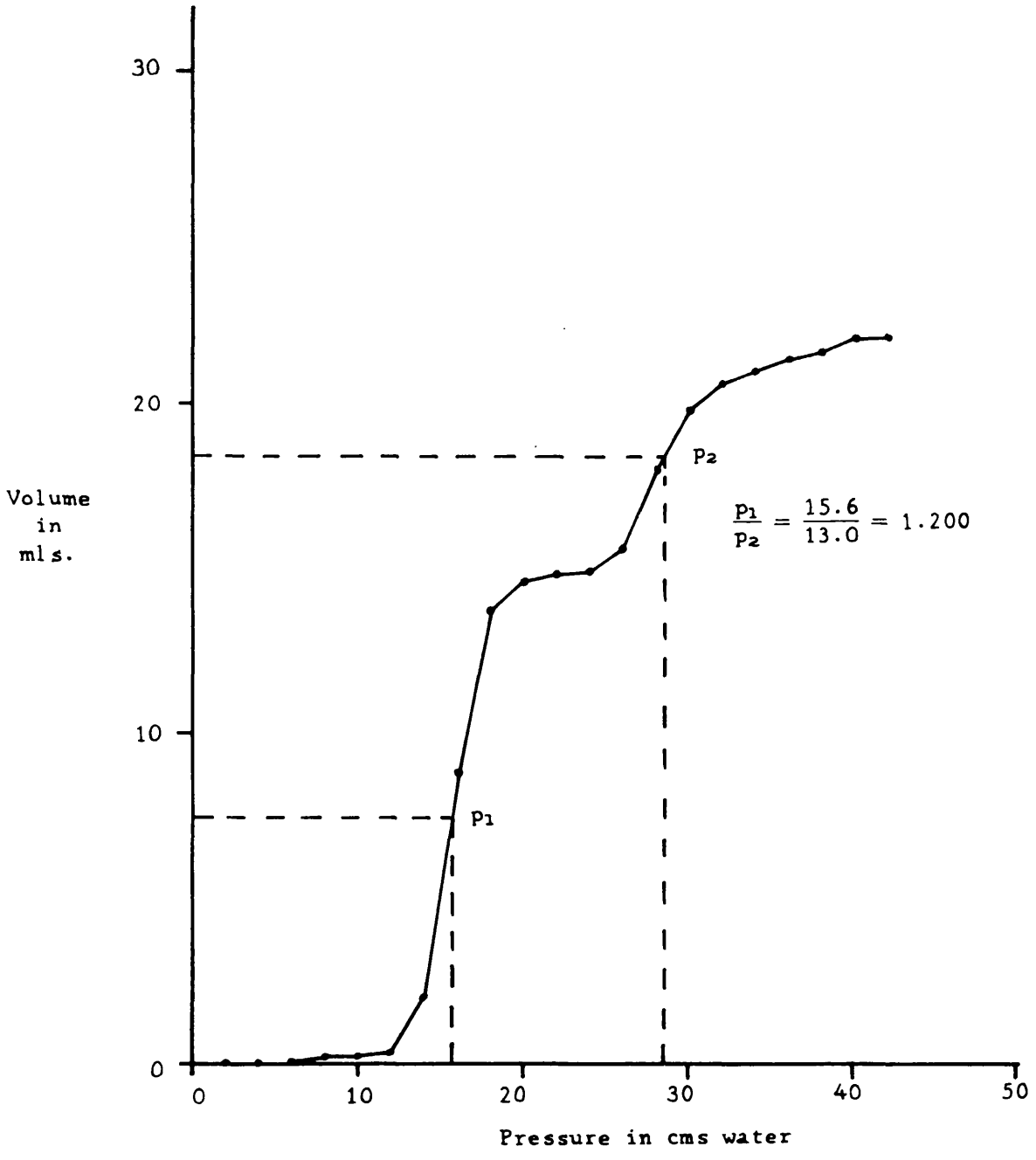

FIG. 25. Pressure/volume relationship for Weathered Morlais Untreated Smalls.

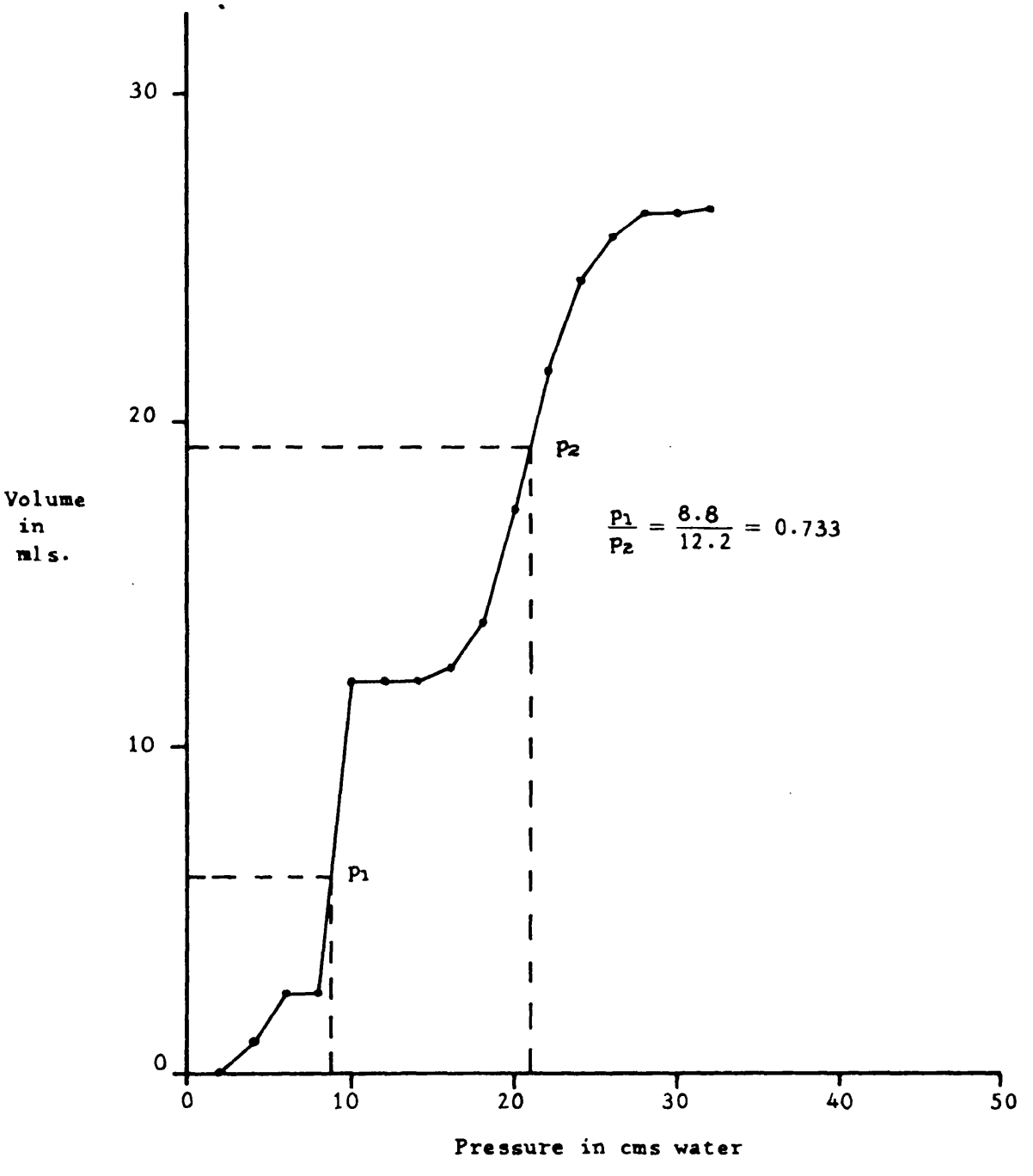

FIG. 26. Pressure/volume relationship for Rhas Untreated Smalls.

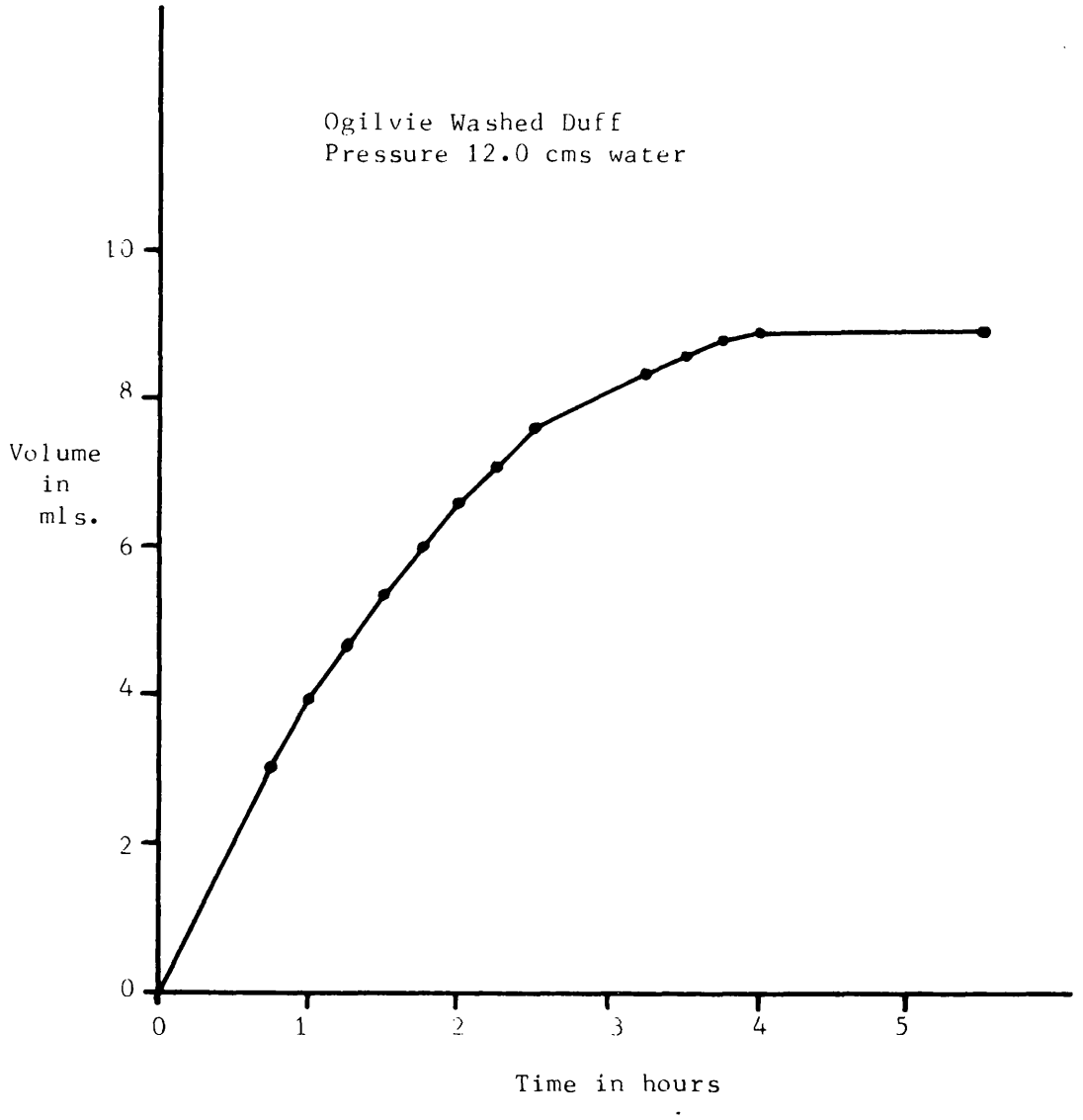

FIG. 27. Rate of equilibration for a step increase in pressure.

REFERENCES

1. Solid Surfaces. J.J. Bikerman. Electrical phenomena at a solid/liquid interface. Proc. 2nd International Conference of Surface Activity. 1957.

2. An essay on the cohesion of fluids. T. Young. Phil. Trans. 54, Pt. 1, 65 (1804).

3. Resistance of solid surfaces to wetting by water. R.N. Wenzel. Ind. Eng. Chem. (Industr.)28, 988, (1936).

4. Growth and form. D'Arcy W. Thompson. Cambridge University Press.

5. Surface tension and the spreading of liquids. R.S. Burdon. Cambridge University Press. 1949.

6. The hysteresis of the angle of contact of mercury. G.D. Yarnold. Proc. Phys. Soc. 58, 120 (1946).

7. Principles of flotation. K.L. Sutherland & I.W. Wark. Brown, Prior, Anderson Pty Ltd. Melbourne. 1955.

8. The bubble machine for flotation testing. I.W. Wark & A.B. Cox. Eng. & Min. J. 137, 641. (1936).

9. Contact angle between mercury and coal. P. G. Sevenster. Fuel. 37, 506. (1958).

10. C. F. Stocker. Thesis. University of Illinois. 1956.

11. The determination of the wetting characteristic of starches and other polymers as measured by contact angles. J. R. Anderson. Thesis. University of Illinois. 1958.

12. An attempt to test the theories of capillary action. F. Bashforth & J.C. Adams. Cambridge. 1883.

13. Contact angle studies on surfaces of coal and other surfaces of low free energy. R.L. Eissler. Thesis. University of Illinois. 1960.

14. The sliding of liquid drops on solid surfaces. D.A. Olsen, P.A. Joyner and M.D. Olsen. J. Phys. Chem. 66, 883 (1962).

15. An investigation of the angle of contact between wax and water. R. Ablett. Phil. Mag. 46, 244 (1924).

16. Moving interfaces and contact angle rate dependence. W. Rose & R.W. Heins. J. Colloid Sci. 17, 39 (1962).

17. Another analysis of capillary rise. W. Rose, N. Chaudhari & H. Fara. Z. physik. Chem. (Frankfurt). 34, 182, (1962).

18. Determination of the wettability of a solid by a liquid. F.E. Bartell & H.J. Osterhof. Ind. Eng. Chem. 19, 1277 (1927).

19. The dewatering of fine coal. V.R. Gray. J. Inst. Fuel, 31, 96 (1958)

20. Studies on the physical properties of soil V. W. B. Haines. J. Agric. Sci. 20, 97, (1930).

21. The suction of moisture held in soil and other porous material. D. Croney, J.D. Coleman & P.M. Bridge. Road Research T.P. 24. H.M.S.O. London. 1952.

22. Measurement and interpretation of capillary pressures in porous media. N.R. Morrow. Ph.D. Thesis. Leeds University. 1962.

23. The determination of surface tension from the maximum pressure in bubbles. S. Sugden. J. Chem. Soc. 121, 858 (1928).

24. The internal flow of granular masses. R.L. Brown & G.W. Hawksley. Fuel. 26, 159 (1947).

25. Notes on the deposition of sands. J. Kolbuszewski. Research (Supplement) 3, 478 (1950).

26. K.H. Roscoe. Private Communication.

27. A new apparatus for measuring surface tension, P. Lecomte du Noüy. J. Gen. Physiol. 1, 521 (1919).

28. Effect of contact angle on the capillary properties of porous masses. C.C. Harris, A. Jowett & N. R. Morrow. Paper read at a meeting of the Surface Activity Group of the Society of Chemical Industry. 24th Feb. 1964.

29. Tables of Physical & Chemical Constants. G.W.C. Kaye & T.H. Laby. 11th Ed. Longmans. London. 1956

CHAPTER FOUR

THE SPREADING OF OIL ON WET COAL

INTRODUCTION

1. Oiling of coal

NOTES ON COAL

1. Rank system
2. Nomenclature
3. Structure variations of single lumps
4. Microporous structure

NOTES ON OIL

1. Oil used in this study
2. Surface active agents in oil

PREPARATION OF COAL SAMPLES

1. Details of coal used
2. Sieving and washing
3. Rewetting and sample size
4. Artificial weathering
5. Details of the runs

INTERPRETATION OF THE RESULTS

1. Details of the results
2. Effect of oiling
3. Difference between fresh and weathered coal
4. Mechanism for oiling
5. Attempt at photographing the mechanism

INFRA-RED ABSORPTION SPECTRA

1. Reason for investigation
2. Main methods of obtaining I.R. spectra
3. Specular reflectance results

INTRODUCTION

1. Wet coal is often a difficult material to handle on a large scale and various additives have been tried to reduce its wet cohesive strength. A common additive has been fuel oil, as experiments proved it to be effective. Oil does not always improve the flow characteristics and coals are termed "responsive" and "non-responsive", depending on their susceptibility to oiling.

A mechanism of the oiling process will depend on whether the oil spreads on the wet coal or, quantitatively, on the contact angle.

NOTES ON COAL

1. Coal is an incredibly complex solid resulting from the coalification of ancient plant forests. The structure is indefinite, not only on a molecular scale, but also on a macroscale. Classification is necessarily broad and a coal is usually referred to by its rank. High rank coals are those which have been very largely carbonised to give anthracites with a carbon content of more than 90%. Next come middle rank coals with a carbon content between 85% and 90%, and finally the low rank coals (lignites) with 70% - 80% carbon. Further sub-divisions can be made and a coal can be classified as to its properties by a numerical system[1]. The coals mentioned in this chapter are all high rank anthracites.

2. The numerical system only grades a coal for type and not for particle size range and ash content. The coals in this study are from the South Wales coalfield and the methods of mining and preparation are of some interest in that they emphasize the inherent variability of the subject material.

The usual labelling index is the coal mine (or washery) name and some other factor referring to size; such as Lady Windsor Fines,

Rhas Untreated Smalls and Brynlliw Dry Duff. Coal is mined from each pit and may come from any of the working faces up any of the several shafts to the stockpile. It is all referred to as the same coal. Fortunately, coalfield types do not vary significantly over a wide area. As van Krevelen[1] puts it, "One of the most remarkable features of a coal seam is its extraordinary extensiveness compared with its slight thickness. It is certainly an astonishing fact that a stratum with a thickness of several feet, sometimes extends over an area of hundreds of square miles".

Nevertheless, the shale bands that split the seams do vary in thickness and cause some changes in the output of the mine. A bag sample of some coal taken this year may differ significantly from a similar sample taken a year later, but both will have the same name.

3. Apart from the body structure of the coal, any attempt at the study of a coal surface is hindered by the non-homogeneity and the differing properties of fissures along the bedding planes and those across them. This implies that studies of individual lumps of coal are somewhat meaningless; a fact emphasised by the sophistication of technique required to obtain a representative sample of a 5,000 ton stockpile[2].

4. Small coal particles are not solid throughout, but contain a microporous structure with pores some 10 Å in diameter[3,4,5]. This structure is usually studied by heats of wetting and gas adsorption methods. The large relative surface areas of coal particles means that slow reactions involving the solid become more noticable. For example, coals are oxidised slowly in the atmosphere, and under certain circumstances spontaneous ignition can take place in a stockpile[2]. Thus the age, and storage conditions can change the surface properties of a coal sample.

NOTES ON OIL

1. In oiling studies of coal the customary oil is light fuel oil mainly because in any large scale application the additive must be cheap. However, almost any light oil will produce a response with a responsive coal[10]. Hence, in these experiments ordinary domestic paraffin was used. This oil is very similar to light fuel oil (diesel fuel, etc.), except that it does not have the same obnoxious smell.

2. There is a possibility that it is not the oil that causes the improvements in flowability, but some trace quantity of surface active agent in the oil. This approach has not been tested here. However, it suffices to point out that since most oils cause a response and none is overwhelmingly better than the others, either this surface active agent is very widespread or does not exist.

PREPARATION OF COAL SAMPLES

1. The samples provided by the Central Electricity Generating Board arrived in a polythene sack inside a conventional sack in case of rupture of the polythene. They were transferred to polythene dustbins with locking lids for ease and convenience of handling.

The suction potential method of contact angle determination (see Chapter 3) demanded a narrow particle size range and a clean sample containing no dust which might clog the sinter and slow down the rate at which equilibrium was approached.

2. Each sample was sieved in batches and the sieved sizes stored in Kilner jars, which had sealing tops. When about a kilogram of the most plentiful size had accumulated, the samples were washed with tap water by placing the sample on the sieve through which it would not pass and swirling tap water over and through it. This was continued until no further fines were washed from the sieve. The samples were then rinsed with distilled water and dried at $90^{o}C$ in an oven. It was noticed that after this treatment, the coals were pleasant, free-flowing, dust free powders.

Name	Rank Number	Other Details
Felinferan Untreated Smalls	2011	Ash 12.9% Volatiles 11.0% Sulphur 0.8% Chlorine 0.06%
Morlais Untreated Smalls	2011	Ash 11.4% Volatiles 9.9% Sulphur 1.7%
Brynlliw Dry Duff	2011	Ash 13.7% Volatiles 8.7%
Ogilvie Washed Duff	2030	Ash 8.8% Volatiles 13.3% Sulphur 0.9%
Lady Windsor Fines	2030	Ash 12.0% Volatiles 13.0%
Rhas Untreated Smalls	1020	Ash 15.0% Volatiles 9.1%

FIG. 1. Details of samples of coal.

3. The contact angle results were taken for the 36 - 72 B.S. sieve mesh range (422 - 211 microns). This was an abundant range and gave convenient pressures on the suction potential apparatus. The sample size could not be as small as that investigated by Morrow[6], because the apparatus would not respond to such small liquid volumes and also two interfaces had to be accommodated instead of Morrow's[6] single interface. 50 gms was decided upon, as it provided a bed some 3 cms thick with reasonable economy of the sieved fractions. The sample was prepared for the sample bed by adding 100 mls of distilled water to the 50 gm sample and de-gassing either by boiling or evacuation until the water boiled under reduced pressure. Gray[7] had demonstrated the need for de-gassing as otherwise it was possible for the gas to be released when the suction was applied, causing unusual draining curves. Also, the de-gassing removed any small air bubbles in the mass of the powdered sample. In the discussion[8] of Gray's[7] paper it was pointed out that coal reacts with water at 100°C producing small quantities of carbon monoxide, carbon dioxide and hydrogen[9]. Gray[8] replied that he considered boiling to be merely the speeding of a reaction that would take place slowly anyway, and any bed of wet coal would, in practice, approximate to his boiled samples rather than the unboiled ones. The results obtained here using both vacuum de-gassing and boiling seem to indicate that boiling does not alter the surface properties of the sample.

4. Cuttress and Walker[10,11] in their study of the response of wet coal to oiling showed that coal which had been oxidised with potassium permanganate[6] or by stoving for three days at 140°C in a ventilated oven no longer improved in flowability when oiled. Other tests with oxidised coal which was freshly ground and responded to oiling further confirmed this viewpoint. In these experiments results

have been obtained for the same coal both oxidized and fresh. The oxidation was performed by stoving in a ventilated oven.

5. One of the objectives of measuring the contact angle of oil against wet coal was to decide whether it was related to the response of the coal to oil. Consequently, samples of both fresh and oxidized coals were used and the contact angles measured for both. The details of each run are given in the results section of Chapter 3.

INTERPRETATION OF THE RESULTS

1. It has been shown in Chapter 3 that using a uniform capillary theory, the advancing contact angle of oil upon wet coal can be calculated from the suction potential curves. The equation derived was

$$\frac{\cos\theta_{o/w}}{\cos\theta_{o/a}} = \frac{Po/w}{Po/a} \times \frac{\gamma_{o/a}}{\gamma_{o/w}} \qquad \ldots\ldots\ldots\ldots\ldots\ldots (1)$$

The ratio $\frac{\gamma_{o/a}}{\gamma_{o/w}}$ was found to be 0.808 by measuring both these surface tensions with a du Nuoy tensiometer. Assuming the receding angle of the oil/air interface to be 0^{o}, the maximum value of $\frac{P_{o/w}}{P_{o/a}}$ is 1.238, since $\cos\theta_{o/w} \leqslant 1$

Thus $\frac{P_{o/w}}{P_{o/a}} \leqslant 1.238$

2. It can be seen from Fig. 2 that in every case $\theta_{o/w}$ is reduced by weathering or oxidising the coal surface. This means that oil does not spread as easily on weathered coal as on fresh coal.

3. Lady Windsor Fines was known to be responsive when fresh[10] yet unresponsive when weathered. Rhas Untreated Smalls was known to be unresponsive when fresh[10]. This would indicate that for a coal to be responsive, the angle $\theta_{o/w}$ must be greater than 36^{o}. No weathered coal exhibits such a value which would indicate that oil would improve none of the weathered samples studied here.

4. Oil does not spontaneously displace water from the coal surface and so any mechanism which relies on oil spreading on a coal surface and thus changing the contact angle must be suspect. It is possible

Coal Name Fig. No. of Results	Fresh or Weathered	$P_{o/w}$ cms. H_2O	$P_{o/a}$ cms. H_2O	$\frac{P_{o/w}}{P_{o/a}}$	$\cos\theta_{o/w}$	$\theta_{o/w}$
Lady Windsor Fines						
11	Fresh	10.8	11.5	0.94	0.760	40°
12	Fresh	13.0	14.2	0.916	0.741	42°
13	Fresh	12.2	13.2	0.925	0.748	42°
14	Fresh	14.6	15.4	0.950	0.768	40°
15	Weathered	15.9	15.8	1.005	0.812	36°
Felinferan Untreated Smalls						
16	Fresh	15.1	15.4	0.982	0.794	37°
17	Weathered	15.4	14.6	1.055	0.854	31°
Rhas Untreated Smalls						
18	Fresh	14.5	14.1	1.030	0.833	34°
19	Weathered	16.3	15.0	1.085	0.876	29°
Ogilvie Washed Duff						
20	Fresh	10.6	11.8	0.890	0.720	44°
21	Weathered	17.0	15.4	1.104	0.892	27°
Brynlliw Dry Duff						
22	Fresh	13.0	14.9	0.879	0.711	45°
23	Weathered	15.8	12.9	1.234	0.998	3°
Morlais Untreated Smalls						
24	Fresh	12.8	15.3	0.836	0.677	43°
25	Weathered	15.6	13.0	1.200	0.970	14°

Fig. 2. Results of contact-angles experiments.

that the oil reduces the cohesive strength of the wet coal by acting in a manner which seems to be unexplored at present.

One per cent is normally considered an appropriate quantity of oil to add by weight to the wet coal. A normal wet coal will have about 12% water by weight and so it can be seen that the liquid content of the coal will be increased by about 10% after oiling. This is more than a mere trace of surface active agent and it is more like a four phase system (coal, oil, water, air). If the oil accumulates at at the junction of the water and air phases with the surface and modifies the contact angle locally a reduction in the cohesion of the coal mass will be observed.

Consider Fig. 3. When oil is present, the liquid bridge will be of greater volume, but this will not affect the strength of the bridge (see Chapter 2). The oil will wet the coal surface where there is no water present and have possibly a zero receding contact angle. The oil/water interface will have an angle of 45^{o} with the coal surface for a responsive coal and this will change the profile of the oil/water interface, reducing its curvature. With this reduction in curvature comes a reduction in pressure differential and hence a reduction in the cohesive force. It is possible that the oil on the water surface will not reduce the surface tension by any appreciable amount, (Antonow's Rule[14]), although experimentally a reduction of 15 dynes/cm was observed between the total surface tensions of oil/air and oil/water and the surface tension of the water/air interface. This mechanism requires that the oil is added in sufficient quantity to form the subsidiary rings at the coal/air/water junctions. An excess of oil does not continue to reduce the cohesive force.

5. It was attempted to observe directly with a 35 mm Contaflex single lens reflex camera with an extension bellows, whether oil did accumulate at the junctions and to photograph the effect. However,

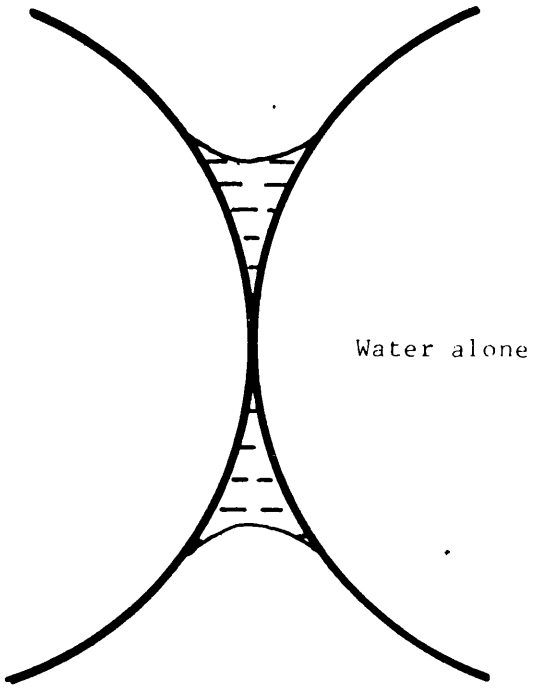

FIG. 3.

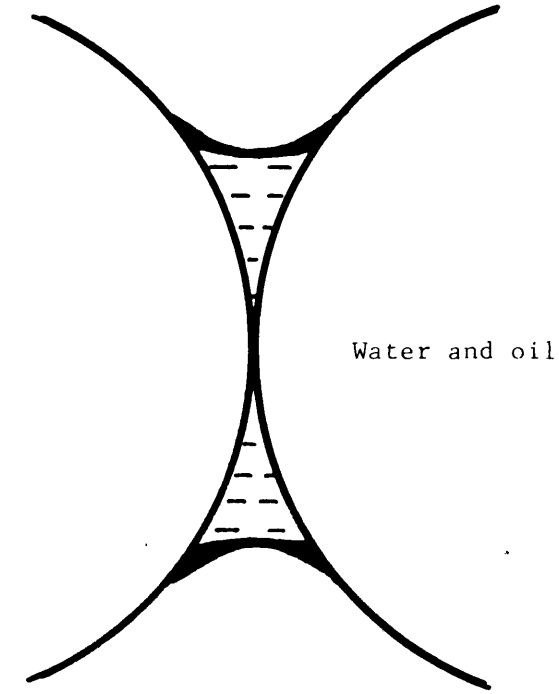

the lighting of the system proved to be somewhat critical and almost any effect seemed to be observable by variations of the lights. The coal surface used was a cleavage plane in a small piece of Rhas, mainly because this sample split with larger planes than any other sample.

INFRA-RED ABSORPTION SPECTRA

1. It is possible that differences in the surface structure might account for responsive and non-responsive coals. Since oxidation seemed to affect responsive coals the presence of C-O bonds in the structure would appear to be vital. Consequently, the size of the C-O absorption band in the infra-red region seemed an obvious property to investigate.

2. However, infra-red spectra of coal are difficult to obtain because the preparation of the sample requires skill and care. There are three basic techniques. Thin sections of between 0.1 and 0.01 mms thickness can be prepared, but the difficulties of preparing such sections with a brittle material such as coal speak for themselves. Sample preparation is lengthy and oxidation of the thin section and contamination with abrasives can occur. Nujol mulls have been popular as the sample is easily prepared, but the Nujol absorbs in the same region as the coal causing some confusion. Pressed potassium bromide discs have been used, but again the preparation is difficult due to particle size effects. Lowry[2] gives a review of the results of these main methods.

3. A further technique is that of specular reflectance and Fig. 4 gives an illustration of the optical set-up. The method seemed to be of much greater potential simplicity with respect to sample preparation than the alternatives. A specular reflectance head for a Unicam SP200 machine was used and the sample of coal was finely ground and dusted upon the mirror of the head. This was all the preparation needed.

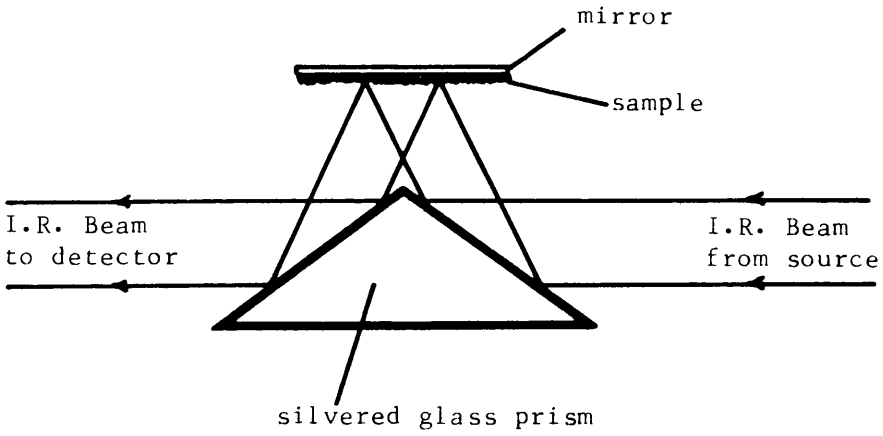

FIG. 4. Optical arrangement of the specular reflectance head.

As little energy reached the detector all the slits had to be wide open and the gain at a maximum. The spectra obtained are of absorption by the sample which is held on the mirror by surface forces. It is rather like holding a thin layer up for transmission spectra without an absorbing support material. The results were rather promising, giving the characteristic coal absorption bands, but no further time could be spent perfecting the technique. Two typical spectra are produced as Fig. 5 and Fig. 6.

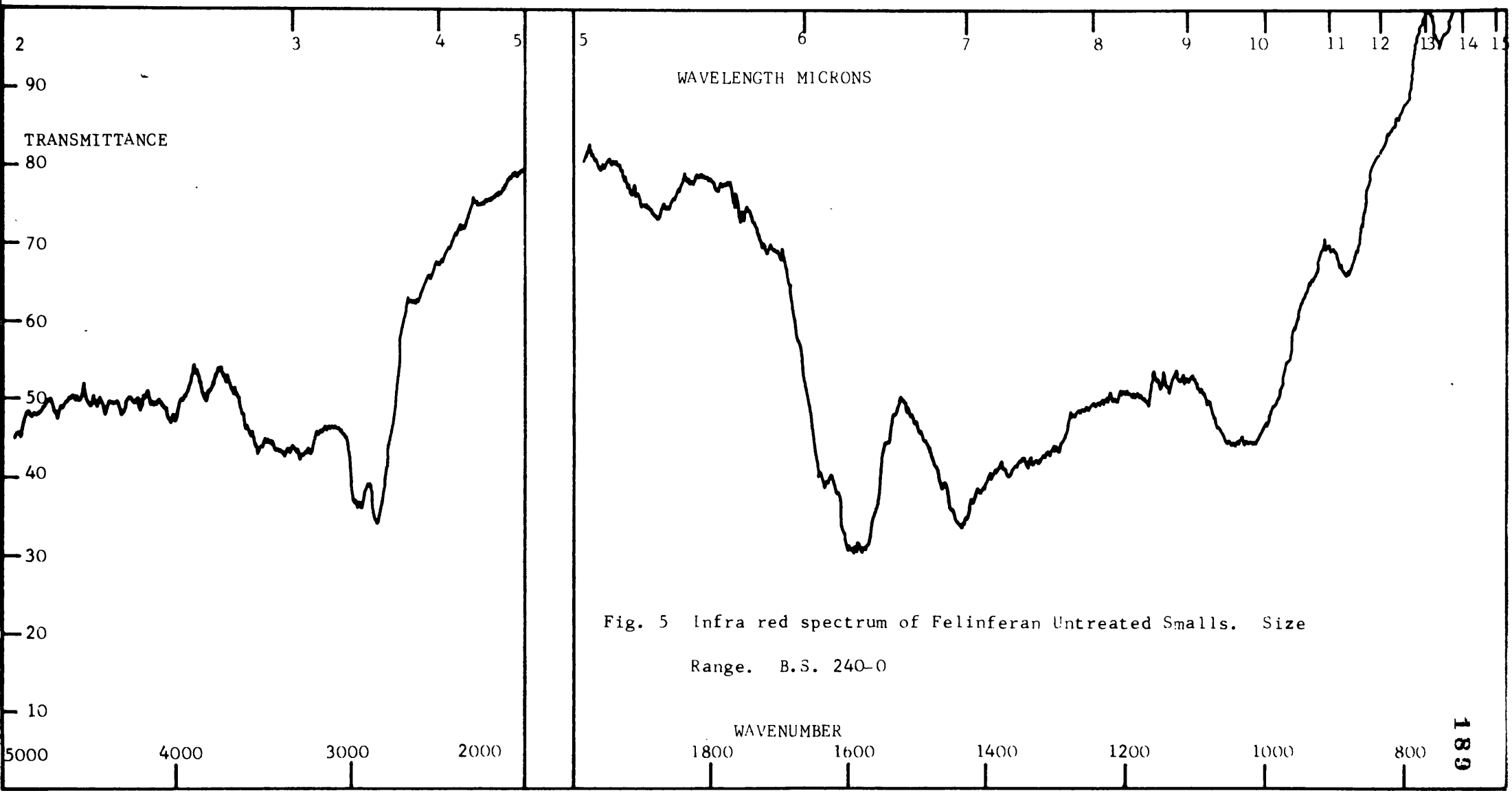

Fig. 5 Infra red spectrum of Felinferan Untreated Smalls. Size Range. B.S. 240-0

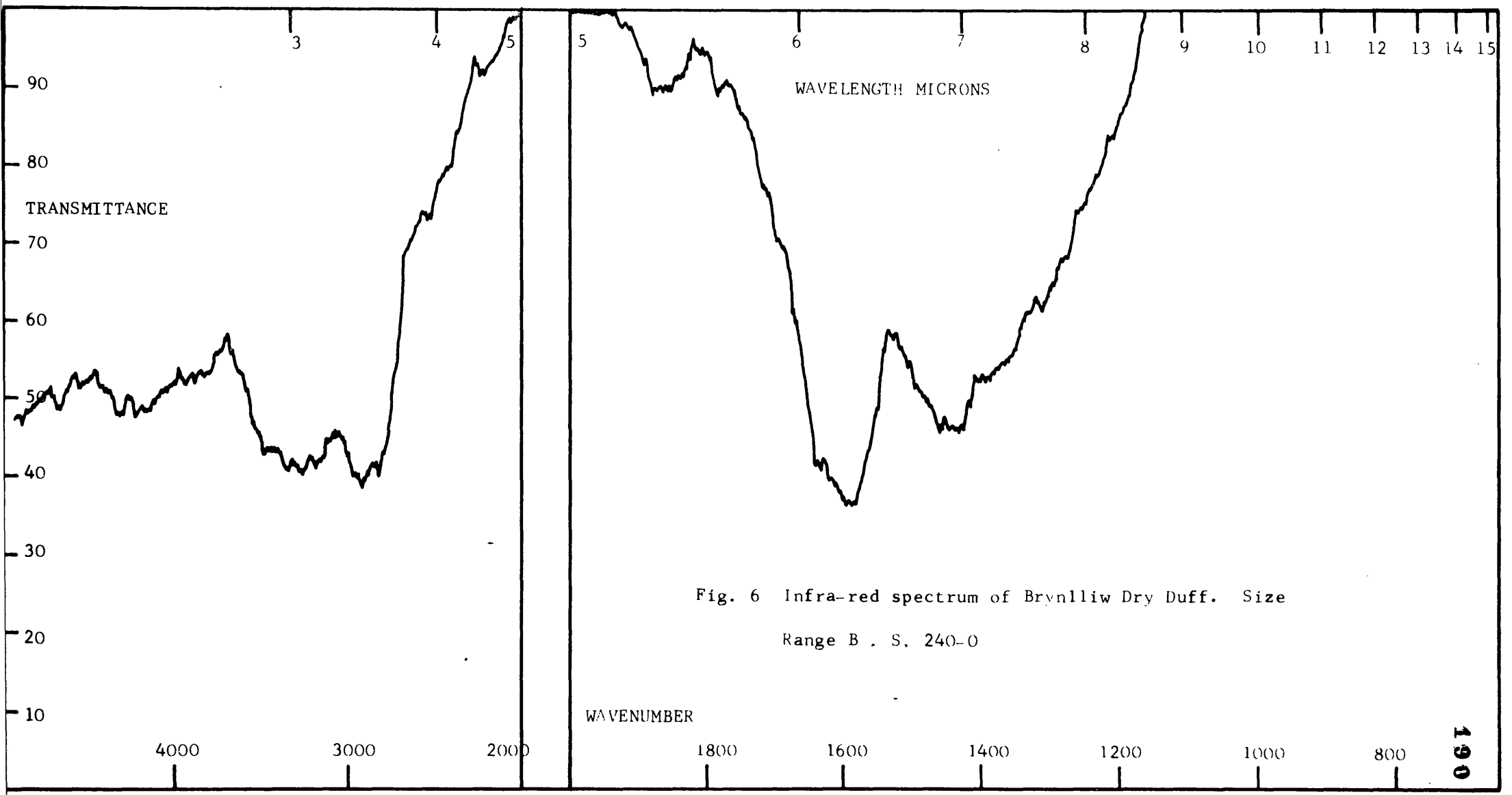

Fig. 6 Infra-red spectrum of Brynlliw Dry Duff. Size Range B . S. 240-0

REFERENCES

1. Coal Science. D.W. van Krevelen & J. Schuyer. Elsevier. 1957.

2. Chemistry of Coal Utilisation. H. H. Lowry. J. Wiley. N.Y. 1963.

3. A structural model for coal substance. D. H. Bangham, R. E. Franklin, W. Hirst and F.A.P. Maggs. Fuel 28, 231 (1949).

4. Some observations on the specific surface of coals. S. G. Gregg & M. I. Pope. Fuel. 38, 501. (1959).

5. Some properties of water adsorbed in the capillary structure of coal. R. L. Bond, M. Griffith, & F.A.P. Maggs. Disc. Farad. Soc. No. 3. 29. (1948).

6. Measurement and interpretation of capillary pressures in porous media. N. R. Morrow. Ph.D. Thesis. Leeds University. 1962.

7. The dewatering of fine coal. V. R. Gray. J. Inst. Fuel. 31, 96. (1958).

8. Discussion on "The dewatering of fine coal". J. Inst. Fuel. 32, 72. (1959).

9. The interaction of water and coal at low temperatures, P. N. Mukherjee & A. Lahiri. Fuel. 36, 176, (1957).

10. The effect of additives on the handling of wet South Wales coals. J. O. Cutress & D. M. Walker. J. Inst. Fuel. 37, 537, (1964).

11. An investigation into the effect of additives on the flowability of damp coal. D.M. Walker. C.E.G.B. South West Regional Research and Development Internal Report No. 9.

12. A new apparatus for measuring surface tension. P. Lecomte du Noüy. J. Gen. Physiol. 1, 521. (1919).

13. Tables of physical and chemical constants. G.W.C. Kaye & T. H. Laby. 11th Ed. Longmans. London. 1956.

14. Surface tension at the limit of two layers. G. N. Antonow. J. Russ. Phys. Chem. Soc. 93, 342. (1907). Reprinted J. Chim. Phys. 5, 372. (1907).

CHAPTER FIVE

SOME PROPERTIES OF GRANULAR MATERIALS CONTAINING FREE MOISTURE.

THE SIEVE TEST

1. Raison d'etre and simple description
2. Sieving theory
3. Unusual features of sieve test
4. Experimental results
5. Initial sieving rates
6. Effect of removal of fines
7. Obvious deficiencies of sieve test
8. Visual examination of the test
9. Apparent mechanism of the test
10. Properties of a high speed shaker
11. Results on sand with various liquid contents

TENSILE STRENGTH OF WET GRANULAR MATERIAL

1. Introduction
2. Split sample cells
3. The tensile tester
4. Compaction of a sample
5. Results
6. Reasons for large random errors

THE SIEVE TEST

1. In an attempt to find some qualitative test of the effects of surface active agents on wet coal, Cutress and Walker[1] devised the sieve flow test. Basically the idea was to place a weighed sample of coal on a coarse sieve through which all the coal would pass and sieve on a mechanical shaker for a fixed period of time. The quantity of coal which passed through the sieve was taken as some measure of the "flowability". The sieve aperture and time were arbitrary and fixed at ¼" square mesh and ten minutes respectively.

2. The variables in any sieve analysis are complex, although studies have been attempted. Fagerholt[2] accomplished a theoretical statistical analysis and also studied size distributions as sieving was continued. It was clear that the rate of sieving depended upon the area of the screen cloth and, in some complex way, on the ratio of the mixture of particles that could and could not pass the cloth[4]. Furthermore, the number of times that the particles were presented to the screen per second had an effect together with the violence of this presentation[3]. Detailed studies of the errors in the fabric of the screening cloth have been made[5,6], but the effect is small unless the sieve is very lightly loaded.

3. The Cutress and Walker[1] sieve test differs in many aspects from a standard sieve analysis. All of the sample could pass the screen if it were not in the form of cohesive lumps and the load of 500 gms would normally be considered a gross overload for an eight inch diameter sieve[4]. As yet, no theory seems applicable to this special use of sieving.

4. In the work described here, the standard Cutress and Walker sieve test[1] was used to study the flow of various coals and attempts were made to discover the significant variables. An Endrock sieve

shaker was used which both shook the sieve up and down and tilted it in a regular manner. The up-and-down mechanism raised the sieve half an inch and then allowed it to drop onto a hydraulic stop arresting its motion rapidly. The tilting mechanism, designed to prevent the sieve load accumulating in one place made the tilted sieve stack slowly precess around the vertical axis. A whole precession took about 30 seconds and the machine made about 120 vertical oscillations to the minute.

5. Samples of different moisture contents were made up by adding water to 500 gms dry weight of coal. As a variation the sieving machine was stopped every 30 secs., and the quantity of coal on the sieve determined by weighing. Fig. 1 shows the results graphically. It was noted that the initial gradient of the line was a better indication of the rate of flow than the intercept at a time of ten minutes, because it extended over a wider flow rate. Fig. 2 shows a comparison of the results plotted to compare these two methods.

6. Fig. 3 shows two separate sieve test runs and shows that the small quantity of dust that adheres to particles when they are dry sieved has an effect. The "without fines" sample was dry sieved, washed on a sieve under the tap, dried, weighed and remoistened.

7. The actual effect of the sieve action did not appear to be simple. During these sieve tests several phenomena occurred which obviously affected the results of the percentage which passes the sieve. The most obvious was when the coal sample was very wet. A quantity of free water passed the sieve and the moisture content of the coal on the sieve was obviously reduced. Sometimes, after sieving, the portion below the sieve would be a slurry, whilst that on top would be rather dry.

8. Other sieve tests were observed visually in a search for a mechanism. It was noted that the sample was initially one large

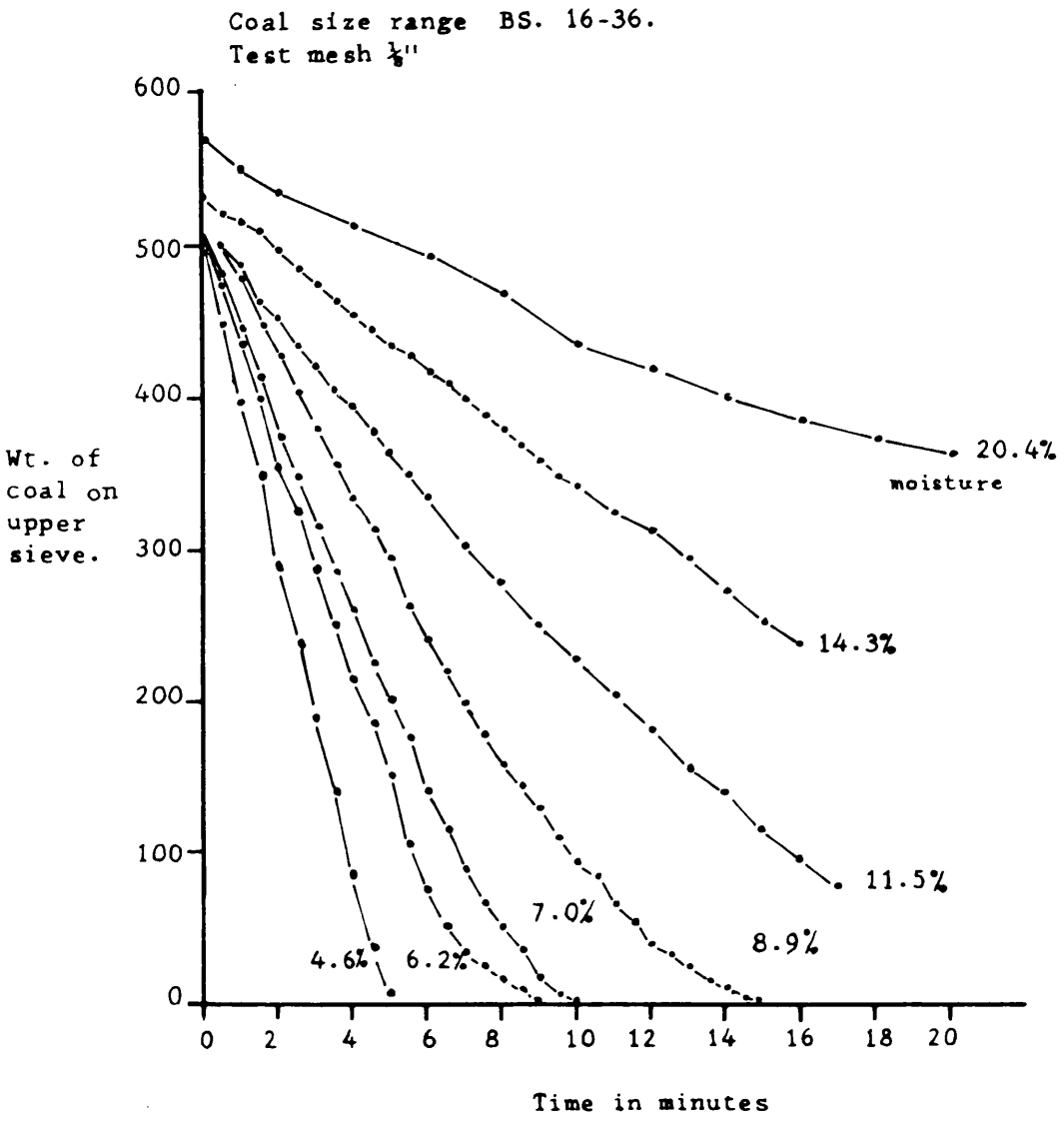

FIG. 1. Sieve flow test. Wt. remaining after certain times.

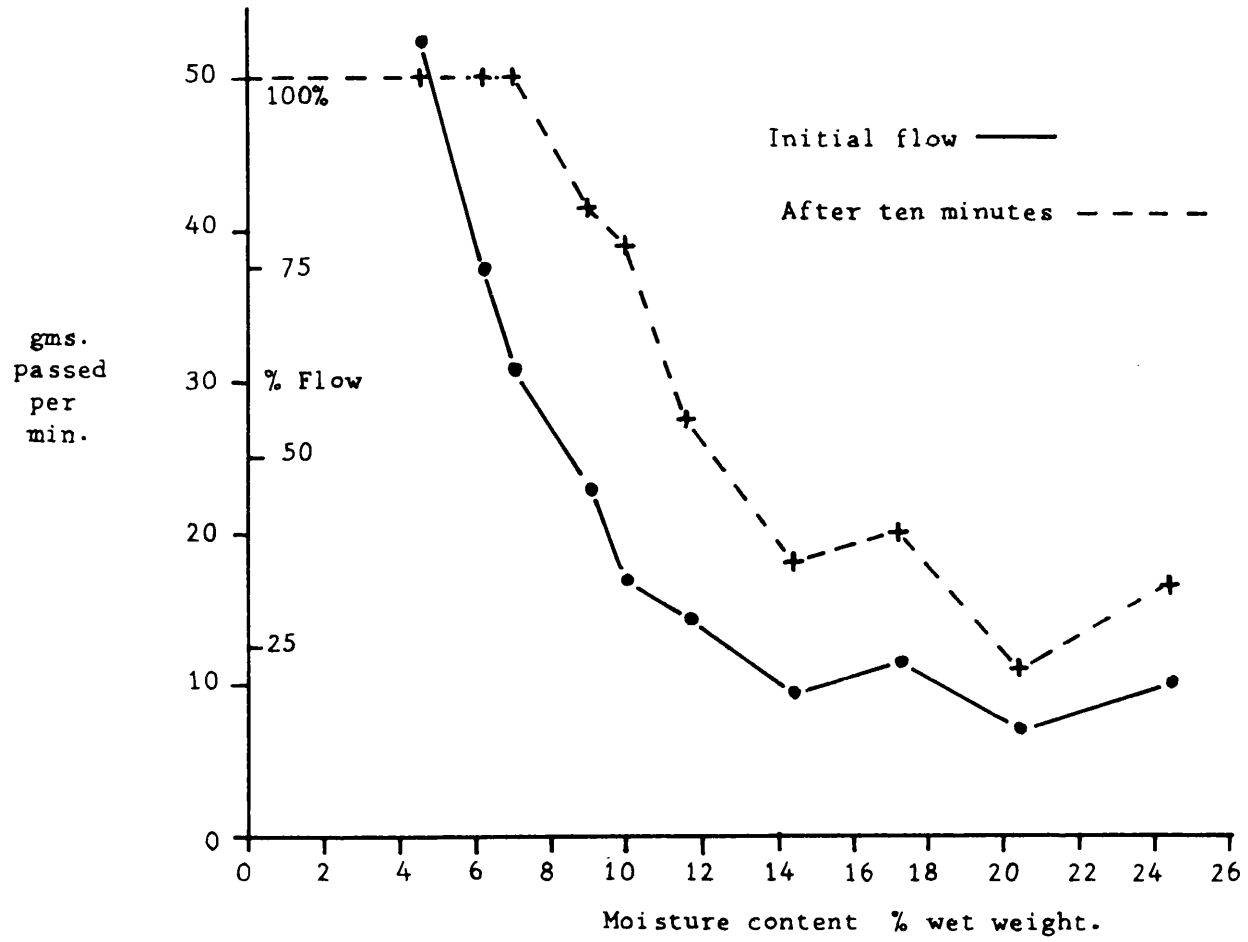

FIG. 2. Sieve flow test. Comparison of initial gradient with the "ten minute" flow rate.

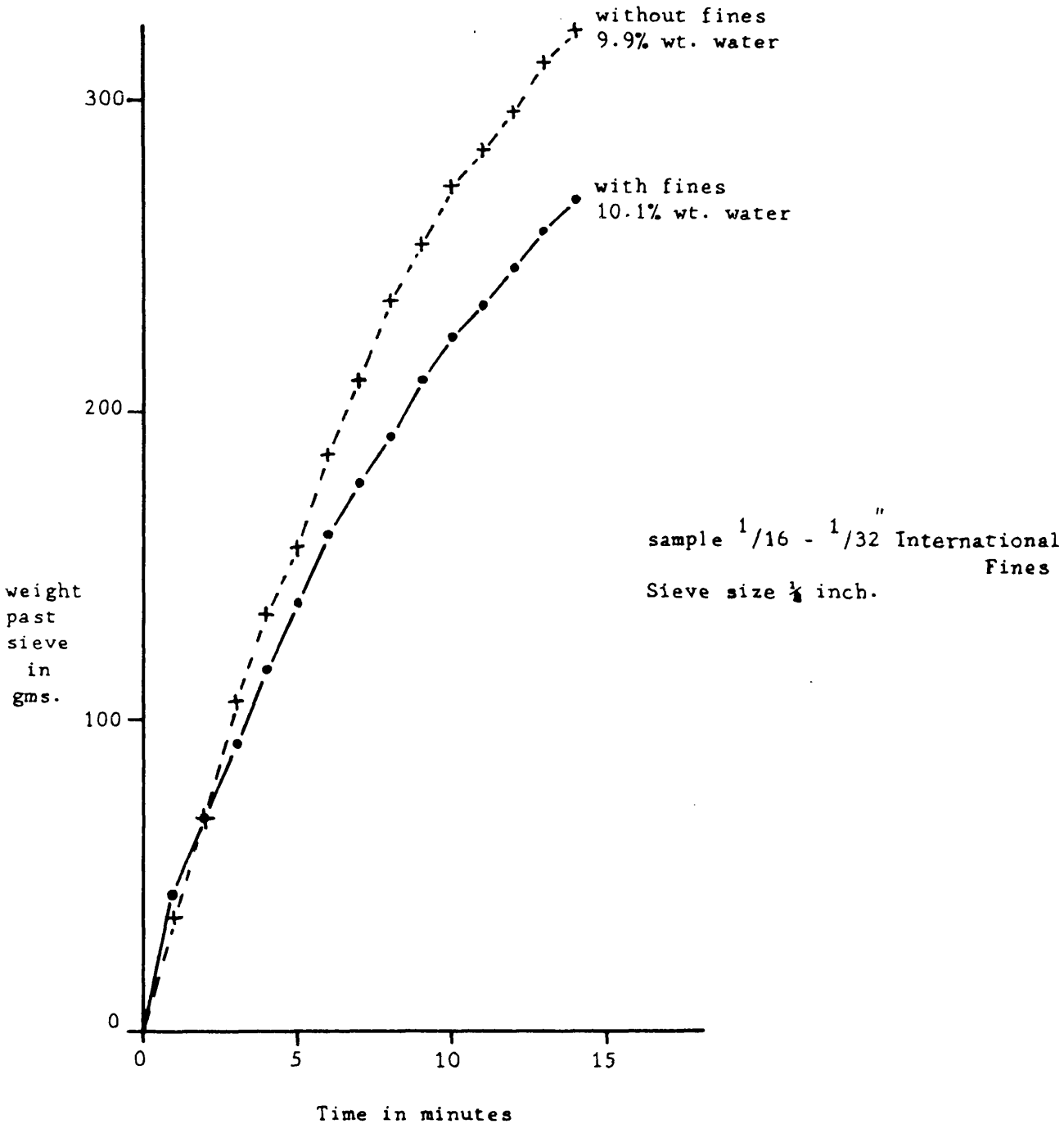

FIG. 3. Sieve flow test. Effect of fines.

pancake-like lump. As the test proceeded this vibrated up and down on the sieve screen and slowly broke up into lumps too large to pass the mesh. A lot of smaller fragments were produced and these passed the sieve screen. Eventually lumps formed which could vibrate on the screen indefinately without breaking up. At high moisture contents the sieve shaker did not have enough energy to break the adhesive force between the sieve screen and the coal pancake and so this large pancake did not break up. Consequently, little flow was observed. At high moisture contents the pancake still would not bounce on the screen but the vibration appeared to compact the sample sufficiently for free moisture to appear. It then behaved somewhat like a slurry and flow rates were high.

9. Obviously the sieve shaker was acting as a kind of mill, breaking the wet coal into small enough particles to pass the screen. However, the efficiency of the milling action was affected by the energy transfer between the sieve and the particles which was in turn dependent on the size of the agglomerates of coal.

10. The results of these experiments were deemed unsatisfactory because it was not at all certain what was being measured, even if it was being measured reproducibly. Some further experiments were performed, this time using an Endrock High Speed Shaker. This consisted of a heavy base with three steel strips such that they rose at an angle of 45^{o} to the plane of the base. They were fastened regularly around the perimeter of the base and were also fastened on to the vibrating platform, supported by them above the base, in a similar way. If the vibrating platform were moved up and down then it also had to rotate through a small angle about the centre - the steel strips bending slightly in the process. A 1450 rpm induction motor drove a cam which vibrated the platform up and down. Initial experiments

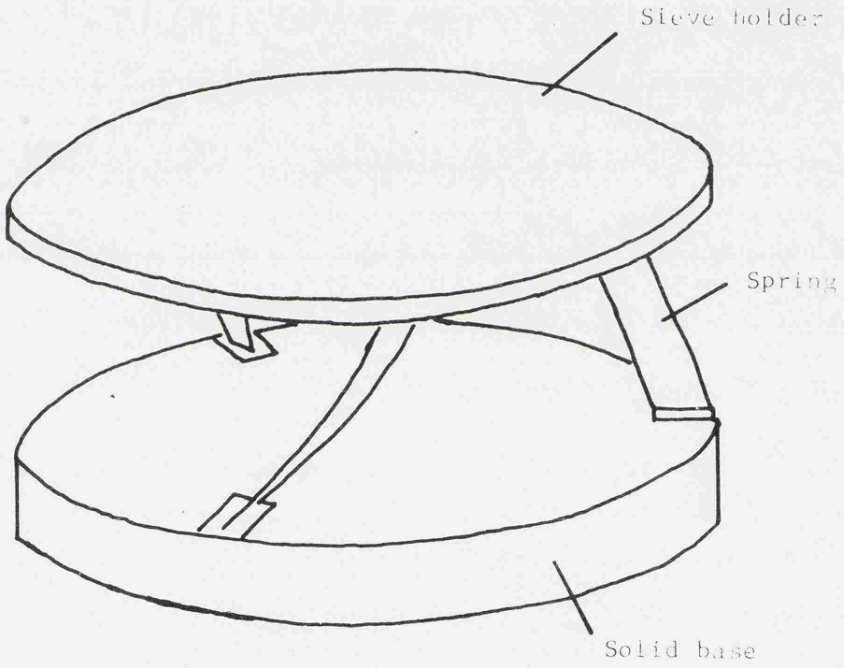

FIG. 4. Diagram of construction of the high speed sieving machine

showed that due to the sieving action the whole sample accumulated in a heap in the centre of the sieve where it remained motionless. In order to overcome this tendency a 4" diameter cylinder was bolted to the middle of the sieve so as to form a channel 2 ins wide round which the sample moved. Sieving times had to be cut from ten minutes to about thirty seconds, otherwise the entire sample passed the sieve.

In order to investigate the sieve test more fully, liquids of different viscosities and surface tensions were used and an inert material selected because coal is chemically attacked by most liquids. Domestic building sand was chosen as this was readily available in large quantities. Several kilograms were sieved, washed and dried in the size fraction which passed a 36 mesh sieve but remained on a 72 mesh (B.S.) sieve. Samples of different liquid contents were made up by mixing in the correct weight of liquid into individual samples and these samples were stored in Kilner jars until used.

11. The results for sand with water, dibutyl phthalate and domestic paraffin are reproduced graphically (Figs. 5,6,7). All results show a minimum flowability at about 14% wet weight. The various physical properties of the wetting liquids are shown in Fig. 8 and a comparison of the flow properties with these physical properties showed no outstanding connection. Surface tension did not appear to be of great importance in determining the mass of material which passed the sieve.

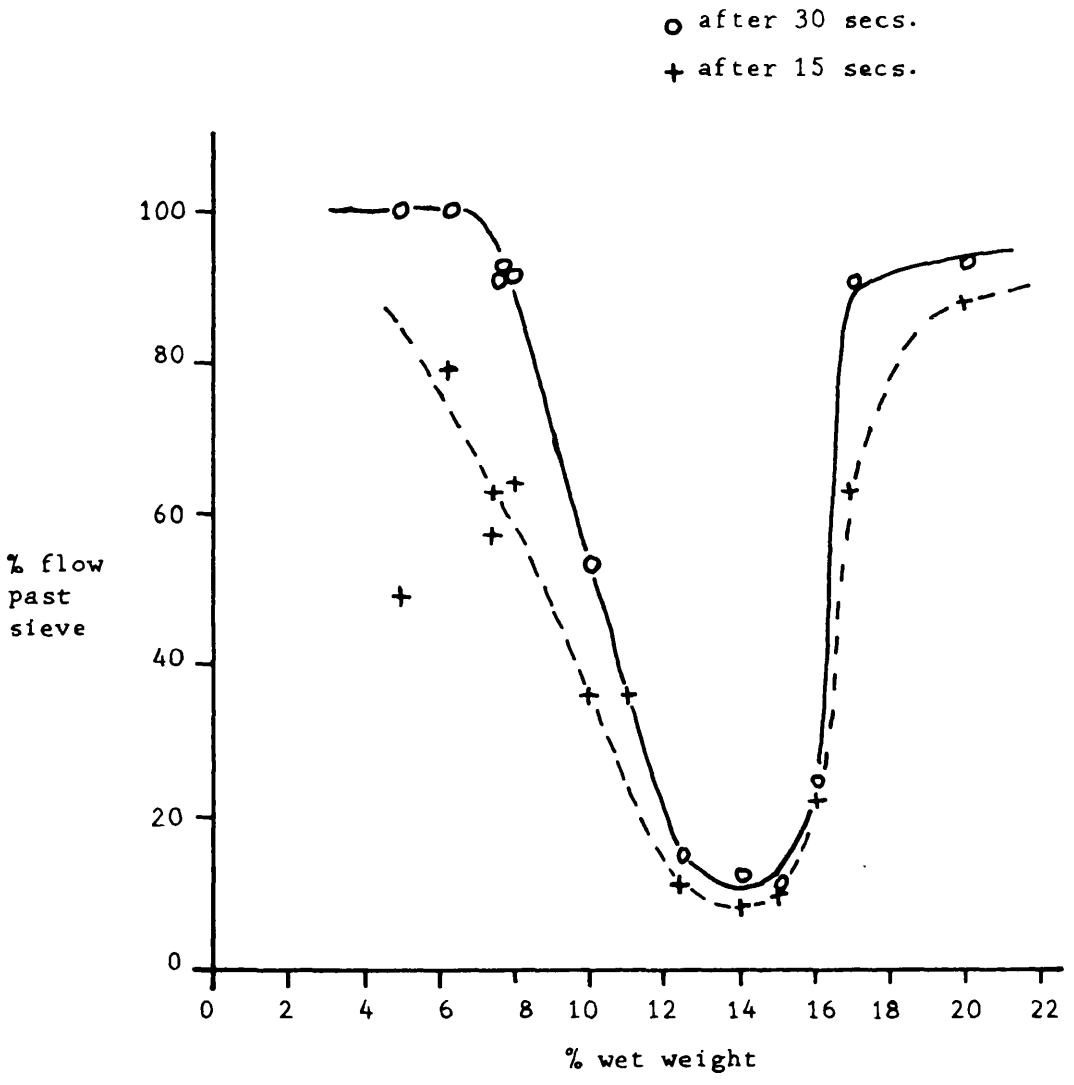

FIG. 5. High speed sieve test. Water in 36-72 mesh sand samples.

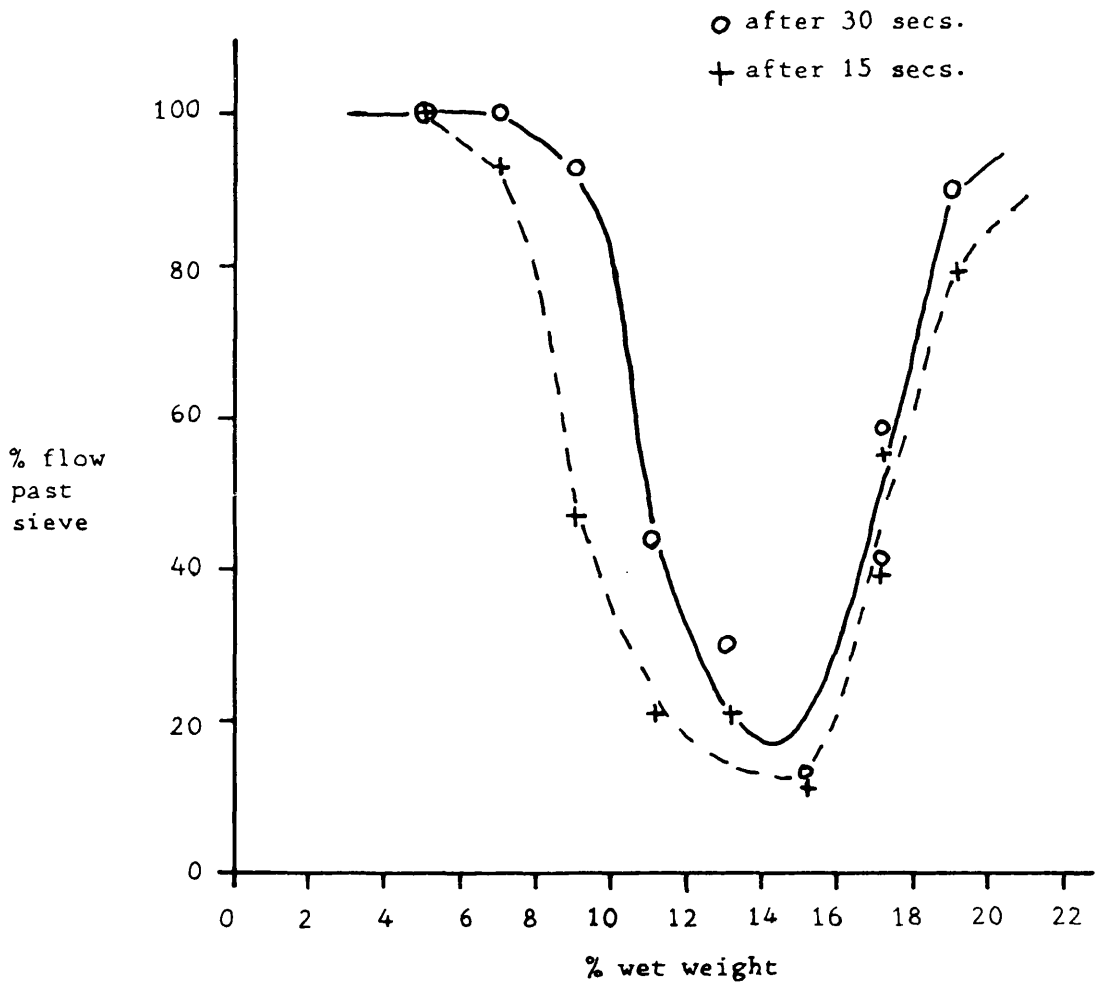

FIG. 6. High speed sieve test. Di-n-butyl phthalate in 36-72 mesh sand samples.

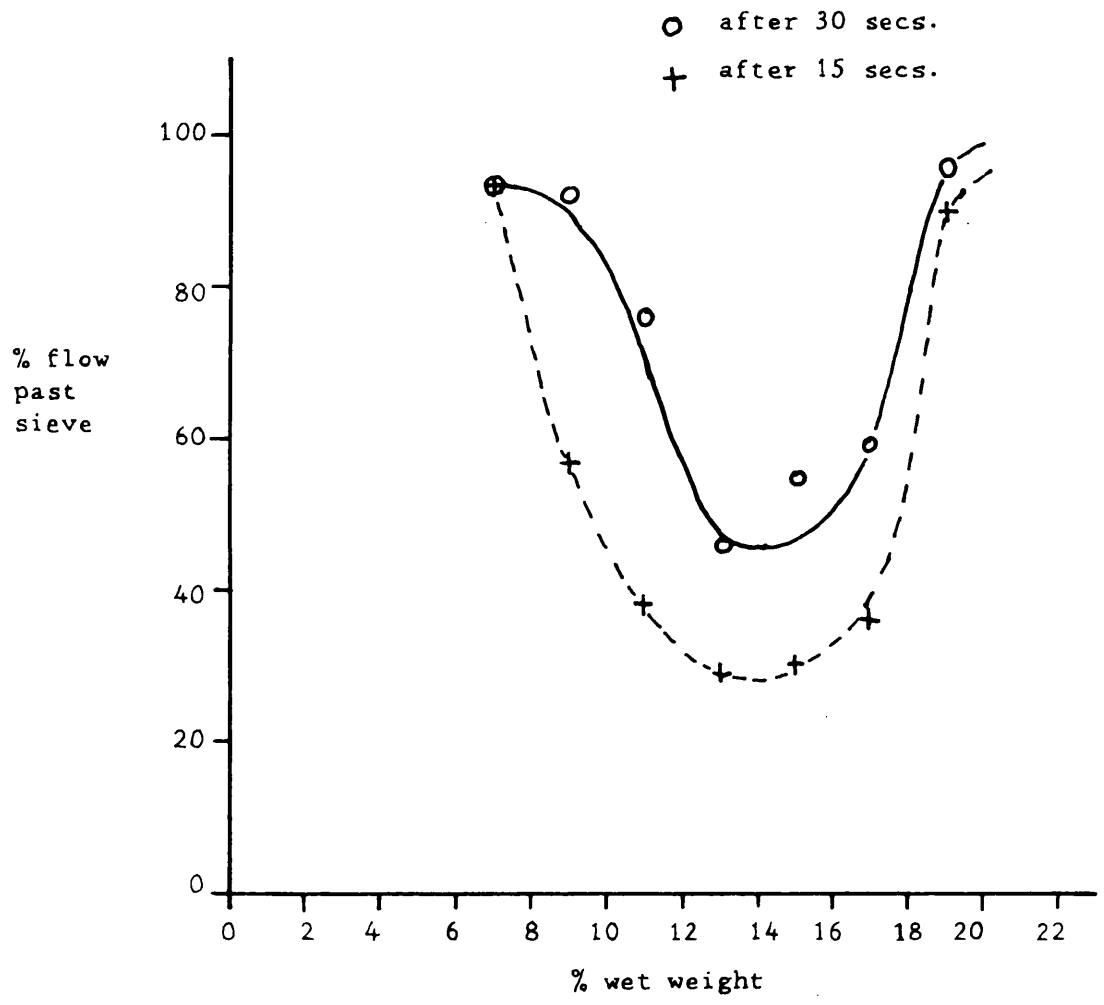

FIG. 7. High speed sieve test. Domestic paraffin in 36-72 mesh sand samples.

Liquid	Surface Tension dynes/cm.	Density gms/cc	Viscosity centipoise
Paraffin	25	0.78	1.39
Water	73	1.0	1.0
Di-n-butyl phthalate	34	1.0	20.0

FIG. 8. Properties of the various liquids at 20°C.

TENSILE STRENGTH OF WET GRANULAR MATERIALS

1. As the mechanism of the sieve test could not be properly elucidated, an attempt was made to measure a different property, the tensile strength, of a bed of wet sand to see if this parameter could be related to the sieve test.

2. Various methods have been used for measuring tensile strength[7][8][9][10][11] but most rely on applying a tension to a split cell of known geometry. This tension is slowly increased until the sample in the cell ruptures. The construction of split cells has often involved designing fairly complex tracks for the cell halves to run on as frictional forces must be kept to the minimum. Any design is further complicated by the need to compact the wet granular material into the cell by a force which is relatively large compared with the tensile strength. If the tracks of the split-cell deflect under this load then as they relax when the load is removed minute cracks can be formed in the bed. When tension is applied to the cracked bed, a low tensile strength is observed. One thus needs very strong, yet friction-free tracks.

3. The design of the tensile tester used in these experiments was novel, in that it resembled a ballistic pendulum apparatus. Two flat boards were suspended each by four chains, from a frame such that, as they were moved back and forth the plane of the boards was kept horizontal. The cell was circular in section and the split ran across the whole diameter of the cell. The sample was thus cylindrical and ruptured along a diameter plane containing the axis of circular symmetry. One side of the cell was fitted to one of the swinging boards and the other side to the other board and the whole arranged so that with no sample the two cell halves just mated.

4. The two halves of the cell were clamped together, whilst the cell was filled and the sample compacted by placing a piston in the top of the cell and loading this with, typically, a one kilogram weight. The piston was then twisted an arbitrary, but consistent number of

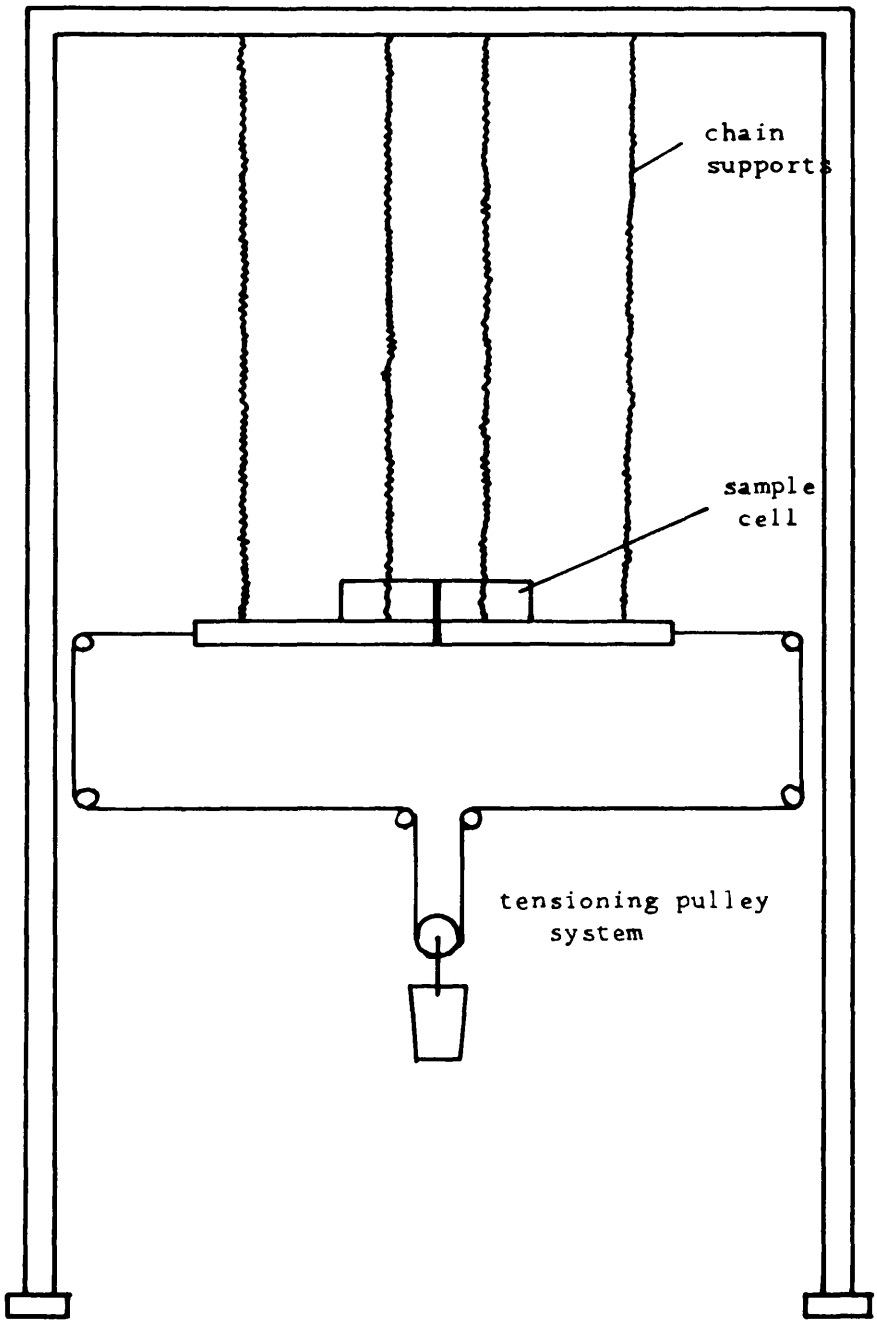

FIG. 9. Diagrammatic representation of the tensile tester.

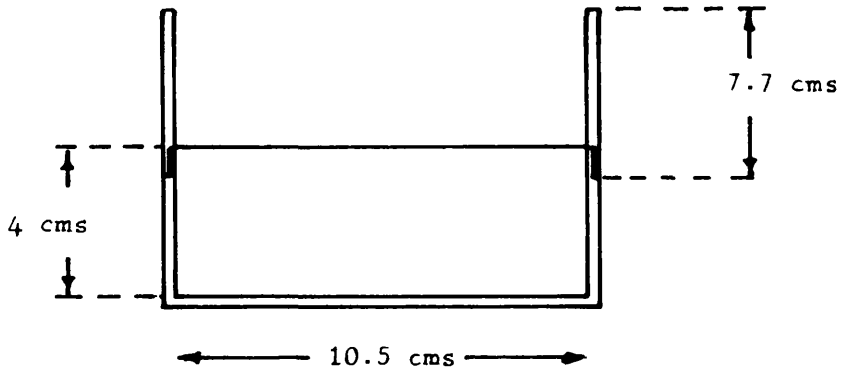

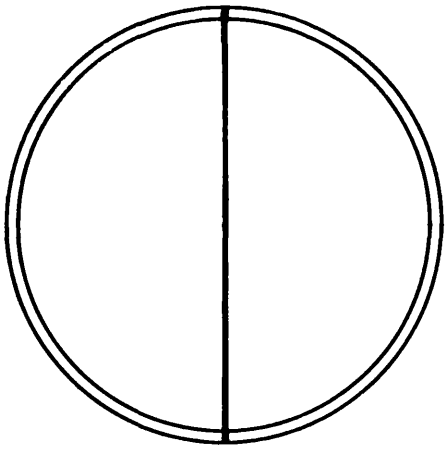

FIG. 10. Diagram of tensile tester sample cell. Rupture area = 42 sq. cms.

times, usually twenty, before the piston and weights were removed. The top retaining ring of the cell was removed and the sample scraped down until plane with the outer edge of the cell. The whole cell assembly was unclamped and left hanging free from the chains. A tensile force was applied to opposite sides of the cell by a thread and pulley system and this force was slowly increased by running water into a small bucket until the sample cell ruptured. The tensile strength could then be calculated from the weight of water in the bucket and the cell geometry.

5. Unfortunately, it was found that the results were most irregular and irreproducible. Some of the preliminary results with wet building sand (see also the sieve test) are reproduced in Figs. 11, 12, 13, 14, as an illustration.

6. Tensile strength measurements usually show this wide scatter[7,12] and the cause seems to lie in the sample preparation. There were arbitrary parameters in this preparation, such as the weight used to compact the sample and the number of twists imparted to the compacting piston - both of which had a profound effect. The more carefully the sample was prepared and compacted, the stronger it appeared to be. Results are therefore a measurement of the experimental technique, rather than the material being tested.

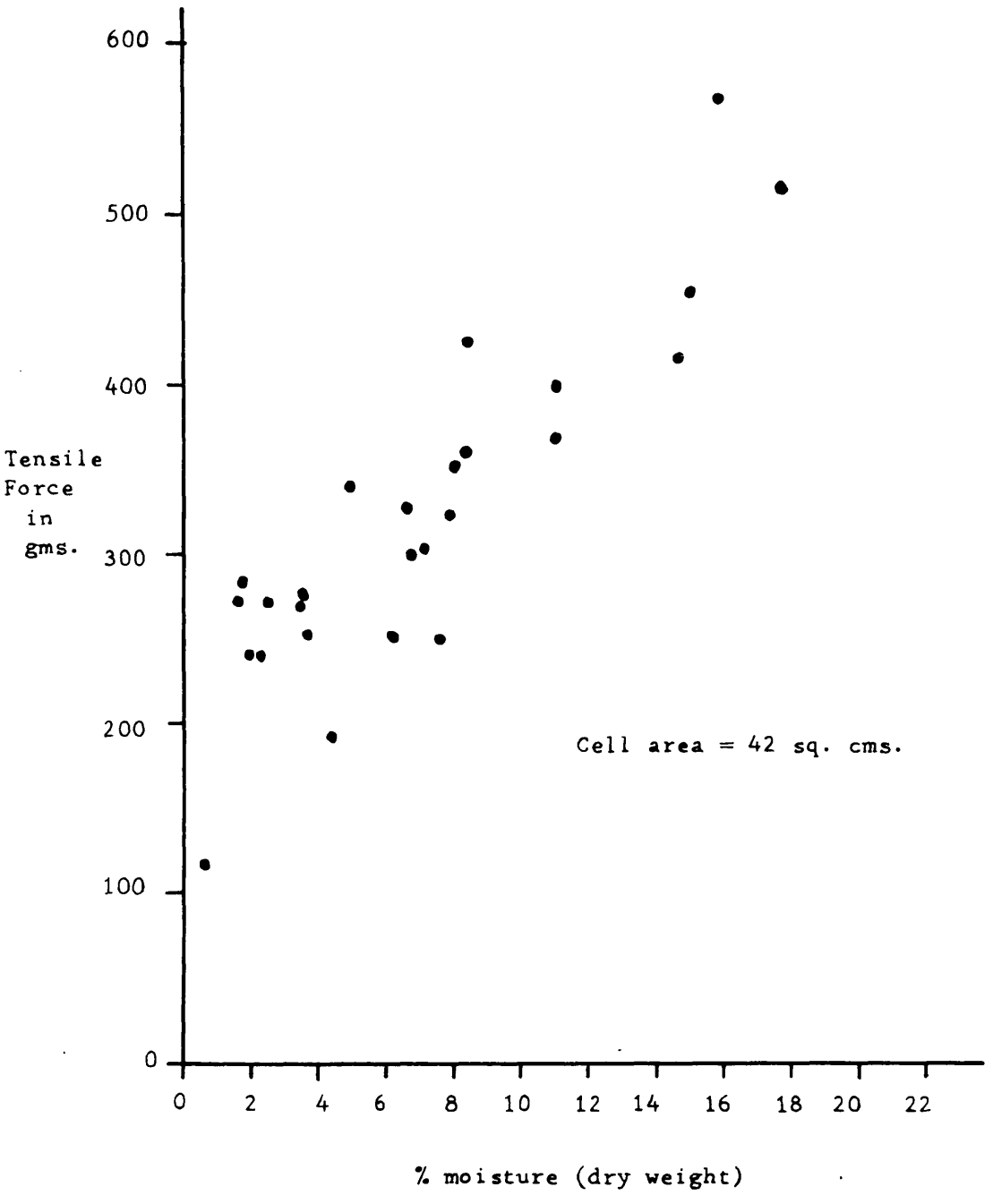

FIG. 11. Rupture forces of beds of wet sand.
Size range as received - about 50% passes 72 mesh.

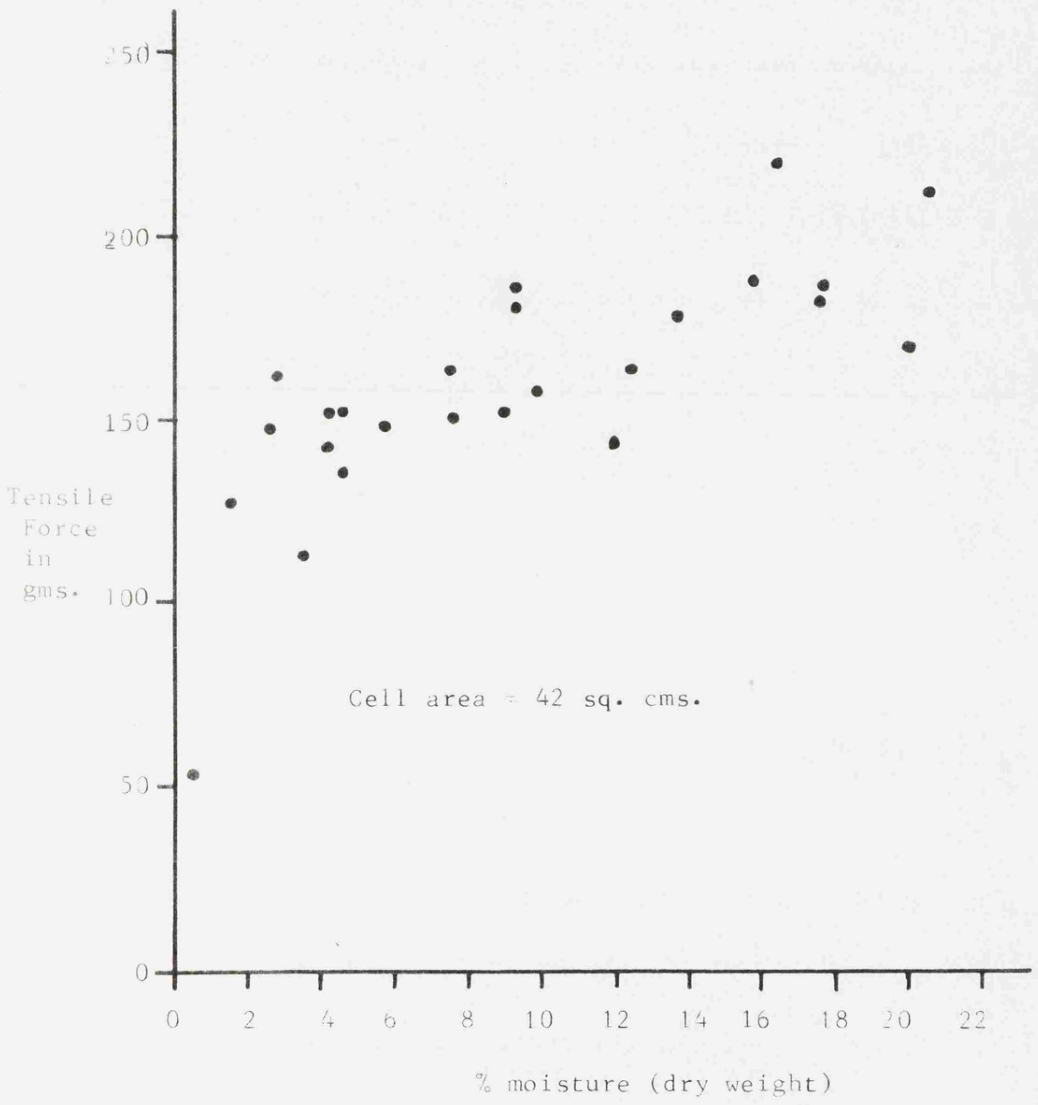

FIG. 12 Rupture forces of beds of wet sand.
Size range through 36 mesh on a 72 mesh

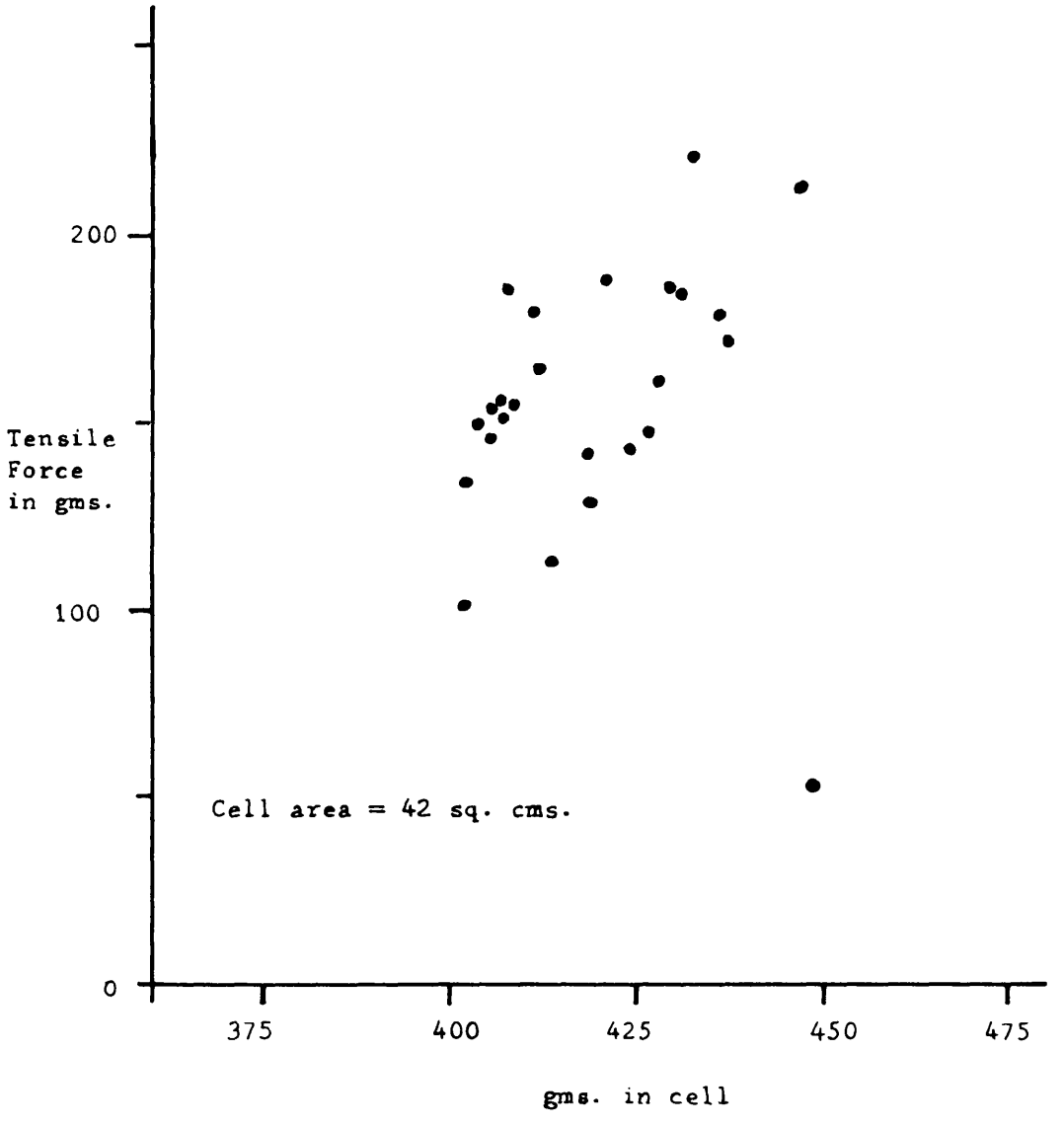

FIG. 13. Rupture forces for beds of wet sand.
Size range through 36 mesh on a 72 mesh.

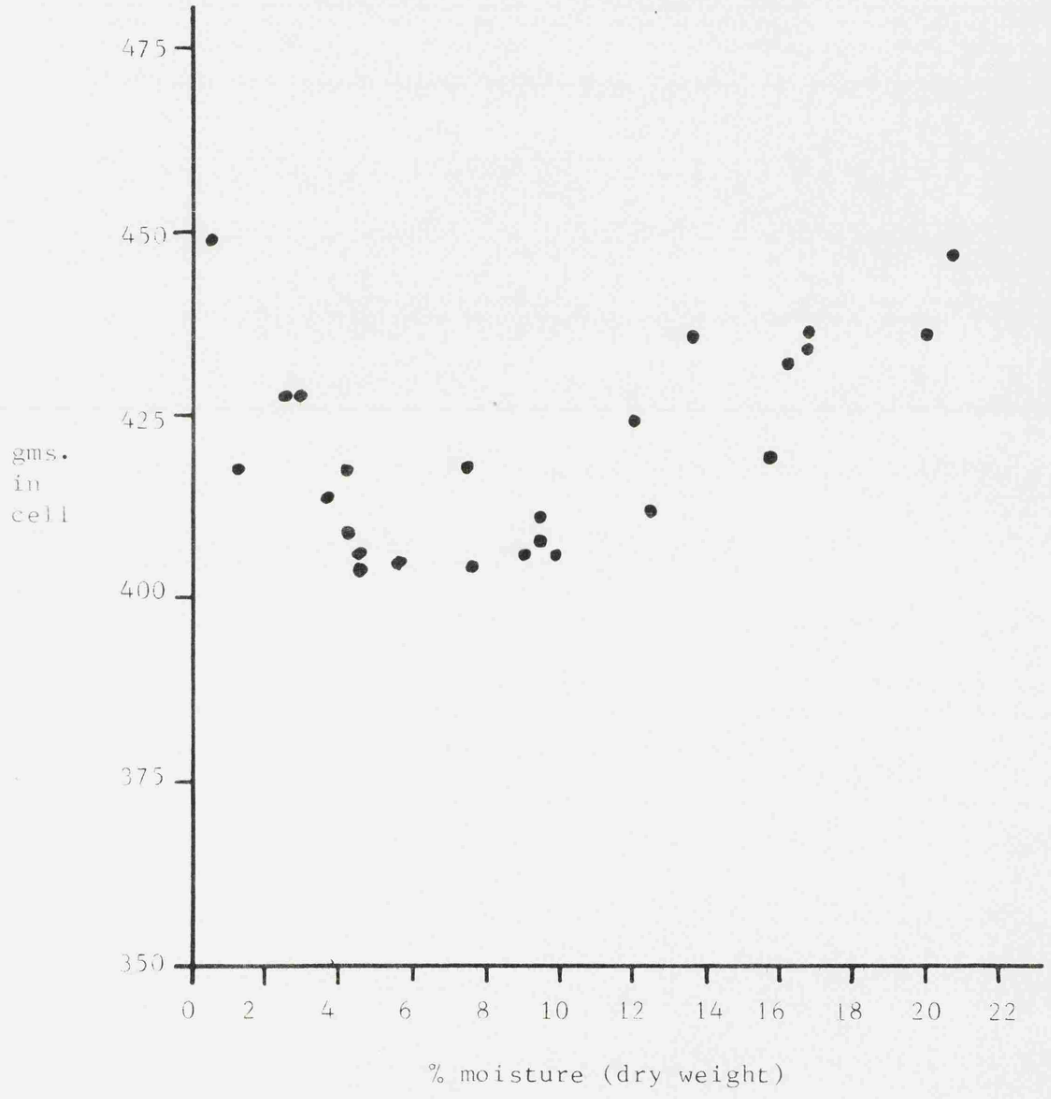

FIG. 14. Wt. of dried sand in cell packed at different moisture contents.

REFERENCES

1. The effect of additives on the handling of wet South Wales coals. J.O. Cutress & D. M. Walker. J. Inst. Fuel. 37, 537, (1964).

2. Particle size distribution of products ground in the tube mill. G. Fagerholt. Copenhagen 1945. G.E.D. Gads Forlag.

3. Effect of sieve motion on screening efficiency. A. W. Fahrenwald & S. W. Stockdale. U.S. Bureau of Mines Rpt Investigations. 2933. Washington. 1929. (Dept. of the Interior).

4. Effect of sieve loading on the results of sieve analysis of natural sand. F.A. Shergold. J. Soc. Chem. Ind. 65, 245, (1946).

5. Study of sieves for coarse aggregates. A.H.D. Markwick. J. Soc. Chem. Ind. 59, 88, (1940).

6. A precise method for sieving analysis. M. Weber Jr. and R.F. Moran. Ind. Eng. Chem. Anal. Ed. 10. 180. (1938)

7. An improved apparatus for measuring the tensile strength of powders. M. D. Ashton, R. Farley & F.H.H. Valentin. J. Sci. Inst. 41, 763. (1964).

8. Gravity Flow of bulk solids. A. W. Jenike. Bull. Utah. Engng. Exp. Stn. No. 108. 1961.

9. Dispersion of dust deposits by blasts of air. J. G. Dawes. Research Report. Nos. 36, 46, 49. (1952). Sheffield. Safety in Mines Research Establishment.

10. The physical properties of colliery stone. G. Thouzeau & T. W. Taylor. Research Report No. 197. (1961) Sheffield. Safety in Mines Research Establishment.

11. Cohesion of powder and the effect of atmospheric moisture. H. S. Eisner, G. Fogg & T. W. Taylor. 3rd. Int. Congress on Surface Activity. 1960. Vol. 2. Herstellung: Universitatsdruckerei Mainz GmbH.

12. Basic studies of coal flow. Surface tension forces in wet powders. J. F. Carr. C.E.G.B. S.W. Region Research Memorandum No. 14. 1964.

CHAPTER SIX

THEORETICAL TENSILE STRENGTH

1. Introduction.
2. Experimental facts.
3. Calculation of tensile strength.
4. Calculation of moisture content.
5. Comparison with experiments.
6. Observations of Fisher.
7. Another way of calculating tensile strength.
8. Detailed mechanism of rupture.
9. Calculation of energy to rupture packing.
10. Conclusions.

1. It is possible, knowing the geometrical properties of sphere packings, the tension forces and distance interactions of liquid bridges, to calculate the tensile strength of a random packing of spheres.[1, 2].

2. Experimentally, the variation of force with separation for a large liquid bridge between spheres can be approximated by a linear decay from a maximum at contact to zero at the rupture point. (viz. Chapter 2).

Experimentally, the relation between the separation when the bridge ruptures and the initial neck diameter appears to be a straight line (Fig. 1), and can therefore be extrapolated to give the separation at rupture for any bridge. (viz. Chapter 2).

Fisher[3] calculated exactly the initial forces at contact and the bridge neck diameter, and by applying both of the above experimental approximations it is possible to produce force/separation triangles for bridges of different volumes. (Fig. 3). The situation can be expressed by the following equation:

$$F = F_{max} - F_{max} \cdot \frac{x}{x_{max}} \qquad \ldots\ldots\ldots\ldots\ldots (1)$$

where F is the attractive force of the bridge at a sphere separation of x and x_{max} is the separation at rupture.

The variation of co-ordination number with distance has been studied in Chapter 1, and, assuming that the variation is linear, (Fig. 4), the following equation may be obtained:

$$N = 7.6 + 14.4\ x \qquad \ldots\ldots\ldots\ldots\ldots (2)$$

where N is the co-ordination number of spheres within a distance x. x is the gap between the spheres expressed in diameters.

Differentiating (2) gives

$$\frac{dN}{dx} = 14.4 \qquad \ldots\ldots\ldots\ldots\ldots (3)$$

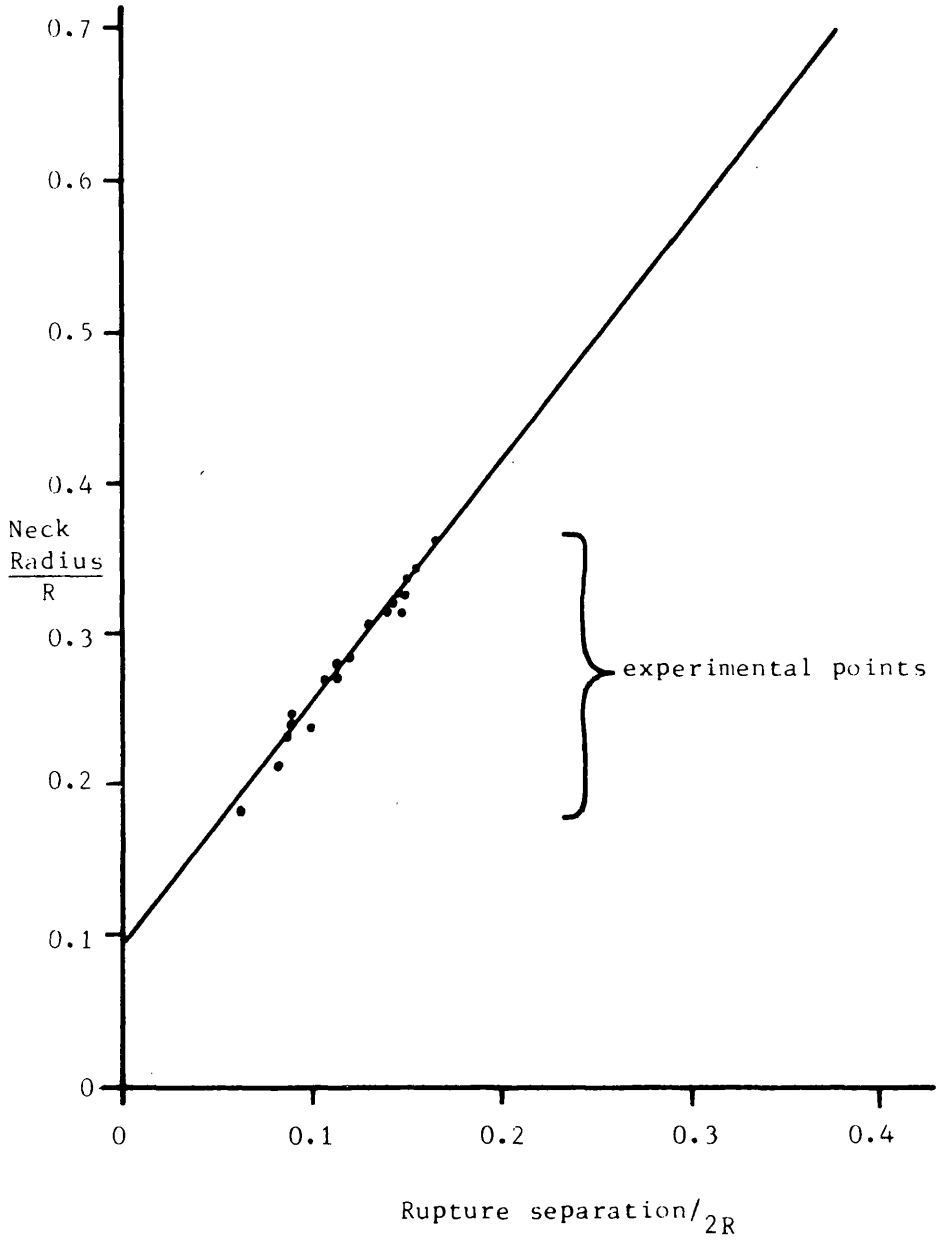

FIG. 1. Extrapolation of experimental rupture separations to larger liquid bridges.

$\frac{\text{Neck Radius}}{R}$	$\frac{\text{Force}}{2\pi R\gamma}$	$\frac{\text{Rupture Separation}}{2R}$
0.168	0.931	0.046
0.213	0.912	0.074
0.261	0.890	0.103
0.310	0.868	0.134
0.360	0.845	0.165
0.410	0.821	0.197
0.460	0.797	0.228
0.508	0.772	0.259
0.555	0.749	0.288
0.599	0.725	0.316
From Fisher[3]		Extrapolated from Fig. 1.

FIG. 2. Properties of liquid bridges related with the rupture separation.

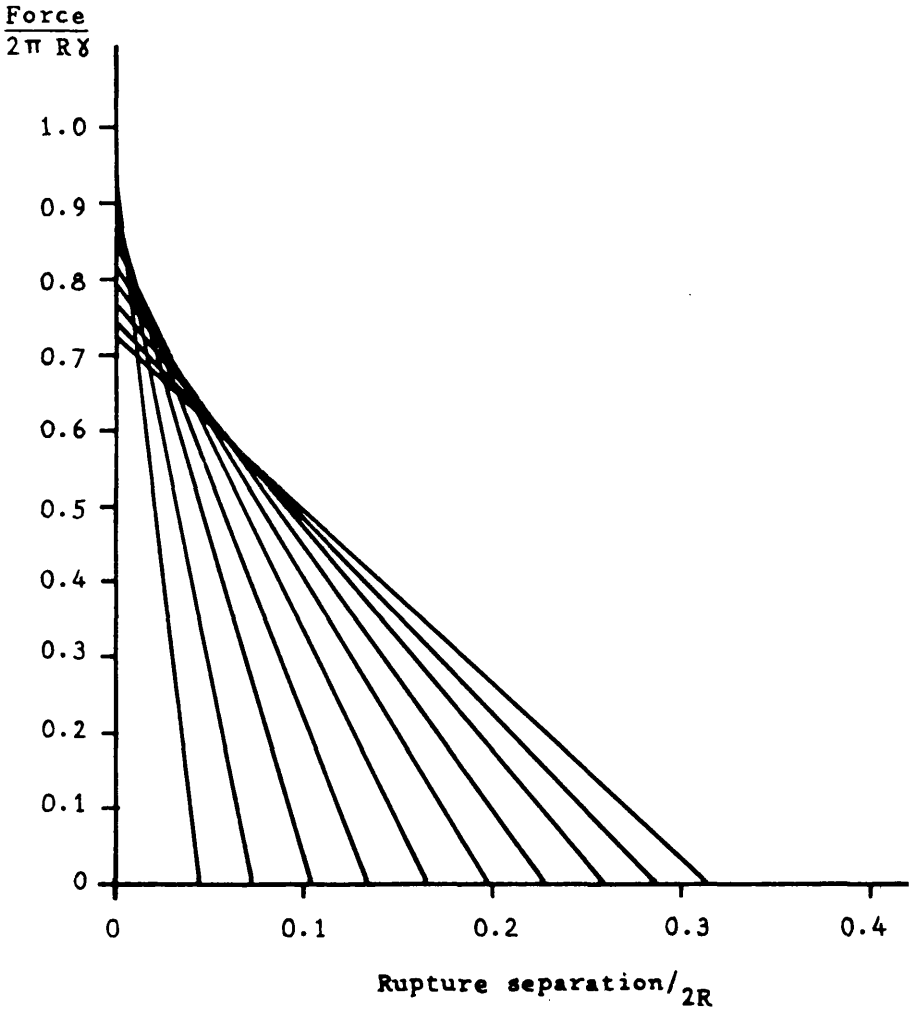

FIG. 3. Some calculated Force/separation triangles.

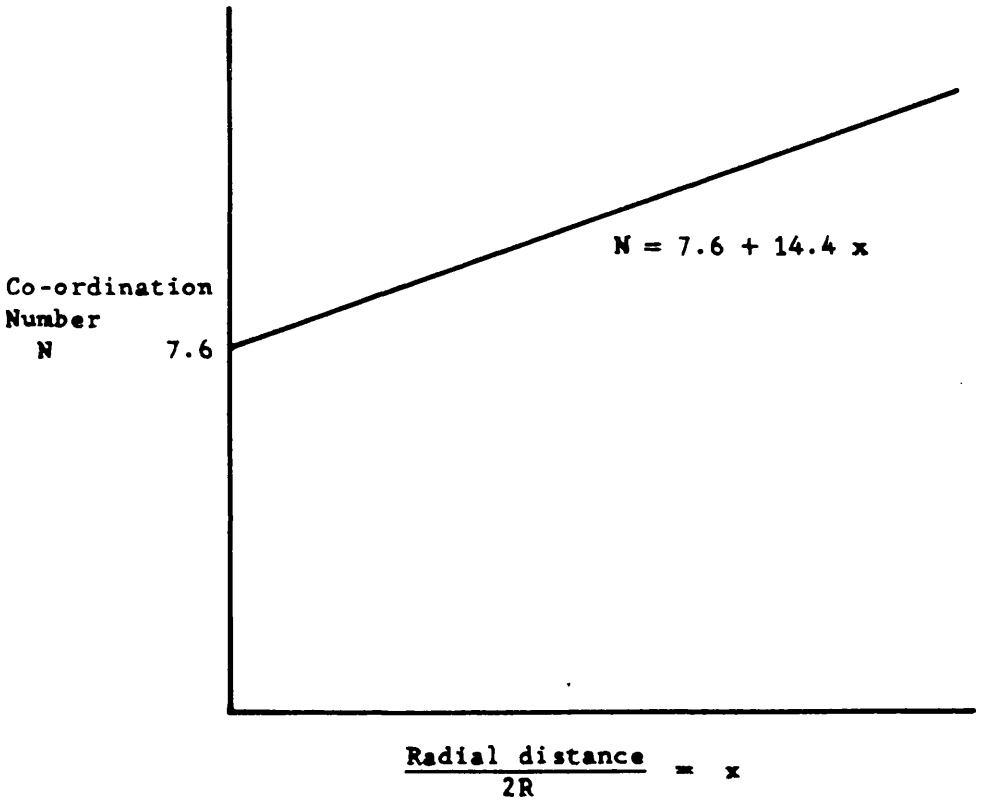

FIG. 4. Approximation of variation of co-ordination number with radial distance.

3. Assuming that all the bridges have an equal volume, and that every gap smaller than the rupture distance is spanned by a liquid bridge, then an equation for the overall tensile strength can be written:

$$TS. \quad \alpha \quad 7.6\ F_{max} + \int_{o}^{x_{max}} \left(F_{max} - F_{max} \cdot \frac{x}{x_{max}}\right) .14.4\ dx \qquad (4)$$

Evaluating:

$$TS. \ \alpha\ F_{max} \cdot (7.6 + 7.2\ x_{max}) \qquad \ldots\ldots\ldots\ldots\ldots\ldots (5)$$

However, to obtain a useful equation, the constant of proportionality has to be found. In a tensile strength determination only the force components parallel to the line of tension are involved. If the "average" sphere is considered with the forces pulling at random over its surface then the average force per unit area can be calculated. This average force per unit area will be the tensile strength.

Hence:

$$TS = \frac{F_{max}}{4\pi R^2} (7.6 + 7.2\ x_{max}) \qquad \ldots\ldots\ldots\ldots\ldots\ldots (6)$$

Fisher's[3] theoretical results give normalised values of F_{max} with a factor of $2\pi R\gamma$ by which they have to be multiplied. x_{max} can be found for the volume values of Fisher[3] by extrapolation from experimental results. (See Fig. 1).

4. Since all the bridges were assumed to have equal volume, the moisture content (% volume solids) can be calculated as both the number of bridges and their volume are known.

The calculated tensile strengths at different moisture contents are listed in Fig. 5.

It will be seen that the value of the tensile strength is virtually unchanging at a numerical value of about 7.3, and so the tensile strength of a wet granular material should be constant at about for a packing density of 0.63.

$$3.65\ \gamma / R \quad \text{dynes/cm}^2 \qquad \ldots\ldots\ldots\ldots\ldots\ldots (8)$$

$$TS = \frac{F_{max}}{4\pi R^2} \quad (7.6 + 7.2\ x_{max})$$

$$TS = \frac{\gamma}{2R} \cdot F_{calc} \cdot (7.6 + 7.2\ x_{max})$$

$$\text{Vol \% liquid} = \frac{\text{No. bridges x vol. bridges}}{2 \text{ x vol of one sphere}} = \frac{Vol_{calc} \cdot (7.6 + 14.4\ x_{max})}{\frac{4}{3}\pi}$$

Fisher[3]		Extrapolated from Fig. 1.	Number of bridges per sphere	$F_{calc} \cdot (7.6 + 7.2x_{max})$	% age liquid by volume
Volume of half of each bridge / R^3	Attractive Force / $2\pi R\gamma$	Rupture Separation / x_{max} 2R	$7.6 + 14.4\ x_{max}$		
0.000679	0.93	0.046	8.22	7.34	0.13
0.00178	0.91	0.076	8.67	7.40	0.367
0.00407	0.89	0.103	9.08	7.41	0.882
0.0826	0.87	0.134	9.53	7.45	1.88
0.0154	0.85	0.165	9.98	7.47	3.67
0.0265	0.82	0.197	10.44	7.37	6.60
0.0426	0.79	0.228	10.88	7.30	11.60
0.0647	0.77	0.259	11.33	7.26	17.40
0.0933	0.75	0.288	11.75	7.18	26.5
0.129	0.72	0.316	12.15	7.12	37.0

FIG. 5. Some tensile strengths calculated for different moisture contents using equation 6.

5. However, Carr's[4] results for spheres and coal indicate that this equation gives a tensile strength about five times too large, and in this way it is similar to Rumpf's[1] equation which errs by a similar amount.

A better equation can be derived by the somewhat irrational method of ignoring the contacts altogether as regards their contribution to the tensile strength. This gives:

$$TS = \frac{\gamma}{2R} \cdot F_{calc} \cdot 7.2 \cdot x_{max} \quad \ldots\ldots\ldots\ldots\ldots (9)$$

where F_{calc} is the peak force from Fisher's[13] calculations. This equation is compared with Carr's[14] results in Fig. 6.

6. Quite why this equation is in better agreement is not at all clear, but a limited case can be made for the suggestion. When Haines[5] and Fisher[3] were unable to explain the rise in cohesive strengths of soils with moisture content, Fisher[3] suggested that the apparatus (a wedge system) was not measuring the static stress but "the work required to rupture the connecting moisture" and pointed out that moist soil is relatively tough and dry soil relatively brittle. This statement was qualitative but what Fisher[3] had noted was that the graphs of tensile strength and potential energy of a bridge had similar shapes. Thus, he reasoned, the apparatus was not measuring tensile strength as he understood it, but some more complex factor. The difficulty was to discover why this apparent relation held and to derive theoretically quantitative values for the measured tensile strengths. In order to do this some way of converting the potential energy back into tensile strength is required and this proved rather difficult.

7. If the tensile strength is not at a maximum when the packing is unextended but remains at a constant value until some critical extension is reached then, if this critical extension can be found the tensile strength can be found from the potential energy of each

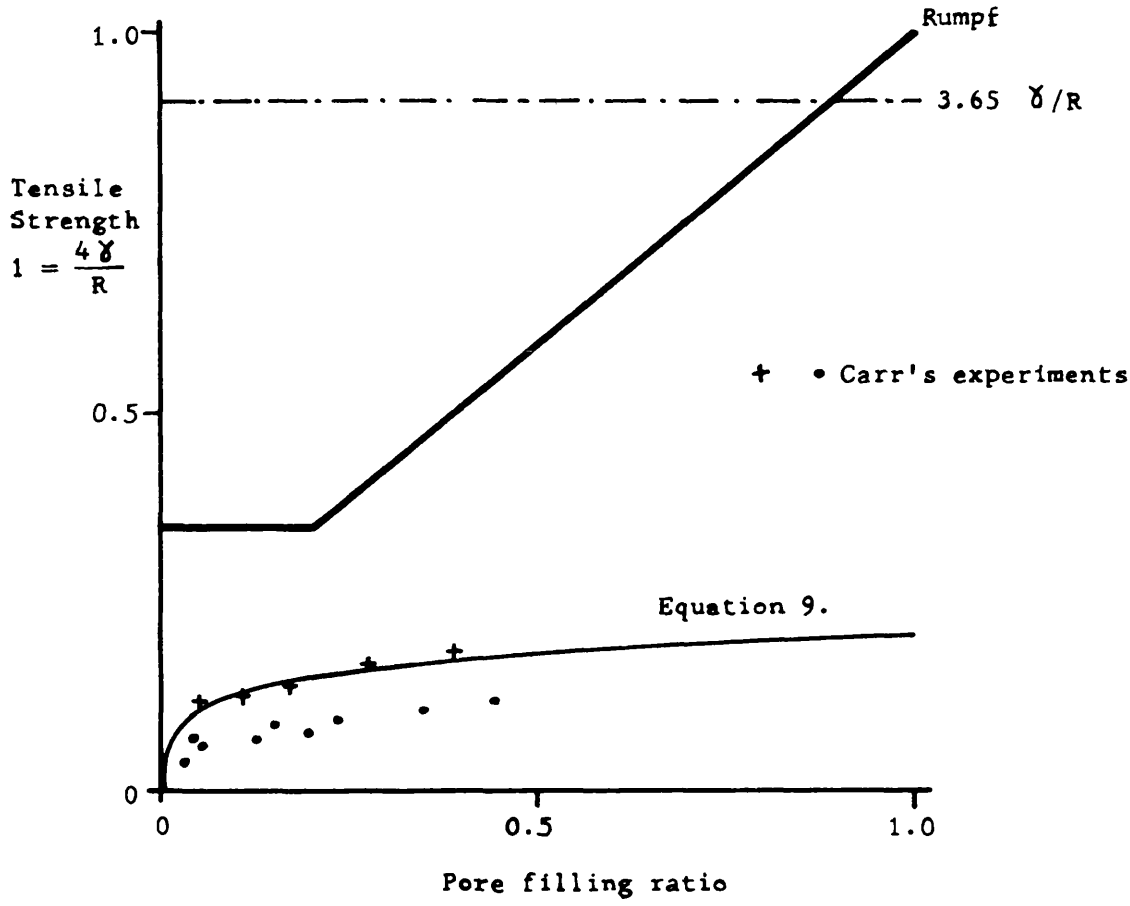

FIG. 6. Comparison of Equations 8 and 9 with that of Rumpf[1] and the experiments of Carr[4].

bridge. The problem is now that of finding the critical extension of the shear plane. Unfortunately this is very difficult to observe or measure, and an "intelligent guess" of its magnitude has to be made.

8. In the experimental work on liquid bridges (viz. Chapter 2), a rise to a maximum force was observed as the separation was increased. This was explained as misalignment of the spheres in the initial stages. It is possible that this is a real effect in packings of particles and that any pair of spheres that are not being pulled axially do not contribute to the tensile strength. Any such pair of spheres merely slide round each other, maintaining the liquid bridge until they are tensioned axially, when they stretch the bridge until it ruptures. Figs. 7, 8, 9. demonstrate this diagramatically. On this basis it would appear that the critical extension of the shear plane would be of the order of one diameter or possibly a little larger as the bridge has to stretch some way before it ruptures.

9. The energy required to rupture all the bridges around an average sphere will now be calculated.

The energy required to rupture the contacts (7.6 of them) is easily calculated as

$$= 7.6\ F_{max}\ \frac{x_{max}}{2} \qquad \ldots\ldots\ldots\ldots\ldots (10)$$

from the area beneath the line in Fig. 10.

The energy required to rupture the bridges of length 'x' is more difficult. The number of contacts between the separations 'x' and 'x + δx' will be δN, and it can be seen from equns. 2 & 3 that

$$\delta N = 14.4\ \delta x \qquad \ldots\ldots\ldots\ldots\ldots (11)$$

The energy required to rupture one of these bridges is the shaded area in Fig. 10. which can be shown to be

$$= \frac{F_{max}}{2x_{max}} (x_{max} - x)^2 \qquad \ldots\ldots\ldots\ldots\ldots (12)$$

FIG. 7.

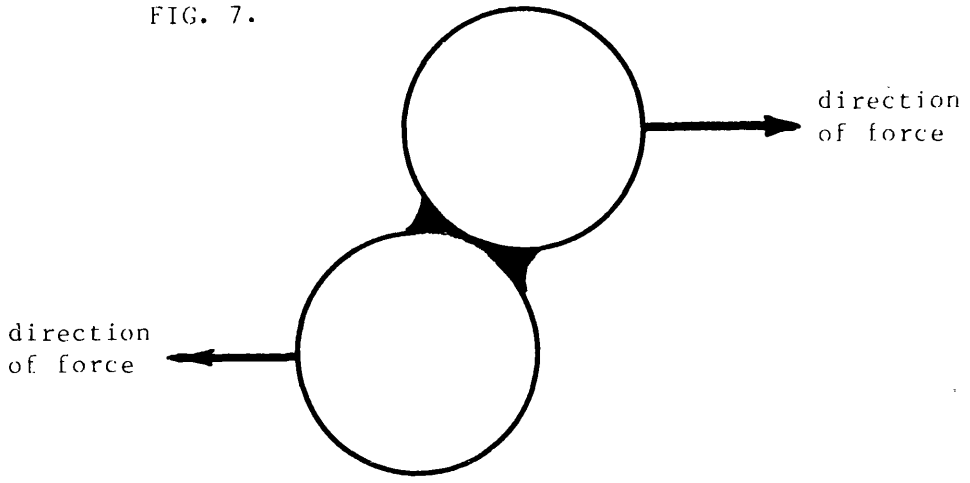

FIG. 8.

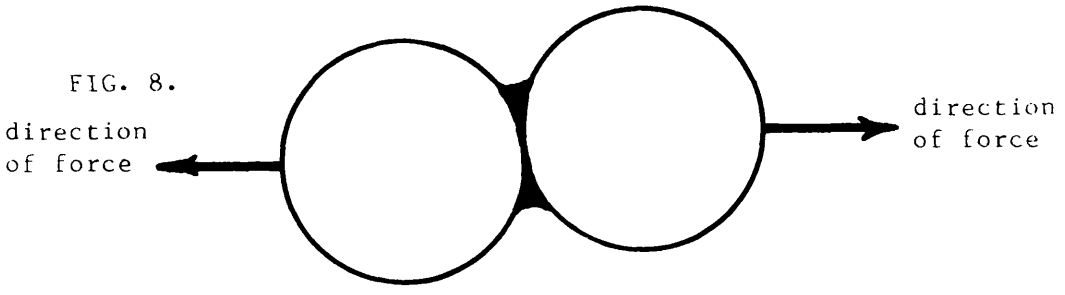

FIG. 9.

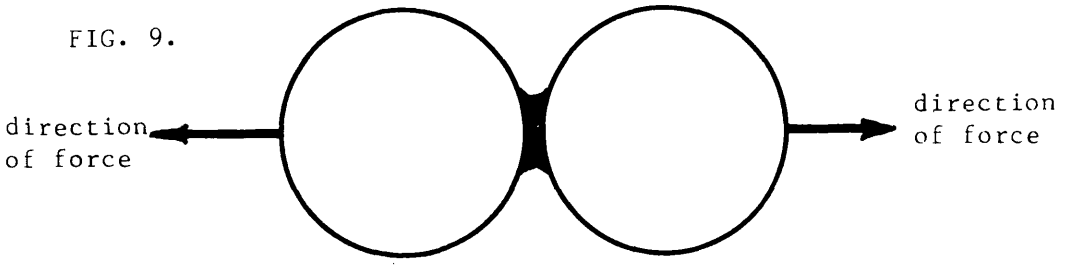

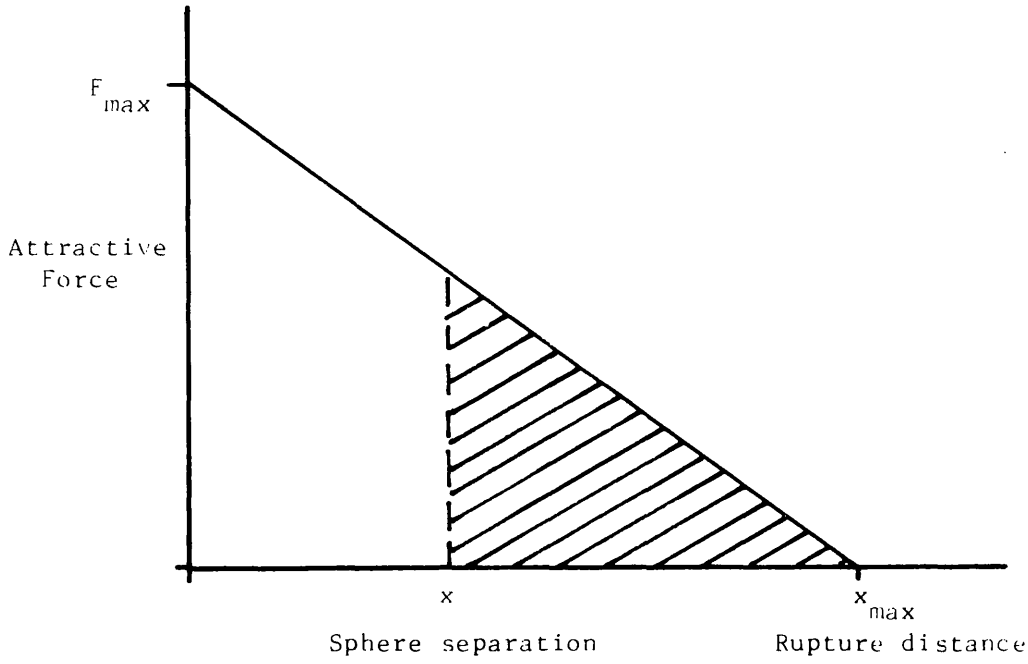

FIG. 10. Force/separation triangle for the liquid bridge between two spheres. The shaded area represents the work required to rupture a bridge of length 'x'.

Hence, the energy required to rupture δN bridges will be

$$= \frac{F_{max}}{2x_{max}}(x_{max} - x)^2 \cdot \delta N \quad \ldots\ldots\ldots\ldots\ldots (13)$$

$$= \frac{F_{max}}{2x_{max}} (x_{max} - x)^2 \; 14.4 \; \delta x \quad \ldots\ldots\ldots\ldots\ldots (14)$$

The energy needed to rupture all of the bridges around the average sphere will thus be

$$= 7.6 \; F_{max} \; \frac{x_{max}}{2} + \int_0^{x_{max}} 14.4 \; \frac{F_{max}}{2x_{max}} \; (x_{max} - x)^2 \, dx \quad \ldots\ldots (15)$$

Giving

$$E_{tot} = \frac{7.6}{2} \; F_{max} \; x_{max} + \frac{14.4}{6} \; F_{max} \; x_{max}^2 \quad \ldots\ldots\ldots\ldots\ldots (16)$$

where E_{tot} is the total energy associated with one sphere.

If a constant force acts over a distance of one particle diameter then, in order to rupture all the bridges this force will have to be

$$= E_{tot}$$

as separations are expressed normalised in diameters.

This force acts over an effective projected area of πR^2, the cross sectional area of one particle, but only ruptures half of the bridges of any one sphere on the rupture plane. Thus the tensile strength

$$= E_{tot} \cdot \frac{1}{2\pi R^2} \quad \ldots\ldots\ldots\ldots\ldots (17)$$

$$= (7.6 \; F_{max} \; x_{max} + \frac{14.4}{3} \; F_{max} \; x_{max^2}) \; \frac{1}{4\pi R^2} \ldots\ldots\ldots\ldots\ldots (18)$$

Replacing F_{max} by Fisher's[3] constant $F_{calc} \times 2\pi R$

$$TS = F_{calc} \cdot \frac{\gamma}{2R} \cdot (7.6 \; x_{max} + 4.8 \; x_{max}^2) \ldots\ldots\ldots\ldots (19)$$

As x_{max} is always less than 0.3, then x_{max}^2 will be a small term and

$$TS \simeq F_{calc} \cdot \frac{\gamma}{2R} \cdot 7.6 \; x_{max} \quad \ldots\ldots\ldots\ldots\ldots (20)$$

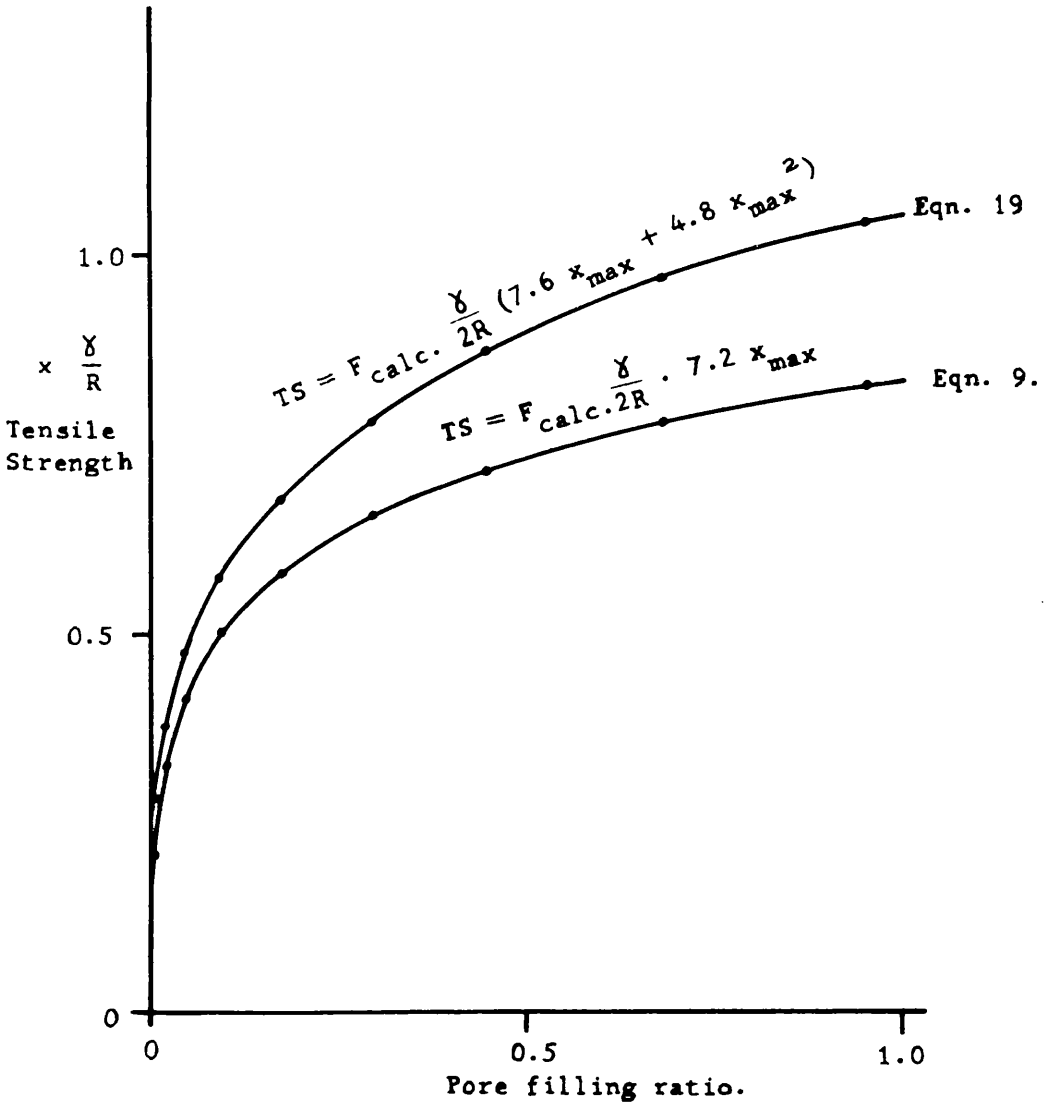

FIG. 11. Comparison of the theoretical tensile strength for Eqn. 19 and the approximation Equn. 9.

which is similar to equation (9) which gives a much better fit to Carr's experimental results than equation (8).

10. It would therefore seem that in order to obtain a theoretical equation for tensile strength of both the correct form and magnitude the assumption has to be made that the rupture plane expands by one particle diameter before the sample breaks, and that the tensile strength is constant in this region.

Alternatively, it could be argued that all experimental values of tensile strength are an under-estimate because of cracks and defects in the packing. This argument has been advanced before to account for theoretical over-estimates of tensile strength.

The properties of the individual liquid bridges in the random packing are known precisely, as are the geometrical properties of individual spheres in the packing. Furthermore, individual bridges are known to occur, as experiments with corrosive or setting liquids in sphere packing have demonstrated.

However, the combination of both these accurately known properties in the simplest manner yields an equation which considerably over-estimates tensile strength, and one has to postulate an exact mechanism before a reasonable equation can be derived.

Perhaps the answer lies in experiments which measure the extension of the packing as well as the tensile strength. Also tests which measure the energy required to break the sample may show that the mechanism of "tensile strength" is not as simple as it appears, and that the observation of Fisher[3] that dry soil is brittle and wet soil relatively tough is the key to the problem.

REFERENCES

1. The strength of granules and agglomerates.
H. Rumpf. Agglomeration. 379-481. Interscience. 1962.

2. Tensile strength of granular materials.
V. Smalley & I.J. Smalley. Nature 202, 168. (1964).

3. On the capillary forces in an ideal soil.
Correction of formulae given by W.B. Haines.
R. A. Fisher. J. Agric. Sci. 16, 492. (1926).

4. Basic studies of coal flow. Surface tension forces in wet powders. J.F. Carr. C.E.G.B. S.W. Region Research Memorandum. No. 14. 1964.

5. Studies on the physical properties of soils II.
W. B. Haines. J. Agric. Sci. 15, 529. (1925).

CONCLUSIONS

1. There are many small gaps in a dense random packing of equal spheres. The average number of spheres touching a typical sphere is about equal to the average number within a maximum sphere centre separation of 1.4 diameters, but not touching the typical sphere.

2. The calculations by Fisher of the properties of liquid bridges between contacting spheres have been compared with experiments and have in every way proved adequate.

3. The properties of liquid bridges between a sphere and a plane, calculated using the toroid approximation, have been compared with experiments and have, in most cases, proved adequate. The approximation overestimates the neck radius for a given bridge volume.

4. Liquid bridges spanning small gaps between spheres <u>increase</u> in strength as the bridge volume increases.

5. Liquid bridges between contacting spheres <u>decrease</u> in strength as the bridge volume increases

6. The increase in tensile strength with increasing moisture content of random packings of spheres cannot be explained by the number of bridges increasing with moisture content or by the bridges spanning small gaps increasing in strength with bridge volume because the combination of these two effects is almost exactly equalled by the decrease in strength with increasing bridge volume of the bridges between contacting spheres.

7. The increase in tensile strength with increasing moisture content of random packings of spheres can be explained by a rupture mechanism in which the packing expands at a constant tensile strength by about one particle diameter before rupturing.

8. The contact angle of paraffin displacing water from high rank coals is probably related to the response of these coals to oiling.

9. Paraffin does not spread spontaneously on wet weathered high rank coals.

10. Specular reflectance is a particularly simple method of determining the infra red spectra of finely ground coals.

SUGGESTIONS FOR FURTHER WORK

There is scope for more work on packings of equal spheres. The co-ordination numbers and near neighbour distribution functions for packings of different density would be particularly useful.

A study of packings of different sized spheres, in particular of their co-ordination numbers and near neighbour distribution functions, would enable an ideal model, which more nearly resembled a real powder, to be constructed.

Details of liquid bridges between spheres of different sizes would have to be obtained if the tensile strength of packings of different sized spheres were to be calculated.

The measurement of extension before rupture of a packing would enable the hypothesis of packing extension, proposed in Chapter 6, to be tested experimentally.

The effect of the solid/liquid contact angle on the tensile force exerted by liquid bridges between spheres should enable properties of non-wetted powders to be inferred.

In respect of coal, the effect of temperature on the coal/water/oil contact angle is probably worth studying because temperature has been shown to have a considerable effect on coal/water/air contact angles.

The work on the sieve test, although unsatisfactory from a theoretical aspect, could be easily and quickly pursued. In particular, studies on an inert solid, using liquids with different surface tensions, viscosities and densities might enable a mechanism for this quick and easy test to be formulated.

Most important of all is the need for some accurate and reproducible method for studying the tensile strength of wet powders. There is scope for the development of the apparatus described in Chapter 5; the chains could be replaced by rods and the framework made more stable. A powerful means of clamping the cell while the sample is made, but a means that can be released without straining the sample, might be arranged magnetically.